EXCITATION-CONTRACTION COUPLING IN HAMSTER MODEL OF CARDIOMYOPATHY

by

TONY SUNGNAN MA

A Thesis Presented to the
University of Manitoba
in Partial Fulfillment
of the Requirements for the Degree of
Doctor of Philosophy

Department of Pharmacology and Therapeutics

University of Manitoba

1977

To All of my Family
and Loving Friends

EXCITATION-CONTRACTION COUPLING IN HAMSTER MODEL OF CARDIOMYOPATHY

BY

TONY SUNGNAN MA

A dissertation submitted to the Faculty of Graduate Studies of the University of Manitoba in partial fulfillment of the requirements of the degree of

DOCTOR OF PHILOSOPHY

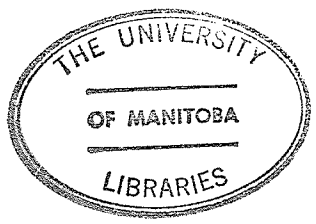

ACKNOWLEDGEMENTS

I am grateful for the financial assistances provided by the University of Manitoba and Dalhousie University Graduate Fellowships during the period of this study.

I would like to thank my supervisor Dr. L.E. Bailey for his introduction to me of the extremely interesting subjects of ion exchange kinetics and primary cardiomyopathy, for his encouragements during my many set-backs, for his continuous critical advices, for his generous allowance to let me use his facilities, and for his patience in supervising the writing of this manuscript.

I would also like to express my appreciation for the many advices and suggestions from Dr. P.E. Dresel and Dr. D. Bose. I wish to acknowledge Dr. I. Innes and the entire staff of the Department of Pharmacology at both the University of Manitoba and Dalhousie University for allowing me to associate with, and to learn from them, throughout my years in graduate studies.

I wish to acknowledge Mr. S. Vivian for writing the computer program for graphical analysis, Mr. J. Delaire for designing and assembling the perfusion set-up and electronics, and Mr. J. Kiekush and his staff for their excellent hamster breeding.

I appreciate very much the kindness from Mrs. Marge Turner of the University of Manitoba and Miss Janet Murphy of Dalhousie University, who have gone out of their ways to make my graduate student days peaceful and worthy of happy memories.

Finally I like to thank Mrs. R. Hayes and Mrs. E. Banfield for typing this thesis.

failure. A 1:1 correspondence was revealed between the concentration of surface sialic acid residues and Ca bound to the sarcolemma. Cardiomyopathic hearts had a simultaneous reduction of surface sialic acid residues and Ca binding capacity. There was also an indication of a reduced sialyltransferase activity. The results suggested a close relationship between the sarcolemmal sialic acid residues, sarcolemmal Ca binding capacity, fast exchanging Ca pool size from kinetic studies and contractility of the hamster hearts.

It is proposed that the basic fundtional defect of this cardiomyopathy is a deficiency of surface membrane sialic acid residues. This hypothesis not only accounts for the depressed contractility in the myopathic hearts but also suggests a mechanism for the observed supersensitivity of the heart to the necrotic action of catecholamines based on the Ca permeability regulating function of the surface sialic acid residues. Spontaneous myolysis is suggested to result from reflex elevation of cardiac sympathetic tone due to genetic-predisposed depression of cardiac contractility.

ABSTRACT

It is well known that extracellular and surface bound Ca are intimately involved E-C coupling in cardiac muscle. It is also known that cardiac contractility is depressed in cardiomyopathic hamster hearts during the stage of hypertrophy and failure. The purposes of this investigation were threefold: (1) to study the changes in cardiac contractility and Ca exchange kinetics as a chronological function of the disease process, (2) to relate changes in the binding properties of an isolated cardiac sarcolemmal fraction to superficial Ca compartment size and cardiac contractility, and (3) to relate changes in surface sialic acid residues to Ca binding capacity.

From non-steady state Ca exchange kinetics and contractility changes it was concluded that a rapidly exchanging superficial Ca pool was responsible for regulation of contractile force in the hamster heart. The same conclusion was reached in both Ca washout and Ca uptake studies although different kinetic models were necessary. In washout studies, an in-parallel model between rapidly and slowly exchanging Ca compartments adequately described Ca efflux. An in-series model described the kinetics of Ca movement in the uptake studies. In all age groups examined, there was a reduction of the Ca content of the rapidly exchanging compartment. This depression was correlated with reduced cardiac contractility and was particularly pronounced during the stage of congestive

TABLE OF CONTENTS

LIST OF FIGURES

LIST OF TABLES

SECTION I

INTRODUCTION

A. DEFINITION AND INCIDENCE OF PRIMARY CARDIOMYOPATHY

The concept of cardiomyopathy developed slowly. Clinicians and pathologists first paid attention to this group of diseases in the 1930's when several observers reported cases of what were called for lack of a better term "idiopathic myocardial hypertrophy", "idiopathic cardiomegaly", or "cardiac hypertrophy of unknown causes" (Mattingly, 1965). Microscopic observations in these reports indicated degenerative changes of the myocardium, but not the changes of cellular infiltration or proliferation associated with myocarditis (inflammation), while clinical and necropsy findings ruled out the possible involvement of hypertension, coronary or vascular diseases. The disease entity, however, was relatively slowly realized as indicated by its absence from the program in the First National Conference on Cardiovascular Diseases in 1950.

At the Second National Conference on Cardiovascular Diseases in 1965, the term "cardiomyopathy" was used interchangeably with "primary myocardial disease" and designated those diseases which when they involve the cardiovascular system attacked primarily the heart muscle and minimally involve the endocardium, pericardium, blood vessels, valves and other cardiovascular structures (Burch et al, 1965).

This definition has been accepted in large part up to the present with the reservations that endocardial involvement occurs in some cases (eg. endocardial fibrosis) and that pri-

mary cardiomyopathy encompasses only one sub-group of the more general cardiomyopathies.

No single classification of cardiomyopathy has been accepted by all, the present trend is to categorize the cardiomyopathies in terms of their possible etiological factors. Table I summarizes the major sub-groups of cardiomyopathies as proposed by Burch and DePasquale (1970). Although this is by no means completely satisfactory, as recognized by its authors, the distinction between primary and secondary heart muscle diseases makes the classification less ambiguous and more understandable. In this classification, the primary cardiomyopathies represent a sub-group of cardiomyopathies, which, because of lack of information, could not be localized to the possible etiological factor. Thus, the primary cardiomyopathy may not be a single entity of heart disease but a syndrome; the diagnosis is made by exclusion of the heart diseases of known etiology.

In the following review of the literature, a slightly modified version of the preceding classification is adopted. Since progressive muscular dystrophy is associated with (primary) cardiomyopathy in the majority, if not all cases (see below), and since the etiological factor assigned is by association only, the cardiac lesion in this desease will be treated as a primary cardiomyopathy.

The world wide incidence of primary cardiomyopathy is not known because diagnosis of the disease is arrived at by elimination (of other heart muscle diseases) and thus requires exhaustive patient history, clinical and necropsy findings.

Table 1

Heart Muscle Disease

I. Primary heart muscle disease

- A. Familial cardiomyopathy
- B. Non-familial idiopathic cardiomyopathy
- C. Endomyocardial fibrosis

II. Secondary heart muscle disease

- A. Infectious myocarditis
- B. Alcoholic cardiomyopathy
- C. Puerperal cardiomyopathy
- D. Metabolic cardiomyopathy

  (Hyperthyroidism, Hypothyrodism, amyloidosis, glycogen storage disease, nutritional deficiency)

- E. Allergy-related cardiomyopathy
- F. Cardiomyopathy associated with systemic disease of unknown etiology

  (Rheumatoid arthritis, autoimmune disease, collagen vascular disease)

- G. Toxic cardiomyopathy

  (Drugs, anethetic gas, poisons, foods, heavy metals)

- H. Infiltrative cardiomyopathy
- I. Cardiomyopathy due to physical agents
- J. Cardiomyopathy associated with neuromuscular disorders

  (Progressive muscular dystrophy, Friedreich's ataxia)

- K. Primary tumors of the myocardium
- L. Senile cardiomyopathy
- M. Ischemic cardiomyopathy

Increasingly, cardiomyopathies previously considered idiopathic (or primary) are now being classified secondary to viral infection, alcoholism, malnutrition, etc. The continually changing criteria of clinical and necropsy diagnosis makes an estimate of incidence extremely difficult if not meaningless.

Nevertheless, with clinical awareness of this disease, primary cardiomyopathies have been reported from all corners of the world (Fejfar, 1968). Incidence of idiopathic cardiomegaly ranged from 43% in Mombasa, Kenya to 37.5% in Johannesburg, South Africa among patients hospitalized with heart disease. The incidence of endomyocardial fibrosis in the same geographic zone was 10-11% (Fejfar, 1968). In Japan, from 1958 to 1967, 4.4% of patients with heart disease that were autopsied were classified to have been inflicted with idiopathic cardiomyopathy (Okada & Nasu, 1970). The incidence of idiopathic cardiomyopathy in the United States is not clear. McGill and Thatcher (1955) reported a 7-8% incidence of children with idiopathic heart muscle diseases in New Orleans during the interval from 1949 to 1953. Lyon (1966) reported an incidence of 1.1% in Bronx VA Hospital in 15 years.

B. ANIMAL MODELS OF PRIMARY CARDIOMYOPATHY

By definition, a primary cardiomyopathy precludes any experimental manipulation. Hence, reproducible experimental models with spontaneous myocardial lesions can only be

obtained through hereditary cardiomyopathic strains of animals. Fortunately, a number of hereditary animal cardiomyopathies have been recognized.

Jasmin and Bajusz (1962) were the first to recognize myocardial lesions in strain 129 of dystrophic mice. However, the muscular lesions, though severe in skeletal muscle, only occurred occasionally in the myocardium. In the same year, Homburger and co-workers (1062) reported the occurrence of a muscular dystrophy-like lesion associated with cardiac necrosis in an inbred line of Syrian hamsters. The subsequent pedigreed BIO 14.6 strain of hamsters with a 100% incidence of hereditary disease, spurred voluminous investigations in the field of hereditary primary cardiomyopathy. This is the animal model I have chosen for my study of excitation-contraction coupling in primary cardiomyopathies.

C. EXCITATION-CONTRACTION (E-C) COUPLING IN THE HEART

The link between the electrical events which occur at the surface of a muscle fiber with the contractile process that takes place within the fiber has been a puzzle that still lacks a complete solution. Although Ringer (1883) recognized the essential role of Ca for the maintenance of cardiac contractility, it was not until the work of Locke and Rosenheim (1907) and Mines (1913) that electrical excitability was dissociated from cardiac contractility. It was then established that electrical excitability of the heart persisted in a Ca-free medium long after the heart had ceased

to contract. This demonstrated the existence of intermediate steps, coupling contraction with excitation, which were Ca dependent.

Much of the early work on the mechanism of E-C coupling has been done on skeletal muscle. Abundant evidence has now accumulated to suggest different mechanisms for E-C coupling between cardiac and skeletal muscle. The observation that skeletal muscle would contract for hours in Ca-free solution, in the presence of lanthanum (La) (Andersson and Edman, 1974), or for many minutes in EGTA buffered solution with external Ca less than 2×10^{-9} M until the resting potential began to decline, suggests that extracellular Ca is not essential to the E-C coupling process of this tissue. On the other hand, removal of extracellular Ca caused rapid reduction of contractility in cardiac muscle with a half time ($t_{\frac{1}{2}}$) of 15-60 sec (Bailey and Dresel, 1968). Similarly, La (0.5 mM), which is known to specifically displace Ca from the extracellular binding sites (Langer and Frank, 1972), caused reduction of cardiac contractility with a $t_{\frac{1}{2}}$ of 22 sec (Ong, 1972). These observations demonstrated the important participatory role of extracellular Ca in cardiac muscle E-C coupling.

Increasing evidence is now accumulating to suggest that the Ca involved in E-C coupling of the heart is not only derived from the interstitial free form of Ca, but is also supplied from a superficially bound form of Ca external to the cardiac sarcolemma. The following review demonstrates the gradual development of this concept in E-C coupling of the heart muscle.

The important role of a rapidly exchanging superficial Ca in cardiac cell E-C coupling is deduced from both kinetic and electrophysiologic data. However, the concept that superficial Ca represents both bound and free Ca is based primarily on histochemical and ultrastructural studies.

1. Ca flux and exchange kinetics: role of a superficial Ca pool

In early studies on the interaction of Ca and Na on the contractility of amphibian heart muscle, it was observed the cardiac contractility remained constant if extracellular $[Ca]/[Na]^2$ was kept constant. This led Luttgau and Niedergerke (1958) to propose that Ca and Na ions competed for a hypothetical site or molecule R at the cell surface, but that only the CaR complex could initiate contraction. This hypothesis of Ca entry being responsible for the initiation of contraction was supported by the observation of increased Ca uptake during augmented cardiac contractility brought about by lowering the external Na or increasing the external Ca (Niedergerke, 1963). A similar correlation between contractility and Ca flux has been reported by Winegrad and Shanes (1962) in guinea pig atria.

In their study of guinea pig atria, Winegrad and Shanes defined kinetically the exchangeable Ca into fast and slow components. The former had a $t_{\frac{1}{2}}$ of 4.5 min and was considered to include superficial ("intermediary") Ca, in addition to extracellular Ca, similar to "activator Ca" proposed earlier by Luttgau and Niedergerke (1958). Langer (1964) introduced

the arterially perfused isolated dog papillary muscle and resolved the exchangeable Ca kinetics into five components. It was proposed that the component which had a $t_{\frac{1}{2}}$ of 6 min corresponeded to the superficial Ca important in E-C coupling. In 1968, Bailey and Dresel, showed that the washout of Ca from a kitten heart was characteristic of a three compartment system; the second compartment washout with a $t_{\frac{1}{2}}$ of 43 sec was similar to the interstitial (inulin) compartment washout and was correlated with the decay of contractility. Furthermore, the Ca content of this compartment, upon changing perfusate Ca concentration, positively correlated with the cardiac contractile force. Subsequent work from the same laboratory indicated the $t_{\frac{1}{2}}$ of the exchange of this compartment to be 12-22 sec (Ong, 1972; Pang, 1976).

With consideration given to different preparations and procedures (eg. perfusate flow rate), different laboratories also have reported a superficial Ca pool which is primarily interstitial in origin and has a $t_{\frac{1}{2}}$ of around 60 sec or less (Shine et al, 1971, $t_{\frac{1}{2}}$ = 83 sec; Saari and Johnson, 1971, $t_{\frac{1}{2}}$ = 16 sec). In 1972, Langer and Frank reported the Ca exchange kinetics of cardiac tissue culture cells. The rapidly exchanging compartment in this study had a $t_{\frac{1}{2}}$ of 54 sec which was abolished by the addition of 0.5 mM La. La abolished the contractile activity although regenerative depolarization of the cells was maintained. This again supported the concept of an important role for rapidly exchanging superficial Ca pool in cardiac cell E-C coupling.

2. Electrophysiological evidence for a superficial Ca in E-C coupling

In mammalian myocardium, prolongation of the action potential at the level of the plateau by means of voltage clamp decreases the rate of relaxation and causes a secondary component of tension to develop which is maintained for the duration of depolarization (Morad and Trautwein, 1968). The initial rapid development of tension is called the "phasic tension" whereas the maintained tension is called the "tonic tension".

The voltage-tension relationship of the phasic tension component is highly sensitive to alteration of extracellular Ca ($[Ca]_0$). In contrast, tonic tension appears to saturate at $[Ca]_0$ of approximately 2 mM. Catecholamines or low $[Na]_0$ both potentiate the phasic response while supressing the tonic response. This divergent behavior by two components of tension development suggest separate functional sources of activator Ca (Morad and Goldman, 1973).

Since tonic tension is maintained for the duration of depolarization and relaxes only after repolarization, it has been suggested that the source of activator Ca is extracellular pool and/or the surface membrane bound Ca (Morad and Goldman, 1973). Phasic tension, on the other hand, although proportionately affected by $[Ca]_0$, is nevertheless independent of continuous membrane depolarization, suggesting an intracellular site may be "triggered" in some way to release Ca. Failure of continuous membrane depolarization to affect phasic tension is explained in terms of depletion of the store of Ca involved

in maintaining phasic tension.

Ionic movements during the phasic contraction have been explored by voltage clamp experiments. Under a variety of conditions in which the influence of the fast initial Na current is essentially abolished, such as in the presence of tetrodotoxin or in Na-deficient medium, a small inward current carried by Ca ion (I_{Ca}) was observed (Beeler and Reuter, 1970 a, b, c). This current is increased by epinephrine (Reuter, 1973) but is greatly reduced or abolished by Ca antagonists, Mn, La, verapamil or D600 (Kohlhardt et al, 1973).

The dominant role of I_{Ca} in the E-C coupling of cardiac muscle is indicated by the identical threshold for eliciting a contraction and I_{Ca}. Phasic contraction cannot be observed without I_{Ca} and vice versa (Trautwein, 1973).

3. Ultrastructural localization of cardiac superficial Ca

It has been known for years that many different kinds of cells have a surface coating rich in polysaccharides which is thought to reside in membrane glycoproteins (Cook, 1968; Hughes, 1973). Fawcett and McNutt (1969), in their extensive ultrastructural description of cat myocardium, emphasized the presence of a protein-polysaccharide moiety on the muscle cell membrane which continue to line the T-tubule invagination. They speculated that this might be one of the morphological differences between cardiac and skeletal muscle (which has narrow T-tubules, unlined with glycoprotein) which contribute to their functional differences in E-C coupling. Subsequently, extensive surface coating of cardiac muscle cells has been demonstrated in different species and in different stages of

cell development (Howse et al, 1970; Manasek, 1976).

The composition of the membrane glycoprotein was initially shown to contain high concentration of sialic acid on erythrocyte membranes. Sialic acid residue, which has a carboxy group of low pKa (pKa = 2.6), is thought to confer negative charges to the membrane glycoprotein. Indeed, tryptic degradation and release of a sialomucopeptide caused concommitant reduction of cell electrophoric mobility, indicating the removal of net surface charges (Seaman, 1960). The acidic nature of the glycoprotein end groups is also responsible for a variety of cationic staining such as Hale stain (Gasic and Berwick, 1963), colloidal iron (Revel, 1964) and colloidal thorium (Rambourg and LeBlond, 1967) reaction in which the acidic end groups caused local precipitation of the staining agent. Cook et al (1961) demonstrated that neuraminidase treatment which removes the sialic acid also removes the staining properties of the cell coat.

Bennett has suggested as early as 1963 that the surface anionic sites can bind cation and serve as a site for the regulation of cationic movements. Fawcett and McNutt (1960) further emphasized a functional role of the surface bound polysaccharide of the cardiac basement membrane. From the kinetic studies of ionic exchange ion cardiac muscle, it was noted that the capacity of the superficial pool is greater than combined interstitial and vascular Ca which prompted Langer (1973) to propose the basement membrane as the binding site for additional superficial Ca. La ion, which has high affinity

for Ca binding sites, not only binds to the basement membrane but physically displaces the superficial Ca and uncouples excitation from contraction (Langer and Frank, 1972). The evidence therefore suggests not only the presence of an anionic site on the surface of cardiac sarcolemma which has the affinity for Ca ion, but also that the displacement of the superficially bound Ca deprives the ability of the muscle to contract. It is unfortunate that although many investigators have studied the Ca binding characteristics of isolated plasma membrane (eg. Schlatz and Marinetti, 1972; Williamson et al, 1975; Willet et al, 1976; Dhalla et al, 1976; Sulakhe et al, 1976; Feldnan and Weinhold, 1977),none has attempted to relate quantitatively the amount of Ca bound to the isolated sarcolemma on the one hand to that termed "superficial" derived from ion exchange studies on the other. Similarly, although the enzyme responsible for glycosidically linking sialic acid to glycoproteins, sialyltransferase, has been studied in a variety of cellular functions such as cell to cell adhesion and cellular recognition (Hughes, 1973; Shur and Roth, 1975), no study of its possible involvement in the regulation of cellular excitability and ionic movements has been done.

4. Mechanism of E-C coupling

Although superficial Ca (from kinetic studies) is intimatedly linked with contractile tension (eg. Bailey and Dresel, 1968; Shine et al, 1971) and although I_{Ca} is thought to be derived from the superficial Ca, the size of I_{Ca} does not always correlate with the magnitude of contractile tension. In isolated ventricular preparations from dog hearts, the

first beat of a stair case response is associated with a fully activated I_{Ca} even though contraction is small. Subsequent contraction in such stair case increases in amplitude while I_{Ca} remains unchanged (Beeler and Reuter, 1970 c). Furthermore, low Na augments Ca influx (Langer, 1964) and contractile force but fails to increase I_{Ca} (Beeler and Reuter 1970 c; New and Trautwein, 1972). In addition, the integrated Ca current is thought to be barely enough to reach the mechanical threshold (Langer, 1976; Fozzard, 1977). Thus the data from the tonic and phasic contraction, from the small size of I_{Ca}, as well as from the sometimes incongruent relationship between I_{Ca} and contractile amplitude suggest the presence of a store of Ca which increases upon repetitive depolarization and from which Ca is released, without evidence of trans-sarcolemmal Ca current, to the myofilament.

In skeletal muscle, the source of intracellular Ca is accepted to largely reside in SR. Ford and Podolsky (1968, 1970) have demonstrated that Ca can induce its own release from the SR. A physiological role for Ca-induced Ca release in skeletal muscle, however, appears unlikely: Ca loading of the SR, a low free Mg and a high free Ca ($> 3 \times 10^{-4}$ M) are necessary to induce release (Ebashi, 1976; Endo, 1977). In contrast, Fabiato and Fabiato (1973, 1975, 1977) have shown convincing evidence for Ca-induced Ca release in cardiac cells. In the skinned cardiac cells of rat ventricle, the free Ca necessary for a Ca-induced release of Ca from the SR varies between 3×10^{-8} to 10^{-7} M depending on the medium [EGTA]. The threshold for Ca-induced Ca release is lower than that

for direct activation of the myofilament which is about 2 x 10^{-7} M free [Ca]. No unphysiologic loading of SR with Ca is necessary for this process to occur and Ca-induced Ca release remains observable at free Mg of 3.16 mM which is above the physiological level. The amplitude of the phasic contraction obtained by Ca-induced release of Ca increases when the free [Ca] used to induce the release is increased (Fabiato and Fabiato, 1975). This might be interpreted as a consequence of increasing filling of SR and is compatible with the observed gradation of cardiac contraction as a function of the extracellular Ca.

During the action potential in an intact ventricular muscle cell the trans-sarcolemmal Ca influx could increase the myoplasmic free Ca to 5-8 x 10^{-7} M (assuming 8 μmole Ca influx/kg/beat, Beeler and Reuter, 1970 b; New and Trautwein, 1972; and using the data of Solaro et al (1974) and Fabiato and Fabiato (1975) that this influx is able to generate 10% tension; Langer, 1976) it is clear that Ca-induced Ca release is operable without assuming other electrically neutral Ca influx.

In summary, it is generally accepted that at least two pools of Ca are involved in cardiac muscle E-C coupling. The more labile and rapidly exchanged pool is thought to reside external to the sarcolemma and consists of both interstitial free form of Ca as well as bound form of Ca associated with basement membrane, predominantly to sialic acid residues. The less labile and slowly exchanged pool is thought to reside inside the cell in association with the SR. Action potential on the surface membrane causes an influx of Ca represented by

I_{Ca}. The magnitude of I_{Ca} is directly proportional to the external [Ca] and might also be a direct function of superficially bound Ca, although this has not been carefully explored. The entrance of Ca is thought to cause a "trigger" release of Ca bound to the SR resulting in above-threshold concentration of cytoplasmic Ca for contraction. Processes which abolish the I_{Ca} (eg. Ca antagonists) simultaneously abolish contraction.

D. SYRIAN HAMSTER MODEL OF PRIMARY CARDIOMYOPATHY

1. Course of the disease

Genetic studies of the hamster myopathy indicated the disease, or the susceptibility to the disease, is carried by an autosomal recessive gene (Homberger et al, 1966). The life span of the BIO 14.6 strain is about 146 days, or approximately one-third the normal life expectancy of this species (Bajusz et al, 1966). Continued in-breeding of this strain since then, however, has considerably increased the life span of these animals to 187 days (Bajusz, 1969). My observations confirm the slower progression of congestive heart failure such that animals living beyond the age of 300 days are not uncommon.

The onset of histologically detectable lesions differs in skeletal and heart muscle. Skeletal muscle necroses have been detected as young as six days of age and the incidence of voluntary muscle involvement reaches nearly 100% by the 30th day of age, when the first myocardial lesions usually occur (Bajusz et al, 1966).

The abnormality in the heart muscle, histologically first detectable between the ages of 30 to 70 days, consists of focal myolysis with primary disappearance of the sarcoplasm in the absence of any significant cellular infiltration. Bajusz (1969) subdivided this period into two stages. The first stage (25th-45th day) is characterized by focal myocardial lesions. The second stage (35th-50th day) is marked by progressive myocardial degeneration with numerous fresh lesions. At this time, older foci were already in various stages of healing with secondary calcification which appeared to the naked eye as white streaks that follow the direction of the myocardial fibers. The heart muscle disease is the most severe at this stage, with pronounced cardiac hypertrophy.

Bajusz classified the third stage (80th day onward) as the period when dilatation of the cardiac chambers overtakes the hypertrophy. Liver congestion becomes pronounced with eventual destruction of over three fourths of its cells. During the advanced stages of heart involvement, auricular thrombi occurred quite frequently. These were observed often to fill completely the swollen atrium and were attached to both the endocardium and to the muscular atrial wall. Death, believed to be caused by congestive heart failure, occurred between the 100th day to over 400th day of age.

Associated with the development of myocardial lesions different investigators have observed a corresponding decrease of cardiac contractility. With an isolated perfused heart system (Brink et al, 1967, 1969) and with isolated papillary muscles in a tissue bath (Forman et al, 1972) reduced cardiac

contractility was reported in the hypertrophic and failing stage of cardiomyopathy. Cardiac contractility measurements in young hamster hearts, i.e., before the development of myocardial lesions, has been hampered by a lack of a suitable recording system because of the size of the young hamster hearts. Lockner et al (1970), using a force displacement transducer attached to the apex of the heart, found no difference in cardiac contractility during the myolytic stage of the disease when compared to controls. The large resting tension (5 g) applied in these small hearts (0.17-0.26 g), however, may have induced some mechanical damage.

2. Comparison with human primary cardiomyopathy

With the development of the hamster model of cardiomyopathy, Bajusz (1969) felt confident to state "the possibility exists that investigations in the cardiomyopathic hamsters will help to clarify the genesis of human cardiomyopathies with similar, if not identical, lesions." This optimism in reality is complicated by at least two factors. Firstly, comparative histopathological studies in hamster and human cardiomyopathies, which are essential to validate the animal model, are difficult because necropsy findings from human hearts with primary cardiomyopathy represent the "tombstones" or the end result of a prolonged pathologic process which may be modified by secondary lesions. Secondly and perhaps more importantly, primary cardiomyopathy in the human patient is a collection of diseases of heterogeneous etiologies. Although the outcome of these diseases in general is manifested by congestive heart failure, the demonstration that some of

these are familial while others are non-familial in occurrence, the finding that the lesions can be primarily fibrotic, degenerative or hypertrophic, and the observation that the muscle involvement can be either endocardial, myocardial or both, indicate many different disturbances of the heart muscle that must have been involved. We can expect at the best, therefore, that the disease in hamsters mimics a form of human primary cardiomyopathy, about which remarkably little is known. With this in mind, we may then make the comparisons between cardiomyopathic hamsters and patients with primary cardiomyopathies.

a. Hemodynamic comparisons

Abelmann and co-workers (1973) studied the hemodynamics in two age groups of cardiomyopathic hamsters: 130 days of age in the pre-edematous stage and 250 days of age in congestive heart failure stage. In the pre-edematous stage of the disease, characterized by widespread, active myocardial lesions, cardiac output (CO) was found to be normal or slightly below normal. In contrast, in the edematous stage of congestive heart failure, a tendency for high CO was observed. Heart rate under alphachloralose-urethane anesthesia was found to be 24% lower in the pre-edematous cardiomyopathies and normal in the stage of congestive heart failure.

Cardiomyopathy has been recognized in progressive muscular dystrophy (Globus, 1923; Zatuchni et al, 1951; Perloff et al, 1966; Table 1). Hemodynamic studies in these patients (Gailani et al, 1958; Sundermeyer et al, 1961; Perloff et al, 1966; Sekiguchi, 1974) indicate higher than normal

CO in 31 out of 43 patients (taking the normal level at 3.5 $1/m^2/min.$) The cardiomyopathy associated with human muscular dystrophy, however, like most other heart failures, differs from that of the hamster in that tachycardia occurs in the majority of the patients (Boas & Lowenburg, 1931; Zatuchni et al, 1951; Weisenfeld & Messinger, 1952; Gailani et al, 1958; Gilroy et al, 1963; Perloff et al, 1966) and can account for the increased CO (Perloff et al, 1966).

b. Light and electron microscopic comparisons

The initial cardiac lesions of the cardiomyopathic hamster appear as minute, disseminated foci of myolysis with no significant amount of necrotic tissue. The microfocal lesions are pronouced and widespread. Fiber disintegration is marked by a dissolution of myofibrils so that the sarcoplasm becomes filled with a more or less amorphous material. The myofibrils eventually disappear. The remaining sarcolemmal remnants are often indistinguishable from the surrounding connective tissue (Bajusz et al, 1966). The lesions reported resemble that of the "focal myocytolysis" characterized by Schlesinger and Reiner (1955).

The lesion of focal myocytolysis is usually not larger than 1500 μ and resembles a miliary infarct without stromal necrosis (Schlesing and Reiner, 1955). In this form of myolysis the muscle fibers disintegrate within a small and discrete territory. Their myofibrils seem simply to disappear. The sarcolemma is preserved but it collapses and becomes increasingly difficult to distinguish from the intact stroma. It looks as though the muscle fibrils have lost their syncytial

integrity and had melted or "fallen out" of the stromal envelopes. Focal myocytolysis has been produced experimentally by oxygen deprivation, adrenline injection, induction of hyperthyroidism, tachycardia, protein deficient and vitamin B free diet, and by hypopotassemia (Schlesinger and Reiner, 1955). Focal myocytolysis terminates in a fibrous tissue scar. This scarring is brought about largely by collapse and condensation of the preserved stroma rather than by proliferation of fibroblasts and elaboration of collagen. The same type of fine-spotted scar pattern is also found in hypertrophic heart muscle (Buchner, 1971).

A review of some of the cases of human idiopathic cardiomyopathy and cardiomyopathy associated with progressive muscular dystrophy indicate that myocytolysis or its healed fine-scarred tissue were present in a number of the reported necropsy findings. Levin and co-workers (1959) reported a case of cardiomyopathy associated with pseudohypertrophic muscular dystrophy (Case 1) and they observed that in some areas, the endomysium surrounded an empty space devoid of muscle tissue, whereas in other areas there was some fibrous replacement. These descriptions were similar to those used by Schlesinger and Reiner (1955) in describing the end stage of myocytolysis. Pare and co-workers (1961) reported two cases of familial cardiomyopathy (cases 13 and 14) and observed that many fibers showed disintegration of cytoplasmic components and loss of striations; in some areas, only shadow structures of the sarcolemma remained. This again indicated myocytolysis. Cannon (1962) reported several cases of cardiomyopathy associated

with myotonic muscular dystrophy, one of which (patient M.G.) he described to have small areas of focal interstitial fibrosis and occasional minute areas in which the myocardial fibers seemed to have "dropped out". Van der Walt (1973) did comparative histopathological studies in hamster cardiomyopathies and human endomyocardiopathies and observed frequent occurrence of myocytolysis in both. It appears, therefore, that myocytolysis is not a unique feature of hamster cardiomyopathy. The objection voiced by some (eg. Norris et al, 1966) that the myolytic component seen in hamster histology does not appear in human cardiomyopathy seems to be unfounded. It is also possible that the small focal lesions heal without collagenous scar formation; the loss of muscle bands leads to a collapse of the surrounding hypertrophic fibers upon the interstitium resulting in an undetectable form of the original lesion. This has been shown to be the fate of many myolytic lesions in the hamster cardiomyopathy (Bajusz et al, 1969 b).

Dystrophic calcifications usually are present after myocardial necrosis in the cardiomyopathic hamster hearts. Calcification occurs in two different forms: deposited either in the degenerating muscle fibers only or in the fibers and the surrounding connective tissue (Bajusz, 1969c). Although calcification of cardiac muscle fibers in human primary cardiomyopathy rarely occurs, the process is secondary to necrosis (Gore and Arons, 1949) and can be dissociated from it (Bajusz and Jasmin, 1963a; Bajusz et al, 1963b; Bajusz, 1969c), and therefore the prominent presence of dystrophic calcification in the cardiomyopathic hamster heart does not rule against it being a

valid animal model for human primary cardiomyopathies.

Electron microscopic observations of the myocardium in patients with idiopathic cardiomyopathy reveal many subcellular abnormalities. The morphological changes are not always all present in any one case and many of these are likely due secondary to injuries or mechanical disturbances (eg. fibrosis and hypertrophy). Some of the more consistent findings include the following: mitochondrial proliferation (especially involving smaller sized mitochondria) and degeneration, widening and proliferation of the sarcotubular system, myofilament fragmentation and lysis, increased glycogen deposition, widening of intercalated discs and increase of dense bodies or lysosomes (Sekiguchi and Konno, 1971; Ferrans et al, 1972, 1973; Sekiguchi, 1974; McKinney, 1974; Maron et al, 1975). Maron et al (1975) also observed basement membrane thickening of the myocardial cells and a distinct population of smaller myocardial cells.

Electron microscopic examination of the cardiomyopathic hamster hearts shows abnormalities similar to those discussed in the preceding paragraph. Buchner (1971) reported poor development of myofilaments in multiple small cardiomyoblasts in the cardiomyopathic hamster heart muscle 10 days after birth. Even at this stage the majority of cardiac mitochondria showed severe cristolysis, distension and vacuolation (Buchner, 1971; Nadkarni et al, 1972). Mitochondria were observed to increase in number (<25 days) with many of smaller size (Schwartz et al, 1972); the sarcoplasmic reticulum (SR) was dilated, and myolysis was detected (Nadkarin et al, 1972). At the hypertrophic phase (60-80 days of age), mitochondria showed enlargement, swelling,

vacuolation and clumping, and the SR was dilated (Nadkarni et al, 1972). During the stage of dilatation and terminal failure, the alterations in many cells resembled those caused by hypoxia. The membranes of may intercalated discs were separated, the SR was significantly dilated and mitochondria showed swelling and loss of matrix density. Intracellular edema was evident (Schwartz et al, 1972)

3. Biochemical abnormalities of the hamster cardiomyopathy: relation to striated muscle dystrophy and heart failure

a. Sarcoplasmic reticulum (SR)

The SR is believed to regulate the intracellular concentration of Ca for contraction and relaxation in skeletal muscle (Weber et al, 1963; Ebashi and Endo, 1968). In heart muscle, it has been suggested that the SR has both the speed and capacity for Ca binding to account for muscle relaxation (Carsten, 1964; Katz and Rapke, 1967; Weber et al, 1967; Pretorius et al, 1969; and Schwartz, 1971). Two types of ATP-dependent Ca accumulation can be shown: (1) a rapid binding and subsequent release; and (2) a rapid and extensive accumulation with no release. The former process occurs in the absence of inorganic phosphate or oxalate and is termed binding. The latter occurs in the presence of phosphate or oxalate(resulting in precipitation of Ca inside the SR lumen) and is termed uptake.

A number of reports have appeared since 1966 linking disorders of cardiac contraction to an altered Ca binding activity of the SR. It has been postulated that depressed SR Ca accumulation (binding and uptake) would lead to a loss of

Ca from SR and eventually to less Ca acailable for contraction. A reduced Ca uptake by SR was observed in barbiturate induced heart failure of an isolated dog heart preparation (Briggs et al, 1966; Lain et al, 1968), failing human hearts obtained at the time of transplantation (Harigaya and Schwartz, 1969), and failing isolated rat hearts after substrate depletion (Muir et al, 1970).

In pre-symptomatic cardiomyopathic hamster (10 days of age), neither SR Ca uptake rate (μmole/mg protein/min) nor capacity (μmole/mg protein) were different from normal (Gertz et al, 1970, 1972b). During the stages of myolysis and necrosis (60 days of age), McCollum et al (1970) observed no difference in the capacity or rate of Ca binding whereas Gertz et al (1972 b) observed a decrease in the capacity and rate of Ca uptake. In the older age groups, during compensated hypertrophy and congestive failure, most investigators agree that although binding rate, binding capacity and uptake rate were depressed, the uptake capacity was not altered or slightly reduced (McCollum et al, 1970; Gertz et al, 1970; Schwartz et al, 1972 b; Gertz et al, 1972; Dhalla, 1972; Owen et al, 1973, 1974, 1975). Using calcium oxalate capacity of the whole heart homogenate as an index of SR volume, Briggs et al (1971) and Gertz et al, (1972 b) concluded that there was a "dilution" of SR by the hypertrophy process. Lazarus et al (1976), on the other hand, employing stereological analysis of electronmicrographs, concluded that there was SR proliferation in the late stage of cardiomyopathic hamster disease.

The fact that SR Ca binding and uptake are not depressed

before the onset of clinical lesions and the fact that SR Ca uptake capacity remains constant throughout the disease process suggests that the SR is probably not the etiological focus of the hamster cardiomyopathy. The observation that SR Ca binding and uptake rate are progressively depressed as the disease progresses may indicate a secondary injury due to the myolysis, hypertrophy and failure.

b. Mitochondria

Heart muscle derives most of its required energy from the tricarboxylic acid cycle, electron transport, and oxidative phosphorylation associated with mitochondria. Over the years, many investigators have reported defective oxidative phosphorylation in mitochondria accompanying heart failure (Szekeres and Shein, 1959; Gertler, 1961; Schwartz and Lee, 1962; Bing et al, 1964; Argus et al, 1964; Wollenberger et al, 1965; Fox et al, 1966; Lindenmayer et al, 1968), although others have reported negative findings (Olson, 1964; Chidsey et al, 1966; Sobel et al, 1967). The discrepancies are not resolved.

The indices of oxidative phosphorylation in the mitochondria are as follows: (1) ADP:O (the ratio of ADP phosphorylated to the amount of oxygen consumed; an index of the efficiency of phosphorylation), (2) RCI (respiratory control index; the ratio of the rate of oxygen consumption in the presence and absence of ADP; an index of the tightness of coupling of oxidation to phosphorylation), and (3) QO_2 (the rate of oxygen consumption in the presence of ADP and substrate, this reflects the capacity of mitochondria per unit protein to utilize oxygen).

It is generally agreed that the mitochondria from cardiomyopathic hamster before the development of spontaneous cardiac lesions (<30 days of age) phosphorylate ADP and utilize oxygen normally (Wrogemann et al, 1972; Schwartz et al, 1972 b). Even at the myolytic stage, Lochner et al (1970) reported normal oxidative phosphorylation. However, there is lack of agreement when hypertrophy begins to develop. Lochner et al (1970) observed decreased ADP:O, KaKo et al (1974, 1975) reported depressed QO_2, while Wrogemann and co-workers (Blanchaer and Wrogemann, 1968; Wrogemann and Blanchaer, 1968; Wrogemann et al, 1972),and Lindenmayer et al (1970) observed no change in either ADP:O or QO_2. Lindenmayer et al (1970) and Schwartz (1971 b) even suggested that respiratory control was better in the hypertrophied hearts than in normal. As congestive heart failure became more pronounced, Wrogemann et al (1972) could not detect a defect in oxidative phosphorylation provided appropriate substrates were used. Contrary to these findings, Lindenmayer et al (1970), Lochner et al (1970), Schwartz et al (1972) and Dhalla (1972) reported marked loss of respiratory control and oxidative phosphorylation.

This discrepancy cannot be easily resolved. Wrogemann and co-workers (1975), extrapolating from findings on skeletal muscle of cardiomyopathic hamsters (Mezon et al, 1974), suggested that different populations of mitochondria existed in the cardiomyopathic hearts; some were normal, others were defective. The defective mitochondria were loaded with Ca which is known to cause uncoupling of phosphorylation (Lehninger, 1949). The abnormal accumulation of Ca could move into

the test medium of the oxygraph cuvette and damage the normal population of mitochondria. Indeed, ruthenium red, which prevented Ca movement in mitochondria, changed the uncoupled state of phosphorylation in the cardiomyopathic skeletal muscle mitochondria to normally coupled oxidative phosphorylation. It was suggested that the initial injury resulted from a sarcolemmal defect which led to increased net influx of Ca from the interstitial fluid. Mitochondria were thought to actively excess Ca which rendered them functionally and eventually structurally damaged. Depletion of intracellular energy stores was then thought to produce cellular necrosis. This hypothesis was consistent with the earlier observation that mitochondria from young cardiomyopathic hamster hearts functioned normally and therefore could not be the etiologic factor in the spontaneous cardiac lesion.

Mitochondria accumulate Ca against a gradient, in a process energetically coupled to electron transport. When this is taking place, no oxidative phosphorylation of ADP occurs (Lehninger, 1975). Thus the energy delivered by electron transport can be used to carry out either Ca accumulation or ATP formation but not both simultaneously. Since in cardiac muscle, active Ca accumulation by the SR is much less than in skeletal muscle, both in the presence (Fanburg et al, 1964; Inesi et al, 1964) and absence of oxalate (Katz and Repke, 1967; Pretorius et al, 1969; Weber et al, 1967), and since heart muscle contains more mitochondria than does skeletal muscle, it has been suggested that the energy-dependent mitochondrial Ca uptake plays a role in the cardiac contraction-

relaxation process (Chance, 1964; Lehninger et al, 1967; Haugaard et al, 1969; Patriarca and Carafoli, 1968; Carafoli, 1972, 1975).

Ca can be accumulated by mitochondria via three processes: (1) energy independent, permeant anion (such as phosphate or acetate) independent passive binding; (2) energy dependent, permeant anion independent active binding, and (3) energy dependent, permeant anion dependent Ca uptake. Assuming 80 mg mitochondria protein per g heart tissue (Scarpa and Graziotti, 1972) and using the binding data of Carafoli (1972), the above three process can bind respectively, 6 μmole (0.4 μmole high affinity, 5.6 μmole low affinity), 12 μmole and 240 μmole of Ca per g heart tissue. Assuming further that 100 nmoles of Ca per g of heart are exchanged between the sarcoplasm and troponin per beat, it has been suggested that mitochondria have more than adequate capacity for Ca removal. Carafoli and Azzi (1972 b) have presented data which suggest 400 nmoles of Ca can be sequestered by mitochondria per g of heart tissue per beat. Kubler and Shinebourne (1971) on the other hand, argued that mitochondria can take less than 1 nmole per g during the cardiac relaxation cycle (200 msec). Similarly, although Carafoli and Azzi (1972 b) have indicated a Km of the active binding to be 1 μM, Scarpa and Graziotti (1972) have concluded it to be ten fold larger. It is clear that the role of mitochondria in cardiac contraction-relaxation is not yet established. With this in mind, we may then examine the published data on mitochondria Ca accumulation in the cardiomyopathic hamster.

Although Wrogemann and co-workers (1975) reported preliminary data on an elevated Ca content of the mitochondria from very young cardiomyopathic hearts, there have been no studies on mitochondrial Ca transport at the stage before myolytic lesions develop. From the necrotic stage onward, there is general agreement that mitochondria Ca transport is depressed (Lindenmayer et al, 1970; Schwartz et al, 1968; Schwartz, 1971 b, 1972; Dhalla, 1972). Since mitochondria Ca content of the cardiomyopathic hearts in these age groups were known to be markedly elevated (Wrogemann et al, 1975), it is not clear how much of the reduced capacity reported is due to the higher level of basal content already present. In any case, available data do not permit a conclusive statement on the contributory role of mitochondrial Ca transport in the genesis of hamster heart disease.

c. Sarcolemma

Heart muscle, like other excitable tissue, is dependent on cation-flux for E-C coupling. The maintenance of functional integrity and selective ionic permeability of the sarcolemma is essential for the cell to maintain an ionic balance across the membrane and electrical excitability. Needless to say, the viability of the cardiac muscle cell depends on the ability of the cell membrane to keep important substrates and enzymes within its confine.

Skeletal muscular dystrophy in the cardiomyopathic hamster has been regarded to be an adequate model of human muscular dystrophy (Homburger et al, 1966). In human progressive muscular dystrophy, as in the hamster model of dystrophy, myo-

cardial lesions are revognized to occur in close association with the occurrence of skeletal muscle dystrophy, (Globus, 1923; Zatuchini et al, 1951; Perloff et al, 1966). At present, it is generally assumed, in the absence of contrary evidence, that the same genetic defect(s) cause(s) the cardiomyopathy and the skeletal muscle lesion. It stands to reason, therefore, to review the literature on both the hamster and human primary cardiomyopathy and dystrophy in the delineation of the participatory role of sarcolemmal abnormalities in the genesis of the disease.

Muscle membrane damage is associated with a loss of its permeability regulation integrity. The resultant membrane leakiness, for example, causes elevation of serum glutamic oxaloacetic transaminase (GOT) activity in acute myocardial infarction (LaDue et al, 1954). This enzyme is believed to be most concentrated in heart muscle (Awapara and Seale, 1952). Similarly, catecholamine induced muscle injury results in deposition of an extracellular macromolecular tracer, horseradish peroxidase, in myocardial cells with an otherwise normal sarcolemma (Rona et al, 1975; Boutet et al, 1976).

Wendt and co-workers (1962) demonstrated release of malic acid dehydrogenase (MDH) from the heart into the coronary sinus in patients with idiopathic and alcoholic cardiomyopathies. Sundermeyer et al (1961) reported myocardial release of MDH and aldolase in several patients with progressive muscular dystrophy. Perloff et al (1966) reported elevated serum LD_5 fraction (heart isoenzyme) of lactic dehydrogenase (LDH) and GOT activity in the majority of the patients examined with

Duchenne muscular dystrophy.

In cardiomyopathic hamsters (BIO 14.6) with muscular dystrophy, Homburger et al (1966) reported elevated serum levels of all of those enzymes reported as high in human muscular dystrophy: LDH, MDH, aldolase, and phosphocreatine kinase. The elevated serum enzymes pertaining to heart and skeletal muscle in hamsters as well as in patients with progressive muscular dystrophy suggests that perhaps the dystrophic muscle cell membrane is "leaky", or has abnormal permeability. Direct electron microscopic examination of muscle cells have indicated the presence of focal sarcolemmal discontinuity and breakdown in non-necrotic skeletal muscle membrane in congenital muscular dystrophy (Pearce, 1965), Duchenne muscular dystrophy (Mokori and Engel, 1975), and various forms of myopathy (Schmalbruch, 1975). This defect may account for part of the enzyme leakage. Other evidence supports that abnormalities in membrane permeability alone may play some part in the loss of enzyme from the muscle cells. Electrophysiological studies on dystrophic patients (Farmer et al, 1959) and carriers (Caruso and Buchthal, 1965) have shown shortening of the absolute refractory period of the muscle action potential, suggesting abnormal ionic permeability of the cell membrane. Howland (1974) demonstrated a five fold increase of K efflux from erythrocytes of patients with Duchenne muscular dystrophy as compared to control. Erythrocyte surface deformation has been reported in patients and carriers of Duchenne and other progressive muscular dystrophy (Matheson and Howland, 1974), as well as in mice with genetic muscular dystrophy (Morse and

Howland, 1973). These observations, however, have not been reproduced by other investigators (Miale et al, 1975; Miller et al, 1976). More recently, Schotland et al (1977) demonstrated alterations in muscle plasma membrane structure in Duchenne muscular dystrophy with the freeze-fracture technique. Using fluorescent polarization techniques which measure the mobility of a lipid soluble fluorescent dye, Shaafi and co-workers (1975) noted an increase in membrane microviscosity of dystrophic chicken muscle sarcolemma and erythrocyte plasma membrane. Kunze and co-workers (1973) demonstrated abnormalities in the lipid profile of the erythrocyte membrane (increased sphingomyeline content, altered fatty acid pattern associated with phospholipids, and increased incorporation of linoleic acid into phosphotidylcholine in vitro). The literature thus contains extensive documentation which suggest an alteration of sarcolemmal function in primary cardiomyopathy and dystrophy.

The sarcolemma contains hormonal receptors and other specific enzyme systems. Thus, changes in the microenvironment of these receptors may be reflected in altered enzyme function. In heart failure induced by constriction of the ascending aorta of guinea pigs, Sobel and co-workers (1969) showed a 36% depression of fluoride (0.01M) activated adenylcyclase activity. This depression was not accompanied by a change in the activity of another enzyme of the same system, phosphodiesterase, which argues against a non-specific dilution of adenyl cyclase enzyme activity by hypertrophy of cardiac muscle. Gertler et al (1970), using the same experimental model, on the

other hand, failed to measure the depression of adenyl cyclase activity of the heart.

In cardiomyopathic hamster, LaRia and co-workers (1971) observed a consistent decrease of basal cardiac adenyl cyclase activity from 20 to 220 days of age. Sulakhe and co-workers (1972) find no alteration of basal adenyl cyclase activity both with moderate and advanced degrees of heart failure in cardiomyopathic hamsters. In the latter stage, however, fluoride stimulated activity was reduced while epinephrine stimulation was absent. To complicate the picture further, Nair and co-workers (1972, 1974) found marked elevation of adenyl cyclase activity after 50 days of age in the same strain of animal. In Duchenne as well as facioscapulohumeral dystrophy, Mawatari et al (1974) observed normal basal adenyl cyclase activity in skeletal muscle but the response to epinephrine and sodium fluoride were depressed more than 50%. Thus, it is premature to conclude that alteration of sarcolemmal adenyl cyclase activity is the causal factor in hamster (or Duchenne) cardiomyopathy. Not only are the data conflicting, but also it is not clear what is the participatory role of adenyl cyclase in membrane integrity. Moreover, studies on human fetal muscle (17 to 19 weeks) have indicated ten times as much of basal adenyl cyclase activity, as normal adult level. The high level of enzyme activity, however, is insensitive to epinephrine stimulation and less sensitive to Na fluoride activation (Mawatari et al, 1974). Thus lack of response to epinephrine and sodium fluoride *per se* is not pathological in nature.

Skeletal and cardiac muscle sarcolemma both contain a relatively high concentration of Na,K-ATPase in comparison to other subcellular organelles in the muscle cell. Na,K-ATPase is thought to be involved in the transmembrane active transport of Na and K (Shou, 1965; Albers, 1967). Lindenmayer et al (1971) reported a depressed Na,K-ATPase activity in human cardiac tissue obtained during transplantation as compared to that from a variety of animal heart preparations. The study however was of doubtful value as the patients had all been digitalized prior to surgery which invariably causes Na,K-ATPase inhibition. Mead et al (1971) showed a decrease of ouabain sensitive ATPase (or Na,K-ATPase) in dogs with right ventricular hypertrophy and congestive failure induced by progressive pulmonary artery stenosis. Depressed Na,K-ATPase activity was also observed in isolated heart made to fail either by hypoxic (Balasubramanian et al, 1972) or by substrate-lack (Dhalla et al, 1974). In strain UM-X 7.1 cardiomyopathic hamster with heart failure, Singh et al (1975) observed depression of Na,K-ATPase activity. In addition to its role in membrane excitability, intracellular Na concentration has also been suggested to directly modify intracellular Ca concentration and hence cardiac contractility through Na-Ca exchange (Langer, 1968, 1973). In this sense, it is perhaps paradoxical that a reduced Na,K-ATPase activity is associated with a depression of cardiac contractility. For an elevation of intracellular Na is thought to promote Na-Ca exchange and provide more Ca for E-C coupling. In contrast, in rats fed vitamin E deficient diet for 10 weeks when cardiac contractility (of the isolated heart preparation

at half optimal resting tension) was depressed by 40%, Na,K-ATPase activity was increased two-fold (Fedelesova et al, 1971). Similarly, in cardiomyopathic hamster BIO 14.6 strain in moderate degree of heart failure Na,K-ATPase activity was observed to be elevated two fold (Sulakhe and Dhalla, 1972). It is possible that the increased Na,K-ATPase activity is a cellular adaptation for a "leaky" membrane. Elevated Na,K-ATPase activity might have also contributed to the reduction of cardiac contractility by diminishing Na-Ca exchange involved in E-C coupling.

Because of the diverse alterations in Na,K-ATPase activity associated with different types of heart failures, it appears that changes in Na,K-ATPase activity are not directly related to heart failure. Its role in the genesis of the genetic cardiomyopathy and dystrophy is obscure. Wrogemann and co-workers (1974) reported no difference in skeletal muscle sarcolemmal Na,K-ATPase activity in the young age of BIO 14.6 strain cardiomyopathic hamster. Insofar as the disease in skeletal muscle is more severe than cardiac muscle in this animal model these results suggest that Na,K-ATPase activity alteration was not a primary factor in the genesis of dystrophy in the muscle.

It has been shown that dystrophic cell membranes have altered composition of phospholipid and cholesterol. Owens and Hughes (1970) reported elevated cholesterol content in dystrophic mouse skeletal muscle. Hughes (1972) and Kunze (1968, 1973) extended this observation to patients with Duchenne muscular dystrophy. Owens et al (1972, 1973) further reported

an elevated cholesterol:phospholipid molar ratio for whole ventricular tissue of cardiomyopathic hamsters (BIO 14.6) as well as from isolated sarcoplasmic reticulum and mitochondria. Borowski et al (1974) demonstrated an elevated cholesterol: phospholipid ratio in both skeletal muscle and cardiac muscle of strain UM-X 7.1 cardiomyopathic hamster. Shaafi et al (1975) postulated that a higher cholesterol:phospholipid ratio could cause a tighter packing of lipid molecules resulting in an enhancement of the Van der Waals interaction between adjacent lipid molecule and leading to a defect in the polar pathways in the protein moiety of the membrane. This configuration would yield increased ionic movement. They therefore suggested that a lipid-related defect which affected the membrane microenvironment was the underlying genetic disorder of muscular dystrophy. There is no evidence at present to disprove Shaafi's hypothesis. Owens and co-workers (1975) have cautioned that the finding of a high cholesterol content in dystrophic muscle might simply be a reflection of proliferation of lysosomes. However, the activity of one lysosomal enzyme measured by them, p-nitrophenylphosphatase, was not elevated in cardiomyopathic hamster hearts (Owens et al, 1975).

d. Electrolyte balance

The effect of electrolyte imbalance in the pathogenesis of cardiac necrosis has been well documented by Bajusz (1961, 1965 a,b). K, Mg and Cl deficiencies are known to produce cardiac necrosis. In contrast, dietary supplements of K, Mg, Cl or reduction of Na protected the heart against the production of a variety of induced cardiomyopathies.

Several investigators have examined electrolyte homeostasis in the hamster cardiomyopathy. Bajusz and Lossnitzer (1968) observed higher serum Ca and Mg in the cardiomyopathic hamsters before the development of myolytic lesions (<35 days of age). The myocardium, on the other hand, contained more Ca and less Mg than control. However, since Mg supplements were unable to modify the development of the spontaneous myocardial lesions, it was concluded that the demonstrated myocardial Mg deficiency was a secondary consequence of some genetically determined metabolic defect. With the exception of an elevated serum Mg level, the above findings were confirmed by Cantin et al (1972) in the young cardiomyopathic animals 10-25 days of age. In contrast to cardiac muscle, Mg concentration in skeletal muscle was normal at the early stage of the disease (Lossnitzer and Bajusz, 1974). Although necrosis of the myopathic heart is associated with an explosive increase of tissue Ca in the cardiomyopathic hamster, prenecrotic heart tissue does not always have elevated Ca levels. This is demonstrated in BIO 8262 inbred strain of cardiomyopathic hamster which showed no difference in the myocardial Ca content at 30 days of age (Lossnitzer et al, 1975).

e. Cardiac sympathetic activity

Raab (1943, 1960 a, b) have proposed that an excess of cardiac sympathetic nerve discharge and catecholamine release played a decisive role in the development of most heart failures. In 1955, Raab and Gigel reported an elevated concentration of total catecholamine in diseased human hearts especially those obtained after myocardial infarction and congestive failure.

In contrast, Bloodworth and Von Haam (1956), using aluminum hydroxide-arsenomolybdic acid assay for catecholamines, reported normal or below normal concentrations in diseased and failed hearts. In 1963, Meerson and co-workers reported a progressive reduction of myocardial norephinephrine (NE) concentration in experimental aortic stenosis which eventually reached only 25% of normal value at the stage of impending failure (6 months after 75% occlusion of aorta). In the same year, Chidsey and co-workers (1963) reported pronounced reduction of human atrial NE concentration obtained during surgery in chronic congestive heart failure as compared to that in normal subjects. A reduction of cardiac NE concentration in failure was substantiated by others in dogs with experimental tricuspid insufficiency (Chidsey et al, 1964), in guinea pigs (Spann et al, 1964) and in rats (Fisher et al, 1965) with aortic constriction. Depletion of cardiac functional releasable NE was demonstrated using tyramine which normally caused augmentation of isolated cardiac muscle contractility due to release of tissue endogenous catecholamine; it produced negligible effects on papillary muscle from failing heart (Chidsey et al, 1964; Chidsey and Braunwald, 1966). Direct stellate ganglion stimulation also produced less chronotropic and inotropic responses in the animals with congestive heart failure (Covell et al, 1966). It was thus proposed, and has been generally accepted, that chronically augmented sympathetic activity, which is known to occur in compensated and failing hearts, leads to exhaustion of cardiac sympathetic nerve NE stores. In these hearts working below normal efficiency,

cardiac sympathetic tone might be the final mechanism preventing failure. In the event of eventual NE store exhaustion, failure would then ensue. A reduction of the number of normal nerve endings engaged in the re-uptake of released NE (Spann et al, 1965; Chidsey and Braunwald, 1966), a reduction in activity of the rate-limiting enxyme tyrosine hydroxylase in the synthesis of NE (Pool et al, 1967; Sassa, 1971; Yamazaki and Ogawa, 1971; DeQuattro et al, 1973), and an alteration of the metabolizing systems (Sassa, 1971, Yamazaki and Ogawa, 1971; DeQuattro et al, 1973) have been suggested to contribute to the NE exhaustion.

In cardiomyopathic hamster (BIO 14.6), Angelakos et al (1969, 1972, 1973) reported no difference in NE content (per heart) or concentration (per g heart) between normal and cardiomyopathic hearts at 35 days of age. Sole et al (1975), on the other hand, reported a significant increase of NE concentration in the 18-20 day age group. Both groups of investigators observed higher cardiac NE in the cardiomyopathic hearts during the stage of focal myolysis and necrosis as compated to age matched controls. As in human and other animal herat failure, a reduction of cardiac NE was observed during both hypertrophy and failure.

^{14}C-NE synthesis from ^{14}C-tyrosine appeared to be higher in the cardiomyopathic hamster at all ages (Angelakos 1972, 1973). Using the concept that at steady state, the rate of synthesis was equal to the rate of removal, Sole et al (1975) found 75-90% higher NE turnover rate (synthesis) per total ventricular mass in the cardiomyopathic hamster hearts

from 45-65 days of age until failure. Since immobilization stress (24 hrs) elevated the NE turnover rate of the normal hamster to that of the myopathics and since peripheral ganglionic blockade with chlorisondamine in the cardiomyopathic hamster reversed the high turnover rate to normal, it was concluded that there was a progressive increase in cardiac sympathetic tone in the cardiomyopathic hamster, and with worsening of the disease state, the cardiac sympathetic output approached those achieved with severe stress, leaving little cardiac NE reserve. It was hypothesized that when synthesis could not cope with demand, the heart went into failure. In contrast to all other disease state, in human patients as well as in experimental models, cardiac hypertrophy and failure in the hamster was associated with an increased tyrosine hydroxylase activity which approached twice normal in the stage of failure (Sole et al, 1977).

f. Protein metabolism

i. Catabolism

In muscle cells, as well as in other tissue, there exist a group of proteolytic enzymes, loosely termed cathepsins (Fruton, 1960). Among the cathepsins, there are wide differences in pH optimum and substrate specificity. Some of these are thought to be associated with lysosome (DeDuve, 1969), others have obscure sites of localization (Pennington, 1974). In cardiac muscle, three classes of proteases have been identified: acid, neutral, and alkaline proteases (Smith and Bind, 1975). One biological function of cathepsins has been regarded to be the autolysis of dead or damaged cells.

In 1958, Weinstock et al reported marked increase (+87%, per mg non-collagen protein nitrogen) of cathepsin activity in skeletal muscle of dystrophic mice. Tappel et al (1962) measured an increase of cathepsin activity in dystrophic chicken and mice skeletal muscle homogenates. The detergent activation profile indicated lysosomal localization. Pennington (1968) found similarly elevated levels of cathepsin activity in muscle biopsy samples from patients with Duchenne muscular dystrophy. Cathepsin activity has not been examined in the cardiomyopathic hamster. An increase in cathepsin activity is not unique in hereditary muscular dystrophies but has been reported in nutritional dystrophy (vitamin E deficiency) of rabbit (Weinstock et al, 1955) and denervation atrophy (Weinstock and Iodice, 1969).

Because of the localization of the majority of cathepsin activity in lysosome, increases in enzyme activity may be a reflection of proliferation of lysosomes. If such is the case, then other hydrolytic enzymes should also be elevated. In cardiomyopathic hamster (BIO 14.6), Dhalla et al (1974 b) reported an increase of both free and bound acid phosphatase activity from heart homogenate in moderate and late stages of the disease. Owens et al (1965), using zonal centrifugation, did not observe an increase of lysosomal marker β-nitrophenyl-phosphatase. The glucuronidase, which they used as a microsomal marker, exhibited less activity in the myopathic hearts. Bester and Gevers (1973 a, b) observed similar acid proteinase but higher 3'-exonuclease activity in extracts of myopathic muscle as compared to control. As in the hamster (cardiac

muscle), Abdullah and Pennington (1968) also reported an increase of ribonuclease activity in Duchenne muscular dystrophy (skeletal muscle). Although not yet clearly understood, it is likely that an elevated cathepsin and other hydrolytic enzyme activities participate an important role in muscular dystrophies and cardiomyopathies.

ii. Anabolism

Relatively few investigators have looked into RNA and protein synthesis in the cardiomyopathic hamster. In contrast, considerable work has been done in other animal dystrophic models, especially in dystrophic mice. It is profitable, therefore, to compare the findings from each of the different models to see if defferences occur at the gene expression level in otherwise clinically similar disease manifestation.

Comparatively few studies had been done in human muscular dystrophy. In 1966, Monckton and Nihei first reported reduced polyribosome content in human dystrophic muscle. This suggested that there should be a reduced protein synthesis. However, later studies (Nihei and Monckton, 1967; Monckton and Nihei, 1969) indicated a paradoxically higher rate of amino acid incorporation by the reconstituted enzyme system, both in the presence and absence of synthetic messenger RNA (mRNA) polyuridylic acid (Poly-U). This finding was confirmed and extended to Duchenne carriers by Ionasescu and co-workers (1971 a, b) who further documented (1971 b) that the increase of protein synthesis was predominantly collagen in nature. The increased synthesis was the result of the absence of a soluble inhibitory factor in the cytoplasm. Replacement of

the soluble fraction from normal subjects abolished the increased protein synthesis of the dystrophic polyribosome. More recently, Monckton and Marusyk (1976) reported that the increased ^{3}H L-leucine incorporation by the dystrophic muscle was disproportionately reduced after glycerination, which removed cytoplasmic soluble contents, as compared to control muscle. This was interpreted to mean that in spite of the overall increase in protein synthesis, the myofibrillar protein synthesis was reduced in dystrophy.

Reports on protein synthesis of the dystrophic chicken are somewhat conflicting. Baieve and Florini (1970) presented results which suggested a low rate of RNA synthesis in isolated nuclei of dystrophic chicken embryos. This implies less active protein synthesis. However, Weinstock et al (1969) and Weinstock and Markiewicz (1974) reported equal peptide synthesis in 18-day embryos. Protein synthesis was actually above control after hatching. In contrast, Battelle and Florini (1973) observed depressed protein synthesis from ribosome preparations of dystrophic embryo breast muscle as well as those from newly hatched dystrophic chickens. The defect was also observed in the presence of poly-U, suggesting that a lack of mRNA was not the causative factor. At present, the inconsistencies are not resolved.

In dystrophic mice, Bar Harbor strain 129, Simon et al (1962) reported a marked increase in the rate of turnover of muscle protein. This was associated with a higher rate of protein synthesis, but an even higher rate of protein breakdown. This metabolic lesion did not affect the protein meta-

bolism of the liver. Srivastava (1969, 1972) confirmed increased protein synthesis in a reconstituted cell-free system. By separating the polysomes according to size, Srivastava (1972) was able to show that although the total radioactive amino acid incorporation was higher in the dystrophic muscle, true amounts incorporated into myosin was less. In contrast, tropomyosin synthesis was sharply increased in dystrophic muscle. Preferential degradation of myosin by intracellular proteolytic enzymes was not ruled out in this study. More recently, Petryshyn and Nicholls (1976) examined the activity of the pH 5 supernatant fraction (containing the soluble protein synthetic machinery: initiating factor, and elongation factor etc., but no RNA) of skeletal muscle from dystrophic mice. They observed marked depression of the incorporation of ^{14}C phenylalanyl-tRNA into peptide with the synthetic messenger poly-U. This was in contrast to normal activity with brain and liver and higher activity in a heart preparation. The defect was attributed to the presence of an inhibitory factor directed against protein synthesis in dystrophic muscle, since addition of dystrophic pH 5 supernatant fraction to the normal ribosomal RNA (rRNA) depressed amino acid incorporation.

In cardiomyopathic hamsters (BIO 14.6), Bester and Gevers (1973 a,b) examined cell-free protein synthesis in both heart and skeletal muscle. Irrespective of the source of polyribosomes, either from myopathic or from normal heart muscle, when it was combined with the myopathic pH 5 enzyme preparation (containing endogenous mRNA and transfer RNA

(tRNA)), produced less polypeptide synthesis than control. The defect was present in the embryonic heart and skeletal muscle and was also detected at 60 and 180 days of age. Increased amount of pH 5 enzyme improved but could not eliminate the defect in myopathics, indicating both a qualitative and quantitative defect in the system. The defect did not show striated muscle localization but was also present in brain, liver and uterus. Data indicated normal aminoacyl-tRNA synthetase in the myopathics, although the myopathic endogenous tRNA was less effectively acylated. Since the amino acid acceptor capacity of tRNA depended on intact 3'-trinucleotide end-sequences, and since the nucleotide-incorporating enzymes of the myopathics were normal, the authors were led to believe the presence of a more active 3'-exonuclease in the myopathic animals. Indeed, presence of ribonuclease-adsorbant bentonite led to an increased capacity of endogenous tRNA to accept amino acids. The defect in polypeptide synthesis was still evident when bentonite was used during the isolation procedure suggesting that the biochemical lesion was present before the cells were homogenized.

Since the lesion was non-specific in nature, it would be expected that a generalized depression of protein synthesis existed in the tissue cells. This was indeed the case; in a subsequent investigation Bester and Gevers (1975) found that the synthesis of myofibrillar and soluble proteins was reduced in cell-free systems and in intact cultured muscle cells.

In summary, it is apparent that the RNA and protein synthetic pattern deviate from normal in human Duchenne mus-

cular dystrophy and in each of the animal models of dystrophy. Some similarities in the defects are present in that all show an elevated catabolism and a depressed myosin synthesis. However, the mechanism of abnormality is attributed to less efficient rRNA in chicken, to the presence of a soluble inhibitory factor in mice (which is muscle specific), and to a generalized increase of cellular exonuclease activity in hamster (which is tissue non-specific). The abnormality in human Duchenne muscular dystrophy is thought to result from the absence of a soluble inhibitory factor which leads to a disproportionate elevation of collagen synthesis. At the same time, possibly due to excessive degradation, there is a reduced net myosin synthesis.

4. Experimental interventions in hamster cardiomyopathies and heart failure

a. Cardiotonic drugs

Bajusz et al (1969 d) examined the effect of catecholamine and digitoxin administration in the disease course of cardiomyopathic hamster (BIO 14.6). In normal hamster at 25 days of age, epinephrine at a low dose (0.2 mg/100 g/day) administered for 20 consecutive days produced no demonstrable muscle pathology. In contrast, similar treatments in the cardiomyopathic strain intensified more than two-fold the severity of the myocardial lesion. Skeletal muscle lesions were likewise aggravated by epinephrine administration. An acute and total failure occurred in 60% of the treated myopathics. This indicated a supersensitivity of the myopathic animals to catecholamine at the young age. Similarly, iso-

proterenol injection (0.1 mg/100 g s.c.), which produced no change in normal 30 days age group controls, markedly increased the myopathic (BIO 8262) heart Ca content (Lossnitzer et al, 1975). When given during the advanced phase of the disease (>100 days), epinephrine lost its necrotic action on the cardiac muscle, although it precipitated heart failure.

Digitoxin administration (0.12 mg/100 g) in the same regimen as for epinephrine, again produced adverse reactions in the young myopathics, but the effect was selective for cardiac muscle. A comparable percentage of the young cardiomyopathic hamster, as in epinephrine administration, developed heart failure due to digitoxin treatment. In contrast, digitoxin administered in the older age groups ameliorated the symptoms of congestive heart failure and prolonged the life span of the animals.

The toxic actions of epinephrine and digitoxin on the heart or skeletal muscle were blocked by KCl administration suggesting one of the adverse reactions may have been cellular depletion of K.

b. Parabiosis

To study possible humoral involvement of cardiomyopathy Bajusz and co-workers (1969 b) joined pairs of hamsters by surgical union of skin and abdominal muscular walls (parabiosis). Parabiosis allowed direct interchange of substances between the parabionts through anastomosis of capillary sized vessels. It was found that parabiosis between a normal and cardiomyopathic hamster significantly prolonged the life of the latter. This process did not alter the onset and progres-

sion of cardiac and skeletal muscle pathology but prevented the development of congestive heart failure. It was also found that parabiosis must be performed prior to the 58th day of age in order to achieve a protective effect indicating the presence of a critical stage of the disease. The exact mechanism of the beneficial effect of parabiosis was not known.

c. Diet electrolyte manipulation

Low K or low Mg diet produced fatal outcome in young (25-30 days of age) cardiomyopathic hamsters (within 10 days) at a time when similarly treated control hamsters developed no histologically demonstrable muscle lesion. This increased sensitivity to electrolyte imbalance suggested a role for K and Mg deficiencies in the disease process. However, K and Mg salt supplementation failed to prevent the occurrence and/or reduce the progression of the spontaneous cardiac lesions (Bajusz et al, 1969 d).

Two K-salts (K-aspartate and K-orotate) but not others (KCl, K-citrate, K-folate, K-gluconate) were found to prevent the cardiac hypertrophy and the development of congestive heart failure (Bajusz, 1968; Bajusz et al, 1969 d). The effective agents were found to enhance the healing of myocardial lesions but did not reduce their incidence. Insulin plus glucose was found to have an equal protective effect (Bajusz , 1968; Lochner et al, 1973). K-aspartate combined with glucose-insulin treatment appeared to have the best effect (Bajusz, 1968). Glucose-insulin treatment for seven days resulted in a significant increase in the incorporation of lysine and leucine

into the soluble protein and the actomysin fraction of the heart respectively. Addition of K-aspartate into this treatment, however, paradoxically, abolished this increase of protein synthesis (Lochner et al, 1973), despite of its beneficial action on the clinical course of the disease.

The observation that only certain K-salts influenced the healing processes, the development of compensating cardiac hypertrophy, and the incidence of congestive heart failure suggested that the organic moiety of these salts played an important role in the therapeutic affect. However, neither Na-aspartate nor Mg-aspartate was able to produce a beneficial effect on the healing process or reduce the incidence of congestive heart failure. Nevertheless, both treatments produced a slight reduction of the severity of congestive heart failure in the surviving members (Bajusz, 1968).

d. Low Ca diet and Ca-antagonist

Jasmin and co-workers (1975) reported that low Ca diet instituted at 20 days of age for one month markedly lowered the severity of the cardiomyopathy (arbitrary grade, from 2.1 to 0.2 out of a maximum of 3) and reduced the incidence of myocardial lesions to 25 % (UM-X 7.1). Skeletal muscle lesions, however, were found in all animals but of less severity. When low Ca regimen was instituted at 30 days of age, the beneficial effect was reduced but still evident in both the heart and skeletal muscle (Jasmin et al, 1975).

Calcium gluconate alone, reduced severity to 0.18, incidence to 38%, or in combination with low Ca diet, reduced severity to 0.00, incidence to 0%, protected the dystrophic

myocardium but produced little or no effect on skeletal muscle (Jasmin and Solymoss, 1975). The exact mechanism of protection for Ca-gluconate was not known but it might have stabilized the membrane as the serum creative phosphokinase (CPK) activity was dramatically reduced with its administration.

Verapamil treatment for 30 days in cardiomyopathic hamster (UM-X 7.1) of 20-30 days of age reduced the myocardial lesion incidence to 8% and severity to grade 0.08, (Jasmin and Solymoss, 1975). It produced no protection of the skeletal muscle. If, on the other hand, similarly treated animals were maintained without any treatment during 30 additional days, the preventive action of verapamil was no longer demonstable (Jasmin and Bajusz, 1975).

It was thus hypothesized that a reduction of Ca influx, either by lowering the Ca gradient across the cell membrane through Ca-deprivation, or by a Ca antagonist, prevented the cardiac muscle degenerative changes elicited by Ca "overload". The same conclusion was reached by Lossnitzer and co-workers (1975) who found that verapamil treatment prevented both isoproteronal increased ^{45}Ca uptake as well as the explosive Ca uptake during the necrotic stage in the cardiomyopathic hamster (BIO 8262).

5. E-C coupling in cardiomyopathy

No investigation has been conducted on the E-C coupling in hamster cardiomyopathy. Electrophysiologic investigation is perhaps hampered by the lack of good tissue preparation. Thin and long papillary muscle, which is necessary for simultaneous membrane potential and muscle tension measurement, is

difficult to obtain in the hamster heart. The small size of the hearts also poses as a problem for in vitro perfusion and studies of ion exchange kinetics.

There are abundant biochemical data in the literature to suggest abnormal characteristics of cardiomyopathic hamster cardiac sarcolemma such as altered membrane associated enzyme activities (La Ria et al, 197; Sulakhe et al, 1972; Nair et al, 1972; Singh et al, 1975) and altered membrane composition (Owens et al, 1972, 1973; Borowski et al, 1974). Furthermore the supersensitivity of the young cardiomyopathic hamsters to the toxic action of catecholamines (Bajusz et al, 1969 d; Lossnitzer et al, 1975) and digitoxin (Bajusz et al, 1969 d) suggest abnormal membrane function in these animals. E-C coupling of heart muscle is intimately associated with trans-membrane movement of Ca. It is conceivable and highly probable that an altered E-C coupling of the heart muscle occurs in the cardiomyopathic hamster in the face of the many observations of an abnormal cardiac sarcolemma which could affect the movement of Ca

E. STATEMENT OF THE PROBLEM

In human patients with primary cardiomyopathy, the clinical manifestations probably do not result from a single entity of a disease state but rather from a collection of unknown (primary) cardiac lesions which lead to a common out-come: terminal congestive heart failure (CHF). It is thus not only impractical, but moreover probably hopeless to find the causal factor of primary human cardiomyopathy. Homburger

and co-workers (1962) introduced a model of genetic hamster cardiomyopathy (Bajusz et al, 1966, 1968, 1969 a, b) which offers a reproducible animal model of a primary cardiomyopathy in which we may finally have the opportunity of localizing the etiological factor in its pathogenesis.

Since the hamster cardiomyopathy is characterized by a depression of cardiac contractility, it is likely that step(s) involved in E-C coupling is disturbed. Available evidence so far does not suggest a primary disturbance at the mitochondria and SR, two loci that have been suggested to be intimately involved in E-C coupling. Qualitative contractile protein changes have not been demonstrated although quantitative myosin synthesis has been shown to be depressed.

Cardiac muscle E-C coupling is strongly dependent on extracellular and membrane bound Ca. It is likely, in the absence of other major biochemical defects elsewhere in the E-C coupling processes, that the depressed cardiac function may be the result of a disturbance in Ca exchange at the sarcolemmal level.

To investigate this possibility in myopathic hamsters, Ca exchange kinetics established for kitten hearts will be extended to hamster hearts. Chronological examination of cardiac contractility and Ca exchange kinetics will be examined from the pre-symptomatic stage to that during CHF. Isolated cardiac sarcolemma will be studied with respect to sialic acid residues content, sialytransferase activities and Ca binding profiles. It is hypothesized that a correlation exists between cardiac contractility, Ca exchange kinetics and sar-

colemmal Ca binding during the different stages of hamster cardiomyopathy and that depressed cardiac function can be explained both at the physiological (Ca exchange kinetics) and biochemical (sarcolemmal Ca binding) level.

It must be emphasized that the cardiomyopathic hamster will not be used as a model for human primary cardiomyopathy categorically; nevertheless, it would be a windfall if the animal suffers an identical form of heart lesion to that observed in human patients. However, it is hoped that with this genetically transmitted, reproducible and uniform heart disease, we may find a biochemical abnormality whose presence is responsible for the cardiac disfunction and eventual heart failure.

F. APPROACH TO THE PROBLEM

Isolated perfused heart systems will be used both for measurement of cardiac contractility and for the study of Ca exchange kinetics. Cardiac contractility will be measured by a saline-filled balloon inserted into the left ventricle of modified Langendorff perfused hearts. This probably gives a more physiological index of cardiac contractility than that obtained by a force transducer attached to the apex of the heart. Ca exchange kinetics will be studied by non-steady uptake and washout of Ca. This will permit a correlation between Ca movement and changes of cardiac contractility.

One of the inherent problems of uptake and washout methods for measurement of Ca fluxes under non-steady state conditions is that permeability to Ca remains unchanged during

the manipulation. This complication will be examined by comparing the exchange of ^{14}C-mannitol as well as ^{45}Ca under steady and non-steady state of Ca exchange. It is believed that a gross alteration of capillary and membrane Ca permeability would be reflected in an alteration in the exchange rate of the indicators.

To ensure rapid and precise sampling of the effluent from the hearts, a collection technique similar to that introduced by Wilde and co-worker (Effluography, 1956) is adopted. The procedure involves collection of the effluent from the heart on a continuously moving (constant speed) chromatography paper. The activities of the radioactive tracer will be counted by Actigraph (Geiger gas counting chamber). To overcome the problem of personal bias, the data will be analyzed by a computer program which performs curve peeling based on statistical criteria. And finally, to ensure the appropriateness of the model used in interpreting the data, in-series models of Ca exchange will be solved with simultaneous differential equations and compared to an in-parallel model.

Since cardiac E-C coupling is closely associated with extracellular Ca which includes both interstitial and membrane bound Ca, the Ca binding characteristics of isolated cardiac sarcolemma will be examined. A "cell ghost", or membrane sac preparation was chosen over the small vesicle preparation because of the possibilities of an inverted and resealed vesicles in the latter approach. The Ca-binding profile of cardiac sarcolemma will be analyzed by Scathard plot (1949). A computer program of successive approximations, not requiring

prior assumptions will be used to analyze the Ca-binding data.

Since surface sialic acid residues may function as Ca binding sites (Langer, 1973) and may represent the anatomical location for the superficial Ca involved in cardiac muscle E-C coupling, the concentration of surface sialic acid residues will be measured in both normal and cardiomyopathic hamster hearts to determine if a quantitative difference exists. The enzyme, sialyltransferase, responsible for the addition of sialic acid residues to the polysaccharide side chains of the surface glycoprotein will be also assayed.

SECTION II

METHODS

A. ISOLATED HEART

1. Experimental preparation

(a) Perfusion apparatus

The perfusion apparatus used in this study is shown in Figure 1. The perfusion solution was delivered by a Masterflex pump (Cole-Palmer Model 7598) through a condenser maintained at the desired temperature and then via a bubble trap to a cannula in the aorta of the heart. The temperature of the condenser was maintained by means of a Heto-Thermostat (Binkerød, Denmark, Model 623) at a temperature of approximately 35°C which stabilized the temperature of the perfusate at the heart at 30.1±1.0°C. The perfusate temperature was monitored by a thermocouple thermometer (Bailey Instrument Inc. Model BAT-8) inserted just proximal to the aortic cannula. One arm of the bubble trap was connected to a Statham pressure transducer (Model P23AC) to monitor perfusion pressure. An electronic negative feed-back loop between the pressure transducer and the pump allowed constant pressure perfusion when desired. Around the bubble trap was a by-pass controlled by two three-way Teflon valves. This by-pass, when opened, eliminated the dead space of the bubble trap which would otherwise complicate the collection procedures (see below).

The perfusate, after traversing through the coronary circulation, was collected on 4 cm. wide strip of chromatography paper (Whatman Chromatography paper number 4, 0.2 mm thick). The collection of the fluid on the paper was rendered smooth and continuous, rather than dropwise, by moving the paper

Figure 1

The perfusion apparatus (see text for description).

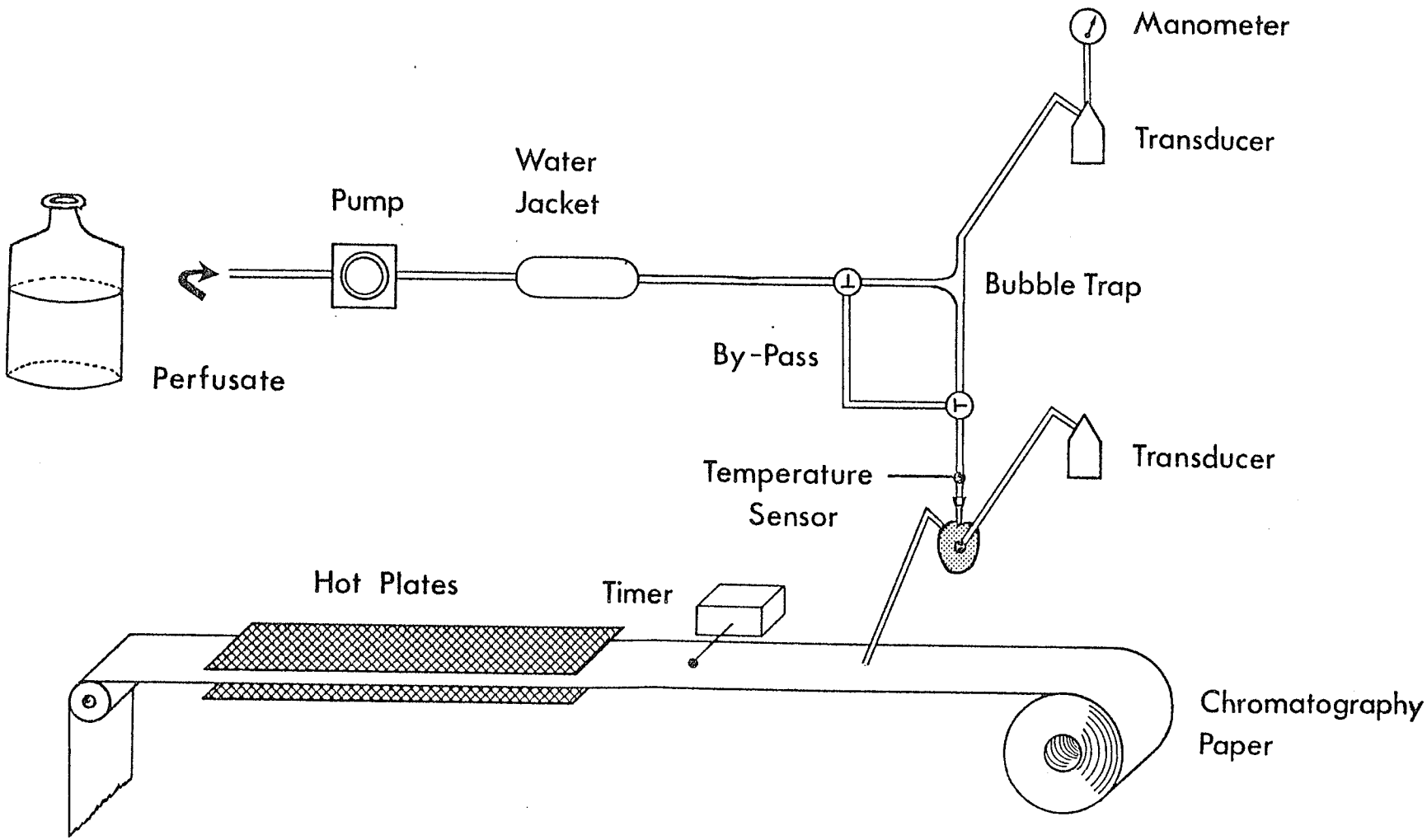
Manometer
Transducer
Water
Jacket
Pump
Bubble Trap
By-Pass
Perfusate
Transducer
Temperature
Sensor
Hot Plates
Timer
Chromatography
Paper

at a constant speed under the heart. This was achieved by a constant speed motor with a variable speed setting of 12, 18.5 and 34 mm/sec. The speed of the paper motion chosen depended on the rate of the perfusate flow. Figure 2 shows the calibration curves of the width of perfusate migration on the chromatography paper, which could easily be measured on a slightly burned strip (see below), at different settings of motor speed. A linear relationship between these two parameters existed between 0.5-2.3, 1.0-2.8 and 1.4-4.3 ml/min respectively for the low, medium and high speed setting of the motor. The reproducible relationship between flow rate and perfusate width on the collecting chromatography paper allowed indirect estimates of the perfusate flow in this system.

The motor driven chromatography paper, moving at a constant speed, was pulled between a pair of drying hot plates. This, together with a high intensity radiant heat projector (Cole-Palmer Model 3151-6, Dyna-lume) distal to it, assured complete drying of the chromatography paper. A time marker with a marking pen provided 1 sec or 5 sec spaced marking on the chromatography paper.

Another Statham pressure transducer (Model P23Dc) was connected via polyethylene tubing to a small latex balloon. This system was filled with saline and was used to monitor left intra-ventricular pressure changes.

Throughout the experiment, recordings were made on a four channel Gould Brush Recorder (Model 440) of the per-

Figure 2

Calibration curves for flow rate as a function of the width of fluid migration on Whatman 4 chromatography paper. The paper speed shown was at 12, 18.5 and 34 mm/sec.

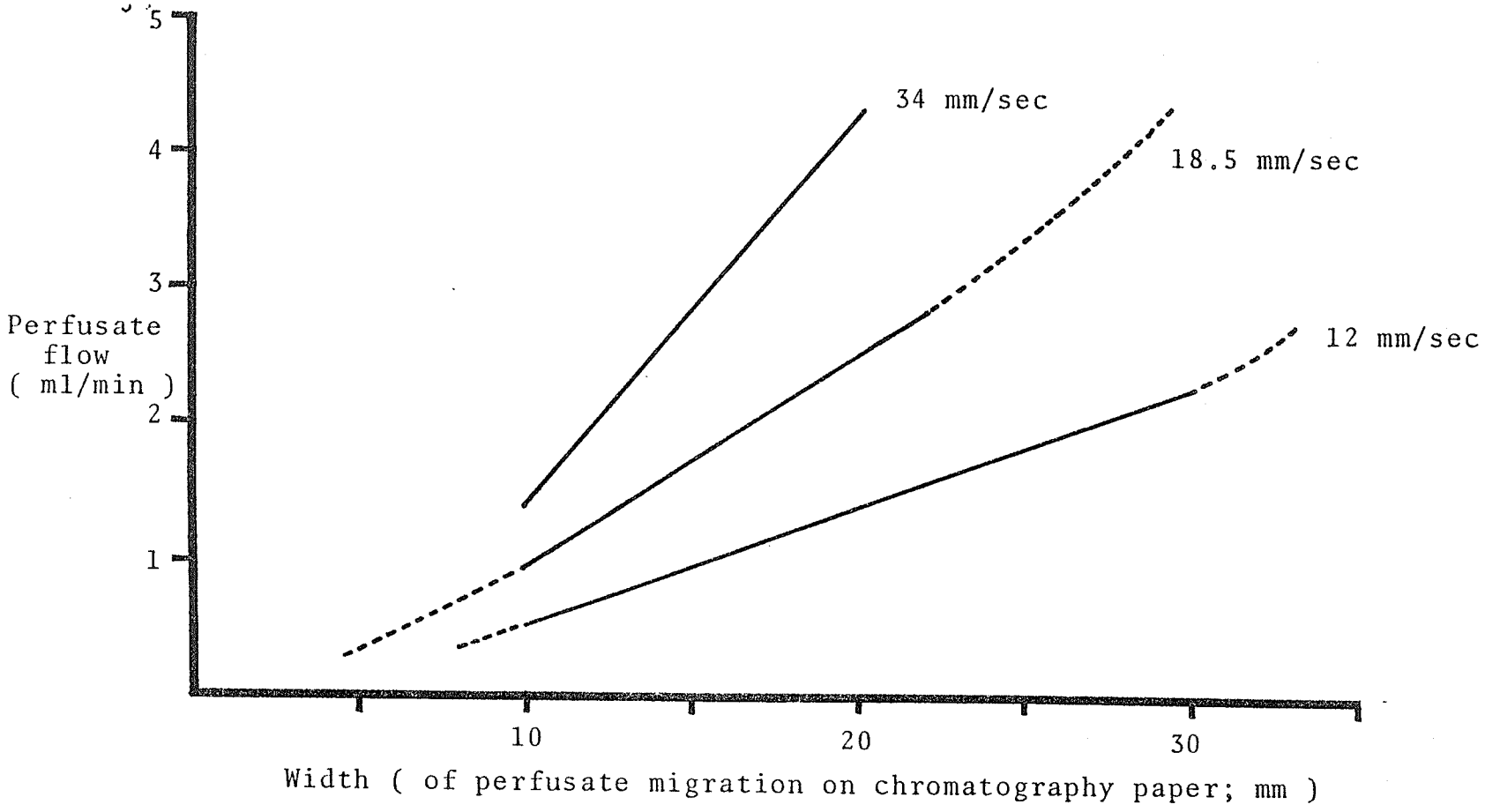
5
4
3
2
1
Perfusate flow (ml/min)
34 mm/sec
18.5 mm/sec
12 mm/sec
10
20
30
Width (of perfusate migration on chromatography paper; mm)

fusion pressure, the left intra-ventricular pressure (IVP) and its first time derivative (dP/dt), and the flow rate. Amplifiers in these experiments were designed and assembled by Mr. John Delaive of the Department of Pharmacology and Therapeutics of the University of Manitoba.

(b) Perfusion solutions

The perfusion solutions used in this study were modified Krebs-Henseleit (1932) solution with 1.8 mM Ca (normal K-H solution) or without Ca (Ca free K-H solution). The solutions were equilibrated with 95% O_2 and 5% CO_2.

On the day of the experiment the solutions were prepared from four stock solutions of the following composition:

	mM	ml
1. NaCl	116.5/4.9	950
2. $CaCl_2$ (or H_2O)	360	5
3. $MgCl_2$	240	5
4. $NaHCO_3/NaH_2PO_4$	655 / 30	40

Glucose was added at 2 g per litre. In the Ca free K-H solution, $CaCl_2$ stock was replaced by equal volume of distilled water. The resultant composition of the perfusion solutions is given in Table 2.

(c) Perfusion protocol

Hamsters of either sex between the ages of 26 days to 220 days were given heparin (4000 u/kg) subcutaneously one hour before being anesthetized with diethyl ether. The hearts were then immediately removed and immersed in cold ($4^{o}C$), pre-oxygenated normal K-H solution. The aorta was

Table 2

Composition of Perfusates (mM)

Components	I Normal K-H	II Ca-free K-H
NaCl	110.7	110.7
KCl	4.7	4.7
$CaCl_2$	1.8	<0.001
$MgCl_2$	1.2	1.2
$NaHCO_3$	26.2	26.2
NaH_2PO_4	1.2	1.2
Glucose	11	11

cannulated and perfusion started on a temporary movable stand at 80-100 mm Hg. This set up facilitated the cannulations. From ether anesthesia to perfusion of the isolated heart, the time lapse was five min or less.

The right atrium was ligated to remove a site of automaticity and perfusion dead space. In the initial experiments, the pulmonary artery was cannulated (Figure 3) for collection of effluent not contaminated by perfusate leaked through the aortic valve. This procedure was later found unnecessary as the analysis depended on the amount of tracer in the effluent per unit time (see Analysis section) rather than its concentration. A small latex balloon, made from the tip of a condom (volume dependent upon heart size) and tied on a short piece of polyethylene tubing, was filled with saline and inserted via an incision in the left atrium into the left ventricle. This was for measurement of left ventricular pressure and its first time derivative. To facilitate insertion into the tiny left ventricular cavity, the balloon was distended from within by a thin, blunt glass rod which extended through the polyethylene tubing. This rod was afterwards removed and the tubing was connected via an appropriate length of the same kind of tubing to the Statham pressure transducer.

After cannulation, the heart was transferred to the perfusion apparatus (Figure 1) and perfused with 30^{o}C Normal K-H solution. This temperature was used because preliminary experiments showed better maintenance of cardiac contractility

Figure 3

Cannulation of the isolated heart (see text for description).

LA = left atrium
RA = right atrium
LV = left ventricle
RV = right ventricle

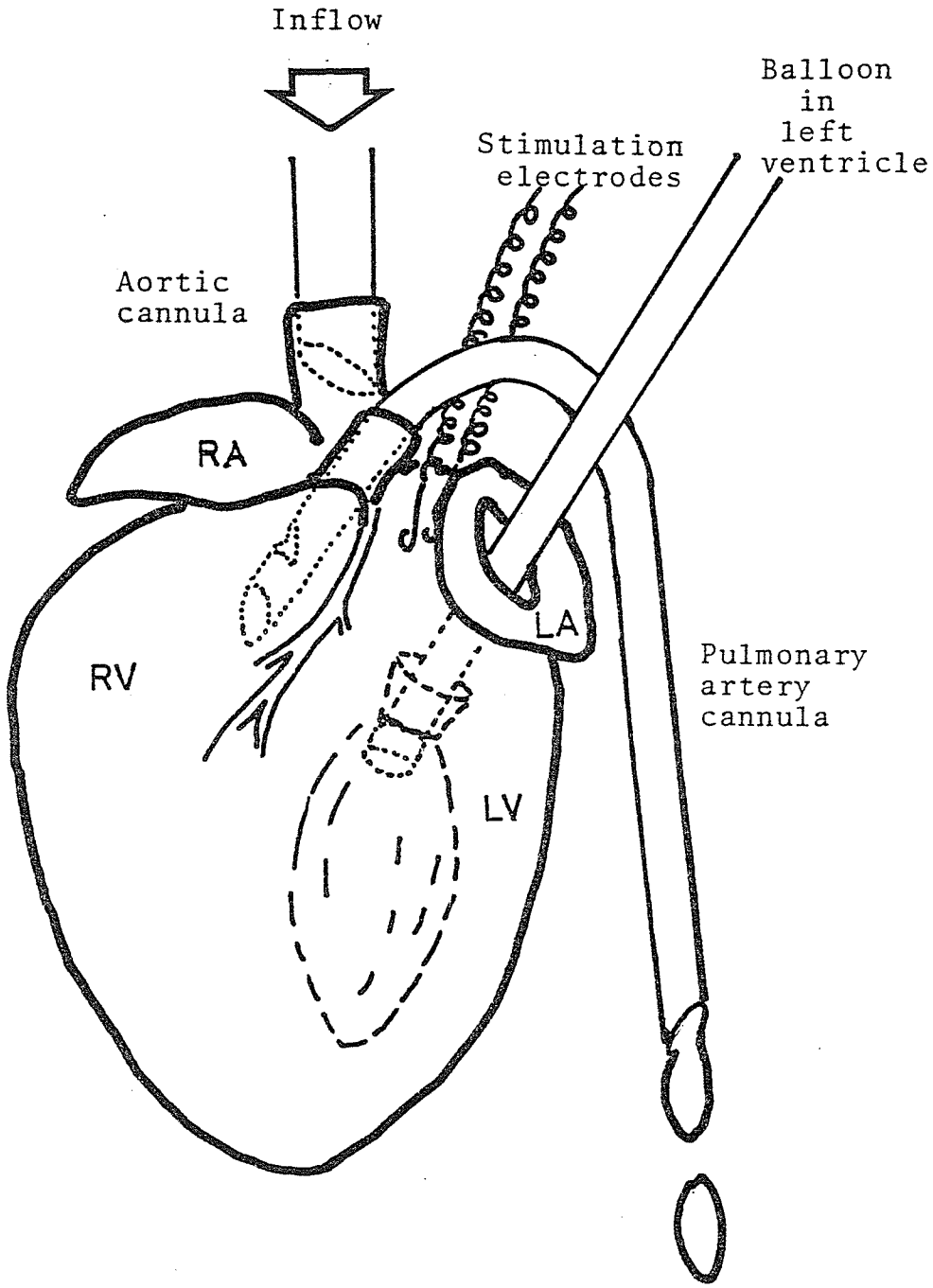
Inflow
Balloon
in
left
ventricle
Stimulation
electrodes
Aortic
cannula
RA
LA
RV
LV
Pulmonary
artery
cannula

and slower heart rate compared to 37°C.

The hearts were allowed to equilibrate for 30 min without contracting against the isometric load at a constant pressure of 80 mm Hg. The hearts were not paced during equilibration. At the end of 30 min, the hearts were driven electrically at 180 beats/min by a Grass S6 Stimulator at twice threshold voltage through bi-polar electrodes attached to the base of the heart. After the hearts had stabilized the perfusion was switched from constant pressure to constant flow which provided a pressure of 80 mm Hg. Perfusate flow was maintained at this rate for the remainder of the experiment.A constant rate of perfusate flow was a necessary condition for the kinetic analysis to be detailed later in the Data Analysis section.

The length-tension relationship of the heart was established by progressive inflation of the balloon to increase end diastolic IVP. The curve was constructed for end diastolic IVP of 0 to 20 mm Hg.

The end diastolic IVP was returned to 5 mm Hg and the by-pass around the bubble trap was opened. An essential procedure utilized in this study was a brief period of gas perfusion between perfusates of different compositions. The removal of the bubble trap eliminated a mixing space for air bubbles and perfusates.

Kinetic studies were initiated by perfusing the hearts for two min with Ca free K-H solution by which time contractile activity had ceased. Analysis of the Ca washout data indicated

that more than 90% of the exchangeable Ca was removed by two min of Ca free perfusion (see Results). Contractility was restored by perfusion of the hearts with normal K-H solution containing trace amounts of ^{45}Ca. This constituted the Ca uptake part of the experiment.

Tracing of IVP, dP/dt, and perfusate flow from a representative experiment during this perfusion procedure is shown in Figure 4.

The uptake of Ca was monitored for five min. Tracer analysis indicated that by this time all the exchangeable Ca involved in excitation-contraction (E-C) coupling had reached equilibrium with the perfusate (see Results). As a routine procedure to prevent intermixing of Ca containing perfusate with Ca-free perfusate, the hearts were perfused for 5-10 sec with 95% O_2, 5% CO_2. Ca free K-H solution was then instituted for five min. This constituted the Ca washout part of the study. The second Ca washout rather than the first Ca washout was used because correct graphical analysis, as will be detailed later, necessitated a precise estimation of the last compartment. This is due to the fact that conventional graph-peeling procedures produce inherent accumulative and cascading errors. Since perfusion with normal K-H solution after 5 min of Ca free K-H solution wash inevitably led to contracture and since a reasonable estimation of the last compartment needed about five min of Ca free K-H solution collection, the first Ca washout was limited to two min and not collected for analysis. The effluent from

Figure 4

Tracing of a standard kinetic experiment (Oct. 26/75, Exp. 2; normal hamster 220 d).

Panel A: LVP

Panel B: Perfusion pressure (shut off after the by-pass loop was opened).

Panel C: dP/dt

Panel D: perfusate flow

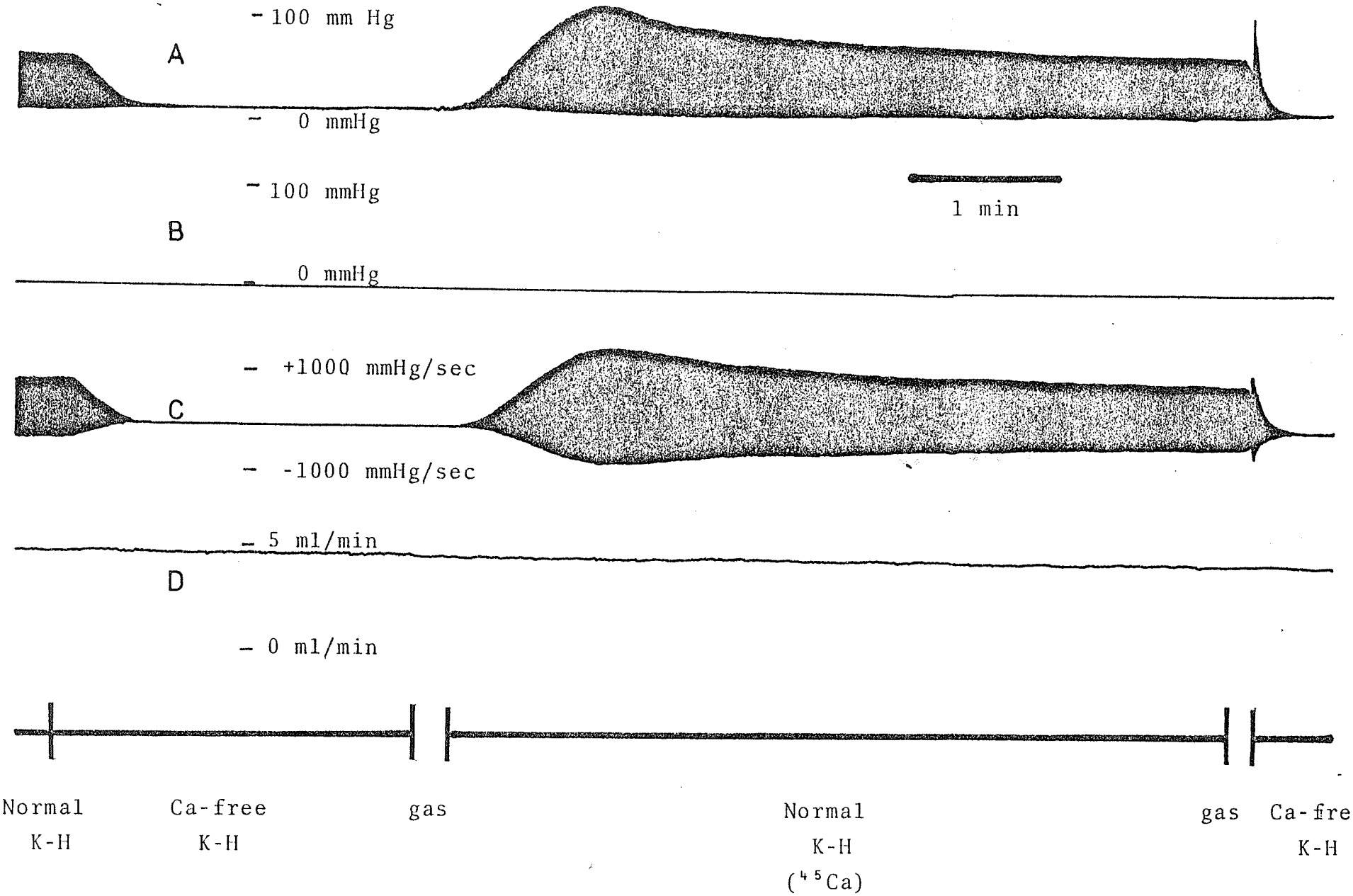
- 100 mm Hg
A
- 0 mmHg
- 100 mmHg
1 min
B
- 0 mmHg
- +1000 mmHg/sec
C
- -1000 mmHg/sec
- 5 ml/min
D
- 0 ml/min
Normal K-H
Ca-free K-H
gas
Normal K-H (^{45}Ca)
gas
Ca-free K-H

the heart during the uptake and washout was collected on the chromatography paper as previously described.

At the conclusion of the experiment, the hearts were cleared of residual perfusate by gas perfusion. The ventricular portion of the heart was blotted dry and weighed. A sample was taken for residual Ca measurement as described below.

The concentration of Ca in the perfusate (in terms of cpm per unit volume) was measured by collecting the perfusate directly on the chromatography paper at a given flow rate and a set paper speed. The amount of Ca extracted in the uptake or washed out of the heart in each experiment was then quantified in relation to this.

Figure 4 illustrates the non-steady state exchange of Ca. Note the associated changes of cardiac contractility. Steady state exchange of Ca (see below), on the other hand, is not associated with changes of cardiac contractility, as only the tracer ^{45}Ca is introduced or removed.

2. Assays

a) ^{45}Ca counting of chromatography paper strip

The ^{45}Ca activity of the dried strip of chromatography paper was determined by counting on a Nuclear-Chicago Actigraph (Geiger gas counting chamber) with helium-butane quench gas at a voltage of 950 volts. The counting window was set at 12 mm to obtain some running average of the ^{45}Ca activity. This width represented less than 0.4 sec sampling rate of the effluent with the high setting of paper speed (see Figure

2) and 1.0 sec sampling rate with the low setting of the paper speed. The system is thus capable of resolving the change of Ca activity to one sec or less.

The scanning speed of the motor and the reaction time of the counting chamber were adjusted in relation to the total activity on the strip that was exposed to the window. For example, at a total count of 50,000 cpm per 12 mm (window width), the scanning speed was set at 60 cm/hr and the reaction time set at 10 sec.

The changes in Ca activity recorded for the experiment illustrated in Figure 4 are shown in Figure 5. To illustrate the conversion of Ca activity to Ca content, assume the perfusate strip was made at a flow rate of 2 ml/min and had a ^{45}Ca activity of 10,000 cpm per 12 mm. Since the perfusate had a total Ca concentration of 1.8 mM, the amount collected for one sec is equal to

$$\frac{1.8 \text{ mmole}}{1000 \text{ ml}} \times \frac{2 \text{ ml}}{\text{min}} \times \frac{1 \text{ sec}}{60 \text{ sec/min}} = 6 \times 10^{-5} \text{ mmole.}$$

If we further assume, for simplicity sake, that the collection was done with a motor speed of 12 mm/sec, then 10,000 cpm is equivalent to 6×10^{-5} mmole. The converted data were then analyzed graphically (see below).

(b) Ca and Mg determination in the plasma

A small volume of plasma (50-100 µl) was mixed with 1 ml of 1% $LaCl_3$ 5% HCl. The diluted sample was read by atomic absorption spectrophotometry at 422.7 nm for Ca and 285.2 nm for Mg (Perkin-Elmer, Model 303). For each set of ion determinations, a standard curve was prepared using

Figure 5

^{45}Ca activity record from Actigraph (Oct. 26/75, Exp. 2; normal hamster 200 d).

Panel A: Effluent during ^{45}Ca uptake.*

Range = 50,000 cpm, scanning speed = 60 cm/hr.

Reaction time = 10 sec.

Panel B: Effluent during ^{45}Ca washout.*

1) Range = 50,000 cpm, scanning speed = 60 cm/hr.
   Reaction time = 10 sec.
2) Range = 5,000 cpm, scanning speed = 60 cm/hr.
   Reaction time = 20 sec.
3) Range = 1,500 cpm, scanning speed = 60 cm/hr.
   Reaction time = 50 sec.

* High voltage = 950 volts.
Counting window = 12 mm.

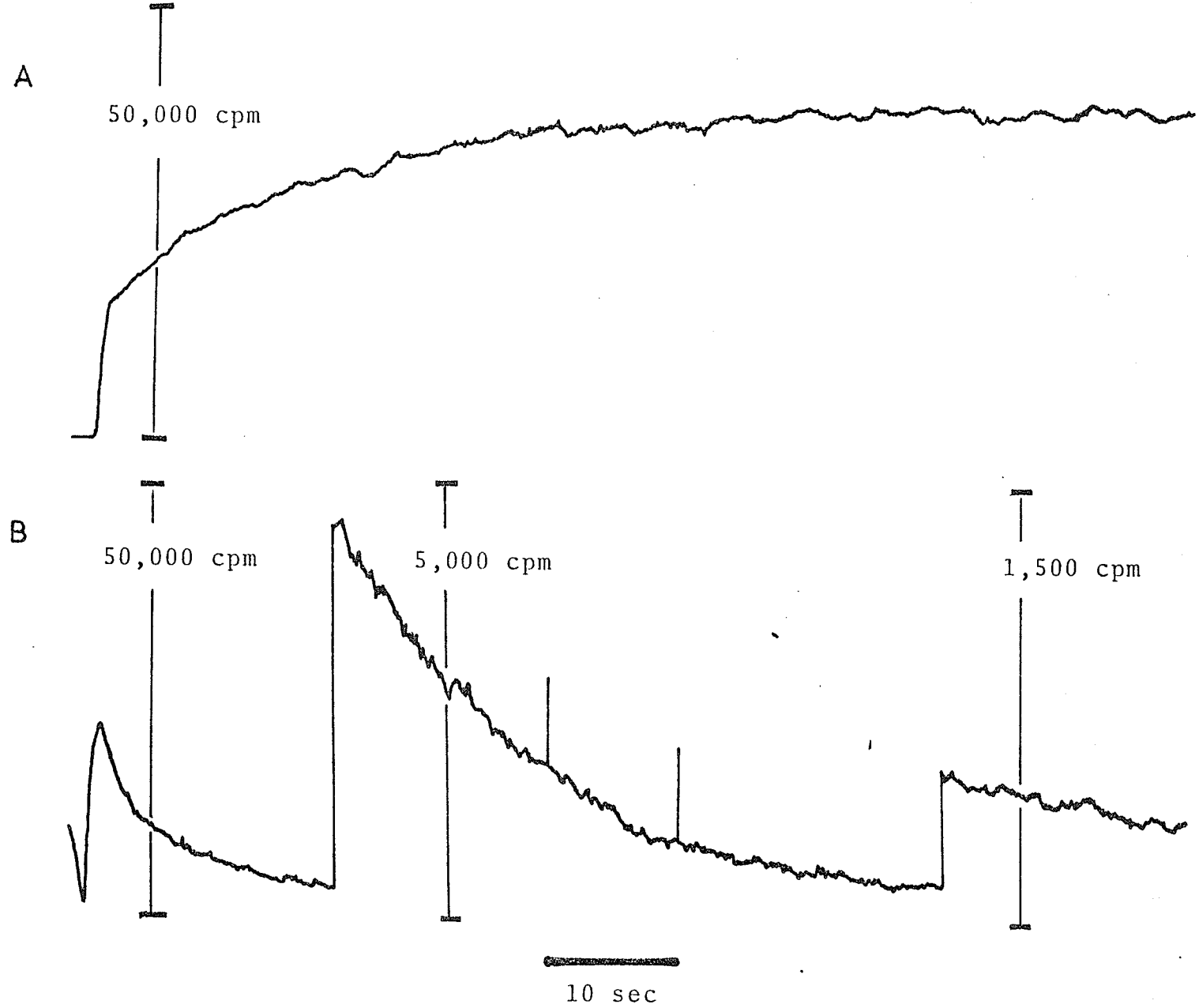
A
50,000 cpm
B
50,000 cpm
5,000 cpm
1,500 cpm
10 sec

a series of different concentrations of Ca and Mg (0, 0.02, 0.04, 0.08, 0.16 mM) in the La solution.

(c) Ca determination of the tissue

A small amount of tissue (0.1 to 0.3 g) was put in a platinum crucible, dried overnight in a heated (80°C) vacuum desiccator (GCA/Precision Scientific) and the ashed for 8 hr at 600°C in a thermolyne muffle furnace (Thermolyne Corp., Type 2000). Temperature was increased in stages to 600°C to prevent spattering of sample. One ml of concentrated HCl was added to the residue to dissolve the inorganic ions. A 0.5 ml aliquot of this sample (or appropriate dilution) was added to 1 ml of the 1% solution in 5% HCl. Ca concentration in this sample was determined by atomic absorption spectrophotometry. The amount of Ca in the muscle was expressed as mmole/kg wet weight.

(d) Determination of the extracellular space exchange kinetics

In order to meaningfully study the Ca exchange kinetics of the isolated heart, it was necessary first to determine the exchange kinetics of the three major compartments of the extracellular space: apparatus space, vascular space and interstitial space. These data could then be used to determine the extracellular compartment in the kinetic analysis and to impose a time constraint on any physiologically meaningful rate of exchange. In other words, a kinetically defined compartment obtained by analysis should not have a half time of exchange less than that of the extracell-

ular space.

To this end, three types of experiments were performed. Firstly, iodinated (^{131}I) albumin uptake and washout of the heart were done to determine the apparatus and vascular space exchange. Secondly, ^{14}C-mannitol uptake and washout were done to include the interstitial space. And finally, ^{45}Ca uptake and washout in the absence of heart were done to examine ^{45}Ca binding to and dissociation from the perfusion apparatus alone.

(i) Preparation of iodinated Bovine serum albumin (^{131}I-BSA)

To prepare the ^{131}I-BSA, 5mCi of ^{131}I (50µl) was reacted with 1 mg of BSA (40 mg/ml, 25 µl) in the presence of freshly prepared Chloramine-T solution (12.5 mg/ml in 0.05 M sodium phosphate buffer pH 7.5, 25 µl). The mixture was vortexed for one min and the reaction terminated by the addition of 50 µl of freshly prepared Na-metabisulfite (12.5 mg/ml) in 0.05 M sodium phosphate buffer. Radioactive ^{131}I bound nonspecifically to BSA was displaced by the addition of 2 mg of KI (10 mg/ml, 200 µl). The mixture was then ready for column chromatography.

The column was prepared by presoaking overnight (with stirring) Sephadex G-50 in 0.07 M sodium barbitone buffer (5 g/100 ml), pH 8.6. This was then poured into a mini-column of inside diameter of 1.0 cm to a height of 10 cm. A disc of No. 3 Whatman filter paper was placed on top of the column. Next, 20 ml of sodium barbitone buffer, 1 ml of BSA

(40 mg/ml), and 10 ml of sodium barbitone buffer were sequentially eluted through the column.

^{131}I-BSA mixture as well as 400 µl of KI washing was introduced on the top of the column. This was eluted with 30 ml of sodium barbitone buffer. The iodination and separation procedure was adopted from Greenwood and Hunter (1963).

The elution pattern, as counted by gamma-scintillation, is shown in Figure 6. Each sample contained 1.5 ml. As the activity was high, only sample number 3 was used in the experiment. This fraction had little or no contamination of free ^{131}I. Note the reaction left little free ^{131}I which could be seen as activity in sample 5 through 9.

(ii) ^{131}I-BSA exchange

^{131}I-BSA from sample number 3 was diluted 50 fold with normal K-H solution and with Ca free K-H solution for the uptake and washout studies. Exposure to ^{131}I-BSA containing solutions was limited to 30-60 sec. Tracer was first introduced to the heart in normal K-H solution and recovered in Ca free K-H solution during Ca washout. The heart was then again exposed to the tracer during Ca free K-H solution perfusion and this time recovered in normal K-H solution during Ca uptake. The recovered effluent on chromatography paper was scanned by the Actigraph.

(iii) ^{14}C-mannitol exchange

^{14}C-mannitol exchange was studied under two kinds

Figure 6

Separation of ^{131}I-BSA from free ^{131}I on Sephadex G-50. The separation was carried out by gel filtration of an iodination reaction mixture containing ^{131}I (5 mCi), BSA (1 mg), chloramine-T (312 µg), Na metabisulfite (625 µg), and KI (2 mg) in a volume of 350 µl. The column (10 cm x 1 cm; 1 g) of Sephadex G-50 was equilibrated with 0.07 M barbitone buffer, pH 8.6, and presaturated with BSA (40 mg). ^{131}I-BSA was eluted first, followed by a small amount of free ^{131}I. Each data point represents 1.5 ml of eluted sample. The radioactivity was counted by gamma-scintillation.

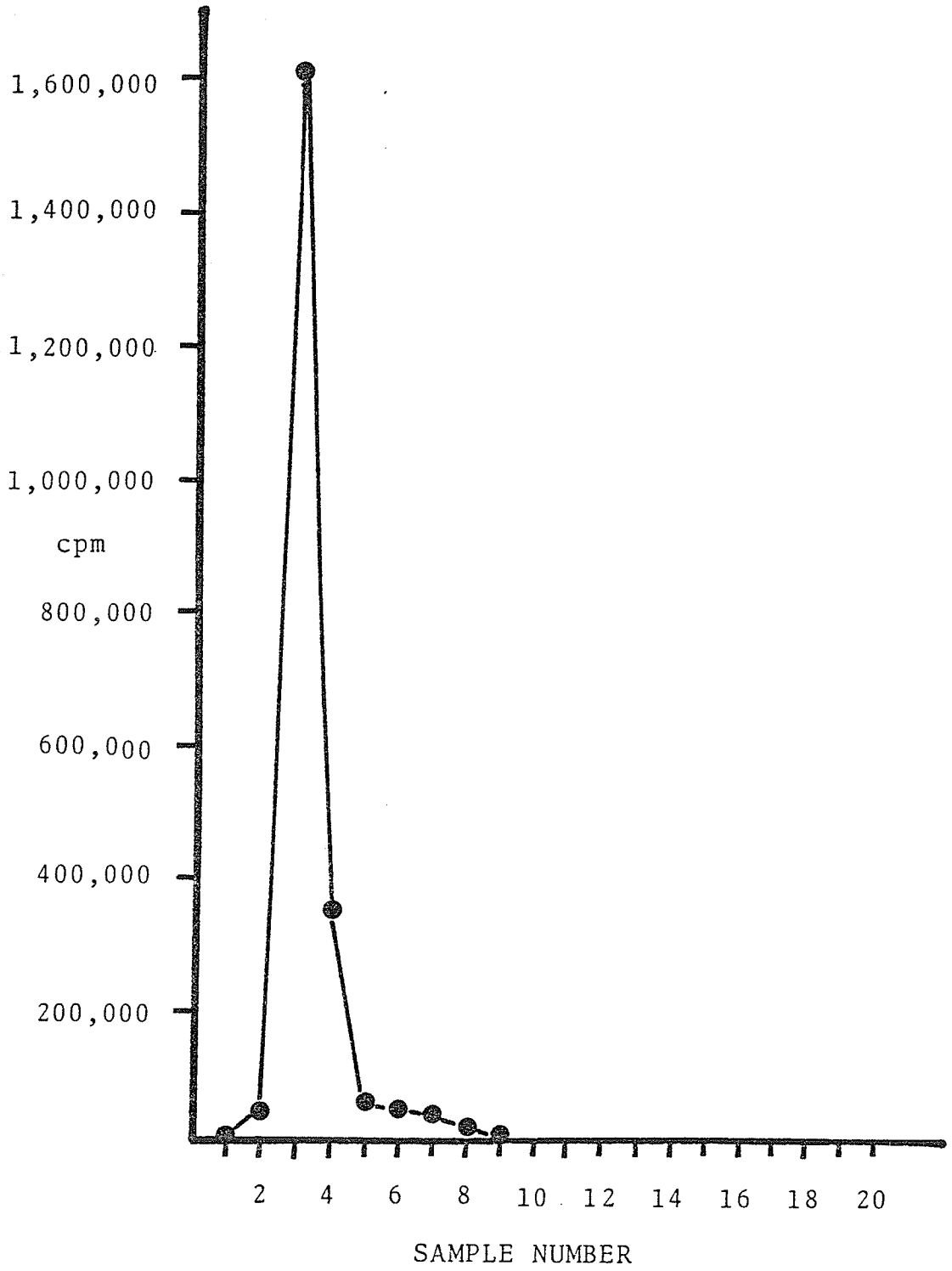
1,600,000
1,400,000
1,200,000
1,000,000
cpm
800,000
600,000
400,000
200,000
2
4
6
8
10
12
14
16
18
20
SAMPLE NUMBER

of conditions. Firstly, the uptake (5 min) and subsequent washout (5 min) of the tracer with normal K-H solution was examined. And secondly, in anticipation of possible changes in cellular permeability following Ca free K-H solution perfusion, ^{14}C-mannitol kinetics were studied under the non-steady state condition of Ca exchange. This was done by a prior two min perfusion with Ca free K-H solution (not collected) which removed most of the exchangeable Ca. The uptake of ^{14}C-mannitol was then followed for five min during normal K-H solution perfusion. The effluents collected on chromatography paper during ^{14}C-mannitol uptake and washout were scanned by the Actigraph to determine the ^{14}C activity.

In order to measure the mannitol space directly, the hearts were cleared of the vascular fluid at the end of this perfusion and samples of 20-30 mg of the ventricles taken for radioactivity measurement. Each sample was dissolved in 300 µl of NCS (Amersham/Searle Corp.) at 50°C in the presence of 20 µl of water. The solubilized tissue was then neutralized with 20 µl of 6N acetic acid to reduce chemiluminescence and mixed with 10 ml scintillation medium consisting of 6 g 2,5-diphenyloxazole (PPO) per 1 of toluene. Radioactivity was measured in a Philips scintillation counter. Radioactive perfusate (50 µl) was treated in the same manner as above before counting.

(iv) ^{45}Ca exchange of the perfusion apparatus

The extraction of ^{45}Ca from the perfusate solution by the perfusion apparatus (in the absence of a heart) and

the subsequent washout of the tracer were studied in order to assess the kinetics of such exchange and the amount of Ca adhering to the apparatus. Identical sequences of uptake (5 min) and washout (5 min) as in previous studies were done and the perfusate collected on chromatography paper. The activity was determined by Actigraph counting.

3. Data analysis of the uptake and washout curves

(a) Two compartments in parallel in an open system: theory and graphical analysis

Compartmental analysis of tracer movements in biological system is designed to describe the system in terms of a simplified model. The compartments so named kinetically do not necessarily have exact anatomical counterparts. A kinetically defined compartment may encompass many structurally distinct entities which nevertheless behave, with regards to the movement of one specific substance (and tracer), indistinguishably from each other. Often in tracer studies the system is resolved into two compartments: extracellular and intracellular. Presumably the cell membrane is the rate limiting barrier and exchange across it kinetically defines two distinct compartments. If the membrane is indeed the rate limiting step, the two compartments, in most cases, can be considered to exchange independently of each other. In most studies, parallel compartments are assumed based on this premise. With this parallel model, extracellular exchange, being outside the membrane, would occur faster than and inde-

pendent of intracellular exchange.

One important assumption in the analyses used in this study, under non-steady state conditions of Ca exchange, is that Ca permeability remains unchanged throughout the uptake and washout process. Some evidence supporting this contention are presented in Results.

Examples of the profiles of Ca uptake rate (mmole of Ca extracted per sec from the perfusing medium by the heart) and washout rate (mmole of Ca leaving the heart per sec and recovered in the effluent) as a function of time are plotted semi-logarithmically as shown in Figure 7 from a representative experiment.

The uptake rate was the difference between the perfusate Ca delivery rate (mmole/sec) and the rate of Ca appearance in the effluent (mmole/sec). The washout rate was just simply the rate of Ca appearance in the effluent. The uptake rate therefore looks like the washout rate (Figure 7) with an initially high value which decreases exponentially as a function of time. Both uptake and washout curves appeared to be bi-exponential and support the two-compartment model of Ca exchange.

Assuming independent, parallel exchange of two compartments, the last part of the curve can be extrapolated to give a single monoexponential decay described by the following equation:

$$\frac{dE(t)}{dt} = A_0 e^{-kt}$$

Figure 7

Bi-exponential profiles of Ca uptake rate and washout rate from a representative experiment (July 11/76, Exp. 2; normal hamster, 44 day, heart wt 0.29 g).

o---o Uptake rate

x——x Washout rate

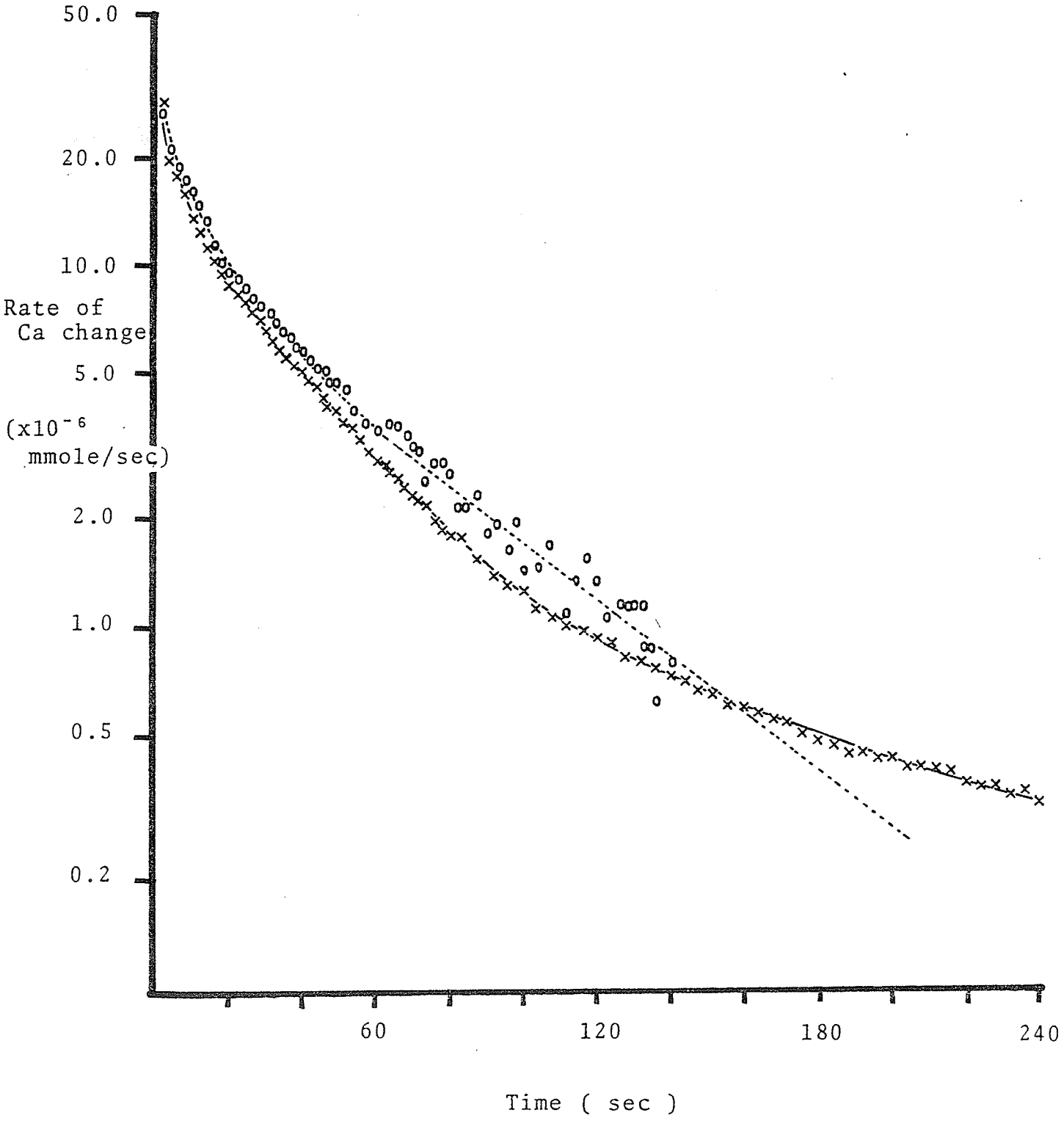
50.0
20.0
10.0
Rate of
Ca change
5.0
(x10⁻⁶
mmole/sec)
2.0
1.0
0.5
0.2
60
120
180
240
Time (sec)

The symbols of equation 1 are defined as follows:

$\frac{dE(t)}{dt}$: mmole of Ca extracted or washed out per sec at time t (mmole/sec)

A_0 : ordinate intercept representing $\frac{dE(o)}{dt}$ (mmole/sec)

K : rate constant of compartmental exchange (1/sec).

The total amount extracted by (or washed out of) this compartment is represented by the area under the curve extrapolated to inifite time. This is represented by the integral of equation 1:

$$D = \int_0^{\infty} A_0 e^{-Kt} = \frac{A_0}{K} , \tag{2}$$

where D is the total content of the compartment in mmole (not normalized for heart wt).

The half time of exchange of the compartment is the time taken to extract (or washout) half the total capacity of the compartment and is described by

$$\int_0^{t_{1/2}} A_0 e^{-Kt} = \tfrac{1}{2} \cdot \frac{A_0}{K} \tag{3}$$

Integration of the left side of equation 3 gives

$$-\frac{A_0}{K} e^{-Kt_{1/2}} - \left(-\frac{A_0}{K}\right) = \tfrac{1}{2} \frac{A_0}{K} ,$$

$$\text{or} \quad e^{-Kt_{1/2}} = \tfrac{1}{2} . \tag{4}$$

This is equivalent to

$$t_{\frac{1}{2}} = \frac{\ln \frac{1}{2}}{-K} = \frac{0.693}{K} \qquad (5)$$

Subtraction of this slow monoexponential compartment from the curve yields the next compartment. It is immediately evident the, from this process of sequential analysis, that a correct determination of this compartment is wholly dependent upon an accurate estimate of the preceding compartment. For this reason, it is important to have data points at a range of time when the contribution from the fast exchanging compartment is negligible so that the estimation of the slow compartment can be reasonably accurate.

If we assume that the rate of exchange of compartment-1 (fast compartment) is at least three times that of the compartment-2 (slow compartment), which is the normally accepted minimal ratio necessary to kinetically differentiate two compartments (Riggs, 1963), then the following table (Table 3) can be constructed to show the degree of contamination by the fast compartment on the slow compartment at different times after the initiation of uptake (or washout). The computations which yield this table are given in Appendix 1.

Assume $K_1 = 3K_2$ where K_1 and K_2 are, respectively, the time constant of compartment-1 and compartment-2. It is then clear from Table 3 that compartment-2 can be reasonably

Table 3

Contamination of fast compartment by the slow compartment as a function of time

D_1/D_2	$A_1(t)/A_2(t)$ at $t=1 \cdot t_{\frac{1}{2}}$ (Comp - 2)	$A_1(t)/A_2(t)$ at $t=2 \cdot t_{\frac{1}{2}}$ (Comp-2)	$A_1(t)/A_2(t)$ at $t=3 \cdot t_{\frac{1}{2}}$ (Comp-2)
2.0	1.500	0.375	0.094
1.5	1.125	0.281	0.070
1.0	0.750	0.188	0.047
0.5	0.375	0.094	0.023
0.1	0.075	0.019	0.005

D_1 = content of compartment-1

D_2 = content of compartment-2

$A_1(t)$, $A_2(t)$ = amount extracted by (or washed out of) compartment-1 and compartment-2 respectively per sec at time t.

$A_1(t)/A_2(t)$ = contamination of Comp - 2 by Comp - 1 at time t.

$t_{\frac{1}{2}}$ (Comp - 2) = time equal to half time of exchange of compartment-2.

estimated with contamination from compartment-1 ($A_1(t)/A_2(t)$ less than 10%, provided the uptake or washout curves are followed to 3 times the half time of exchange of compartment-2 ($t = 3 \cdot t_{\frac{1}{2}}$ (Comp. 2)). This statement holds when the content of compartment-1 is 1/10 the size of compartment-2 ($D_1/D_2=0.1$) and still holds even when it is twice the size of compartment-2 ($D_1/D_2=2.0$).

In this study the usual, manual graph-peeling technique was supplemented by a computerized technique (Vivian & Bailey, in preparation) which minimized much of the personal bias associated with the former. Only in the cases when computer determined boundaries, as displayed on the oscilloscope, appeared to be less than satisfactory due to scattering of data, were boundaries imposed to yield a better fit of the curve. The fitness of the analysis on original data was determined by the least square method.

The computerized compartmental analysis was done on a PDP 11 (Digital Equipment Corp., Maynard, Mass.) as follows. The least square best fit line for the last four data points from an uptake (or washout) curve was calculated and became a "tentative compartment". The next four of the subsequent data points (P1, P2, P3, P4) which were above the best fit line were then tested. If both the third (P3) and fourth (P4) points deviated from the line by more than one standard deviation, another best fit line was calculated for the four data points. The slope of this line was compared with the slop of the "tentative compartment". If the two

slopes did not differ significantly ($P>0.05$), then P1 was included into the current tentative compartment and the four boundary test points were moved one point to the left. Each subsequent data point was tested in the same way. If on the other hand, the slopes were significantly different ($P<0.05$), then the tentative compartment became permanent, and the four data points became a second "tentative compartment". To evaluate the second "tentative compartment" slope, the data were first reduced by subtracting the now permanent compartment from each of the remaining data points and the new data points were tested as described above. After the analysis was completed, each compartment with its associated best fit line were sequentially displayed on oscilloscope for confirmation of the correctness of boundaries setting. Figure 8 and Figure 9 shows the oscilloscope display of sequential compartmental analysis of respectively a washout and an uptake curve by computer program PEEL 65.

The ability of the program PEEL 65 to resolve a generated bi-exponential decay with given intercepts and rate constants (and hence content, where content is equal to intercept divided by rate constant; $D = A/K$) is shown in Tables 4 & 5. In this exercise, pairs of exponentials with half time of exchange respectively of 20 and 100 sec and contents in each pair ranging from 2 = 1 to 0.1 = 1 (D_1/D_2 = 2.0, 1.5, 1.0, 0.5, 0.1) are added together to produce five bi-exponential functions. For each function three sets of data are generated. All data points are three sec apart.

Figure 8

Oscilloscope display of sequential compartmental analysis of a washout curve by the computer program PEEL 65.

Panel A: The straight line portion of the bi-exponential decay is fitted with a single exponential function by PEEL 65. This represents the slow exchanging compartment. The decision on the setting of the boundaries is by statistical test outlined in the text.

Panel B: The mono-exponential function in Panel A is subtracted from the bi-exponential decay curve yielding points which are again fitted by a single exponential function. This represents the fast exchanging compartment.

(A)

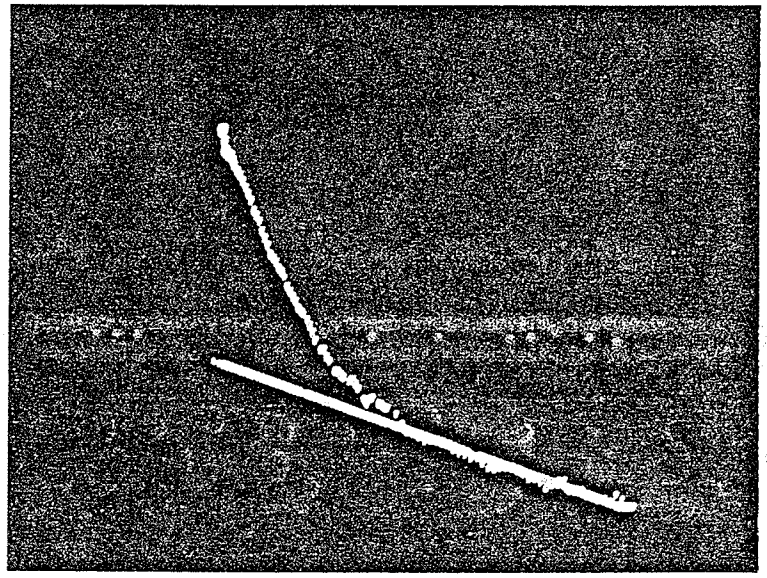

60 sec

(B)

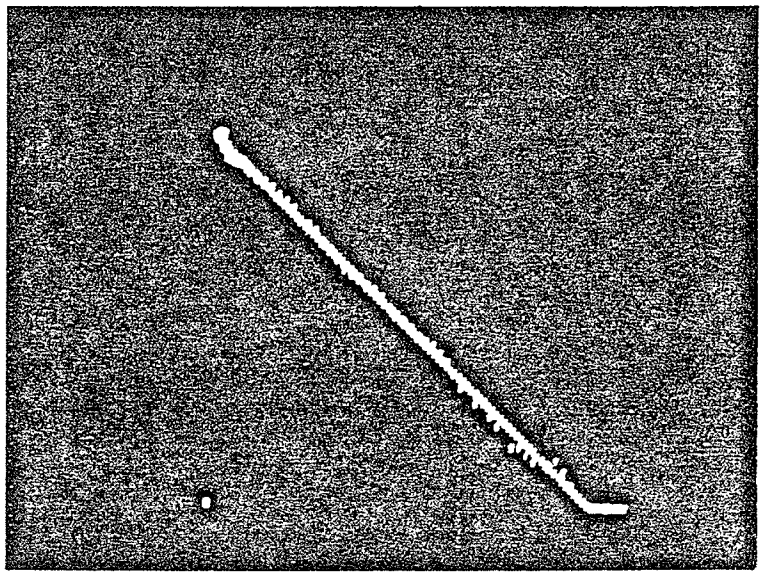

30 sec

Figure 9

Oscilloscope display of sequential compartmental analysis of an uptake curve by the computer program PEEL 65.

Panel A: Resolution of the slow exchanging compartment by PEEL 65. See legend of Figure 8.

Panel B: Resolution of the fast exchanging compartment. See legend of Figure 8.

(A)

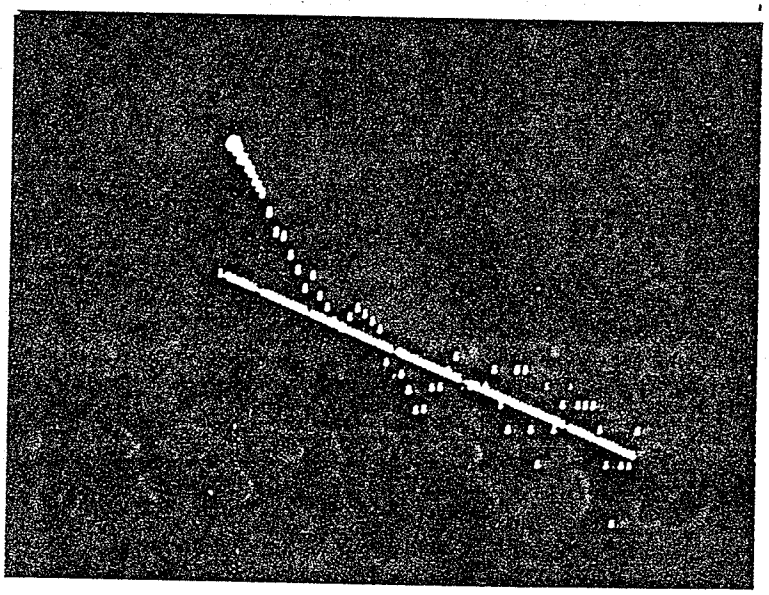

30 sec

(B)

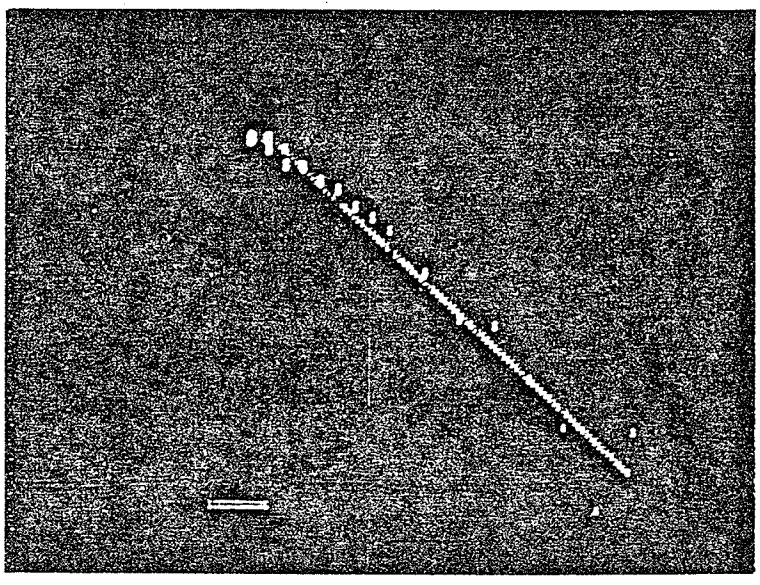

10 sec

The first set of data consists of 33 points (up to 1 x $t_{\frac{1}{2}}$ of compartment-2 or 100 sec). The second set of data consists of 67 points (up to 2 x $t_{\frac{1}{2}}$ of compartment-2 or 200 sec). The third set of data consists of 100 points (up to 3 x $t_{\frac{1}{2}}$ of compartment-2 or 300 sec). Each of these 15 sets of data are analyzed by the computer program PEEL 65. The ratio of the content of each compartment analyzed by PEEL 65 to that originally given is used as an index of the ability of the PEEL 65 program to resolve a generated bi-exponential decay into its two components. A ratio of 1.0 means perfect analysis.

The results in Table 4 & 5 indicate that for two compartments with rate constants differing by five fold, the computer program PEEL 65 is able to analyze quite adequately, provided the sample points are taken to at least two half time (2 x $t_{\frac{1}{2}}$) of compartment-2. This statement holds true over a considerable range of compartment sizes; compartment-1 can be twice that of compartment-2 or one-tenth. Resolution is greatly improved when the sampling points are taken to three half times (3 x $t_{\frac{1}{2}}$) of compartment-2.

(b) Two compartments in series in an open system: theory and graphical analysis

Although the assumption of two compartments in parallel has been accepted for many types of biological study, it lacks factual support and is sometimes inadequate, as is shown by preliminary findings of this investigation, such that a in-series model must be considered.

Table 4

Resolving power of the fast compartment content by computer program PEEL 65

D_1/D_2 (given)	D_1 (analyzed)/D_1 (given) for data points taken to 1 x $t_{1/2}$ (100 sec)	2 x $t_{1/2}$ (200 sec)	3 x $t_{1/2}$ (300 sec)
2.0	0.34	0.89	0.99
1.5	0.37	0.90	0.99
1.0	0.41	0.90	0.99
0.5	0.45	0.90	0.99
0.1	0.48	0.87	0.98

D_1 = content of compartment-1

D_2 = content of compartment-2

$t_{1/2}$ = half time of exchange of compartment-2

Table 5

Resolving power of the slow compartment content by computer program PEEL 65

D_1/D_2 (given)	D_2 (analyzed)/D_2 (given) for data points taken to 1 x $t_{1/2}$ (100 sec)	2 x $t_{1/2}$ (200 sec)	3 x $t_{1/2}$ (300 sec)
2.0	2.07	1.21	1.03
1.5	1.71	1.15	1.02
1.0	1.37	1.09	1.02
0.5	1.10	1.04	1.01
0.1	0.99	1.01	1.00

D_1 = content of compartment-1

D_2 = content of compartment-2

$t_{1/2}$ = half time of exchange of compartment-2

A series exchange model of two compartments may be schemetically depicted in Figure 10. In this model the compartments are described by three variables: D (content in mmole), C (concentration in mmole/l) and V (volume of distribution in l). The exchange kinetics are described by four constants: K_{01}, K_{10}, K_{12}, K_{21} (in 1/sec). In this model an open system is used; this is because in isolated perfused heart the perfusate is continuously renewed. The perfusate is considered to be continuously at 1.8 mM of Ca.

For this model, the following differential equations hold true:

$$\frac{dD_1(t)}{dt} = 1.8\ K_{01} + K_{21}C_2(t) - (K_{10} + K_{12})C_1(t)$$

$$= V_1 \frac{dC_1(t)}{dt} \qquad (6)$$

$$\frac{dD_2(t)}{dt} = K_{12}C_1(t) - K_{21}C_2(t)$$

$$= V_2 \frac{dC_2(t)}{dt} \qquad (7)$$

Under the conditions of this study, the initial content of exchangeable Ca can be assumed to be zero in the uptake process. This is true in the sense that ^{45}Ca is used as the tracer and ^{40}Ca - ^{45}Ca exchange is minimal (due to the prior two min Ca free K-H solution perfusion which removes greater than 90% of the exchangeable Ca). Consequently it may be assumed that

$$C_1(o) = C_2(o) = 0 \ . \qquad (8)$$

Figure 10

Model of series uptake of two compartments in an open system.

D_1, D_2 = compartmental content of Ca (mmole).

C_1, C_2 = compartmental concentration of Ca (mmole/l).

V_1, V_1 = compartmental volume of distribution (l).

K_{01}, K_{10}, K_{12}, K_{21} = exchange constant (1/sec).

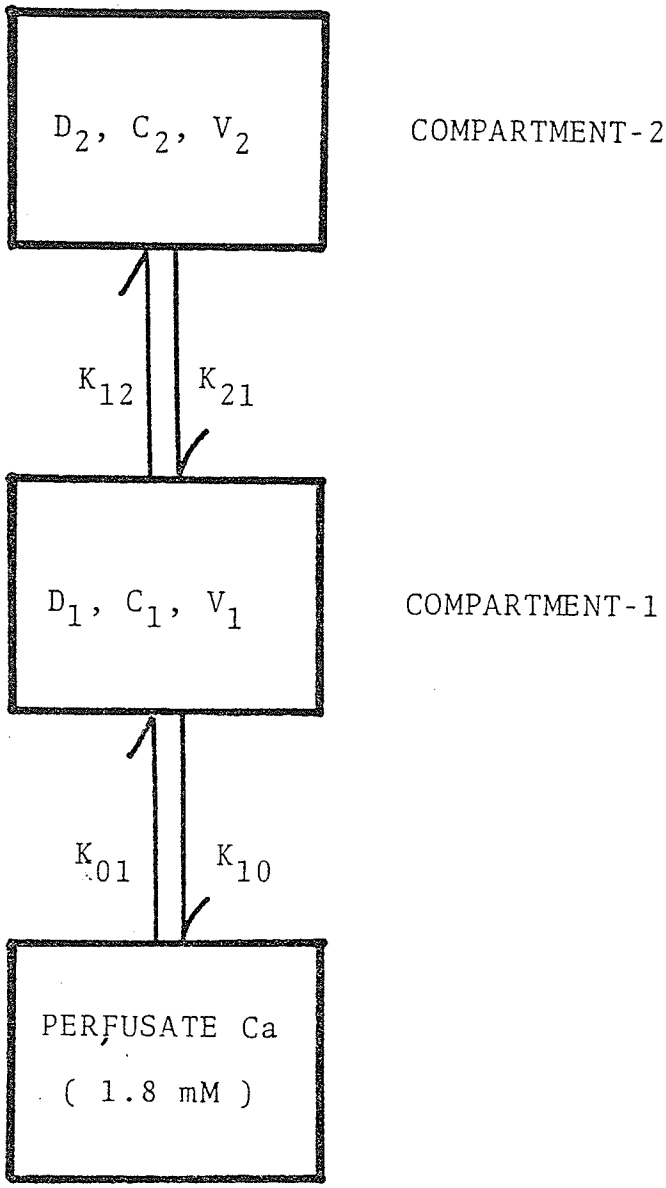
D_2, C_2, V_2
COMPARTMENT-2
K_{12}
K_{21}
D_1, C_1, V_1
COMPARTMENT-1
K_{01}
K_{10}
PERFUSATE Ca
(1.8 mM)

As the uptake process can be graphically resolved into two exponentials each with intercepts A_1 and A_2 (mmole/sec) and rate constants K_1 and K_2 (sec^{-1}), the following equation is valid:

$$\frac{dD_1(t)}{dt} + \frac{dD_2(t)}{dt} = A_1e^{-K_1t} + A_2e^{-K_2t} \qquad (9)$$

which can be integrated to yield

$$D_1(\infty) + D_2(\infty) = A_1/K_1 + A_2/K_2$$

$$= C_1(\infty)\ V_1 + C_2(\infty)\ V_2\ . \qquad (10)$$

At time zero, using equation 6, 7, 8 and 9,

$$A_1 + A_2 = 1.8\ K_{01}\ . \qquad (11)$$

At time equal to infinity, when steady state has been established, the amount of Ca entering and leaving each compartment must be equal, or,

$$1.8\ K_{01} = C_1(\infty)\ K_{10}\ , \qquad (12)$$

and $$C_1(\infty)\ K_{12} = C_2(\infty)\ K_{21}\ . \qquad (13)$$

In addition, by taking the first time derivative of equations 6 and 7 and equating their sum to the first time derivative of equation 9 and setting time to zero then

$$A_1K_1 + A_2K_2 = \frac{1.8\ K_{01}K_{10}}{V_1}\ . \qquad (14)$$

Since $$D_1(\infty) = C_1(\infty)\ V_1\ , \qquad (15)$$

equation 11, 12 and 14 allow us to express $D_1(\infty)$ in terms of

the known constants A_1, A_2, K_1, and K_2 only:

$$D_1(\infty) = \frac{(A_1 + A_2)^2}{A_1K_1 + A_2K_2} \tag{16}$$

The content of compartment-2 can then also be determined:

$$D_2(\infty) = \frac{A_1}{K_1} + \frac{A_2}{K_2} - D_1(\infty) \tag{17}$$

The determination of the contents of compartment-1 and compartment-2 in an in-series model can thus be made in conjunction with the unbiased computer program PEEL 65.

Complete solution for the other variables in the model of Figure 10, however, cannot be obtained numerically, unless we make the assumption

$$K_{12} = K_{21} \ . \tag{18}$$

This is equivalent to assuming that the only driving force for Ca movement between compartment-1 and -2 is the concentration difference between the two. The validity of this assumption could not be tested in this system because compartment-2 was not accessible. However, this assumption permits a qualitative graphical representation of the content changes of each compartment in the in-series model. For purpose of comparison, a synthesized bi-exponential curve representative of the uptake profile of this study is analyzed both in terms of in-parallel model and in-series model in Figure 11 and 12. The approach and computer program for the generation of curve I and II in Figure 12 from those

Figure 11

Ideal compartmental analysis of an uptake curve with an in-parallel model. The solid curve is synthesized by the addition of curve I and II (dotted lines). The half time of exchange of the two compartments are respectively 5.0 and 30.0 sec. Arbitrarily setting the hypothetical heart wt at 0.3 g, the content of the two compartments with this model are respectively:

$$D_1 = 0.12 \text{ mmole/kg},$$

$$D_2 = 1.44 \text{ mmole/kg}.$$

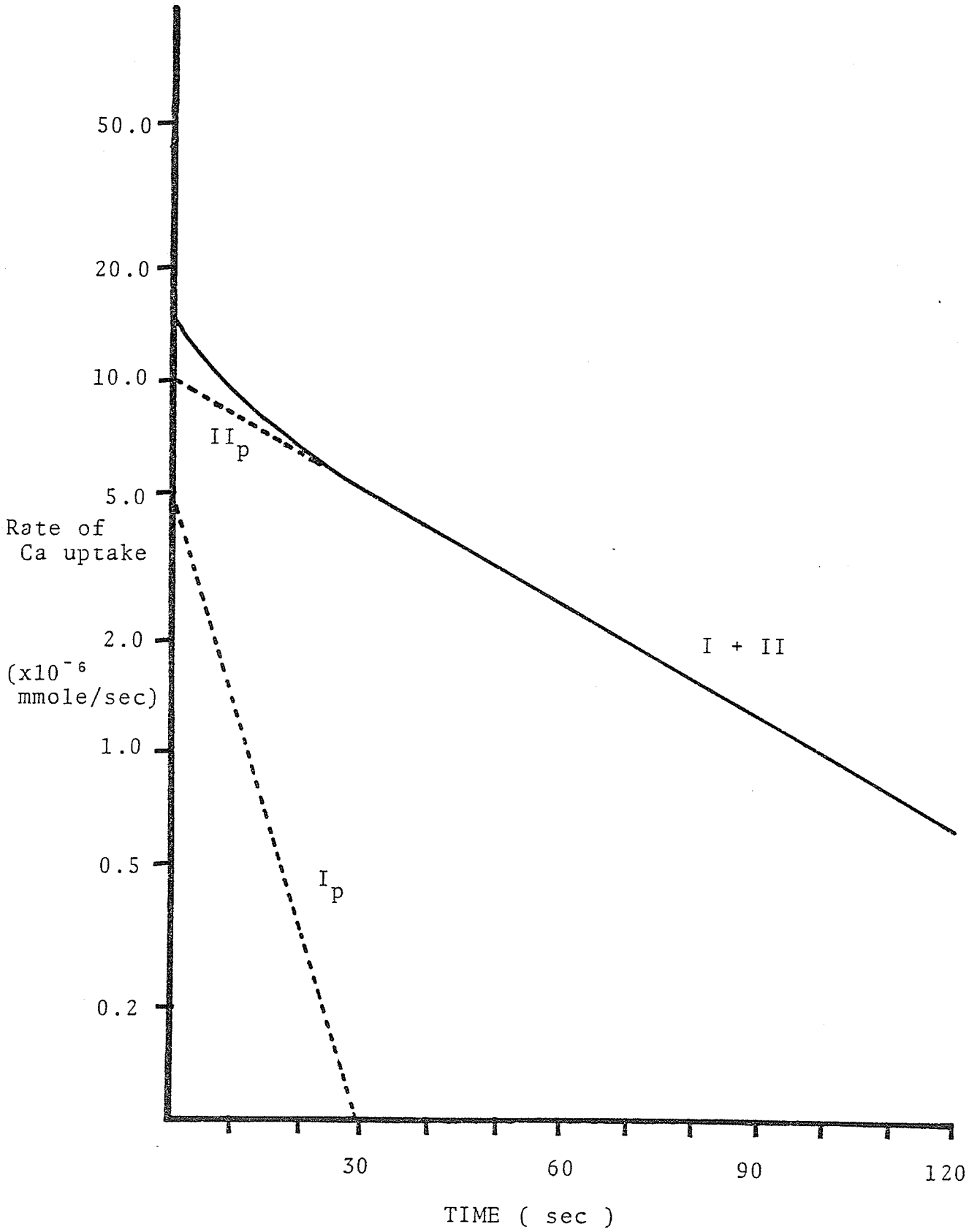
50.0
20.0
10.0
5.0
2.0
1.0
0.5
0.2
Rate of Ca uptake
(x10⁻⁶ mmole/sec)
II_p
I_p
I + II
30
60
90
120
TIME (sec)

Figure 12

Ideal compartmental analysis of an uptake curve with an in-series model. The uptake curve is identical to that in Figure 11. The solid curve is resolved into the two dotted curves I and II using the model in Figure 10 and assuming $K_{12} = K_{21}$ (see text for detail). Arbitrarily setting the hypothetical heart wt at 0.3 g as in Figure 11, the contents of the two compartments with this model are respectively:

$$D_1 = 0.81 \text{ mmole/kg},$$

$$D_2 = 0.75 \text{ mmole/kg}.$$

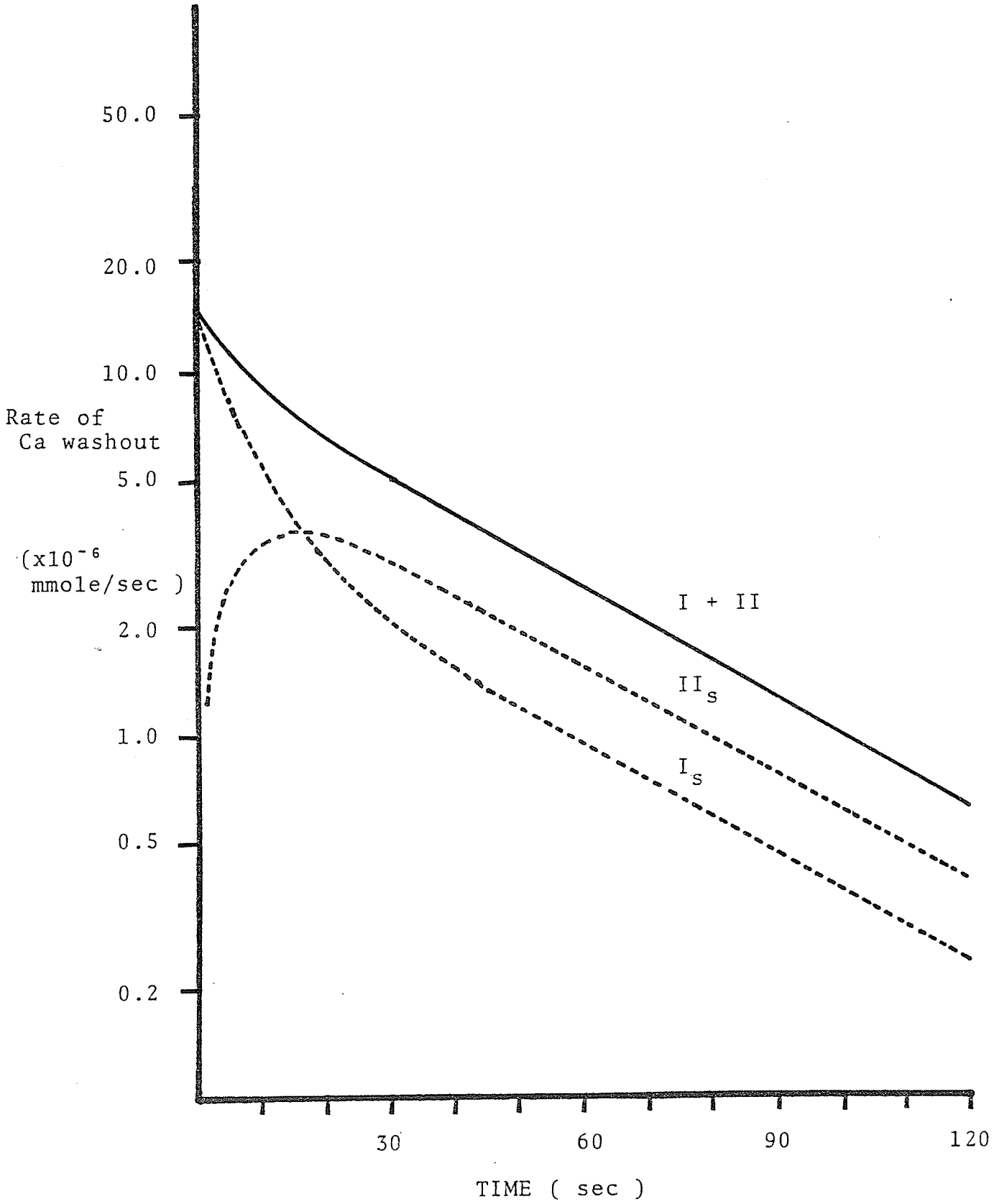
50.0
20.0
10.0
Rate of
Ca washout
5.0
(x10⁻⁶
mmole/sec)
2.0
1.0
0.5
0.2
I + II
II s
I s
30
60
90
120
TIME (sec)

in Figure 11 are detailed in Appendix 2A and 2B.

The washout of a tracer from a two compartment system in an in-series model is given by Figure 13. A further assumption of zero backflux from the perfusate to the heart is made on the basis that the perfusate is continuously renewed in the isolated heart system studied (i.e. $K_{01} = 0$).

A slightly different terminology is used. The content of compartment-1 and compartment-2 are respectively the content at zero time (rather than at infinite time as in the uptake studies), or $D_1(o)$ and $D_2(o)$. With similar reasoning (Appendix 3A), the contents of each compartment can be expressed in terms of the known intercepts A_1, A_2 and rate constants K_1 and K_2; namely,

$$D_1(o) = \frac{(A_1 + A_2)^2}{A_1K_1 + A_2K_2} \tag{19}$$

and

$$D_2(o) = \frac{A_1}{K_1} + \frac{A_2}{K_2} - D_1(o) \ . \tag{20}$$

Again, with the assumption that $K_{12} = K_{21}$ (and setting $V_1 + V_2 = 0.8 \cdot$(wet heart wt), which simplifies calculation for generation of the dD(t)/dt curve, although this is not necessary as the term cancels), the washout profile from each compartment, in this case from a representative experiment, can be shown as in Figure 14. The detailed reasoning, derivation and computer program for the generation of this curve are included in Appendix 3A and 3B.

Figure 13

Model of series washout of two compartments in an open system.

D_1, D_2 = compartmental content of Ca (mmole).

C_1, C_2 = compartmental concentration of Ca (mmole/l).

V_1, V_2 = compartmental volume of distribution (l).

K_{12}, K_{21}, K_{10} = exchange constant (1/sec).

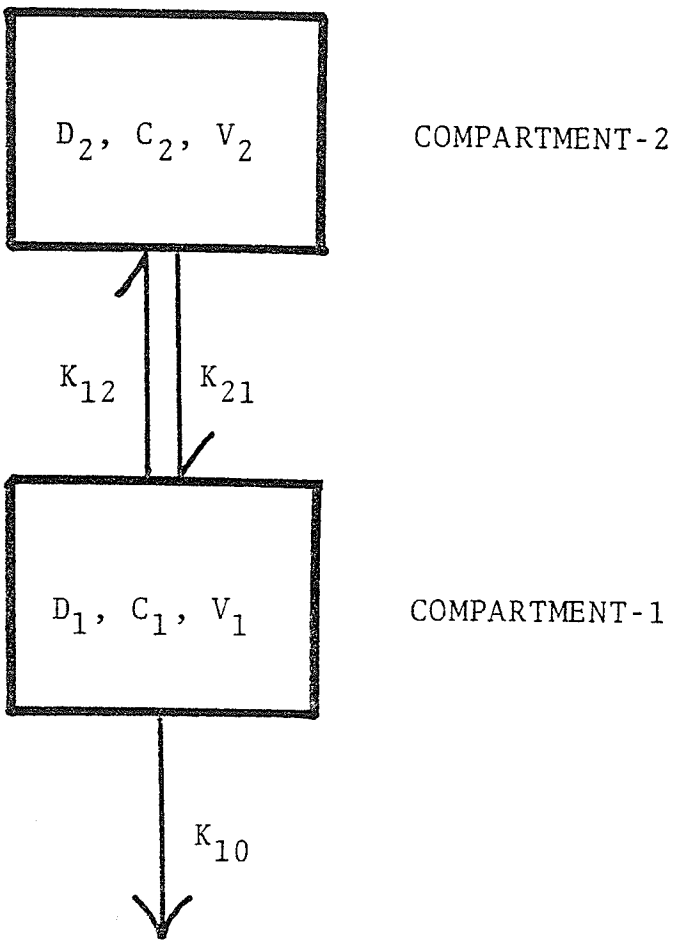
D_2, C_2, V_2
COMPARTMENT-2
K_{12}
K_{21}
D_1, C_1, V_1
COMPARTMENT-1
K_{10}
EFFLUENT

Figure 14

Compartmental analysis of a washout curve with both in-parallel and in-series model. The solid curve is a representative washout curve from Oct. 25/75, Exp. 2 (Myopathic Hamster, 220 d). The two straight line components Ip and IIp are the result of compartmental analysis with PEEL 65 using in-parallel model. The two dotted line components Is and IIs are the result of compartmental analysis with in-series model.

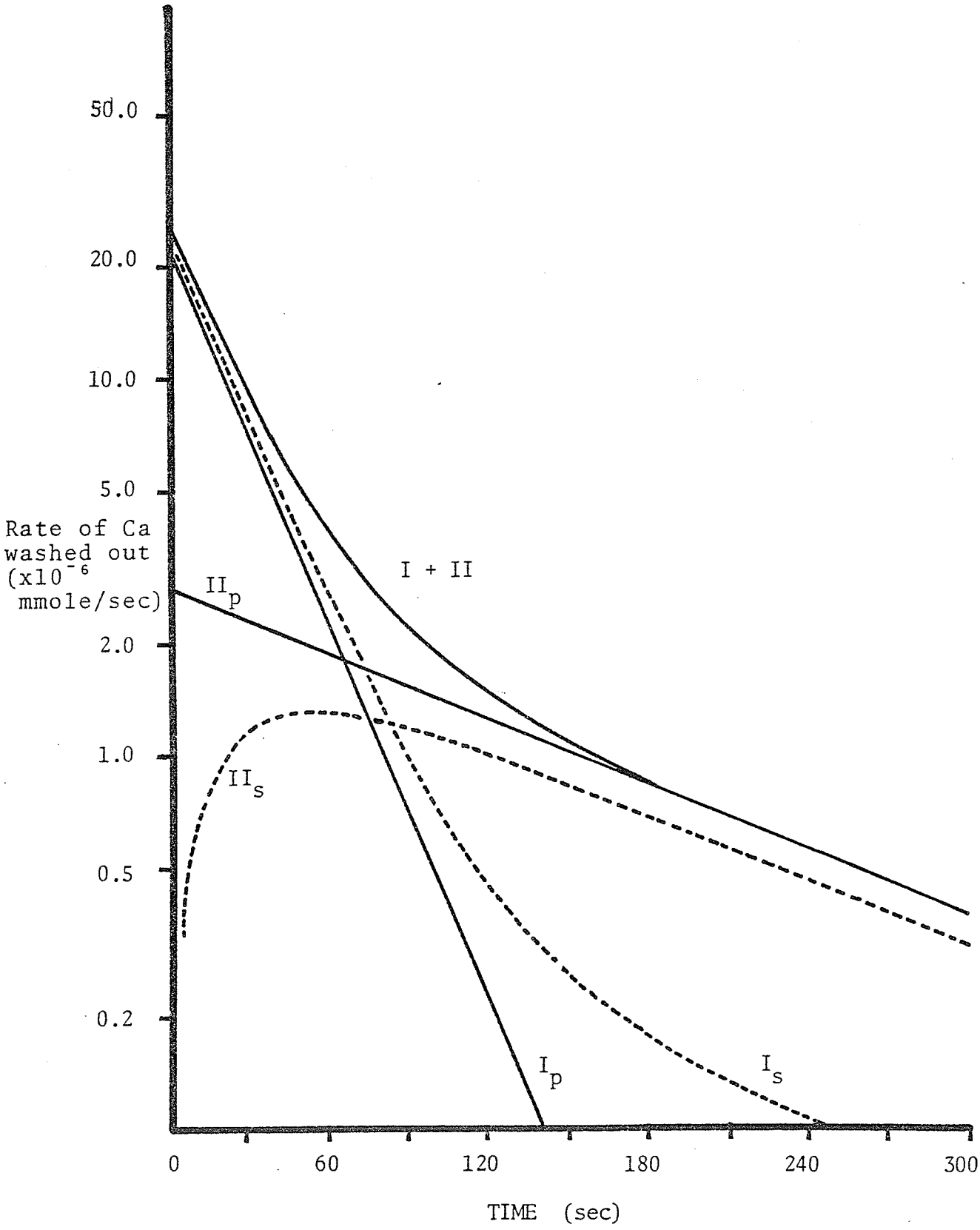
50.0
20.0
10.0
5.0
Rate of Ca washed out (x10⁻⁶ mmole/sec)
2.0
1.0
0.5
0.2
I + II
II_p
II_s
I_p
I_s
0
60
120
180
240
300
TIME (sec)

The concept of half time of exchange, utilized in an in-parallel model, is not meaningful in the in-series model, because the kinetics of exchange are no longer monoexponential. However, an estimate of the half time of exchange of compartment-1 can be obtained when compartment-2 is considered to be absent:

$$t_{\frac{1}{2}} = \frac{0.693}{(A_1+A_2)/D_1} \quad \text{(in-series)}$$

The half time of exchange of compartment-2 in the absence of compartment-1 is the same in the series model as in the parallel model (see Figure 12 and 14).

In all subsequent description of compartmental contents, (s) and (p) will be used to denote series and parallel model respectively; Roman and Arabic numerals will be used to denote washout and uptake respectively; eg, $Ca_I(p)$ indicates compartment-1 of washout Ca in parallel model.

4. Experimental design

Bajusz (1969) classified the hamster cardiomyopathy into four distinct stages based on the gross and histopathological observation on the evolution of the chronic cardiac conditions which might be appropriately named as: preclinic (<30 days of age (d)), myolytic (25-45 d), necrotic and hypertrophic (35-50 d), and compensating on failing (>80 d) stages (see Introduction). Accordingly, four age groups of hamsters from each of the normal and myopathic strain which roughly corresponded to the above classification were studied in this investigation. These are summarized in Table 6.

Table 6

Age groups of the hamster studied

Age	
Normal Hamster	Cardiomyopathic Hamster
26 (3)[a]	30 (5; pre-clinic)
44 (4)	36 (4; myolytic)
60 (4)	53 (4; necrotic & hypertrophic)
220 (5)	220 (8; compensating or failing)

[a]Number inside bracket indicates number of experiments.

B. ISOLATED SARCOLEMMAL FRACTION

1. Experimental design

The flow diagram of the experimental design is shown in Figure 15. Briefly, the ventricular muscle of the hamster heart is homogenized by Virtis Omnimixer (Sorvall) to produce cell fragments about 5 cells in size. This homogenate is subjected to osmotic shock which makes it leaky and facilitates the subsequent salt extraction of the contractile protein. The resultant enriched sarcolemma fraction is assayed for Na-K ATPase, sialyltransferase activity as well as the total and neuraminidase releasable sialic acid. Ca binding characteristics of the sarcolemma was studied before and after neuraminidase treatment.

2. Sarcolemma isolation procedures

Syrian hamsters (B10.RB and B10 14.6) were sacrificed by guillotine and the hearts quickly dissected. The blood within the ventricles and coronary vasculature was flushed through the aorta with ice cold 2.5 mM imidazole (pH 7.4) 0.1 mM - EDTA buffer (I-ED buffer). All the subsequent preparative procedures were done at 4°C.

The atria were removed and the ventricles opened and blotted dry. The tissue was then put in a pre-weighed petri dish containing 10 ml I-ED buffer. For one experiment about 2 gm of heart (5-10 hearts, depending on heart size) was needed.

The tissue was chopped into fine pieces with curved

Figure 15

Flow diagram of the experimental design (see text for detail).

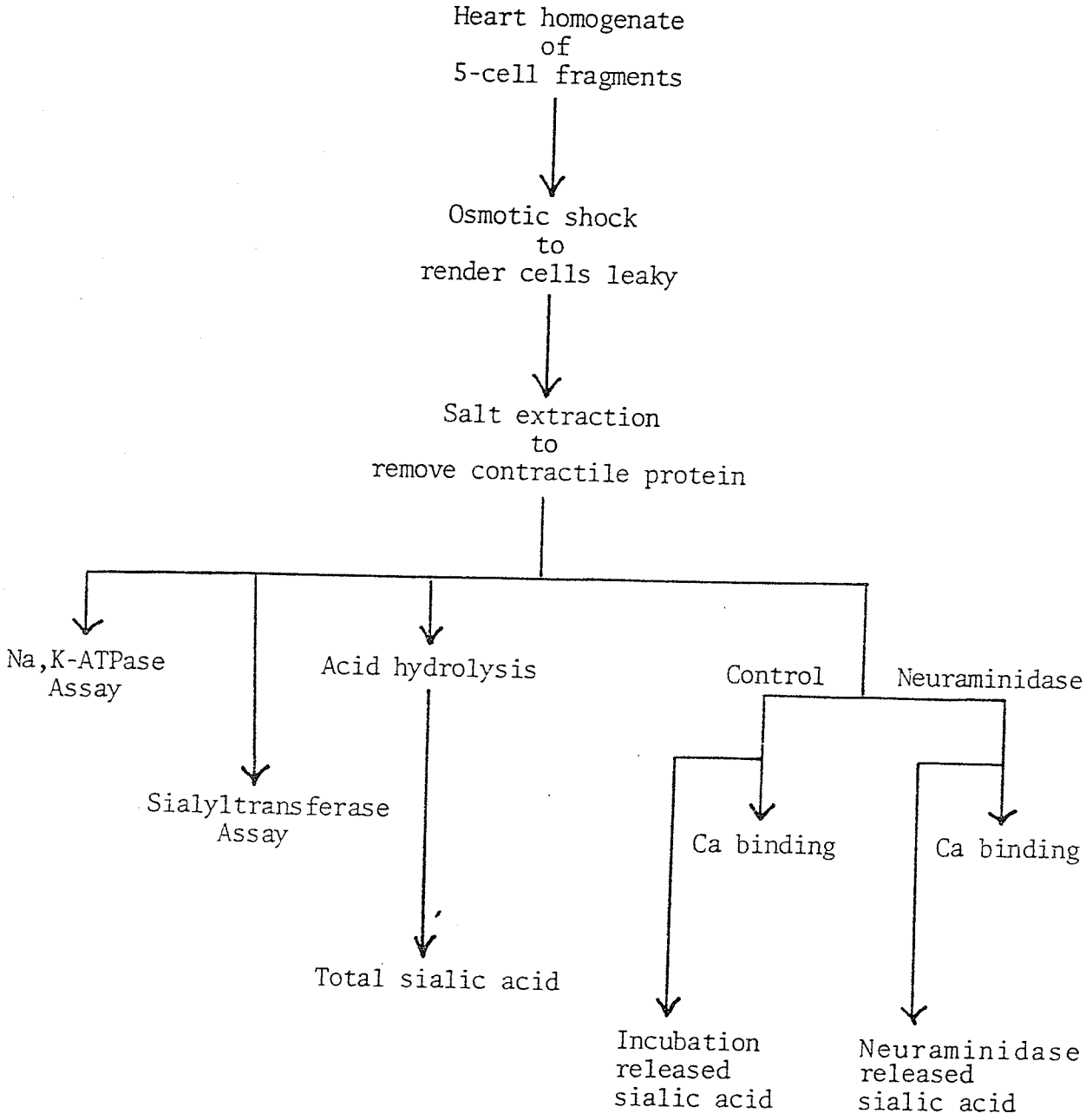
Heart homogenate
of
5-cell fragments
Osmotic shock
to
render cells leaky
Salt extraction
to
remove contractile protein
Na,K-ATPase
Assay
Sialyltransferase
Assay
Acid hydrolysis
Total sialic acid
Control
Neuraminidase
Ca binding
Ca binding
Incubation
released
sialic acid
Neuraminidase
released
sialic acid

scissors and suspended in I-ED buffer (1:10 w/v). The suspension was homogenized with Omin-mixer model 115 (Sorvall) at speed 8 for 2 sec. The homogenate was centrifuged on a bench top centrifuge at speed 5 for 15 sec and speed 4 for another 30 sec (this roughly corresponded to 20 g-min). The supernatant contained only 5 or less cell-segments and was aspirated and saved. The pellet was resuspended in the same volume of I-ED buffer, again homogenized and centrifuged. The homogenization and centrifugation was repeated as necessary to obtain 5 cell-segments of myocardium. Usually, 15-20 repetitions were necessary to homogenize all of the tissue.

After filtration through three layers of gauze to remove large pieces of connective tissue and large cell fragments, the total pooled supernatant was centrifuged at 5000 g for 10 min with a Sorvall preparative centrifuge (Model RC-2, rotor SS-34, 6500 rpm). The pellet was suspended in 20 ml of 10 mM Tris buffer pH 7.4 (1:10 w/v of initial wet wt) by vortexing. This constituted the initial homogenate. The protein concentration at this stage was around 6 mg/ml. Aliquots were taken for enzyme assays and sialic acid determination.

The initial homogenate suspension was centrifuged at 5000 g for 10 min, and the pellet was suspended in 20 ml of 40% sucrose, 0.2 mM EGTA, 10 mM Tris buffer pH 7.4 (or 1:10 w/v of initial wet wt). The hypertonic suspension was osmotic-shocked through 23 gauge needle into 500 ml of 0.25 mM EDTA, 5 mM Tris buffer pH 7.0 (or 1:25 v/v) with

continuous stirring. The preparation was then centrifuged at 5000 g for 10 min. The pellet was washed once with 40 ml of 10 mM Tris buffer pH 7.4 (or 1:20 w/v of initial wet wt) and resuspended in 16 ml of 10 mM Tris buffer pH 7.4 (or 1:8 w/v). This constituted the after shock preparation. The protein concentration, at this dilution, was again 6 mg/ml. Aliquots were taken for enzyme assays and sialic acid determination.

The remaining after shock preparation was mixed 1:3 w/v with 1.3 M KCl, 2.6 mM EGTA, 40% sucrose and 10 mM Tris buffer pH 7.0 to give a final concentration of 1.0 M KCl, 2mM EGTA and 10 mM Tris. This step was the salt extraction step for removing the contractile proteins.

Salt extraction was continued for two hr with stirring. Prolonged extraction (16 hr) of the original preparation (Tada et al., 1972) did not further extract the contractile protein as indicated by a constant yield after two hr extraction . The suspension was filtered through gauze and washed 3 times with 10 mM Tris buffer pH 7.4 (1:20 w/v; 5000 g, 10 min). The pellet after the final centrifugation was suspended in 10 mM Tris buffer pH 7.4 (1:1 w/v of initial wet wt). This constituted the after extraction preparation. The protein concentration at this stage was around 6-8 mg/ml. Aliquots were taken for enzyme assays and sialic acid determination.

3. Assays

(a) Protein determination (Lowry as modified by Hartree)

The protein concentration was determined by the method

of Hartree (1972), modified by a solubilization step with 1 N NaOH for 30 min at room temperature. Bovine serum albmin (1 mg/ml) containing Na-azide (1 mg/ml) to prevent bacteria growth was used as the standard. The photometric assay at 650 nm was linear between 20 to 120 µg of solubilized protein.

(b) ATPase assay

The Na-K ATPase activity was determined by the method of Schwartz et al. (1971). The assay were done in triplicates and the mean taken for comparison.

Basal (Mg) ATPase activity is defined as µmole of inorganic phosphate (P_i) release at 37°C per mg protein per hr in basal buffer (50 mM Tris pH 7.4, 120 mM Na, 2% alcohol and 4 mM MgATP). MgATP (stock 16 mM) was titrated to pH 7.4 with Tris base. The Na-K ATPase activity was expressed in two ways: Na-K activated and ouabain sensitive. The Na-K activated ATPase activity is defined as the increased rate (comparing to basal ATPase activity) of P_i release (µmole/mg/hr) in basal buffer with the modified mono-cation concentration of 100 mM Na and 20 mM K. The ouabain sensitive ATPase activity is defined as the reduced rate (comparing to ATPase activity in the presence of 100 mM Na and 20 mM K) of P_i release in the presence of 1 mM ouabain.

The P_i released was determined by the method of Taussky & Shoir (1953). Potassium phosphate monobasic (KH_2PO_4, 1 mM) was used as the standard. The photometric assay at 690 nm was linear between 0.05 to 0.40 µmoles of P_i.

In a few experiments (see Results), Na-K activated and ouabain sensitive ATPase activity was determined under various conditions: prolonged cold incubation (4°C, 4 hr), veratidine 0.1 mM, Tetrodotoxin 1 μM, Na-azide 5 mM, and a combination of the above.

(c) Sialyltransferase assay

The sialyltransferase activity of the samples was determined by the method of Bernacki (1975). The reaction medium of total volume 200 μl contained: 50 μl of tissue (0.1-0.3 mg), 50 μl of 40 mM $MnCl_2$, 25 μl of 80 mM $MgCl_2$ & 40 mM Tris, 50 μl of asialated feutin (pH 7.4, 0.3 mg) and 25 μl of C^{14}-CMP-sialic acid (159.2 mCi/mmole, 1.8×10^{-5} M, New England Nuclear). Assays were incubated for 30 min to 2 hr at 37°C. The reaction was terminated by adding 2 ml of 1% phosphotungstic acid in 0.5 N HCl. The precipitate was washed twice with 2 ml 10% TCA and once with 2 ml ethanol-ether (2:1 v/v to washout the acid). The resultant precipitate was dissolved in 0.2 ml 1 N NaOH for 30 minutes and neutralized with 0.2 ml 1 N CH_3COOH. A 50 μl aliquot was taken for scintillation counting. The enzyme activity was expressed as pmoles of C^{14}-sialic acid incorporated per mg protein per hour.

Asialofeutin was prepared by mild acid hydrolysis (0.1 N H_2SO_4, 80°C, 1 hr). The hydrosylate was dialyzed overnight against distilled water and neutralized with Tris-base.

The influence of 1 mM UDP, 1 mM Na-oratate and various cation concentration were examined in three experiments.

(d) Ca binding

Ca binding studies were done both on sialic acid rich glycoproteins (mucin & fetuin) and on enriched sarcolemma fractions (sfter extraction preparation). The equilibrium dialysis method was used in the case of soluble glycoproteins whereas the equilibrium centrifugation method was used in the case of the particulate sarcolemmal fraction.

(i) Equilibrium dialysis - Ca binding to mucin and fetuin

To eliminate non-specific binding to the dialysis bag, 8/33 inch (diameter) dialysis tubing was first boiled for 30 min in 3% $NaHCO_3$ solution (Gambhir and McMenamy, 1973) and then thoroughly rinsed, first with boiling water then with distilled water.

The protein (mucin, 0.65 mg; fetuin, 1 mg; asialogetuin, 1 mg) in 1 ml of 50 mM Tris buffer pH 7.4 and 100 mM NaCl was put into the dialysis bag. The external medium (9 ml) of the same composition (minus protein) plus different concentration of Ca (given final concentration of 0.02, 0.05, 0.1, 0.2, 0.5, 1, 2, 3, 5, 10 mM Ca) and 2.5 µCi ^{45}Ca was allowed to equilibrate with the protein at 4°C. After 48 hr equilibrium was established across the semipermeable membrane as was determined by measurement of bags containing no protein.

A 100 µl aliquot of the protein (or equilibrium medium) were mixed with 10 ml of ACS (Amersham/Searle). To circumvent the different quenching effect of the two solutions, 100 µl of an equivalent amount of BSA was added to the medium sample and 100 µl of an equivalent amount of BSA was added to the medium sample and 100 µl of non-radioactive medium was added to the protein sample. The mixture was allowed to stand in the dark for 24 hr and counted by liquid scintillation (Isocap/300, Nuclear Chicago).

Ca binding to the glycoproteins was determined by the ^{45}Ca activity of the protein sample minus the final activity of the equivalent volume of its incubation medium. The results were analyzed as described by Scatchard (see below).

The asialofetuin was made as before but dialyzed against 50 mM Tris buffer pH 7.4 containing 100 mM NaCl.

(ii) Equilibrium centrifugation - Ca binding to sarcolemma

The sarcolemma fraction (in 10 mM Tris buffer pH 7.4) was divided into two portions as shown in the flow diagram of Figure 15. One portion was kept at 4°C and served as the control sample. The second portion was incubated at 37°C for 2 hr in the presence of 0.5 units of neuraminidase per mg of sarcolemmal protein (assuming the enzyme activity at pH 7.4 is only 1/50 of its optimal activity, this amount of enzyme is able to hydrolyze 300 nmoles of sialic acid from 1 mg of sarcolemmal protein in 30 minutes).

After appropriate incubation, aliquots of 100 µl were taken from each of the two portions and assayed for released

sialic acids. Calcium binding studies were done on the remaining portions.

For calcium binding, approximately 0.5 mg of protein was incubated at $4^{o}C$ in a total volume of 5 ml medium which contained: 50 mM Tris buffer pH 7.4, 100 mM Na, 2.5 μCi ^{45}Ca, 2.5 μCi H-inulin and ^{40}Ca (0.02 to 5 mM) for 1 hour in ultracentrifuge tubes presoaked sequentially with 1 N NaOH (overnight), and 8 N Formic acid (2 hr). Calcium binding to the surface of the tubes was assessed by counting a set of tubes at various ^{40}Ca concentration without protein.

At the end of 1 hour incubation, the tubes were centrifuged at 50,000 g for 1 hour in an International preparative ultracentrifuge (Model B-60, rotor A-321, 24,000 rpm). The supernatant was carefully pipetted and a 50 μl aliquot taken for scintillation counting (adding 50 μl H_2O per vial). The pellets were dissolved with 150 μl of 1 N NaOH and a 50 μl aliquot taken for scintillation counting (added 50 μl 1N CH_3COOH per vial). Calcium binding to the membranes was calculated from the specific activity of the added ^{45}Ca and the activity retained by the membrane. The results were analyzed by Scatchard plot (see below).

In two experiments, the influence of different monovalent cations were examined. The original incubation medium of 100 mM NaCl was changed to 100 mM LiCl and to 100 mM KCl.

(e) Sialic acid assay

The sialic acid content of the sample was determined

by the method of Hammond & Papermaster (1976). The sensitivity of the assay was 1/4 that reported because a micro cell was not used, but it was adequate for the purpose of the present study. The fluorometric assay (Aminco-Bowman spectrophotofluorometer, Americal Instrument Co.; excitation: 550 nm; emission: 570 nm) of sialic acid standard (10 μM) was linear in the range from 1 to 4 nmoles. The total sialic acid content was determined after acid hydrolysis as stated before (0.1 N H_2SO_4, 1 hr, 80°C).

In the cases where protein was present in the samples (eg. plasma and membrane suspension), it was removed by precipitation with equal volume of 10% TCA. The possibility of interference from TCA and sucrose (used in the isolation medium) in the fluorometric assay of sialic acid was examined.

4. Scatchard plot of Ca binding

Scatchard (1949) derived a method for plotting data for the binding of small molecules to macromolecules from which the relative affinities and number of binding sites can be extrapolated.

Briefly, if the system contains only one type of ligand and one kind of macromolecular binding site, then the ratio of bound ligand to free ligand is a linear function of the bound ligand. Mathematically (see Appendix 5), this is expressed as follows:

$$\frac{[Ca - Q]}{[Ca]} = K_{eq} [Q_{tot}] - K_{eq} [Ca-Q] \qquad (22)$$

where for this study Ca ion is designated as the ligand, the macromolecular binding sites as some substance Q, the free calcium as Ca, the bound calcium as Ca-Q complex, and the total available binding sites as Q_{tot}. The equilibrium constant is designated as K_{eq}. It is clear that a plot of [Ca-Q]/[Ca] vs [Ca-Q], yields a straight line with a slope of $-K_{eq}$ and an intercept on the abscissa of Q_{tot}. This has been termed the Scatchard plot.

In the case of two binding sites in equilibrium with one ligand, the system can be described by (see Appendix 5):

$$\frac{[Ca\text{-}Q]}{[Ca]} = \frac{K_1[Q_{1\text{-}tot}]}{K_1[Ca]+1} + \frac{K_2[Q_{2\text{-}tot}]}{K_2[Ca]+1} \qquad (23)$$

where K_1,K_2, $Q_{1\text{-}tot}$, and $Q_{2\text{-}tot}$ are respectively the equilibrium constants of component 1 and 2 and the binding capacity of component 1 and 2. A Scatchard plot of this system is given in Figure 16. Berson and Yalow (1959) and Feldman (1972) using different approaches, arrived at the same conclusion (Appendix 5):

$$\text{X-intercept} = Q_{1\text{-}tot} + Q_{2\text{-}tot} \qquad (24)$$

$$\text{Y-intercept} = K_1Q_{1\text{-}tot} + K_2Q_{2\text{-}tot} \qquad (25)$$

Feldman (1972) showed that the hyperbola can be mathematically described by a quadratic equation (Appendix 5). Using this quadratic equation it is possible to resolve the Scatchard plot into its two components using the method of successive approximation (Appendices 6 and 7B). Figure 16 shows that the computer program SKATCH.BA precisely analyzed the curve into its two

Figure 16

Scatchard plot of a system containing two binding sites and one ligand. The solid curve is generated by computer program SCATGN.BA (Appendix 7A) according to the formulation given in Appendix 5. Compartmental analysis by computer program SKATCH.BA (Appendix 7B) resolves the curve into two straight line components, Line-1 and Line-2 whose composite sum is shown by the open circles. The insert shows the given values used to generate the curve and the analyzed corresponding values. The ordinade B/F (Bound/Free or [Ca-Q] / [Ca]) and the abscissa B (Bound or [Ca-Q]) are of arbitrary units.

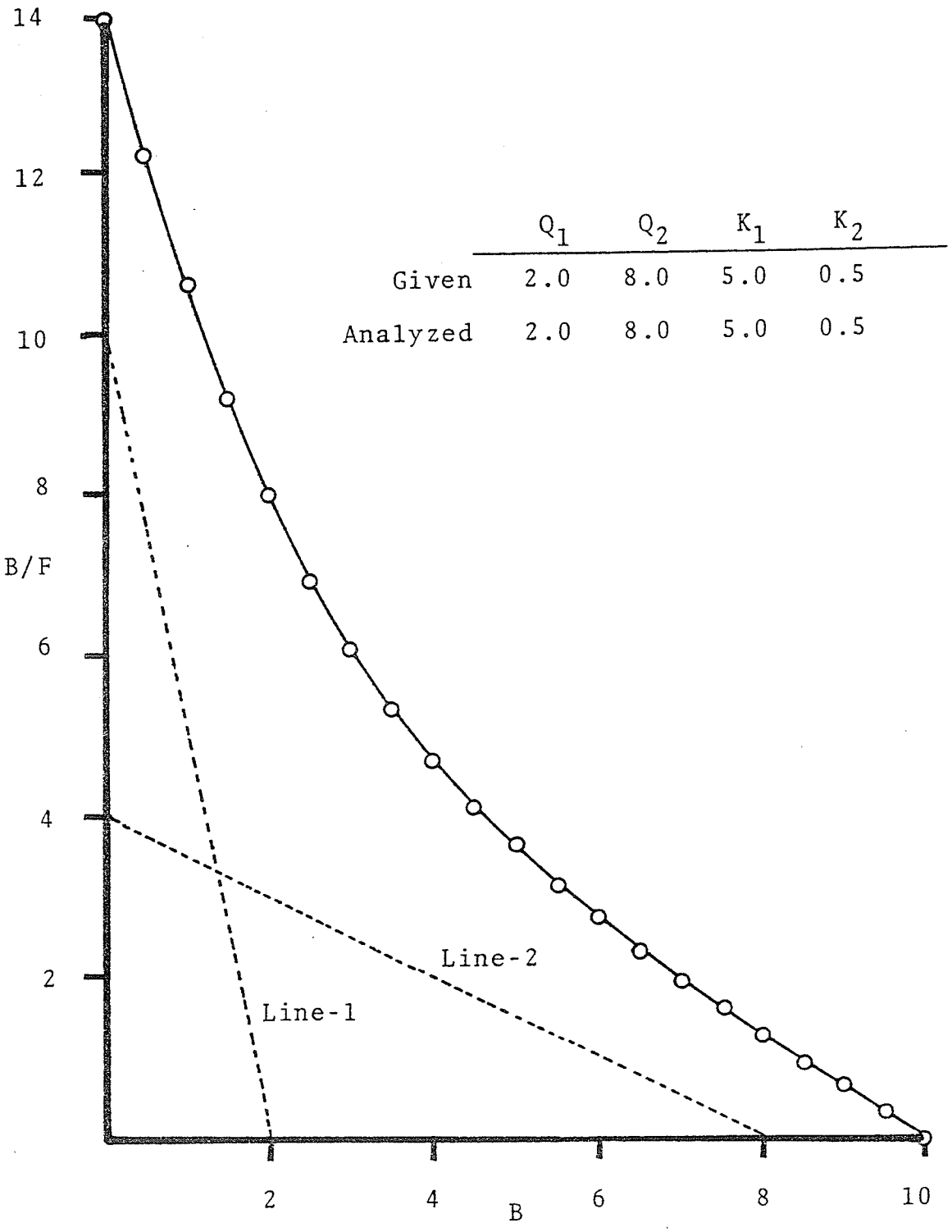

	Q_1	Q_2	K_1	K_2
Given	2.0	8.0	5.0	0.5
Analyzed	2.0	8.0	5.0	0.5

components.

The computer program SKATCH.BA needs two initial estimates of the X-and Y-intercepts which are often difficult to make. To circumvent this and to eliminate personal bias, a modified version of this program (SKATCH.MB; Appendix 8B) has been written. This program uses the data summarized by computer program MAT1.BA (Appendix 8A) and analyzed the data exactly as the program SKATCH.BA. However, only the final analysis is printed out and the program re-enters at the beginning for new estimates of the X- and Y-intercepts. The two intercepts can thus be adjusted to produce a better fit of the curve as judged by the sum of squares of the deviation. The loop is continued until one is satisfied that further adjustments leads to negligible deviation.

SECTION III

RESULTS

A. Evaluation of the method - isolated perfused heart

1. Extracellular exchange kinetics

(a) ^{131}I-BSA exchange

Three experiments were attempted using ^{131}I-labelled BSA as a marker of the vascular space. Of these, two failed as the hearts were in contracture as a result of metal poisoning from a corroded metal valve. The metal poisoning was responsible for a subsequent fifteen to twenty experimental failures until the causative factor was isolated and corrected.

In the successful experiment, ^{131}I-BSA was introduced in two ways, in normal K-H solution (isotope recovered in Ca washout process after brief gas separation) and in Ca-free K-H solution (isotope recovered during Ca uptake process after brief gas separation).

Graphical analysis of the data using the in-parallel model and PEEL65 computer program yielded two compartments. In the ^{131}I-BSA washout experiment, the half times of exchange ($t_{\frac{1}{2}}$) for each compartment were 8.5 and 28 sec. In the ^{131}I-BSA uptake experiment, they were 5.5 and 32 sec. The appearance of two kinetically defined compartments of ^{131}I-BSA was unexpected. Bovine serum albumin is known to adhere to glass and plastic surfaces and this might have been the underlying reason for the emergence of a slowly exchanging compartment. If such was the case, the vascular exchange would have a $t_{\frac{1}{2}}$ of about 7 sec. The alternate explanation, i.e., the slower exchange represented free ^{131}I contamination, was unlikely as

the isotope used contained little or no free ^{131}I (Fig. 6).

Subsequent experiments designed to reduce this adsorption by pre-coating the apparatus with cold BSA were unfortunately not successful because of having metal poisoning.

(b) ^{14}C-mannitol exchange

^{14}C-mannitol was used in a series of five experiments using 200 d normal hamsters both as an extracellular (vascular plus interstitial) marker and as an indicator of capillary and cell membrane permeability changes. The steady state ^{14}C-mannitol exchange followed a bi-exponential pattern in both uptake and washout process. The two compartments analyzed according to the in-parallel model had a $t_{\frac{1}{2}}$ of, respectively, 2.4 ± 0.3 and 16.1 ± 1.5 sec during the uptake and 2.4 ± 0.1 and 15.2 ± 0.4 sec during the washout. The fast compartment appeared to be fluid which had adhered to the perfusion apparatus. As such it had a volume of distribution ranging from 20 to 120 µl which was not correlated with the heart size. This rapidly exchanging compartment was also present in all ^{45}Ca exchange and will only be mentioned in this context. Note that this compartment was absent in the ^{131}I-BSA exchange, possibly because of the fact that the fast compartment in ^{131}I-BSA exchange may have encompassed this compartment as a result of the limited resolving power of this technique.

The ^{14}C-mannitol uptake after two min of Ca-free K-H solution perfusion again followed a bi-exponential pattern

with the slower compartment $t_{\frac{1}{2}}$ of 16.7 ± 1.5 sec. This $t_{\frac{1}{2}}$ was not different statistically from that measured without prior Ca-free washout. The results suggest that Ca-free perfusion of two min or less in duration do not grossly affect capillary and cell membrane permeability.

The mannitol space measured after five min of ^{14}C-mannitol perfusion was 16.9 ± 0.7% of the wet ventricular weight of the heart tissue. This represented the extracellular space minus the vascular space as the vascular space was cleared by the brief gas perfusion.

(c) ^{45}Ca exchange of the perfusion apparatus

^{45}Ca exchange of the perfusion apparatus alone, in the absence of the isolated heart, showed a mono-exponential profile. The $t_{\frac{1}{2}}$ was 9.6 ± 1.0 sec in the uptake as compared to 19.7 ± 1.8 sec in the washout. The two $t_{\frac{1}{2}}$'s were statistically different ($P<0.05$) which suggests that the association of Ca ion is faster than its dissociation from the perfusion apparatus (tubing and glassware). The content of this compartment, using 1.8 mM Ca as the perfusion solution [Ca], was 93.7 ± 4.7 nmole in the uptake and 164.9 ± 4.4 nmole in the washout. The results of the preliminary studies are summarized in Table 7.

2. Comparison of steady state and non-steady state Ca exchange

Steady state Ca exchange is defined as the exchange of tracer ^{45}Ca without modifying the perfusion solution [Ca].

Non-steady state of Ca exchange, on the other hand, describes the uptake or removal of ^{45}Ca, when the perfusion solution [Ca] is altered. Only the latter process is associated with simultaneous changes of cardiac contractility.

The Ca flux data were first corrected for the Ca exchange associated exclusively with the apparatus alone (uptake: 94 nmole, $t_{1/2}$=10 sec; washout: 165 nmole, $t_{1/2}$=20 sec; Table 7) and then normalized by the wet heart weight. In order to establish the validity of comparing Ca exchange kinetics between two different strains of hamster, it was considered necessary to first examine the response of both the normal and the cardiomyopathic hearts to Ca depletion. The Ca exchange profiles of 44 d normal hamster hearts under steady state conditions, versus non-steady state conditions, are shown in Figures 17A & B. Similar exchange profiles from 36 d cardiomyopathic hamster hearts are shown in Figures 18A & B. A paired t-test was used for statistical comparisons.

It is clear that Ca exchange kinetics under non-steady state conditions differs from that under steady state conditions. In Ca uptake experiments (Figures 17A &18A), this is characterized by a larger extraction during the first 30-60 sec under steady state conditions. In Ca washout (Figures 17B & 18B), this is characterized by the removal of a larger amount of Ca during the first 30 sec followed by a reduced removal after 60-120 sec of perfusion in hearts not subjected to Ca depletion.

Table 7

Summary of the extracellular exchange kinetics

Indicator	Exchange site	$t_{1/2}$ (sec)
^{131}I-BSA	apparatus + vascular	7
^{14}C-Manitol	apparatus + vascular	16 (uptake)
	+ interstitial	16 (washout)
^{45}Ca	apparatus	10 (uptake)
		20 (washout)

	Ca bound and adsorbed to the perfusion apparatus
Uptake	94 nmoles
Washout	165 nmoles

Figure 17

Comparison of steady state and non-steady state Ca exchange - normal hamster heart (heart wt=0.30 ± 0.02g, n=3; 44 d).

Panel A: Steady state uptake of ^{45}Ca in normal K-H solution is indicated by solid circles (●——●). Non-steady state uptake of ^{45}Ca in normal K-H solution after 2 min of Ca-free K-H solution wash is indicated by open circles (o---o).

Panel B: Steady state washout of ^{45}Ca in normal K-H solution is indicated by solid circles (●——●). Non-steady state washout of ^{45}Ca in Ca-free K-H solution is indicated by open circles (o---o).

Test of significance is by paired-t statistics

(NS: $P>0.05$; *: $P<0.05$)

The normalized standard error is $S_{\bar{x}} = (S_D^2/2n)^{\frac{1}{2}}$

S_D=standard deviation of the difference

n =number of data pairs

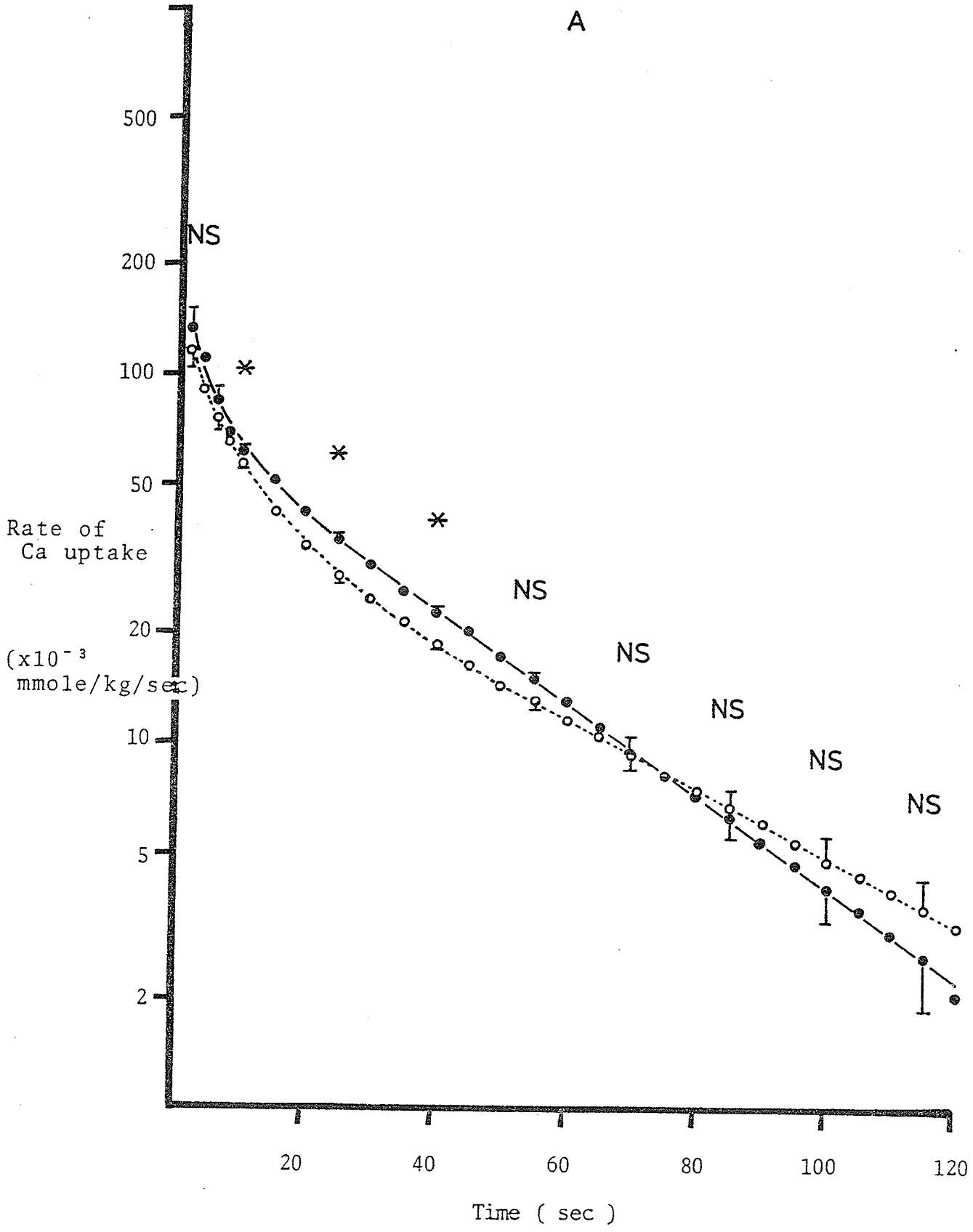
A
500
200
100
50
20
10
5
2
NS
NS
NS
NS
NS
NS
*
*
*
Rate of
Ca uptake
(x10⁻³
mmole/kg/sec)
20
40
60
80
100
120
Time (sec)

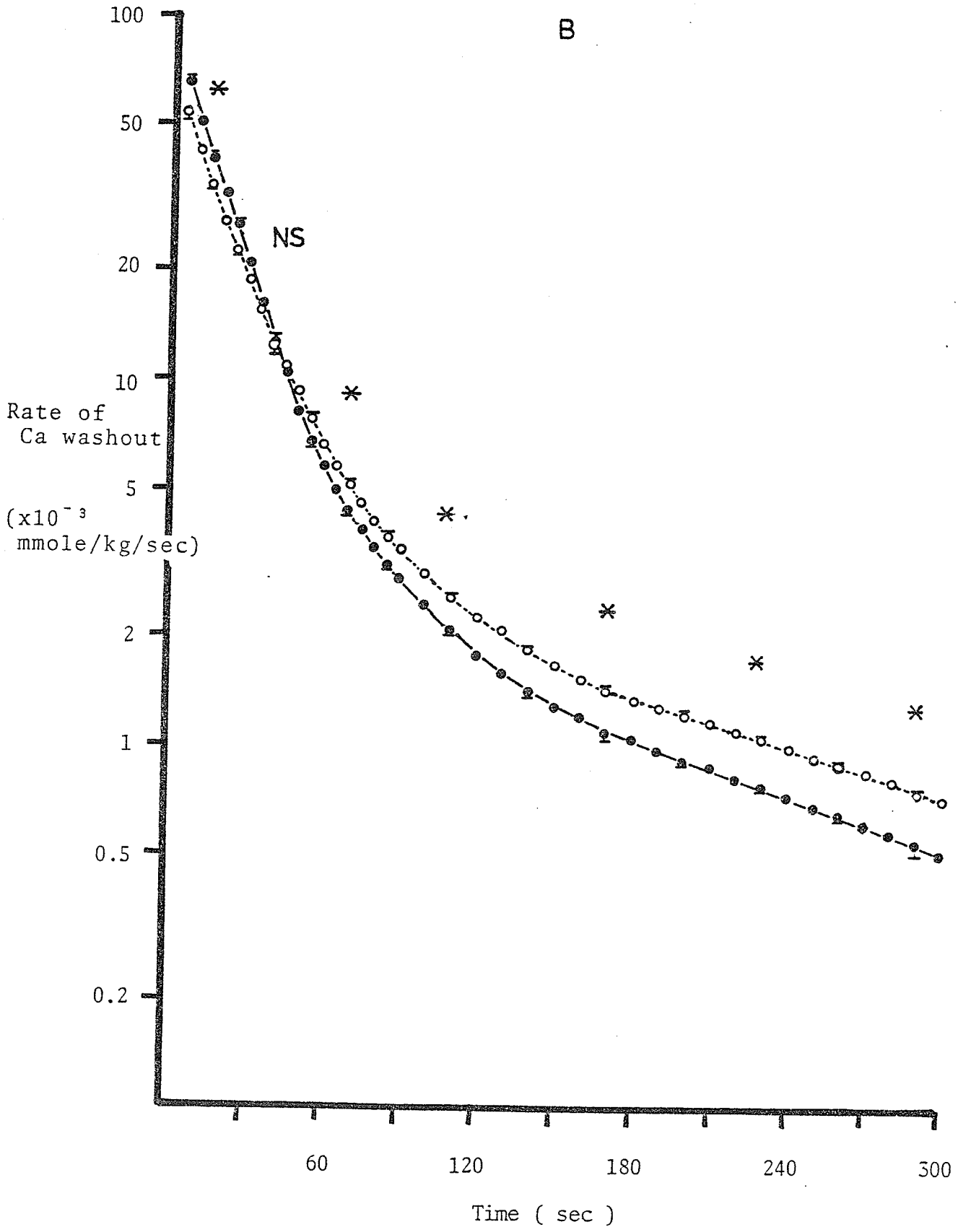
B
NS
100
50
20
10
5
2
1
0.5
0.2
Rate of
Ca washout
(x10⁻³
mmole/kg/sec)
60
120
180
240
300
Time (sec)

Figure 18

Comparison of steady state and non-steady state Ca exchange - cardiomyopathic hamster heart (heart wt = 0.21 ± 0.01 g, n = 4; 36 d)

(Legend as in Figure 17)

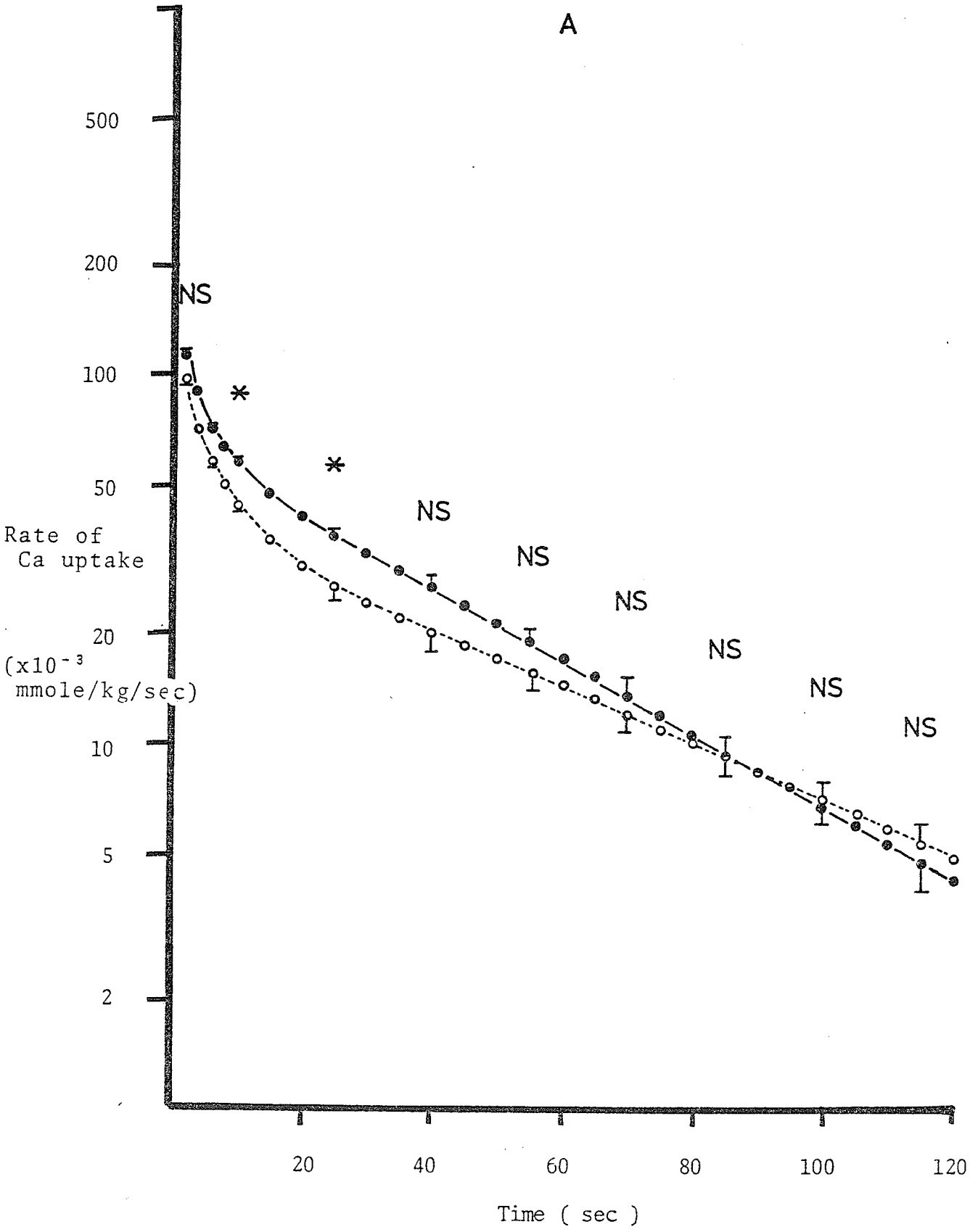
A
500
200
100
50
20
10
5
2
Rate of
Ca uptake
(x10⁻³
mmole/kg/sec)
NS
*
*
NS
NS
NS
NS
NS
NS
20
40
60
80
100
120
Time (sec)

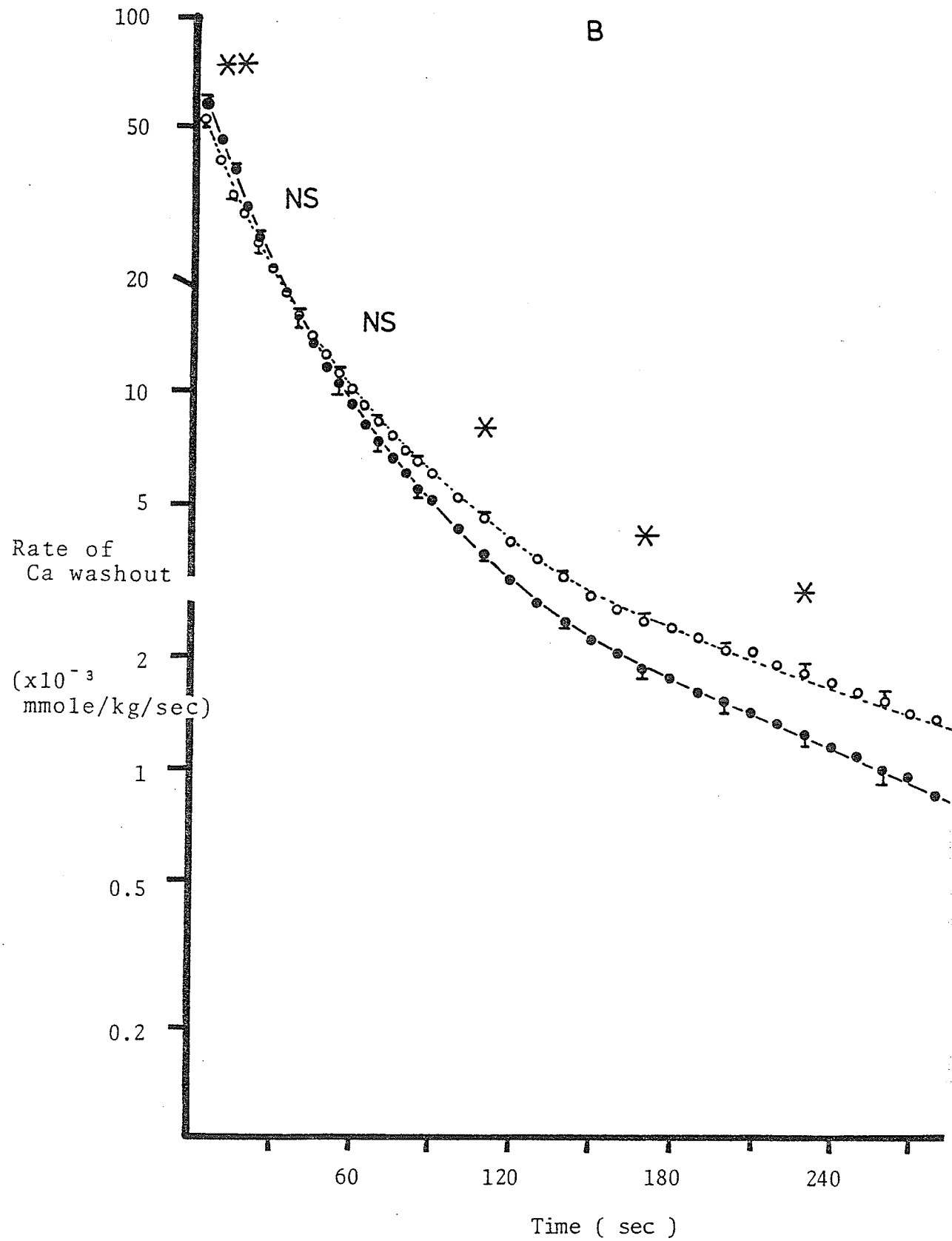
B
100
50
20
10
5
2
1
0.5
0.2
**
NS
NS
*
*
*
Rate of
Ca washout
(x10⁻³
mmole/kg/sec)
60
120
180
240
Time (sec)

During steady state exchange of Ca, the system is not perturbed. On the other hand, during non-steady state exchange of Ca, the system is modified at least with respect to contractile activity, that is, Ca washout is associated with a decline of contractile force and Ca uptake is associated with the re-establishment of contractile force. Consequently, one would expect some difference in the exchange profile of Ca under these two conditions. The important question is whether Ca permeability is continuously altered as a function of time. This question is not easily answered; the previous exchange constant K would no longer be a constant but assumes the role of an unknown variable which might be linear, exponential or some other function of time. Nevertheless, if the kinetics under the non-steady state conditions of Ca exchange do not differ greatly from that under steady state conditions, one may at least assume that no great change of Ca permeability has occured.

Table 8 shows the statistical comparison of the kinetic parameter, $t_{\frac{1}{2}}$, of both rapidly and slowly exchanging Ca compartment, under steady and non-steady state conditions of Ca exchange. The data are taken from the same experiments as those shown in Figures 17 (A & B) and 18 (A & B). The results indicate that although there is a tendency for an increased $t_{\frac{1}{2}}$ under non-steady state exchange conditions, the difference is not statistically significant in either the rapidly or slowly exchanging compartment in Ca washout or uptake studies.

Table 8

Statistical comparison of $t_{1/2}$ of both fast and slow exchanging Ca compartment under steady and non-steady state conditions of Ca exchange

	Compartment	Process	$t_{1/2}$ (sec) Steady State	$t_{1/2}$ (sec) Non-steady State	Statistical Test[c]
Normal[a]	1	washout	14.8± 1.1	15.6± 1.1	N.S.
	2	washout	107.5±12.8	122.5±12.8	N.S.
	1	uptake	3.1± 0.9	5.4± 0.9	N.S.
	2	uptake	28.8± 5.4	31.8± 5.4	N.S.
Cardio-myopathic[b]	1	washout	17.4± 0.5	18.1± 0.5	N.S.
	2	washout	92.1± 7.8	106.2± 7.8	N.S.
	1	uptake	4.2± 1.7	5.9± 1.7	N.S.
	2	uptake	32.9± 3.5	43.2± 3.5	N.S.

[a] Normal hamsters, 44 d (see Figure 17A & B)

[b] Cardiomyopathic hamsters, 36 d (see Figure 18A & B)

[c] Paired-t statistics (N.S. = $P>0.05$). The normalized standard error is $S_{\bar{x}} = (S_D^2/2n)^{\frac{1}{2}}$ where S_D is the standard deviation of the difference and n is the number of data pairs.

Note there is no difference between normal and cardiomyopathic hearts in their response to Ca depletion and subsequent uptake.

3. Identification of a Ca pool responsible for the maintenance of contractile force in the heart

(a) Washout studies

Similar to the findings of Bailey and Dresel (1968) in kitten hearts, it was found in this investigation that the reduction of contractile force during Ca-free perfusion in the hamster hearts also followed mono-exponential decay. The washout of the exchangeable Ca followed a bi-exponential decay as was shown before (Bailey & Dresel, 1968). Using the in-parallel model of Ca exchange and applying the computer program PEEL65, $t_{\frac{1}{2}}$ of the two compartments of exchangeable Ca were calculated. These data are summarized in Table 9.

The $t_{\frac{1}{2}}$ of the slowly exchanging compartment or Ca_{II} (or Ca_{III} according to the previous terminology of Bailey and Dresel, 1968) was approximately ten times that of the contractility decay. This suggested Ca_{II} was not responsible for the maintenance of contractility. The rapidly exchanging compartment, Ca_I, on the other hand, had a $t_{\frac{1}{2}}$ similar to that of the decay of contractility during Ca-free washout.

Indeed, the half time of decay of the contractility was linearly correlated to the half time of exchange of the Ca_I in both the normal and the cardiomyopathic hamster hearts (Figures 19A & B). The correlation coefficient was respec-

Table 9

$t_{1/2}$ of the decay of contractile force and the two compartments of Ca exchange during Ca washout

$t_{1/2}$ (sec)	Normal[a]	Cardiomyopathic[b]
$Ca_I(p)$[c]	14.6± 0.9	16.0± 0.7
$Ca_{II}(p)$	119.8±11.8	114.6±17.7
dP/dt	9.5± 0.9	9.0± 0.7

[a] 26-220 d, 17 hearts

[b] 30-250 d, 28 hearts

[c] $Ca_I(p)$ = compartment I in washout, in-parallel model

Figure 19

$t_{1/2}$ of dP/dt max as a function of $t_{1/2}$ of $Ca_I(p)$

Panel A: Normal hamster hearts 26-220 d.

The equation of the best fit line is :

$t_{1/2}(dP/dt\ max) = 0.72\ t_{1/2}(Ca_I(p)) - 1.07$

Panel B: Cardiomyopathic hamster hearts 30-250 d.

The equation of the best fit line is :

$t_{1/2}(dP/dt\ max) = 0.82\ t_{1/2}(Ca_I(p)) - 4.61$

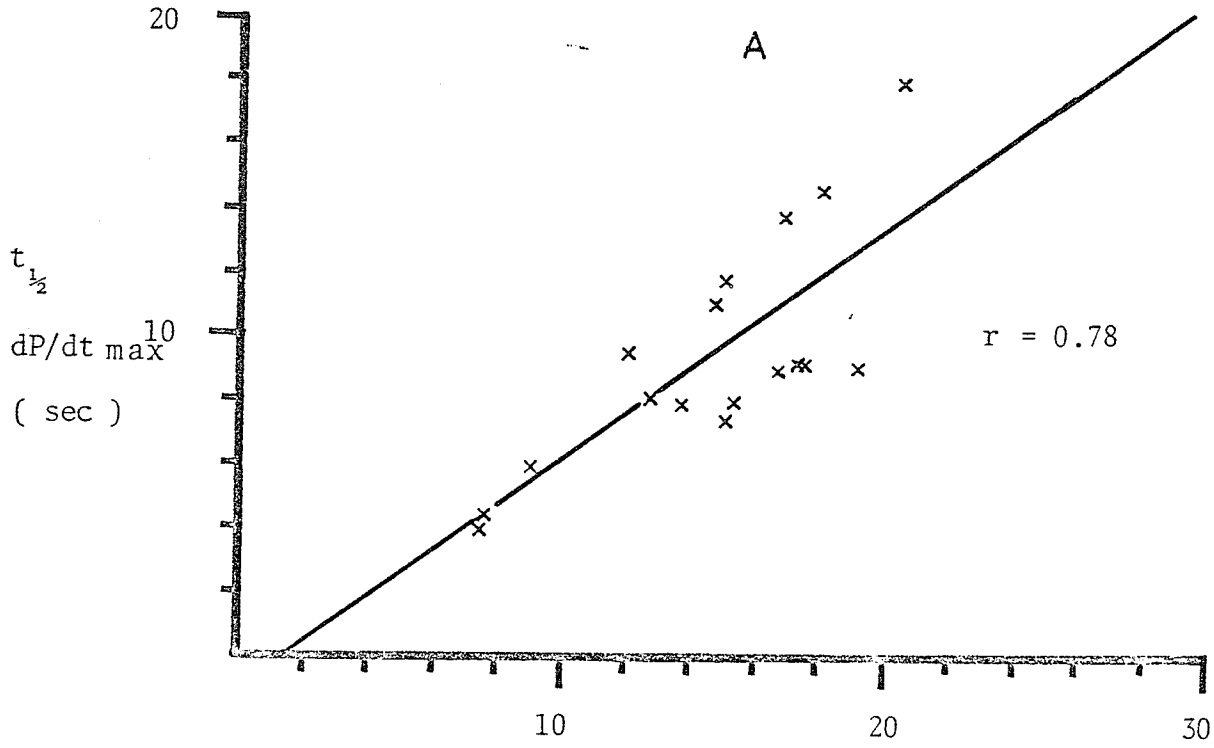
A
20
10
$t_{\frac{1}{2}}$ dP/dt max (sec)
r = 0.78
10
20
30

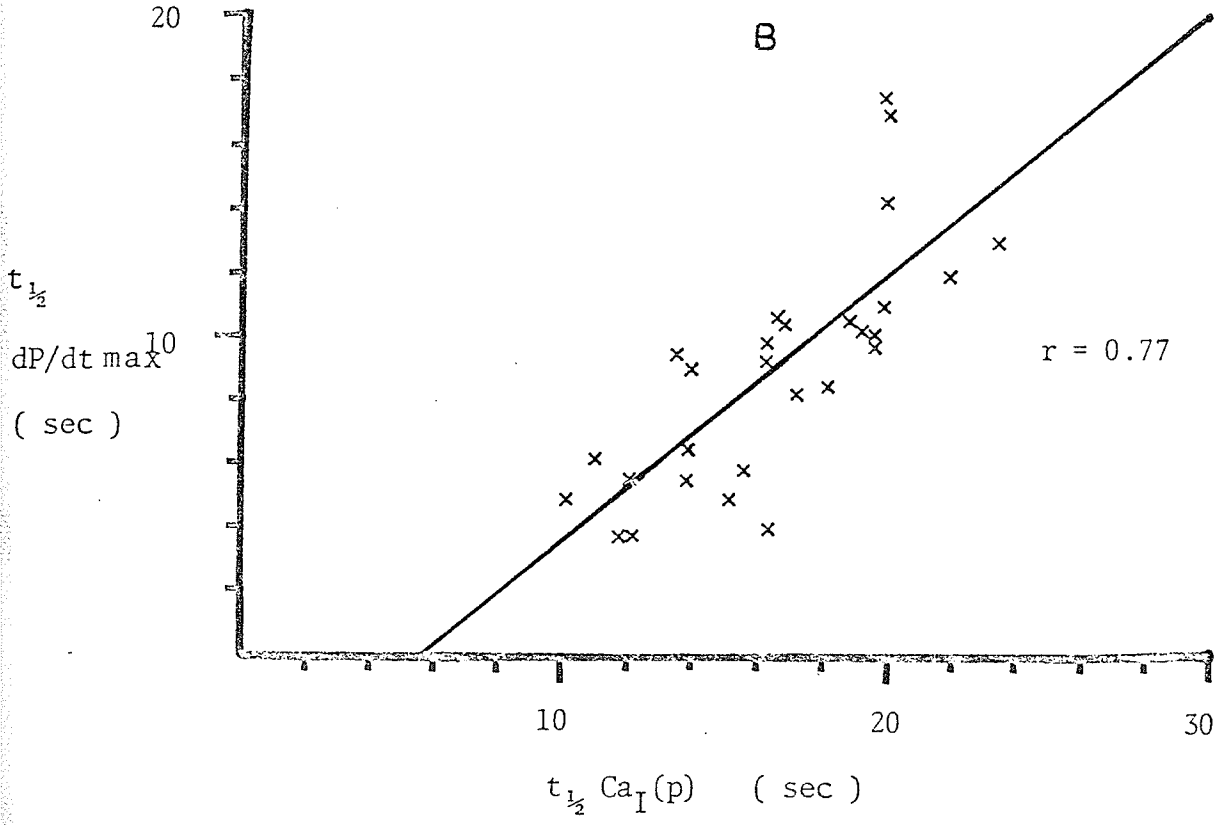
B
20
10
$t_{\frac{1}{2}}$ dP/dt max (sec)
r = 0.77
10
20
30
$t_{\frac{1}{2}}$ Ca_I(p) (sec)

tively 0.78 ($F=22.8$, $dF=16$, $P<0.001$) and 0.77 ($F=38.4$, $dF=27$, $P<0.001$). However, the slopes of the two correlation lines were not unity but were respectively 0.72 and 0.82. The lines also did not pass through the origin, indicating the absence of a one to one correspondence. A possible explanation and the significance of this observation will be found in the Discussion.

The fact that the kinetics of Ca_I exchange approximately paralleled that of the contractility decay in Ca washout studies and that the $t_{1/2}$ of Ca_I was of the same order of magnitude as that of the dP/dt max decay suggested that Ca_I was probably a major determinant in the maintenance of cardiac contractility. The results also suggested that the in-parallel Ca exchange was an adequate model under the condition of Ca-free washout. The observation that the $t_{1/2}$ of Ca_I approximated that of the interstitial space exchange (Table 7) further suggested that the source of Ca_I was probably derived primarily from the extracellular space.

(b) Uptake studies

The return of cardiac contractility during perfusion of Ca containing medium (subsequent to Ca washout) followed a complicated profile. This is illustrated in Figure 20. In general, within 60 sec after initiation of the perfusion with Ca containing medium, cardiac contractility reached a maximum which was about 30% greater than steady state contractility. This apparent overshoot was reproducible in both the normal

Figure 20

Profile of the return of cardiac contractile activity (IVP) during perfusion with normal K-H solution subsequent to Ca-free washout.

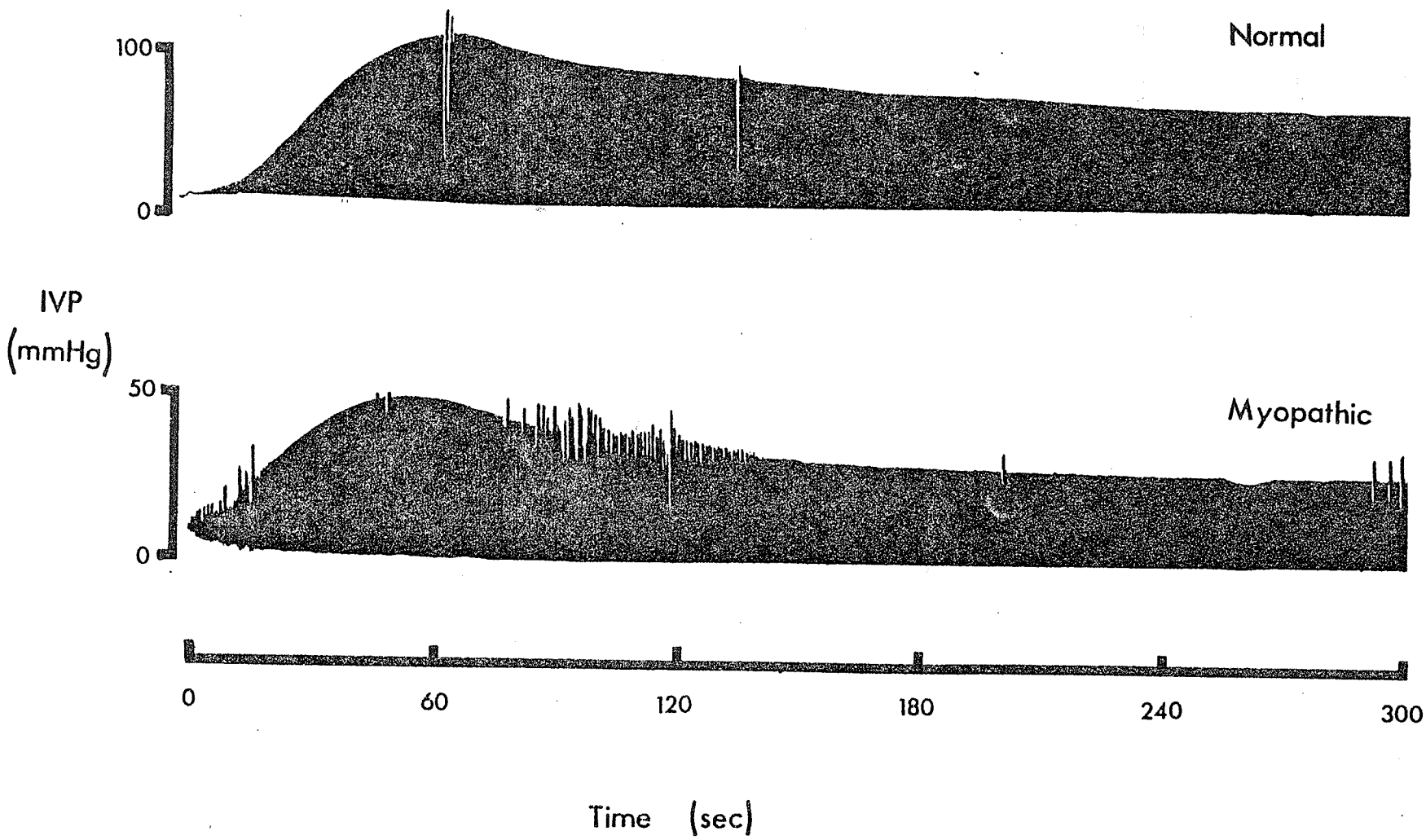
Normal
100
0
IVP
(mmHg)
50
0
Myopathic
0
60
120
180
240
300
Time (sec)

and cardiomyopathic hearts.

Because of the phenomenon of overshoot, the recovery of cardiac contractility could not be described by simple kinetics. The presence of the overshoot and the subsequent re-establishment of the steady state suggested a complicated inter-relationship between the different Ca compartments. The kinetics of exchangeable Ca uptake, however, could still be described as a bi-exponential process.

The accumulation of Ca in the different compartments (both in the in-parallel and in-series models), during Ca uptake, was correlated with steady state dP/dt max. The rational was based on the preceding observation that contractility decayed in an exponential manner with the exponential removal of the Ca in a cellular compartment, suggesting that cardiac contractility was a direct function of the content of Ca in a cellular compartment. The results are summarized in Table 10.

Examination of Table 10 indicates that the best correlation between steady state dP/dt max and the content of a Ca pool was obtained with the rapidly exchanging superficial Ca_1 in the in-series model. The next best correlation was with the total Ca uptake content. Statistically significant correlation was also found with both of the rapidly and slowly exchanging pool content of the in-parallel model, although the correlation coefficients were markedly lower. Figure 21A shows the steady state dP/dt max as a function of the $Ca_1(s)$.

Table 10

Correlation of quantity of Ca uptake by the compartments to steady state dP/dt max

Uptake[a]	r	
Ca_1(s) vs dP/dt max	0.83	* [b]
Ca_2(s) vs dP/dt max	0.36	NS
Ca_1(p) vs dP/dt max	0.54	*
Ca_2(p) vs dP/dt max	0.59	*
Ca_T vs dP/dt max	0.71	*

[a]Normal hamster hearts 26-60 d and cardiomyopathic hamster hearts 30-53 d.

[b]NS = $P>0.05$

* = $P<0.05$

Figure 21

Correlation between uptake Ca_1(s) content and the steady state dP/dt max

Panel A: Open circles(o) indicate normal(26-60d) and crosses (x) indicate cardiomyopathic (30-53d) hamster hearts.

Panel B: Open circles (o) indicate normal (26-220d) and crosses (x) indicate cardiomyopathic (30-220d) hamster hearts.

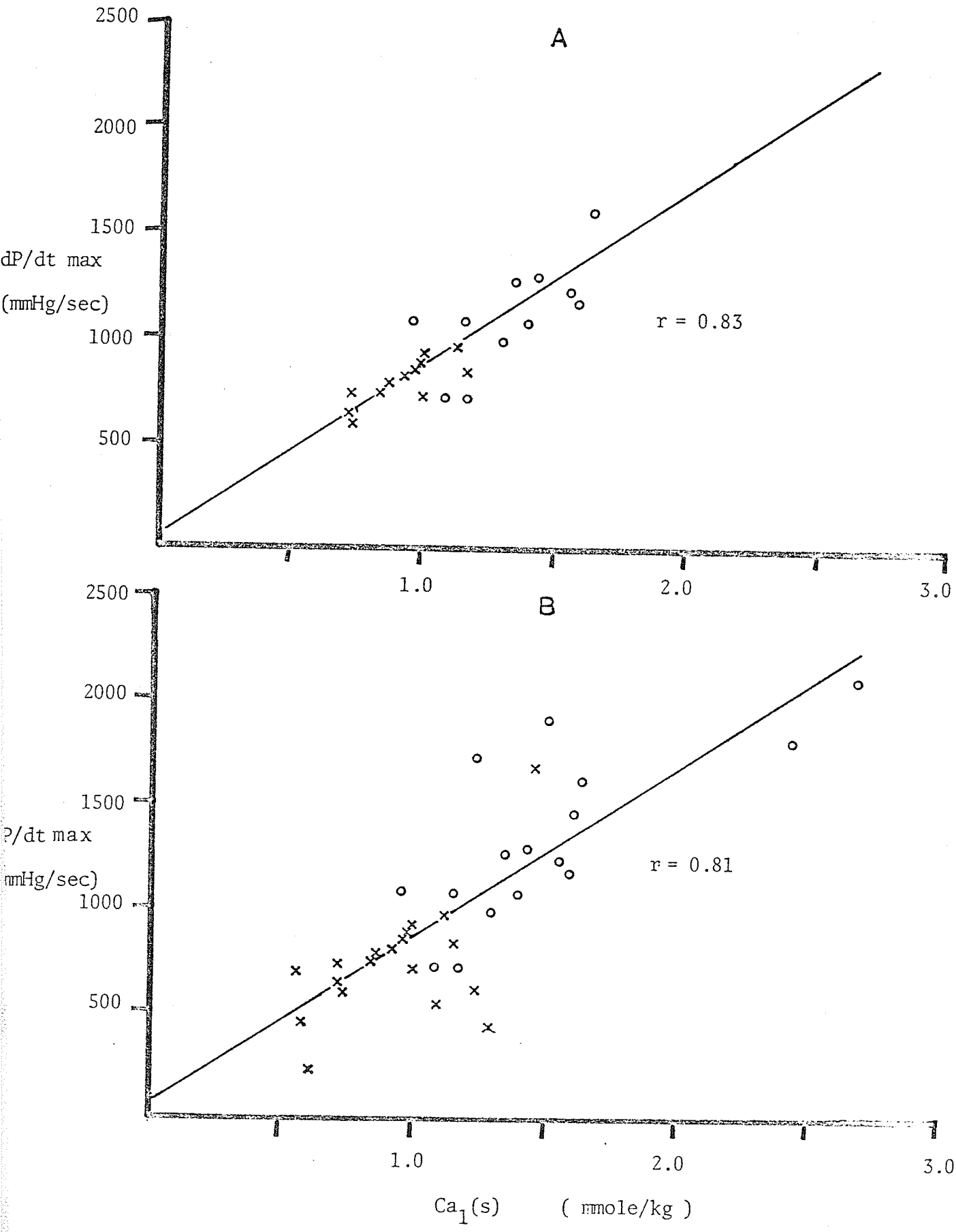
A
2500
2000
1500
1000
500
dP/dt max
(mmHg/sec)
r = 0.83
1.0
2.0
3.0
B
2500
2000
1500
1000
500
P/dt max
mmHg/sec)
r = 0.81
1.0
2.0
3.0
Ca1(s) (mmole/kg)

The small dispersion from the regression line indicated that the populations were homogeneous; in other words, $Ca_1(s)$ from both the normal and cardiomyopathic hearts correlated in the same way to cardiac contractility in these two different strains of hamsters. The results suggested that in the uptake studies, the in-series model may be more appropriate than the in-parallel model, because the content of the rapidly exchanging $Ca_1(s)$ was correlated with cardiac contractility. The relationship between steady state dP/dt max and the $Ca_1(s)$ content was also examined in the total population of hamsters (Figure 21B). Again, a highly significant correlation was found between the two parameters, with a coefficient of correlation of 0.81. The regression line showed little difference from that in Figure 21A. Note that the normal hamster hearts showed consistant higher values of both dP/dt max and $Ca_1(s)$ content.

4. Relationship between the Ca compartments in the washout studies and those in the uptake studies

The kinetic studies of the exchangeable Ca indicated that two compartments could be defined both in the washout and in the uptake studies. The concept that the cell membrane serves as an exchange barrier for Ca leads one to speculate that the rapidly exchanging Ca pool must be superficially located, probably bound primarily to extracellular sites, and might be identical in both the washout and uptake studies. The total exchangeable Ca was calculated with equation 2 of

the Methods section. Paired-t comparison between the content of uptake and washout Ca of the same experiment indicated that the total content of exchangeable Ca differed significantly in the uptake and washout studies. In the young age groups (26-60 d normals and cardiomyopathics inclusive), the content of uptake Ca was 0.28 ± 0.08 mmole/kg larger than that of the corresponding washout Ca. In the old age groups (220 d normals and cardiomyopathics), the difference was 1.35 mmole/kg. Possible explanation for this discrepancies of the quantity of Ca washed out and taken up by the heart in the same experiment will be given in the Discussion section.

Although the total content of exchangeable Ca differs in the uptake and washout studies, the equivalence of the fast exchanging Ca pool is still evident as shown in Table 11. With the exception of the 220 d normal hearts, the close agreement between the two estimations for the content of the rapidly exchanging pool ($Ca_1(s)$ in uptake and $Ca_I(p)$ in washout) is striking. In contrast, the two estimations for the slowly exchanging Ca pool ($Ca_2(s)$ in uptake and $Ca_{II}(p)$ in washout) showed statistically significant differences in two of the six young age groups and in both of the 220 d age groups (Table 12) .

B. Characteristics of cardiomyopathic hamsters

1. Changes in ventricular wet weights of the normal and cardiomyopathic hamster hearts as a function of age

Table 11

Statistical comparison of the content of $Ca_I(p)$ and $Ca_1(s)$

Age	$Ca_I(p)$	$Ca_1(s)$	Statistical significance[b]
N-26	1.34±0.19[a]	1.35±0.12	N.S.
M-30	0.92±0.04	0.84±0.09	N.S.
N-44	1.30±0.13	1.40±0.15	N.S.
M-36	1.21±0.12	1.12±0.12	N.S.
N-60	1.21±0.03	1.25±0.07	N.S.
M-53	0.90±0.07	0.97±0.03	N.S.
N-220	0.93±0.10	1.90±0.28	*
M-220	0.89±0.07	0.90±0.14	N.S.

[a] mean ± SEM; mmole/kg

[b] t-test for 2 means with equal variance

N.S. = $P>0.05$

* = $P<0.05$

Table 12

Statistical comparison of the content of $Ca_{II}(p)$ and $Ca_2(s)$

Age	$Ca_{II}(p)$ [a]	$Ca_2(s)$	Statistical significance [b]
N-26	0.60±0.06	0.95±0.13	N.S.
M-30	0.56±0.18	0.98±0.14	N.S.
N-44	0.72±0.13	1.48±0.28	*
M-36	1.25±0.15	1.47±0.21	N.S.
N-60	0.69±0.03	0.99±0.12	N.S.
M-53	1.08±0.11	0.63±0.07	*
N-220	0.32±0.02	1.40±0.28	*
M-220	0.76±0.10	1.56±0.23	*

[a] mean ± SEM; mmole/kg

[b] t-test for 2 means with equal variance
N.S. = $P>0.05$
* = $P<0.05$

The disease course of the cardiomyopathic hamster in this study appears to parallel those reported previously (Bajusz,1969; Gertz,1972). Hamsters before the 4-5th week of age (<30 d) appear to be free of necrotic lesions (pre-clinic stage). In general, multiple macroscopic calcified lesions can be observed at the 40-50 d hamster hearts. Hypertrophy and ventricular dilatation follows. The chronology of the changes in ventricular wet weights of hearts from the normal and cardiomyopathic hamsters is shown in Figure 22. At 220 d, gross congestive heart failure is evident in the cardiomyopathic hamsters as shown by edema, liver cirrhosis and ascites. Marked ventricular dilatation and frequent auricular thrombi were observed after 220 d.

2. Changes in cardiac contractility and maximum rate of relaxation as a function of age of the hamsters

In the hamster model for genetic cardiomyopathy, congestive heart failure was preceded by a long standing cardiac functional impairment. Forman et al. (1974) reported impairment of cardiac function at 60 d using papillary muscle, when the myopathic hearts were undergoing the necrotic phase of the disease. Cardiac contractility was examined in a working heart preparation to extend the investigation to an age before the development of spontaneous cardiac lesion. The chronological changes in cardiac contractility and maximum rate of relaxation (as measured by the positive and negative dP/dt max of the isovolumic contraction) are shown in Figures 23A & B.

Figure 22

Changes in ventricular wet weights of the normal (o——o) and cardiomyopathic (●----●) hamster hearts. The vertical bars represent standard error of the mean. Each point consists of five or more hearts.

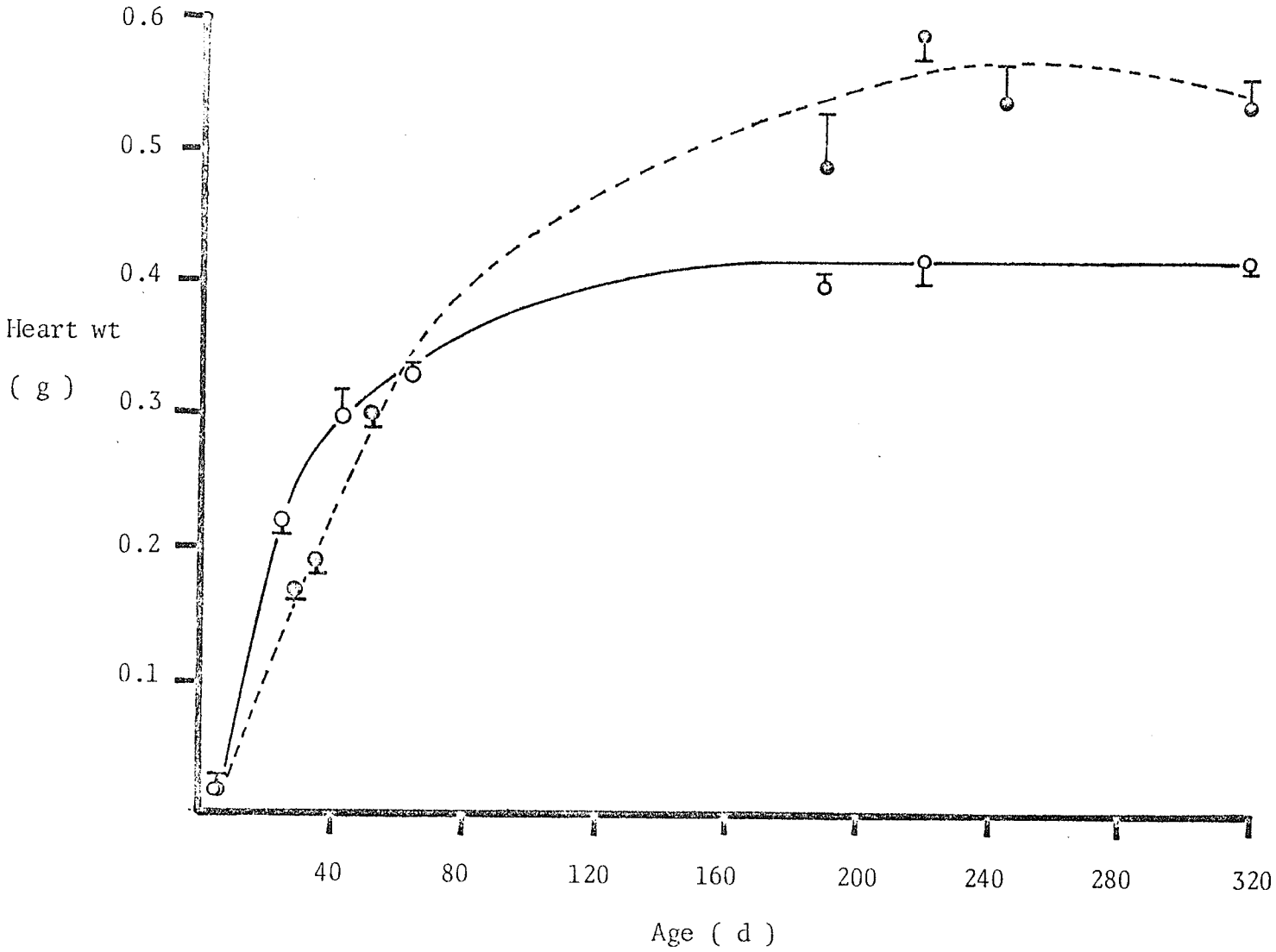
0.6
0.5
0.4
0.3
0.2
0.1
Heart wt
(g)
40
80
120
160
200
240
280
320
Age (d)

Figure 23

Changes in cardiac contractility and maximum rate of relaxation of normal and cardiomyopathic hamster hearts as a function of age

Panel A: Normal hamster cardiac contractility (positive dP/dt max) is indicated by the solid circles(●). Cardiac contractility in the cardiomyopathic hamster is indicated by the open circles (o).

Panel B: Normal hamster cardiac maximum rate of relaxation (negative dP/dt max) is indicated by the solid circles (●). Maximum rate of relaxation in the cardiomyopathic hamster hearts is indicated by the open circles (o).

The verticle bars represent standard error of the mean. Test of significance is by t-test of equal variance (* = $P<0.05$).

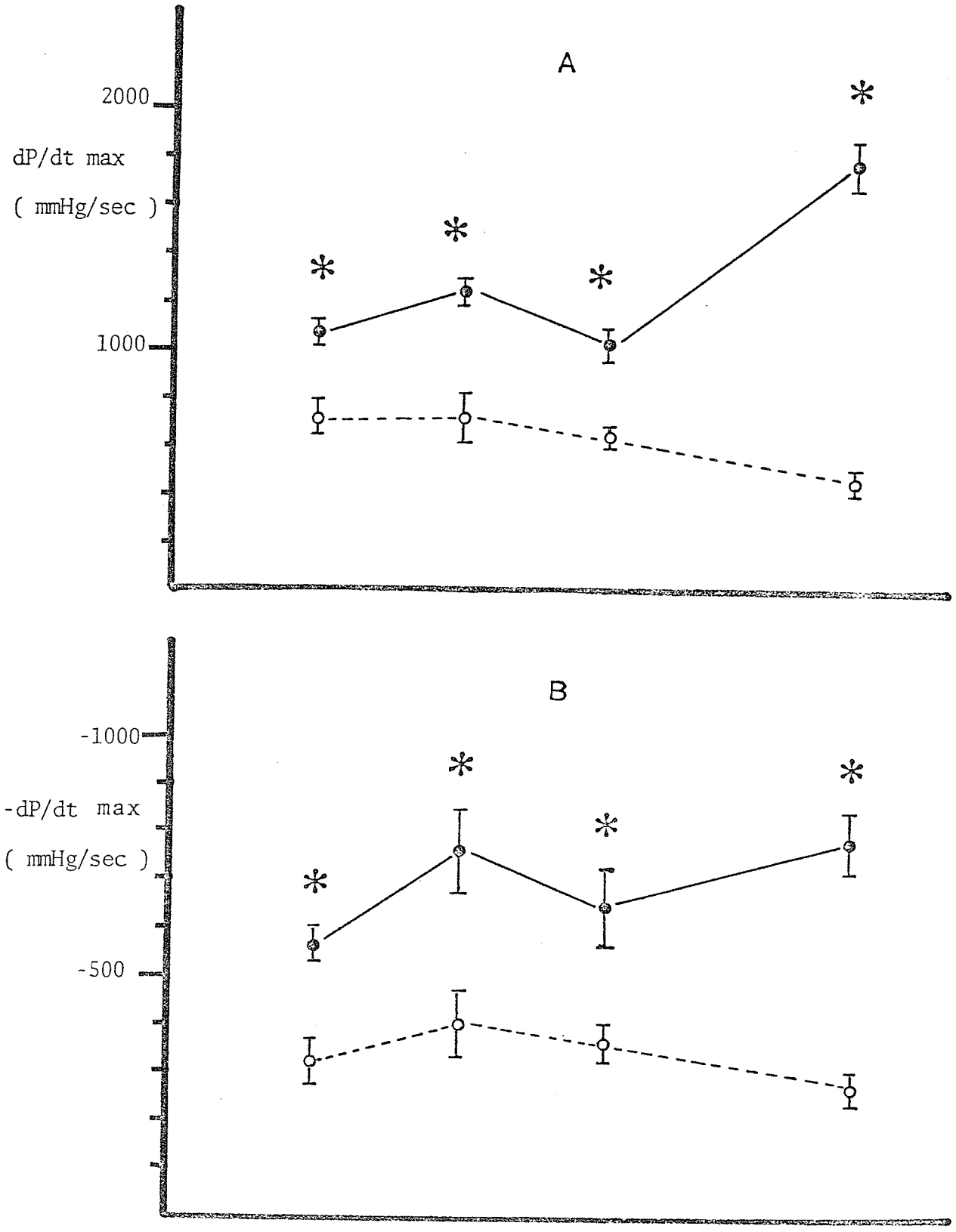
A
2000
dP/dt max
(mmHg/sec)
1000
B
-1000
-dP/dt max
(mmHg/sec)
-500
Pre-clinic
Myolytic
Hypertrophic-nectrotic
Failing

The results show that both cardiac contractility and maximum rate of relaxation are depressed throughout the life span of the cardiomyopathic hamster, even in the pre-clinic stage (30 d) and is most severe at the stage of congestive heart failure (220 d).

3. Ca washout kinetics of the normal vs. the cardiomyopathic hearts

The kinetics of Ca washout in the normal hearts were essentially the same in the 26, 44, and 60 d age groups. This is shown clearly in Figure 24A. There was a marked difference between the Ca efflux pattern of the young normal hearts and the 220 d normal hearts (Figure 24B). For this reason, cardiomyopathic hearts of the 30 (pre-clinic), 36(myolytic), and 53(hypertrophic-necrotic) d groups respectively were each compared with the pooled normal 26-60 d age group, and the 220 d cardiomyopathics were compared with the 220 d normals. Marked differences in the washout profile were observed between each of the three young age groups of the cardiomyopathic hearts and the young normal controls (Figures 25A, B, & C). The results indicate that total exchangeable Ca (Figure 26A) was significantly below control in the pre-clinic phase. This suggests some basic or developmental difference between the normal and cardiomyopathic hearts. Marked increase of total exchangeable Ca, however, was observed at 36 d when the myolytic phase was beginning to develop. This is consistant with the observation of an increased ^{45}Ca uptake in the cardiomyo-

Figure 24

Ca washout profile from normal hamster hearts

Panel A: Ca washout profile from the young hamster hearts. Solid circles (●) indicate 26 d age group, open circles (o) indicate 44 d age group and crosses (x) indicate 60 d age group.

Panel B: Comparison of Ca washout profile from the young and old normal hamster hearts. Solid circles (●) indicate pooled young normal hamster hearts (26-60 d, n=11). Open circles (o) indicate 220 d normal hamster hearts (n=5). Vertical bar denotes standard error of the mean. Statistical test is by t-test of two means with equal variance (*: $P < 0.05$)

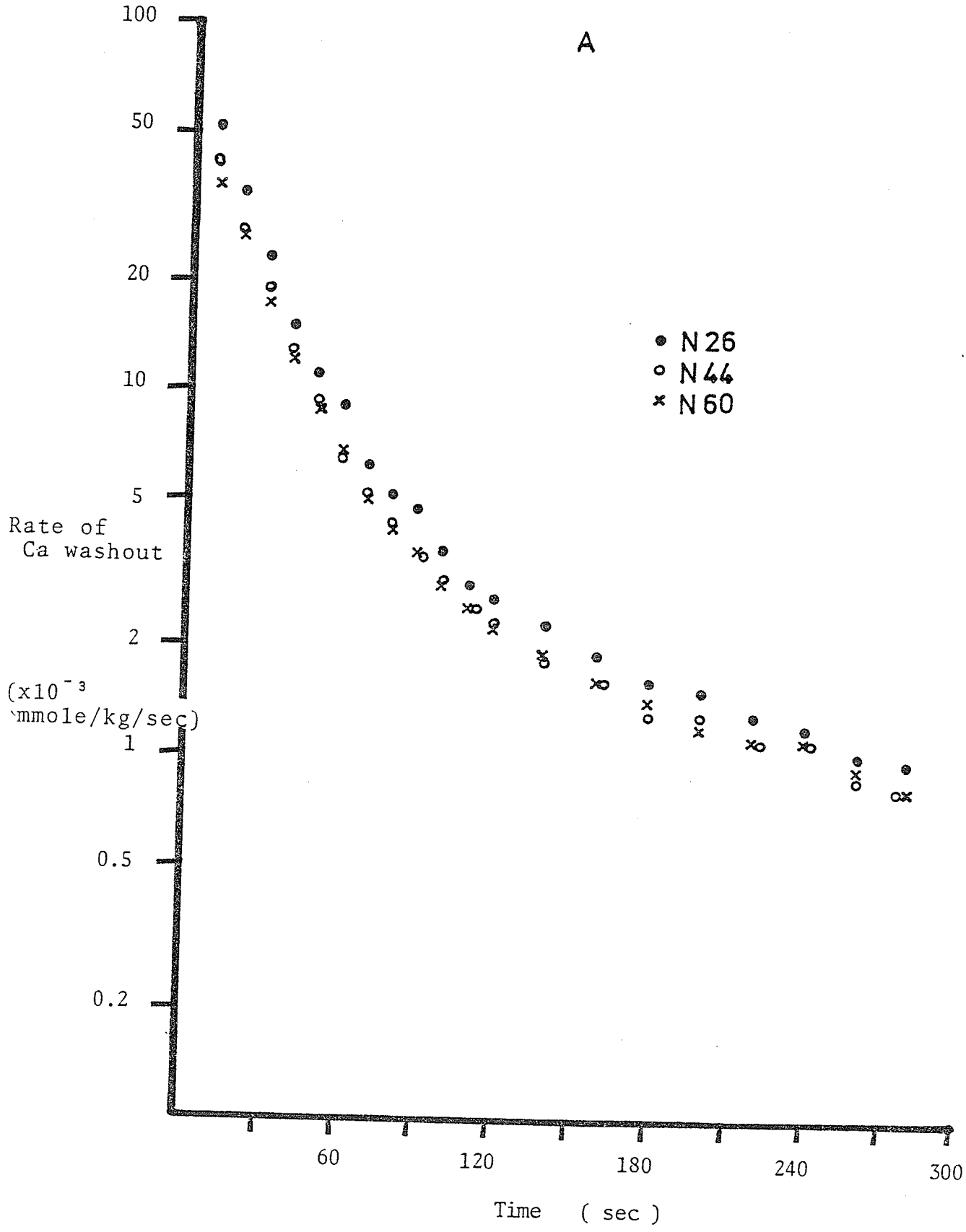
A
100
50
20
10
5
2
1
0.5
0.2
Rate of
Ca washout
(x10⁻³
mmole/kg/sec)
N 26
N 44
N 60
60
120
180
240
300
Time (sec)

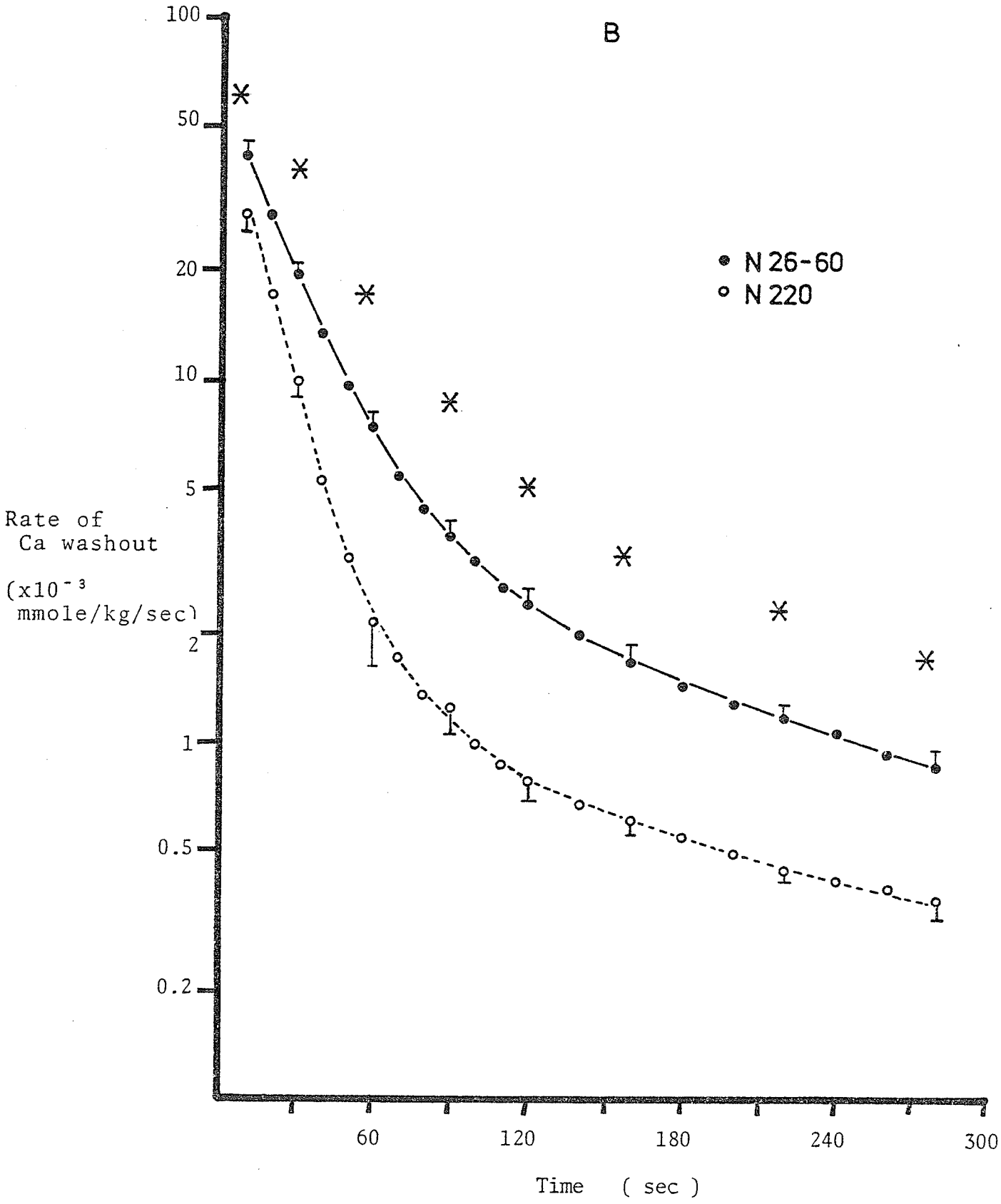
B
100
50
20
10
5
2
1
0.5
0.2
Rate of
Ca washout
(x10⁻³
mmole/kg/sec)
N 26-60
N 220
60
120
180
240
300
Time (sec)

Figure 25

Comparison of Ca washout profile for young normal and cardiomyopathic hamster hearts.

Solid circles and solid line (●——●) indicate pooled 26 to 60 d normals. Open circles and broken line (o---o) indicate 30, 36 and 53 d cardiomyopathics respectively in panel A, B & C. Vertical bar represents standard error of the mean. Test of significance is by t-test of two means with equal variance (N.S.: $P > 0.05$; *: $P < 0.05$).

Panel A: Normals and 30 d cardiomyopathics.

Panel B: Normals and 36 d cardiomyopathics.

Panel C: Normals and 53 d cardiomyopathics.

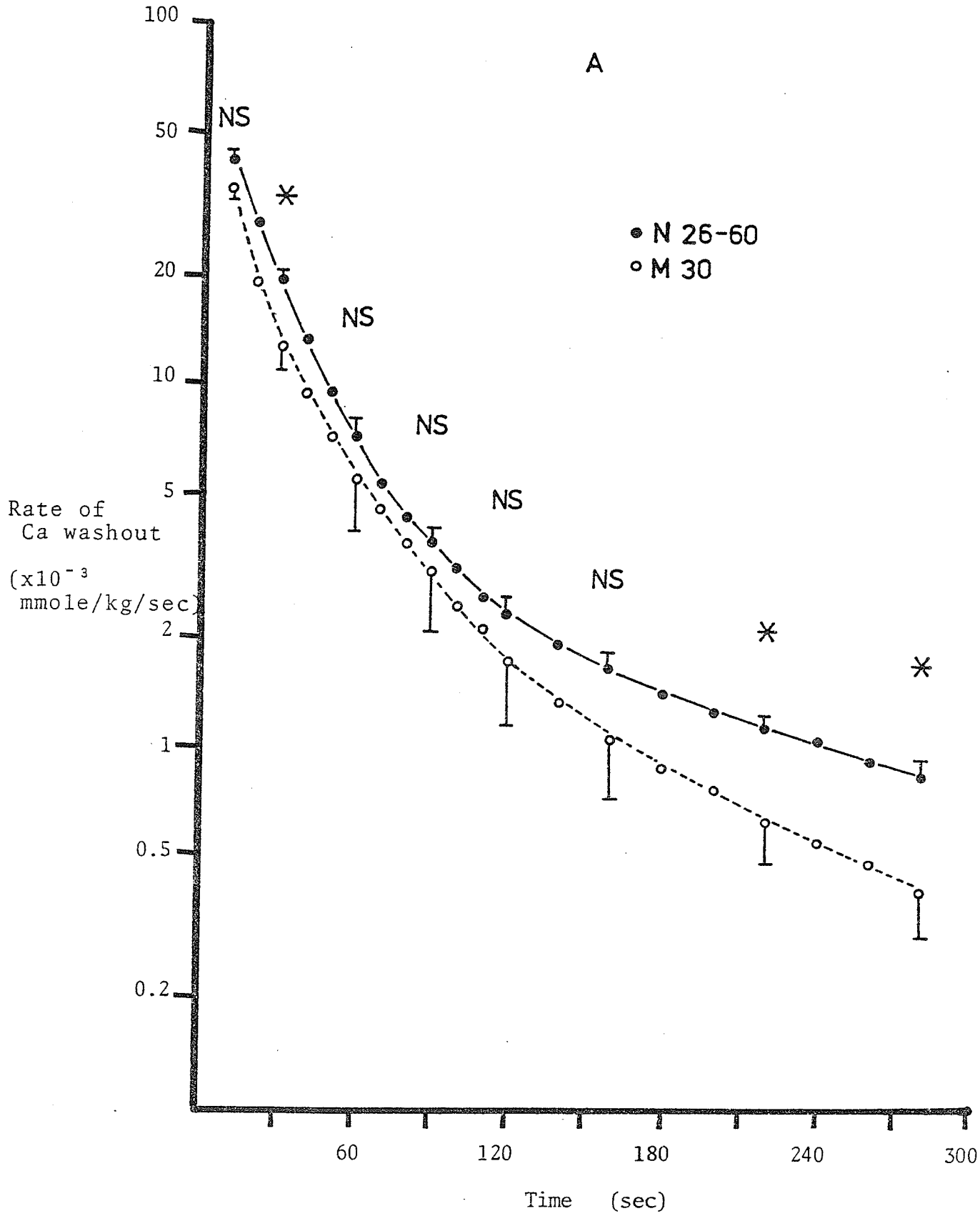
A
100
50
20
10
5
2
1
0.5
0.2
Rate of
Ca washout
(x10⁻³
mmole/kg/sec)
NS
NS
NS
NS
*
*
*
N 26-60
M 30
60
120
180
240
300
Time (sec)

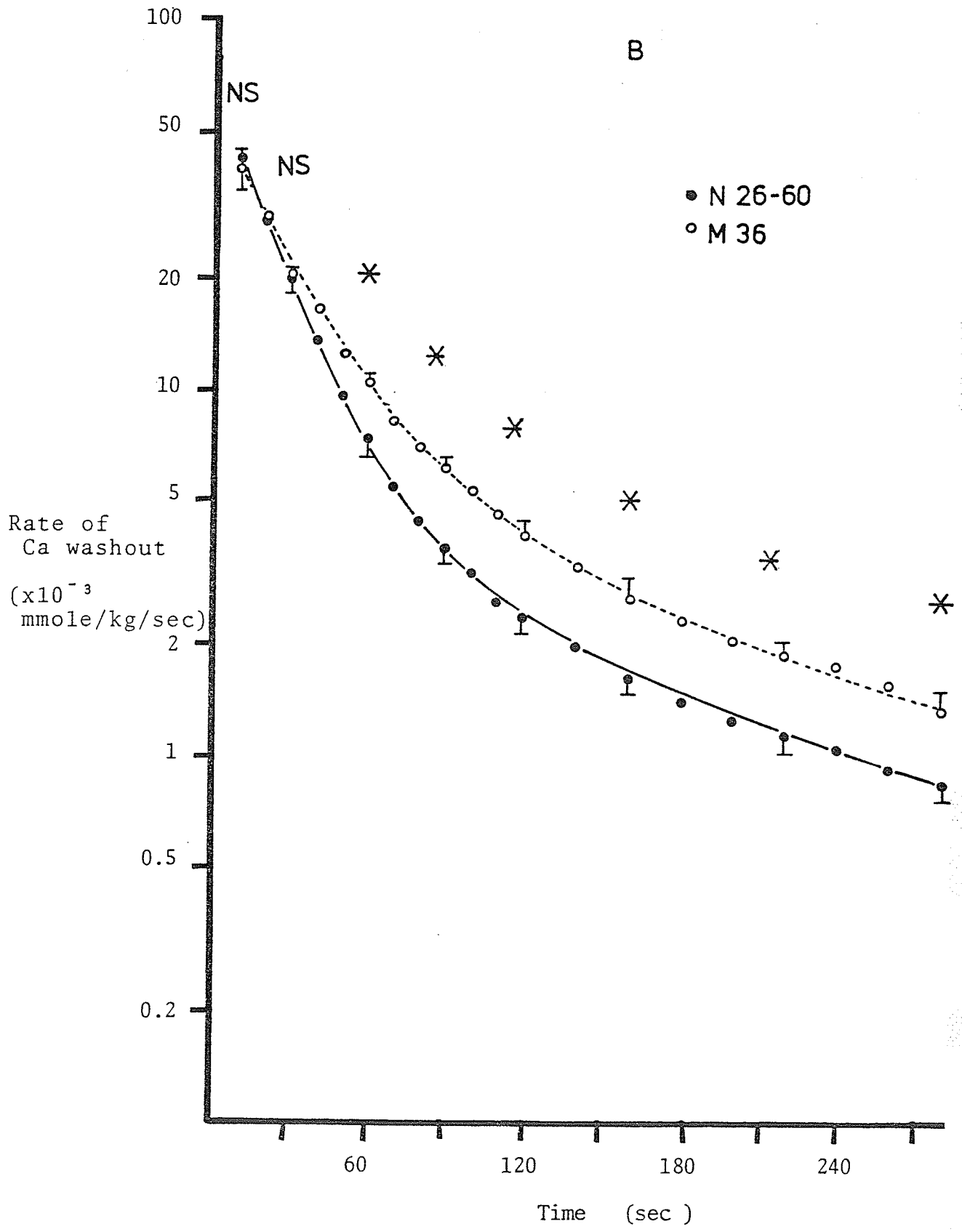
B
NS
NS
N 26-60
M 36
100
50
20
10
5
2
1
0.5
0.2
Rate of
Ca washout
(x10⁻³
mmole/kg/sec)
60
120
180
240
Time (sec)

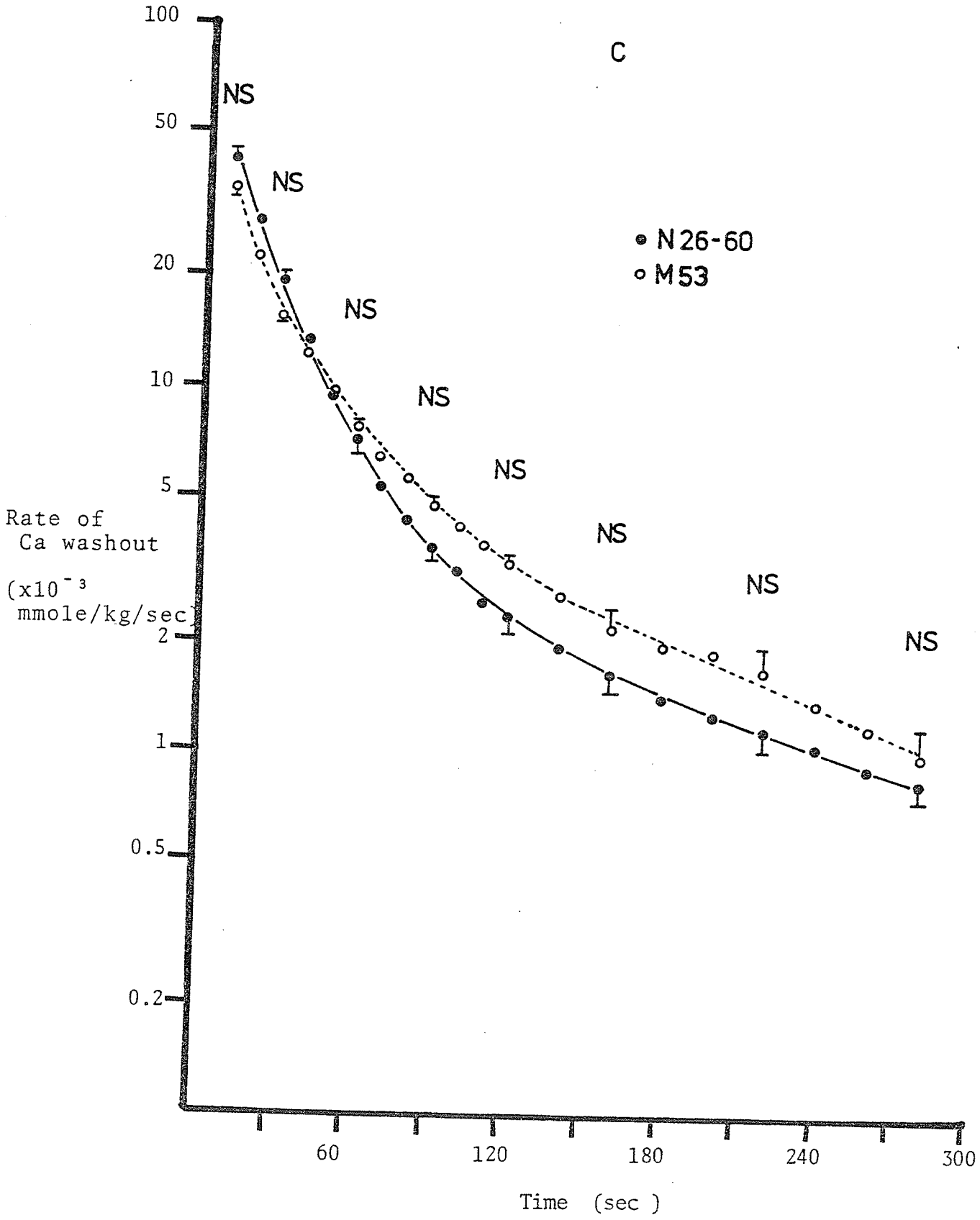
C
N26-60
M53
NS
NS
NS
NS
NS
NS
NS
100
50
20
10
5
2
1
0.5
0.2
Rate of
Ca washout
(x10⁻³
mmole/kg/sec)
60
120
180
240
300
Time (sec)

Figure 26

Total exchangeable Ca, Ca_T, and the compartments $Ca_I(p)$, $Ca_{II}(p)$ measured by Ca free washout in young normal and cardiomyopathic hamster heart

The open rectangles represent Ca content from pooled 26-60 d normals. Shaded rectangles represent Ca contents of cardiomyopathic hearts. Vertical bars indicate standard error of the mean. The broken lines encompass the standard error of the control. Test of significance is by t-test of two means with equal variance (NS: $P>0.05$; *: $P<0.05$).

Panel A: Comparison of total exchangeable Ca content, Ca_T.
Panel B: Comparison of compartment-1 Ca content, $Ca_I(p)$.
Panel C: Comparison of compartment-2 Ca content, $Ca_{II}(p)$.

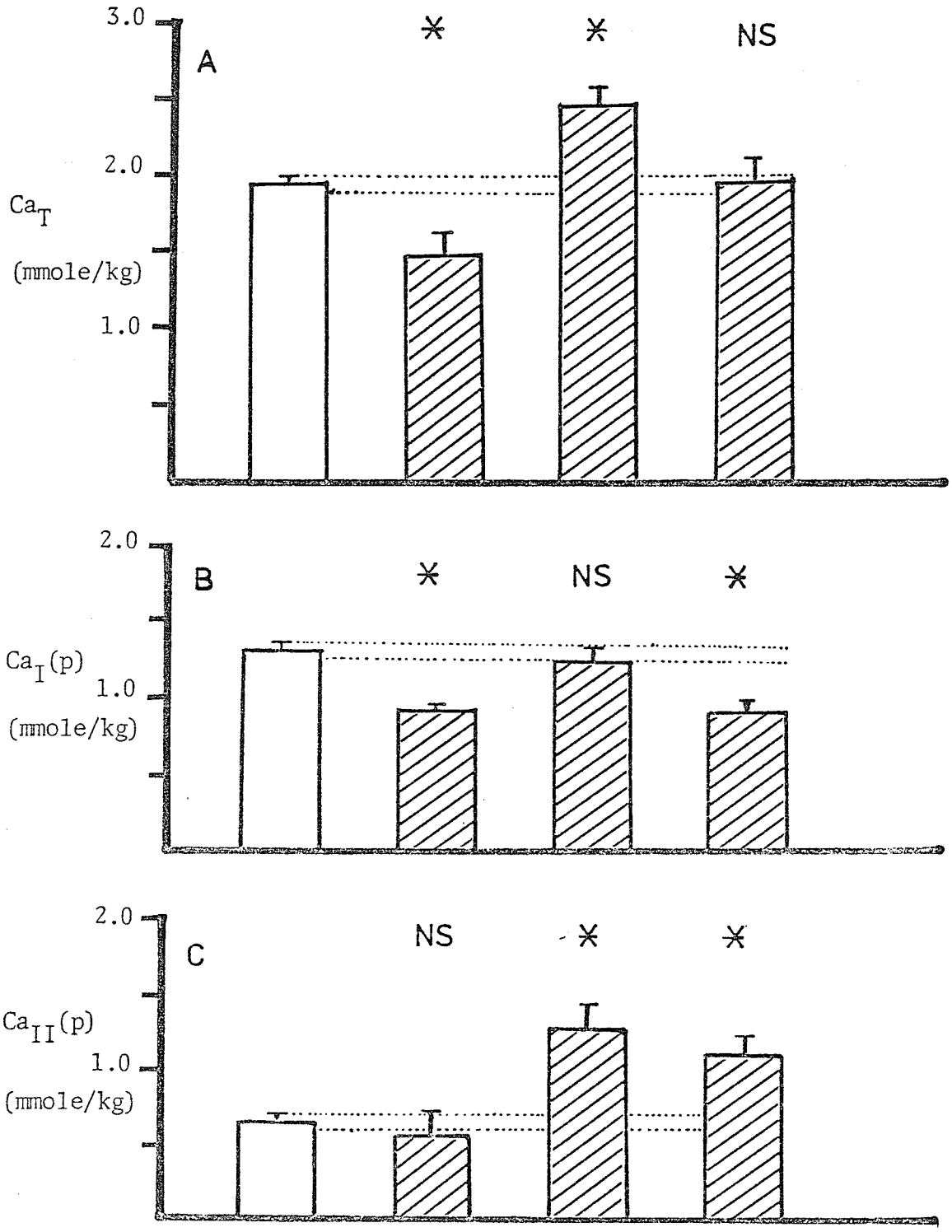
3.0
A
*
*
NS
2.0
Ca_T
(mmole/kg)
1.0
2.0
B
*
NS
*
$Ca_I(p)$
1.0
(mmole/kg)
2.0
C
NS
*
*
$Ca_{II}(p)$
1.0
(mmole/kg)
Pre-clinic
Myolytic
Hypertrophic-necrotic

pathic hearts at this stage of the disease (Lossnitzer et al. 1975). By the 53 d of life (hypertrophic-necrotic phase), when total Ca measured by atomic absorption of the ashed myocardial sample reached 10 to 20 mmole/kg indicating calcified lesions, exchangeable Ca had returned to control levels. This emphasizes the fact that total Ca content bears little relationship to the total quantity of exchangeable Ca, only the latter is important in E-C coupling.

Kinetic analysis showed that the amount of Ca in the rapidly exchanging pool, $Ca_I(p)$, was significantly less in both the pre-clinic (30 d) and hypertrophic-necrotic (53 d) but not in the myolytic (36 d) group of the cardiomyopathic hearts. The reduction of $Ca_I(p)$, whose content has been established in preceding section to be responsible for the development of cardiac contractile activity, suggests one possible reason for the depressed cardiac contractility in the diseased hearts. The normal content of $Ca_I(p)$ in the myolytic hearts coupled with a depressed cardiac contractility may suggest some disturbance in other steps of E-C coupling in the cardiomyopathic hearts. The slowly exchanging Ca pool, $Ca_{II}(p)$, was normal in the pre-clinic phase but was significantly elevated in both the myolytic and hypertrophic-necrotic phase of the disease(Figure 26C). The significance of $Ca_{II}(p)$ in E-C coupling is not clear. The possible involvement of this pool of Ca in relation to cardiac relaxation will be discussed in the Discussion section.

Comparison of the $t_{\frac{1}{2}}$ of $Ca_I(p)$ between normal and

cardiomyopathic hearts (Figure 27A) showed no difference in the three age groups of pre-clinic, myolytic, and hypertrophic-necrotic phase of the disease. There was, on the other hand, a significantly increased rate of Ca exchange, or decreased $t_{\frac{1}{2}}$, of $Ca_{II}(p)$ in the myolytic and hypertrophic-necrotic group of cardiomyopathic hearts (Figure 27B) when compared to controls. In the pre-clinic group, the $t_{\frac{1}{2}}$ of $Ca_{II}(p)$ was also decreased but this decrease was not statistically significant.

The washout profile of the exchangeable Ca of the 220 d normal and cardiomyopathic hearts showed marked differences (Figure 28). At this age, congestive heart failure was pronounce in the cardiomyopathic animals. Taking into account the possible error in the estimation of recovered Ca caused by the collection procedure in the group as pointed out earlier, different kinetics of Ca efflux were clearly apparent.

The exchangeable Ca content was significantly elevated in the 220 d cardiomyopathic hearts as compared to the age matched control (Table 13). This elevation was entirely accounted for by the increase in the slowly exchanging Ca pool, $Ca_{II}(p)$.

The $t_{\frac{1}{2}}$ of the slowly exchanging compartment $Ca_{II}(p)$ did not differ statistically from control. The $t_{\frac{1}{2}}$ of the rapidly exchanging pool, $Ca_{I}(p)$, however, was significantly faster in the normal hearts. When compared to the young

Figure 27

$t_{\frac{1}{2}}$ of $Ca_I(p)$ and $Ca_{II}(p)$ in young normal and cardiomyopathic hamster hearts

Open rectangles represent data from pooled 26-60 d normals. Shaded rectangles represent data from cardiomyopathics. Vertical bars indicate standard error of the mean. The broken lines encompass the standard error of control. Test of significance is by t-test of two means with equal variance.

Panel A: Comparison of $t_{\frac{1}{2}}$ of $Ca_I(p)$.

Panel B: Comparison of $t_{\frac{1}{2}}$ of $Ca_{II}(p)$.

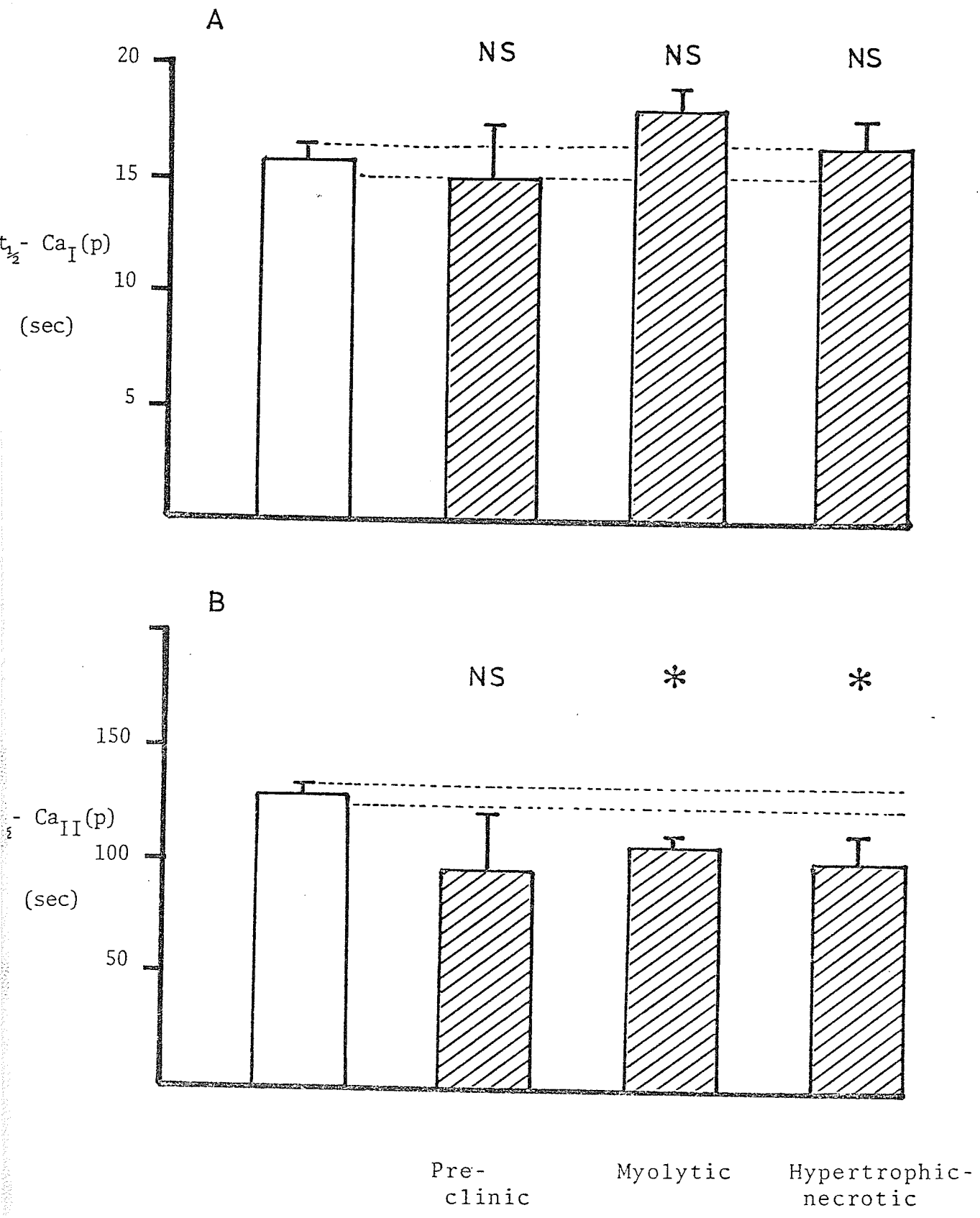
A
NS
NS
NS
20
15
10
5
$t_{1/2}$ - Ca_I(p)
(sec)
B
NS
*
*
150
100
50
- Ca_{II}(p)
(sec)
Pre-clinic
Myolytic
Hypertrophic-necrotic

Figure 28

Comparison of Ca washout profile of 220 d normal and cardiomyopathic hamster hearts

Solid circles and solid line (●———●) indicate 220 d normals. Open circles and broken line (o-----o) indicate 220 d cardiomyopathics. Vertical bars represent standard error of the mean. Test of significance is by t-test of two means with equal variance (NS: $P>0.05$; *: $P<0.05$).

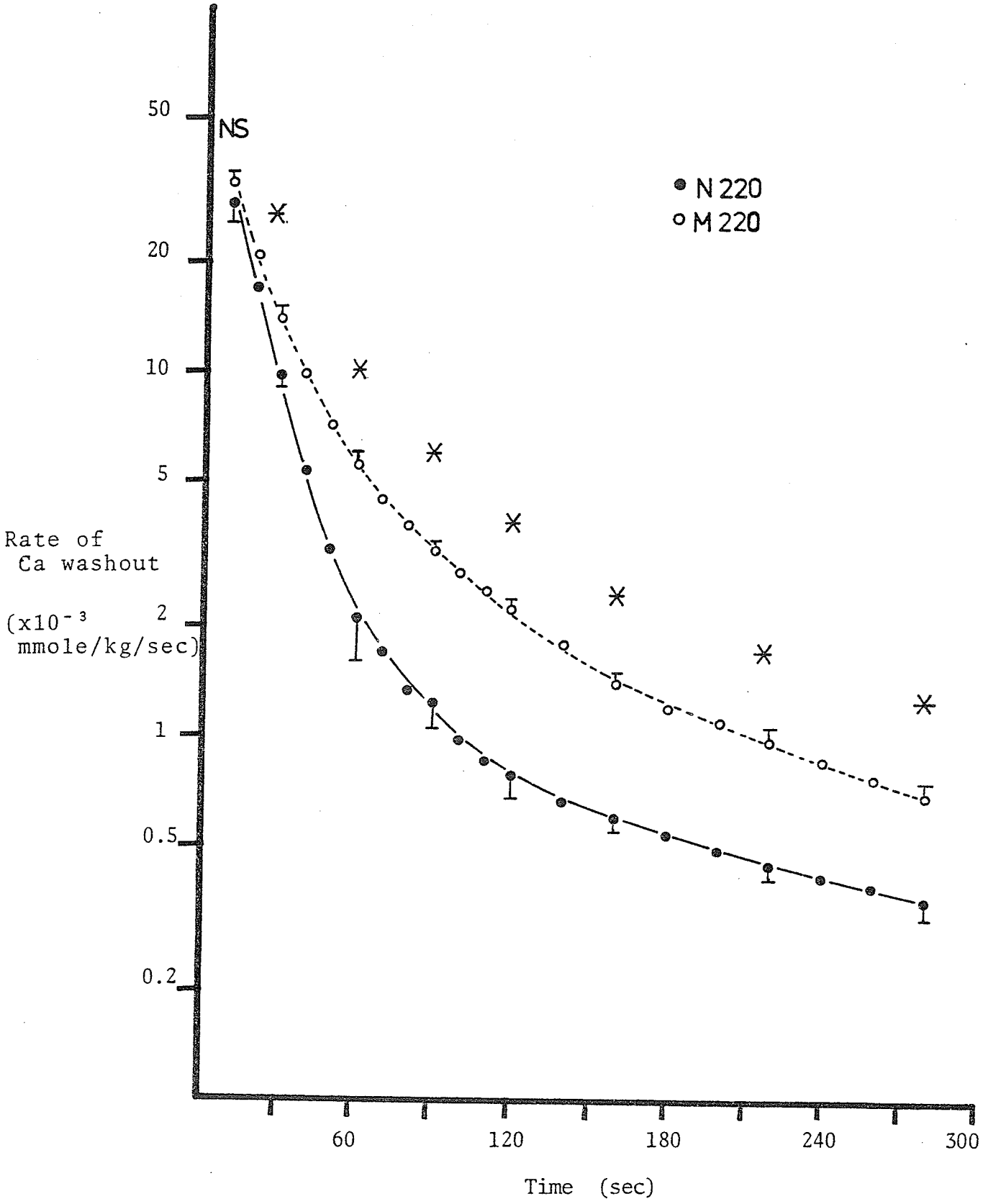
50
20
10
5
2
1
0.5
0.2
NS
N 220
M 220
Rate of
Ca washout
(x10⁻³
mmole/kg/sec)
60
120
180
240
300
Time (sec)

Table 13

Ca content and exchange kinetics in the washout studies of 220d normal and cardiomyopathic hamster hearts

	Normal	Cardiomyopathic	Statistical significance[b]
Content (mmole/kg)			
Ca_T	1.25±0.09[a]	1.65±0.10	*
Ca_I(p)	0.93±0.10	0.89±0.07	N.S.
Ca_{II}(p)	0.32±0.02	0.76±0.10	*
$t_{1/2}$ (sec)			
Ca_I(p)	10.2±1.8	16.1±1.4	*
Ca_{II}(p)	136.2±41.4	156.7±57.1	N.S.
dP/dt max	4.5±0.5	8.2±1.2	*

[a] mean ± S.E.M.

[b] t-test of two means with equal variance

(* : $P<0.05$)

(26-60 d) normal hearts, the 220 d normal hearts again had a haster rate of exchange of the extracellular compartment $Ca_I(p)$. This faster exchange of the extracellular compartment was not an artifact because the $t_{\frac{1}{2}}$ of the decrease of dP/dt max during Ca-free perfusion was concommitantly decreased in this age group of normal hearts (Table 13). Figure 4 shows the typical pattern of the very rapid decay of cardiac contractility in the 220 d normal hearts. This could possibly be due to a higher rate of perfuste flow in the 220 d normal hearts as compared to the age matched cardiomyopathic hearts (Table 14), although the difference was not statistically significant.

4. Ca uptake kinetics of the normal vs. the cardiomyopathic hearts

The uptake profile of the exchangeable Ca in the young normal hamster hearts, as in the washout studies, again showed nearly identical patterns (Figure 29A). Differences, on the other hand, could be seen, as in the washout studies, between the young and old normal hamster hearts (Figure 29B). Comparisons of the Ca uptake kinetics were therefore separated into two groups. The three groups of young cardiomyopathic hearts of the pre-clinic (30 d), myolytic (36 d), and hypertrophic-necrotic (53 d) phases were each compared to the pooled normal hearts (26-60 d). Separate comparison was made between the 220 d normal and cardiomyopathic hearts. Gross differences in the uptake profiles of Ca between the young normal and cardiomyopathic hearts were

Table 14

Perfusate flow of the normal and cardiomyopathic hamster hearts

	Perfusate flow[a] (ml/g/min)		
group	Normal	Cardiomyopathic	
Pre-clinic	7.1 ± 1.0	6.9 ± 0.6	N.S.
Myolytic	6.6 ± 0.6	6.4 ± 0.6	N.S.
Necrotic-hypertrophic	6.0 ± 0.6	5.2 ± 0.4	N.S.
Failing	7.7 ± 0.9	6.2 ± 0.3	N.S.

[a]perfusate flow = coronary flow + aortic leakage

Figure 29

Ca uptake profile from normal hamster hearts

Panel A: Ca uptake profile from the young hamster hearts. Solid circles (●) indicate 26 d age group, open circles (o) indicate 44 d age group, and crosses (x) indicate 60 d age group.

Panel B: Comparison of Ca uptake profile from the young and old normal hamster hearts. Solid circles (●) indicate pooled young normal hamster hearts (26-60 d, n=11). Open circles (o) indicate 220 d normal hamster hearts (n=5). Vertical bar denotes standard error of the mean. Statistical test is by t-test of two means with equal variance (N.S.: $P > 0.05$; *: $P<0.05$).

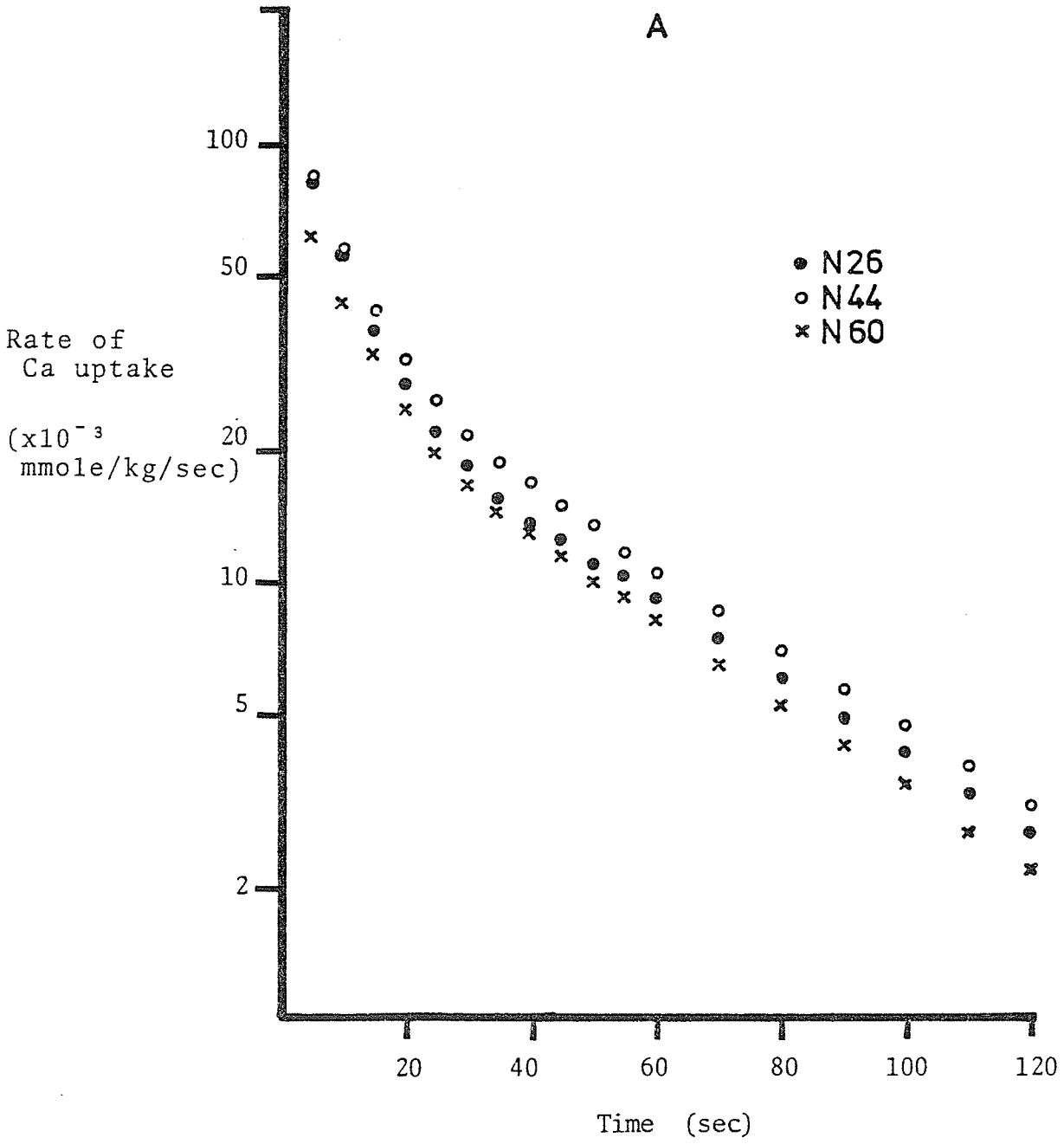
A
100
50
20
10
5
2
Rate of
Ca uptake
(x10⁻³
mmole/kg/sec)
N26
N44
N60
20
40
60
80
100
120
Time (sec)

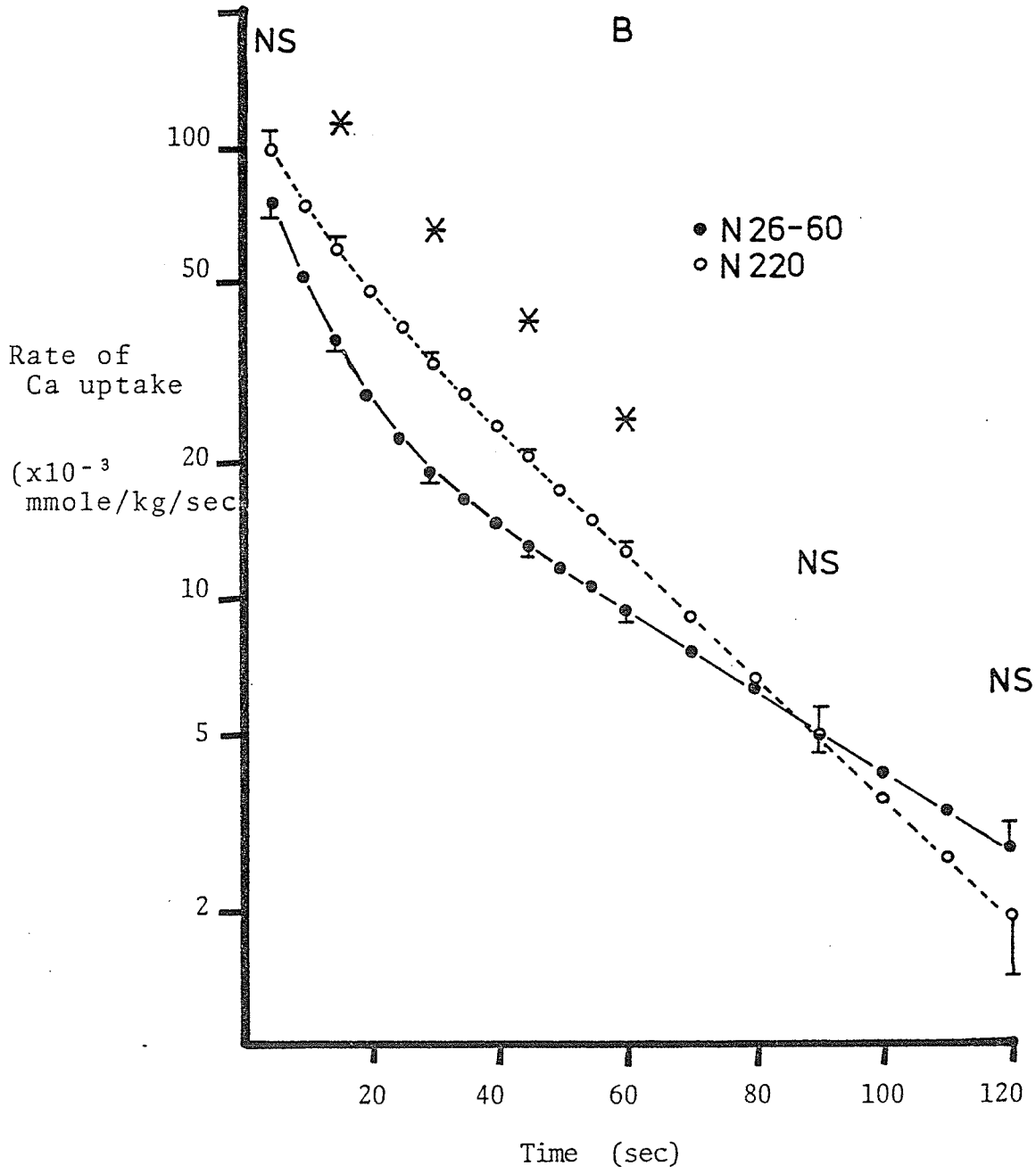
B
NS
NS
NS
N 26-60
N 220
100
50
20
10
5
2
Rate of
Ca uptake
(x10⁻³
mmole/kg/sec
20
40
60
80
100
120
Time (sec)

readily discernable as shown by Figures 30A, B, and C.

The total quantity of Ca taken up by the young cardiomyopathic hamster hearts was significantly decreased in the pre-clinic (30 d) and hypertrophic-necrotic (53 d) stages (Figure 31 A). In contrast to that observed in Ca washout studies, the content of exchangeable Ca at the myolytic stage (36 d) was not significantly above that of the normal control.

The same pattern of depressed Ca content of the rapidly exchanging Ca pool, as shown in the Ca washout studies (as $Ca_I(p)$), is observed in the Ca uptake studies for $Ca_1(s)$ (Figure 31B). This depression was statistically significant in both the pre-clinic and hypertrophic-necrotic but not in the myolytic group of cardiomyopathic hamsters. The content of the slowly exchanging Ca pool, $Ca_2(s)$, was unchanged in the pre-clinic, elevated in the myolytic, and reduced in the hypertrophic-necrotic phase of the disease. With the exception of the last group, the changes observed were similar to those shown for the Ca washout studies.

As $Ca_1(s)$ and $Ca_2(s)$ represent the compartmental content in the in-series model, the $t_{\frac{1}{2}}$ of the two compartments in the usual sense looses its meaning as the filling processes are no longer mono-exponential. However, it is still possible to get an estimate of the $t_{\frac{1}{2}}$ (apparent $t_{\frac{1}{2}}$) of each compartment, when the other compartment is assumed absent, according to equation 21 (see Methods). In addition, the constant K_{01} in

Figure 30

Comparison of Ca uptake profile of the young normal and cardiomyopathic hamster hearts.

Solid circles and solid lines (●——●) indicate pooled 26 to 60 d normals. Open circles and broken line (o---o) indicate 30, 36, and 53 d cardiomyopathics respectively in panel A, B & C. Vertical bars represent standard error of the mean. Test of significance is by t-test of two means with equal variance (N.S.: $P > 0.05$; *: $P < 0.05$).

Panel A: Normals and 30 d cardiomyopathics.

Panel B: Normals and 36 d cardiomyopathics.

Panel C: Normals and 53 d cardiomyopathics.

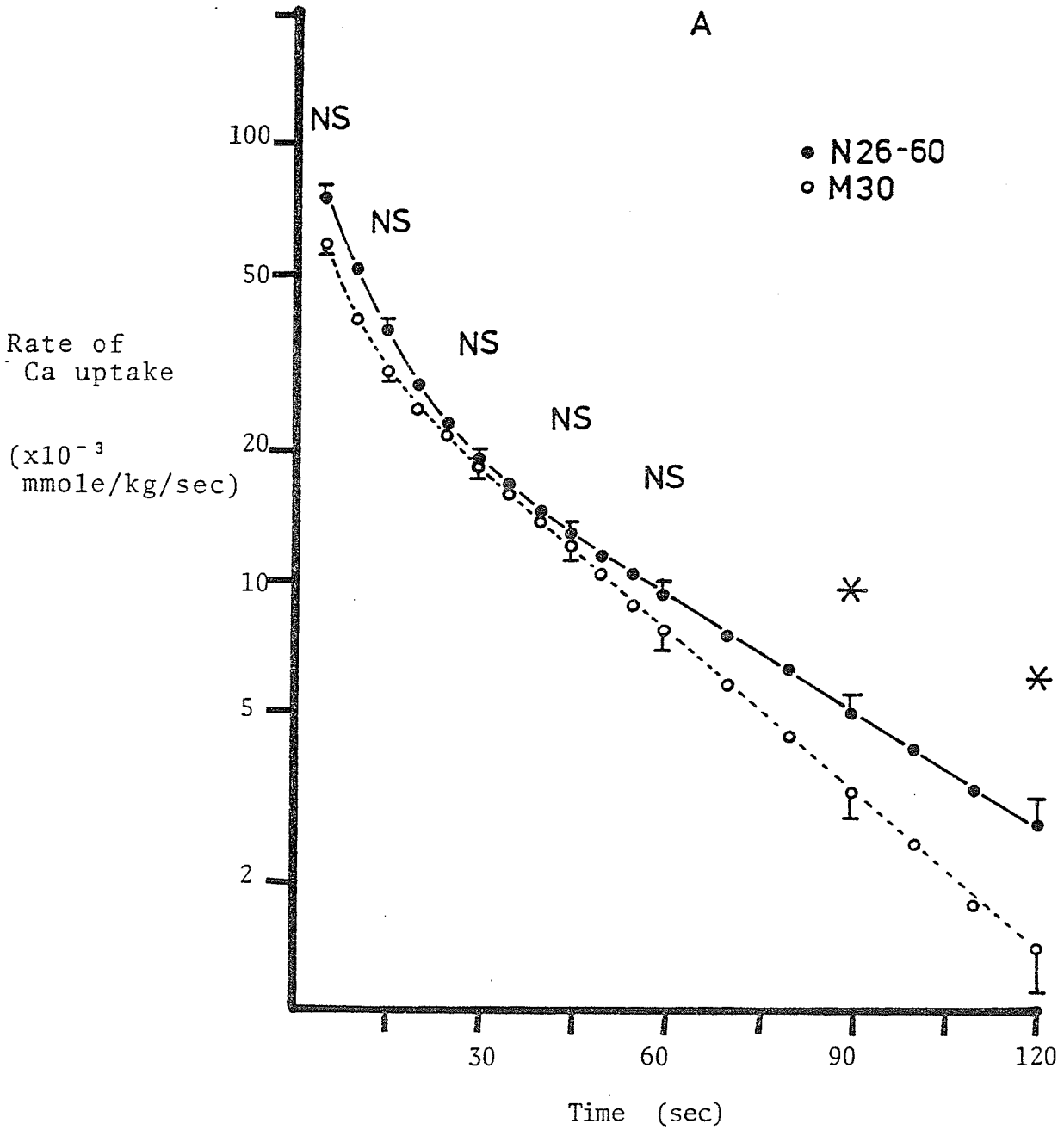
A
NS
NS
NS
NS
NS
100
50
20
10
5
2
Rate of
Ca uptake
(x10⁻³
mmole/kg/sec)
• N26-60
○ M30
*
*
30
60
90
120
Time (sec)

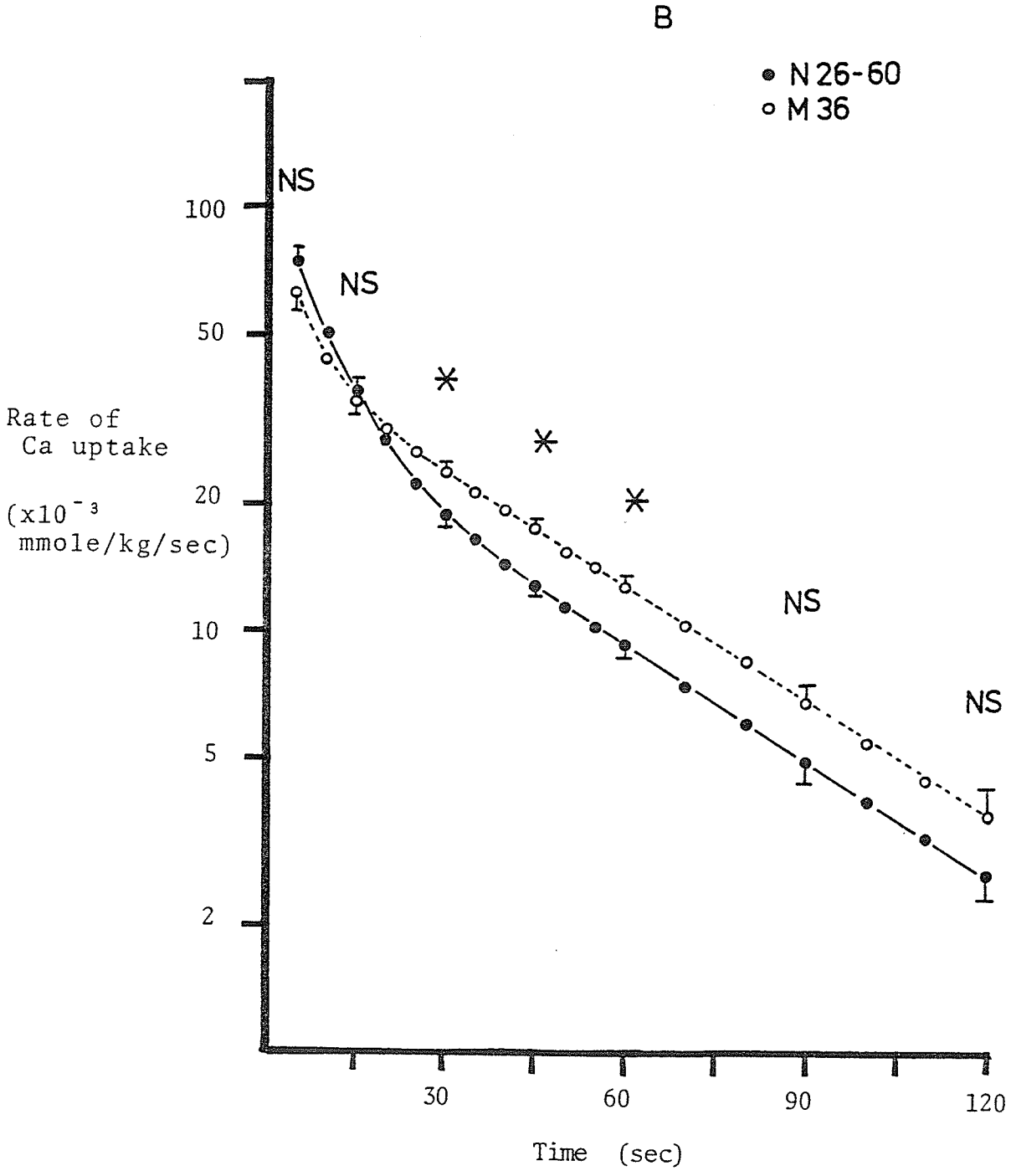
B
N 26-60
M 36
NS
NS
NS
NS
100
50
20
10
5
2
Rate of
Ca uptake
(x10⁻³
mmole/kg/sec)
30
60
90
120
Time (sec)

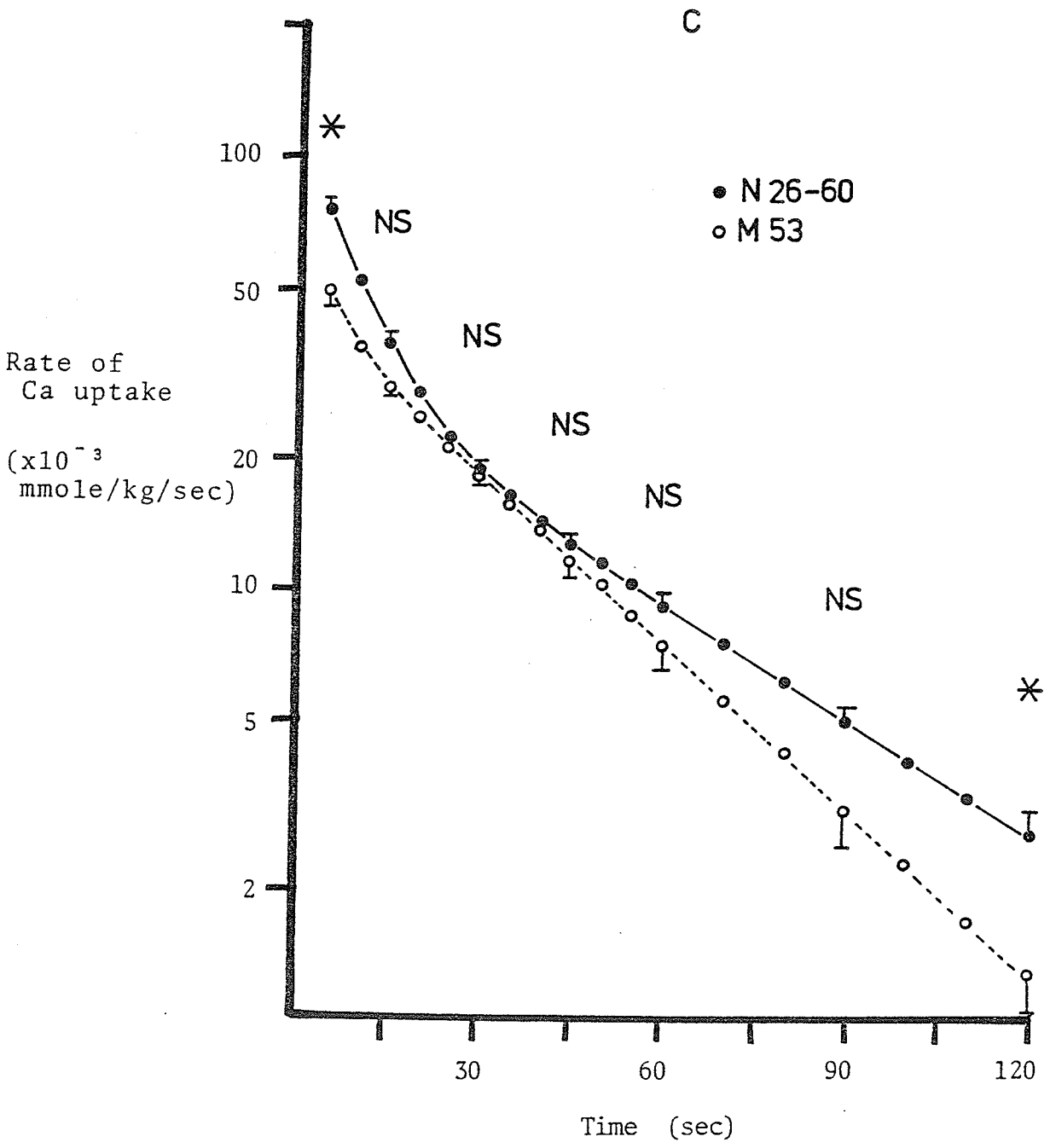
C
N 26-60
M 53
NS
NS
NS
NS
NS
*
*
100
50
20
10
5
2
Rate of
Ca uptake
(x10⁻³
mmole/kg/sec)
30
60
90
120
Time (sec)

Figure 31

Content of Ca_T, $Ca_1(s)$ and $Ca_2(s)$ in the uptake studies of the young normal and cardiomyopathic hamster hearts

Open rectangles represent data from pooled 26-60 d normals. Shaded rectangles represent cardiomyopathics. Vertical bars indicate standard error of the mean. Broken lines encompass the standard error of control.

Panel A: Comparison of total exchangeable Ca, Ca_T.

Panel B: Comparison of $Ca_1(s)$.

Panel C: Comparison of $Ca_2(s)$.

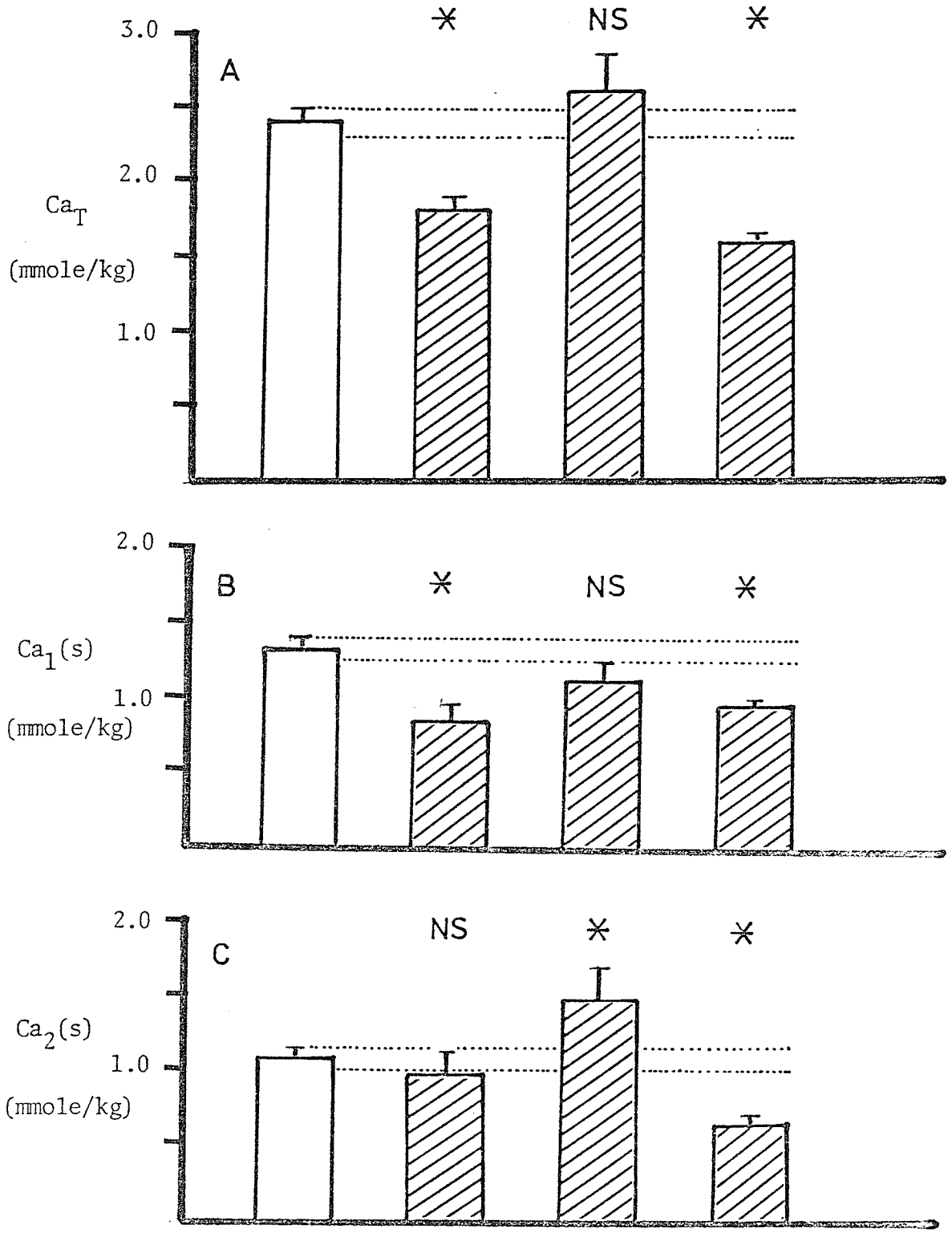
3.0
2.0
1.0
A
Ca_T
(mmole/kg)
*
NS
*
2.0
1.0
B
Ca_1(s)
(mmole/kg)
*
NS
*
2.0
1.0
C
Ca_2(s)
(mmole/kg)
NS
*
*
Pre-clinic
Myolytic
Hypertrophic-necrotic

the in-series model, when normalized by the wet heart weight, has a unit of sec^{-1} and is an index of the rate of Ca extraction from the perfusate. K_{01} may be termed the Ca influx coefficient.

There was no statistically significant difference in the apparent $t_{\frac{1}{2}}$ of both $Ca_1(s)$ and $Ca_2(s)$ between the normal and cardiomyopathic hearts (Figures 32A & B). The Ca influx coefficient K_{01} tended to be depressed in the cardiomyopathic hearts (Figure 33). However, this was statistically significant only in the hypertrophic-necrotic (53 d) age group.

The Ca uptake profile of the 220 d cardiomyopathic hearts showed few differences but a tendency toward general depression throughout the collection period as compared to the normal age matched control (Figure 34). Total Ca extracted was significantly less in the cardiomyopathic hearts (Table 15). The 220 d normals accumulated more Ca ($P<0.05$) than the young normals. The reduction in the Ca content of $Ca_1(s)$ in the 220 d cardiomyopathic hearts was responsible for the depression of total uptake. There was no difference in the size of $Ca_2(s)$ (Table 15). The apparent $t_{\frac{1}{2}}$ of $Ca_1(s)$ was faster in the cardiomyopathic hearts whereas there appeared to be no difference for $Ca_2(s)$. The Ca influx coefficient appeared to be the same for the normals and the cardiomyopathics (Table 15).

5. Serum Ca and Mg in young hamster

The water and electrolyte alterations during the life course of the BIO 14.6 Syrian hamsters have been well

Figure 32

Apparent $t_{\frac{1}{2}}$ of $Ca_1(s)$ and $Ca_2(s)$ in the uptake studies of the young normal and cardiomyopathic hamster hearts

Open rectangles represent data from pooled 26-60 d normals. Shaded rectangles represent cardiomyopathics. Vertical bars indicate standard error of the mean. Broken lines encompass the standard error of control.

Panel A: Comparison of apparent $t_{\frac{1}{2}}$ of $Ca_1(s)$.

Panel B: Comparison of apparent $t_{\frac{1}{2}}$ of $Ca_2(s)$.

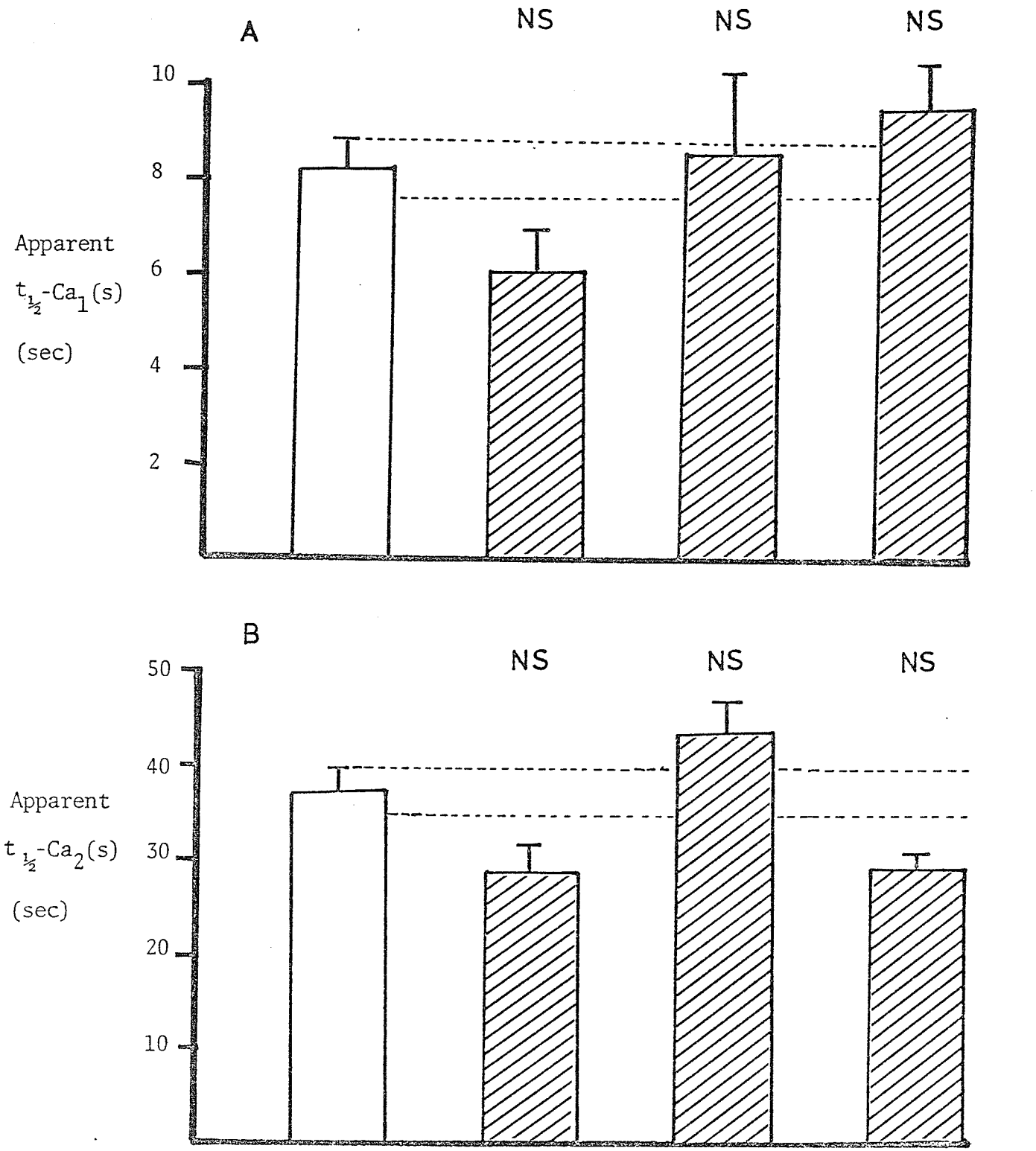
A
NS
NS
NS
10
8
6
4
2
Apparent
$t_{1/2}$-Ca_1(s)
(sec)
B
NS
NS
NS
50
40
30
20
10
Apparent
$t_{1/2}$-Ca_2(s)
(sec)
Pre-
clinic
Myolytic
Hypertrophic-
necrotic

Figure 33

The Ca influx coefficient, K_{01}, of the young normal and cardiomyopathic hamster hearts

Open rectangles represent data from pooled 26-60 d normals. Shaded rectangles represent cardiomyopathics. Vertical bars indicate standard error of the mean. Broken lines encompass the standard error of control.

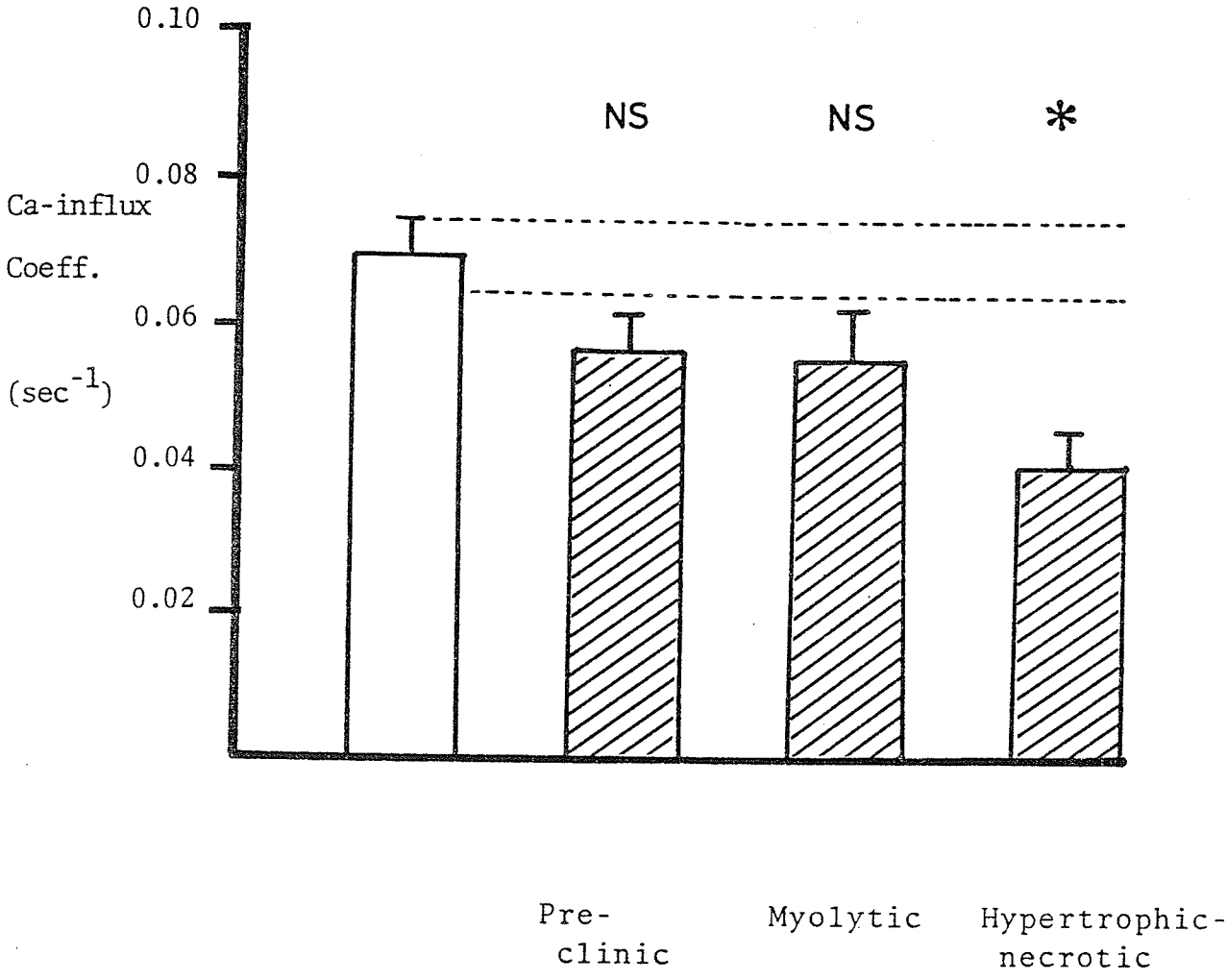
0.10
0.08
0.06
0.04
0.02
Ca-influx
Coeff.
(sec-1)
NS
NS
*
Pre-
clinic
Myolytic
Hypertrophic-
necrotic

Figure 34

Comparison of Ca uptake profile of the 220 d normal and cardiomyopathic hamster hearts.

Solid circles and solid line (●———●) indicate 220 d normals. Open circles and broken line (o-----o) indicate 220 d cardiomyopathics. Vertical bars represent standard error of the mean.

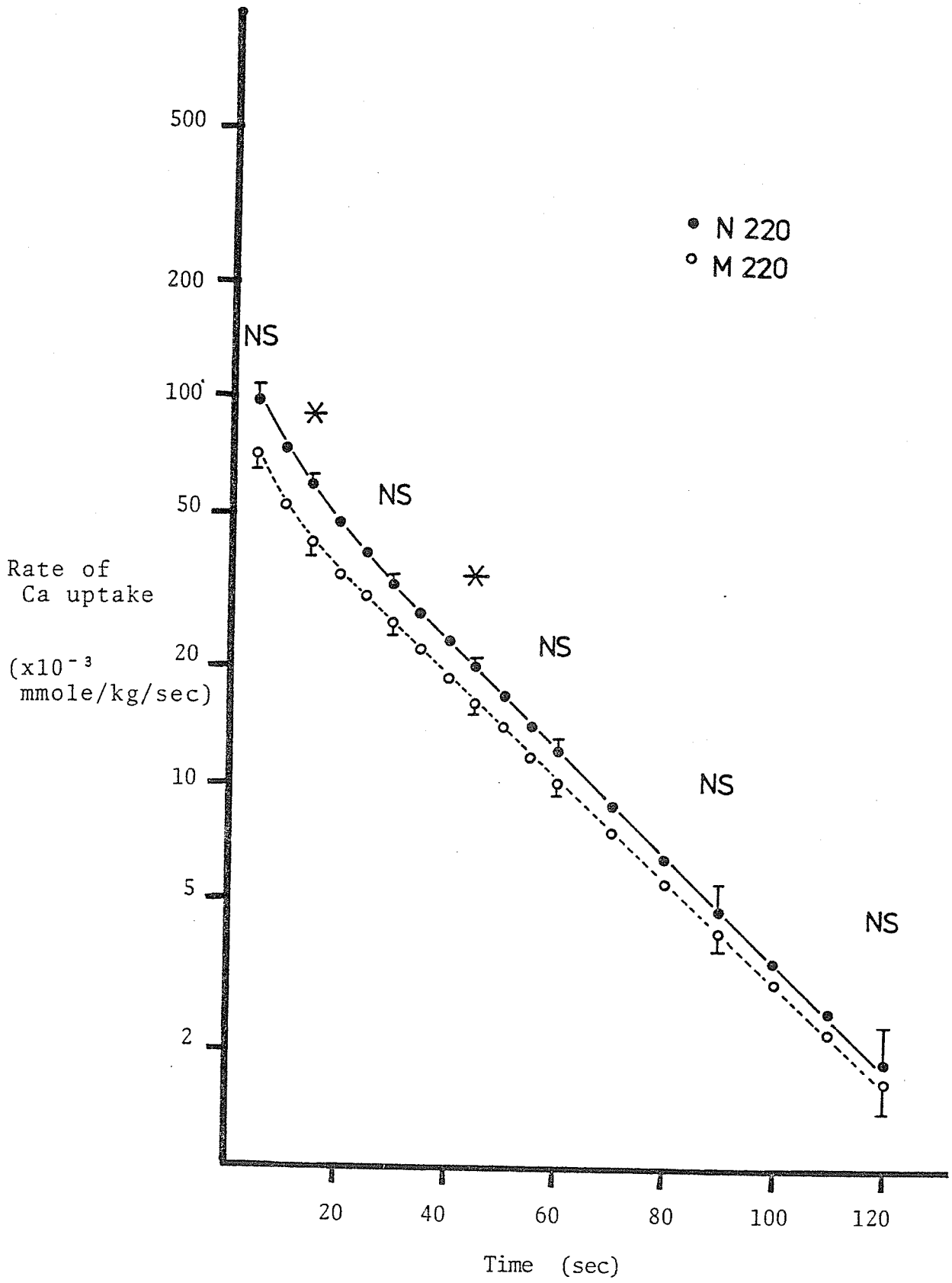
500
200
100
50
20
10
5
2
Rate of
Ca uptake
(x10⁻³
mmole/kg/sec)
N 220
M 220
NS
NS
NS
NS
NS
*
*
20
40
60
80
100
120
Time (sec)

Table 15

Ca content and exchange kinetics in the uptake studies of 220 day age old normal and cardiomyopathic hearts

	Normal	Cardiomyopathic	Statistical significance[b]
Content (mmole/kg)			
Ca_T (uptake)	3.29±0.16[a]	2.47±0.23	*
Ca_1 (s)[b]	1.90±0.28	0.90±0.14	*
Ca_2 (s)[c]	1.40±0.28	1.56±0.23	N.S.
Apparent $t_{1/2}$ (sec)			
Ca_1 (s)	9.3 ±1.6	4.5 ±1.4	*
Ca_2 (s)	26.2 ±2.9	22.0 ±1.7	N.S.
Ca-influx coefficient (sec^{-1})			
K_{01}	0.085±0.014	0.081±0.013	N.S.

[a] mean ± SEM

[b] t-test for 2 means with equal variance
N.S. = $P>0.05$
* = $P\leq 0.05$

documented (Cantin et al. 1972; Lossnitzer and Bajusz, 1974). A significant increase in serum Ca was already present in the youngest animals (10-25 d) and persisted up to the 60 d. In contrast, there was no difference in the serum Mg level at the young age. Serum Ca and Mg were examined as early as one week after birth to determine if electrolyte abnormalities occured which might contribute to the development of cardiac lesion. The results are summarized in Table 16. In contrast to the other reports, no statistically significant changes in serum Ca or Mg level at the pre-clinic stage were observed.

6. Serum sialic acid concentration

Serum sialic acid concentration was examined in four groups of hamsters : normal 120 d, 300 d, cardiomyopathic 250 d, and 300-400 d. The serum was deproteinized with equal volume of 10% TCA. Sialic acid assay values were appropriately corrected for TCA quenching of fluorescence. The results are summarized in Table 17. About 16-20 nmole of sialic acid per ml of serum were found in all of the groups studied. There was no statistical differences between the normals and cardiomyopathics.

C. Isolated sarcolemmal preparation

1. Morphology of the isolated membrane fragments

The initial suspension of cell fragments, after brief homogenization as described in Methods, consisted of 4-6 cell fragments with prominent cross striations (Figure 35A).

Table 16

Serum Ca and Mg in young hamster

Serum Ca (mM)

Age	Normal	Myopathic	Statistical significance[b]
7 d	2.22±0.05[a]	2.22±0.04	N.S.
14 d	2.42±0.06	2.44±0.11	N.S.
30 d	2.64±0.17	2.83±0.30	N.S.

Serum Mg (mM)

Age	Normal	Myopathic	Statistical significance
7 d	1.51±0.18	1.40±0.09	N.S.
14 d	1.05±0.05	1.23±0.07	N.S.
30 d	-	-	-

[a] mean ± SEM

[b] t-test for two means with equal variance
N.S. = P>0.05

Table 17

Serum sialic acid concentration

	nmole/ml	t-test
Normal 130 d	16.9±0.6 (27) [a]	
Myopathic 250 d	16.4±1.2 (10)	P>0.05
Normal 300 d	17.9±1.6 (5)	
Myopathic 300-400 d	20.5±0.9 (10)	P>0.05

[a] number of animals

Figure 35

Morphology of the isolated membrane fragments

Panel A: The 20 g-min supernatant after initial brief homogenization. The suspension consists of 4-6 cell fragments with prominent cross striations.

Panel B: A suspension of the 50,000 g-min pellet after osmotic shock and two hrs of salt extraction. The cross striations are removed although particulate matter can still be observed.

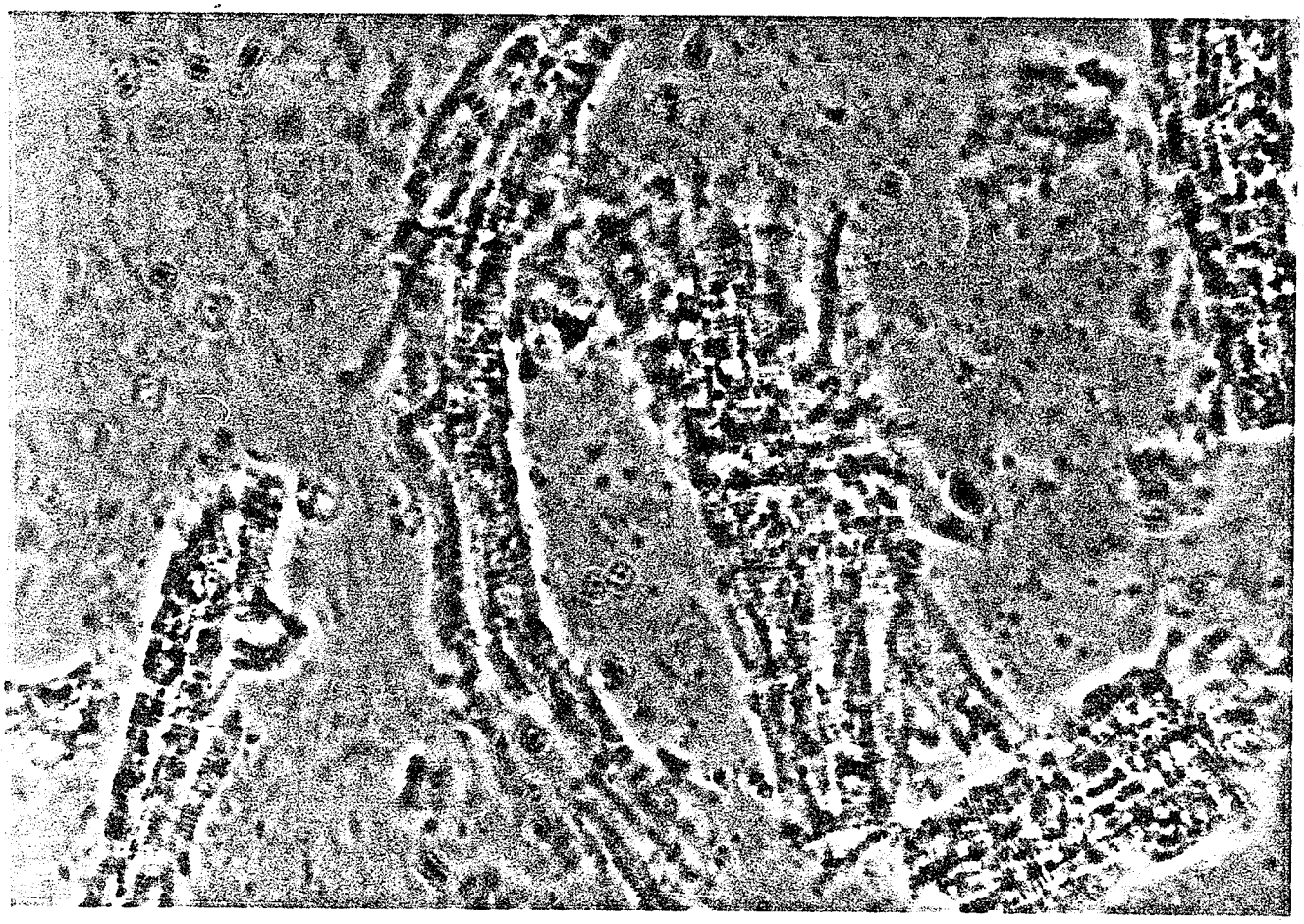

(A)

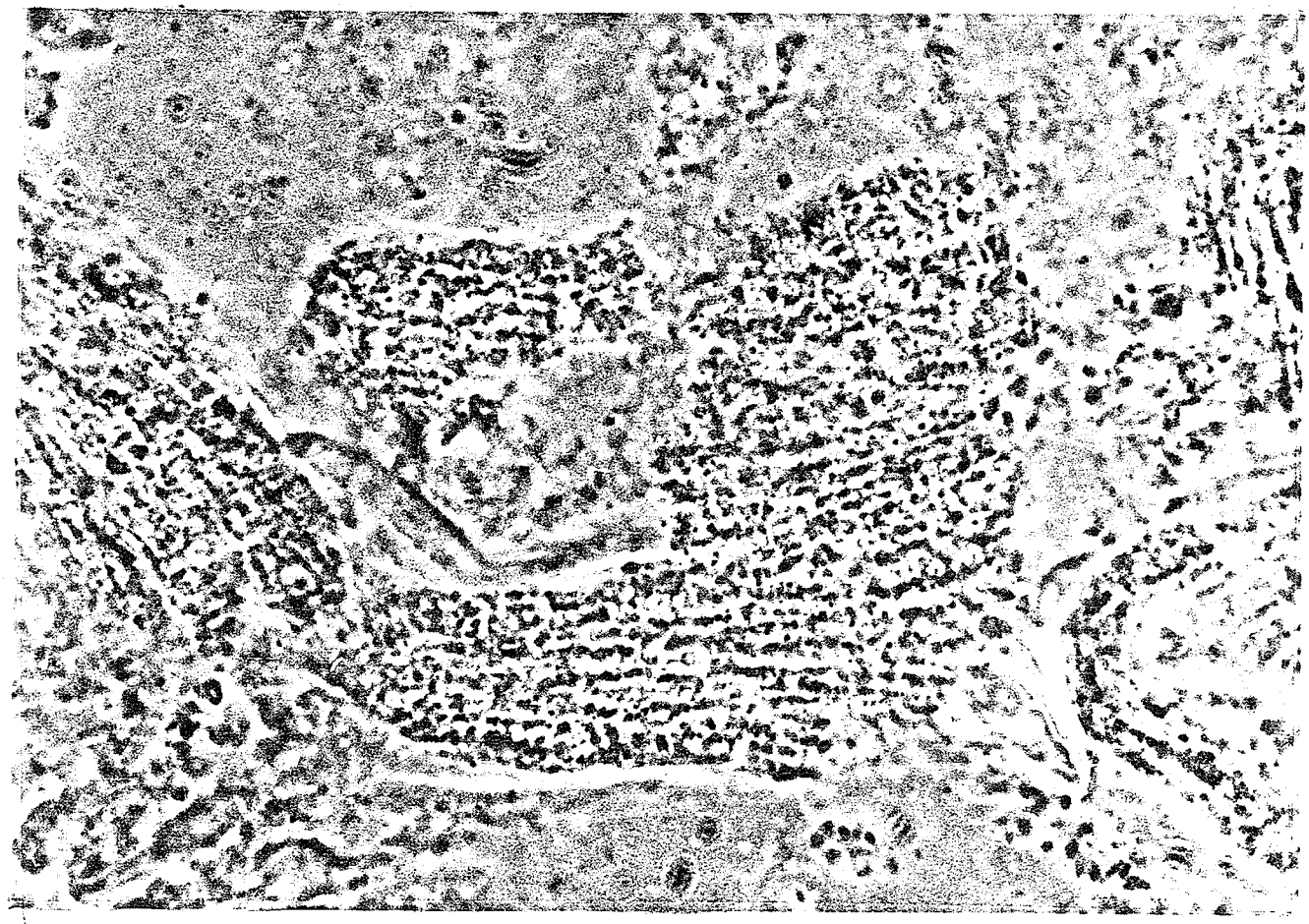

(B)

After osmotic shock and salt extraction, the cross striations were removed although particulate matter could still be observed throughout the preparation (Figure 35B). Gross cell shape was maintained in the final preparation.

2. Evidence for an enriched sarcolemmal fraction

(a) Yield of protein through the procedures

Initial homogenate in 1:10 w/v suspension amounted to 63.4 ± 6.7 mg protein per g of starting wet heart ventricle (Table 18). In contrast to the more than 50% reduction of cell protein by osmotic shock in the guinea pig heart preparation (Tada et al. 1972), this step removed less than 20% protein from the hamster heart homogenate.

Salt extraction of the after-shock sample removed the major proportion of protein. The removal of the cross striations suggests the major source of loss was the contractile protein. Preliminary experiments indicated that two hours of salt extraction removed as much protein as the 16 hr specified in the original method. The final yield was 4.7 ± 0.9 mg protein/g which was about 7% of the initial homogenate protein and approximated the yield of the original method (8%). The amount of final yield in mg/g depends upon how thorough one is in the initial homogenization process. Myopathic hearts also yielded about 7% of the initial homogenate protein as the sarcolemmal enriched fraction.

(b) ATPase activities as the sarcolemmal marker

The ATPase activities of the preparation during

Table 18

Protein yields form normal hamster hearts

Preparation	Yield (mg protein/g ventricle)
initial homogenate	63.4 ± 6.7 (100%)
after shock preparation	49.9 ± 5.3 (79%)
after extraction preparation	4.7 ± 0.9 (7.4%)

different stages of isolation are summarized in Table 19. Mg-ATPase activity (basal ATPase activity) was higher in the initial homogenate but was progressively decreased by each step of isolation. Very low to non-existent amounts of Na, K-activated ATPase activity were detected in the initial homogenate. The activity increased to a mean of 5.1 µmole P_i liberated per mg protein per hr in the final preparation. The variation of the data was large as shown by the standard error of 1.5 µmole P_i per mg per hr. Similarly, the ouabain (1 mM) sensitive Na, K-ATPase activity was very low and variable.

The ATPase activity of the initial homogenate, from one experiment each of normal (80 d) and cardiomyopathic (80 d) hamster hearts, together with that of the rat brain synaptosome preparation kindly provided by Dr. T. White of Dalhousie University, were examined under the influence of azide, veratridine, tetrodotoxin (TTX), prolonged cold incubation and a combination of the above(Table 20 & 21).

More than 60% (mean=63%) of the basal ATPase activities of the initial cardiac homogenate were mitochondrial in origin. In contrast, only 22% of the basal ATPase activity in the brain synaptosomes was contributed by mitochondria (Table 20). Cold incubation produced opposite effects in these two tissues. In cardiac cell fragments, the total basal ATPase activities were reduced to about 70% of the control, and the azide sensitive fraction was reduced to 56% of the total.

Table 19

ATPase activities of the preparation* at different stages of isolation

	Mg-ATPase (basal ATPase)	Na,K-activated ATPase	Ouabain Sensitive Na,K -ATPase
	(μmole P_i liberated/mg protein/hr)		
Initial homogenate	38.3±7.6	0.7±0.6	1.8±1.4
After shock preparation	35.0±5.8	4.6±1.9	5.1±1.6
After extraction preparation	22.7±4.2	5.1±1.5	3.2±1.0

* from 110-300 day normal hearts

Table 20

ATPase activities under various conditions*
(μmole P_i /mg/hr)

	Hamster cardiac cell fragments		Rat Synaptosomes
Control	Normal (80d)	Myopathic (80d)	
basal/(azide-sensitive, %)	24.8/(66%)	42.0/(60%)	13.6/(22%)
Na,K-activated	0	1.2	9.3
ouabain sensitive	0	0	10.4
Veratridine treated			
basal	25.6	42.4	11.7
Na,K-activated	0	4.0	10.9
ouabain sensitive	0.4	3.2	10.1
Veratridine + TTX			
basal	24.0	43.2	15.2
Na,K-activated	0.4	2.4	11.5
ouabain sensitive	0	0	8.0

* basal = Na 120 mM, Tris 50 mM, pH 7.4, MgATP 4 mM
alcohol 2% (used as solvent for ouabain and veratridine)

azide sensitive = basal rate - azide treated

Na,K-activated = (Na 100 mM, K 20 mM) - basal rate

ouabain sensitive = (Na 100 mM, K 20 mM) - (Na 100 mM, K 20 mM, ouabain 1 mM)

veratridine = 0.1 mM

TTX = 1 μM

Table 21

ATPase activities under various conditions* (μmoles P_i/mg/hr) after 4 hours 4°C incubation with substrates and reagents (activity assayed at 37°C)

	Hamster cardiac cell fragments		Rat Synaptosomes
Control	Normal (80d)	Myopathic (80d)	
basal/(azide-sensitive, %)	18.6/(57%)	28.2/(55%)	17.3/(26%)
Na,K-activated	0.2	0.4	9.9
ouabain sensitive	0.8	-no data-	9.3
Veratridine treated			
basal	17.6	27.6	21.3
Na,K-activated	2.0	2.8	6.7
ouabain sensitive	2.0	4.0	10.1
Veratridine + TTX			
basal	19.6	25.8	19.2
Na,K-activated	0	0	9.9
ouabain sensitive	0	0	8.8

* basal = Na 120 mM, Tris 50 mM, pH 7.4, MgATP 4 mM, alcohol 2% (used as solvent for ouabain and veratridine)

azide sensitive = basal rate - azide treated

Na,K-activated = (Na 100 mM, K 20 mM) - basal rate

ouabain sensitive = (Na 100 mM, K 20 mM) - (Na 100 mM, K 20 mM ouabain 1 mM)

veratridine = 0.1 mM

TTX = 1 μM

This indicated that the major loss of the ATPase activities was from that contributed by mitochondria. In contrast, cold incubation produced an increase of basal ATPase activities in the synaptosome from 13.6 to 17.3 μmole/mg/hr and an increase of azide sensitive fraction from 22 to 26%. There was little Na, K-activated and ouabain sensitive ATPase activity in the cardiac cell fragments, confirming the previous observation (Table 19). Pronounced activation by Na and K, on the other hand, was observed in brain synaptosomes. This activation was blocked by ouabain. Cold incubation itself produced minimal effects on Na, K-ATPase activities in both the cardiac and synaptosomal preparations. Veratridine produced no consistent effects on basal ATPase activities either in synaptosomal or cardiac cell preparation. At a concentration of 0.1 mM, which has been shown to depolarize the synaptosomal preparation (White, 1977), veratridine produced no consistent stimulation of Na, K-activated, ouabain sensitive, ATPase activities of this tissue preparation (Table 20 & 21). In contrast, there appears to be a consistent stimulation of Na, K-ATPase activities by veratridine on cardiac cell fragments. This stimulation appeared to be augmented by prolonged cold incubation and blocked by TTX.

(c) Sialyltransferase activity

The first objective was to establish that the assay system according to the method of Bernacki (1975) worked. Serum and liver provided two known sources of sialyltransferase. The incorporation of ^{14}C-sialic acid by the phospho-

tungstic acid insoluble asialofetuin was taken as a functional assay of the enzyme activity in the CMP-sialic acid:asialofetuin: sialyltransferase system. The results from an experiment using normal hamster indicated the assay was indeed capable of measuring the enzyme activity (Table 22). Preliminary experiments with cardiac cell preparations indicated no enrichment of enzyme activities with each step of isolation and in fact salt extraction appeared to diminish the final specific activity. Because of this, sialyltransferase activity of the homogenate was taken as the total cell capacity for the catalytic transfer of sialic acid. Because the initial experiments indicated very low enzyme activity of the cardiac cell preparation, it was necessary to validate the presence of this system further in the preparation. If increasing incorporation of radioactivity followed increasing periods of incubation then one could more confidently rule out the factor of artifact, such as that due to non-specific tracer trapping by the protein. Two such experiments with 200-300 d normal and cardiomyopathic cardiac cell fragment preparations indicated that although the enzyme activity was low, total accumulation of the tracer nonetheless increased linearly for the first 2 hr (Figure 36).

UDP (1 mM) inhibited the sialyltransferase activity (Table 23). Orotate at the same concentration increased the enzyme activity. Various modifications of the medium cation composition did not result in increase of sialyltransferase activity (Table 23).

Table 22

The CMP-sialic acid:asiolofetuin:sialyltransferase system

	CMP-sialic acid incorporation*
Liver homogenate	1 pmole sialic acid/mg protein/hr
Plasma	3.7 pmole sialic acid/ml plasma /hr

*enzyme activity assayed in the absence of Mg & Mn.

Figure 36

Sialyltransferase activity from 200-300 d normal (●) and cardiomyopathic (o) hearts as a function of duration of incubation

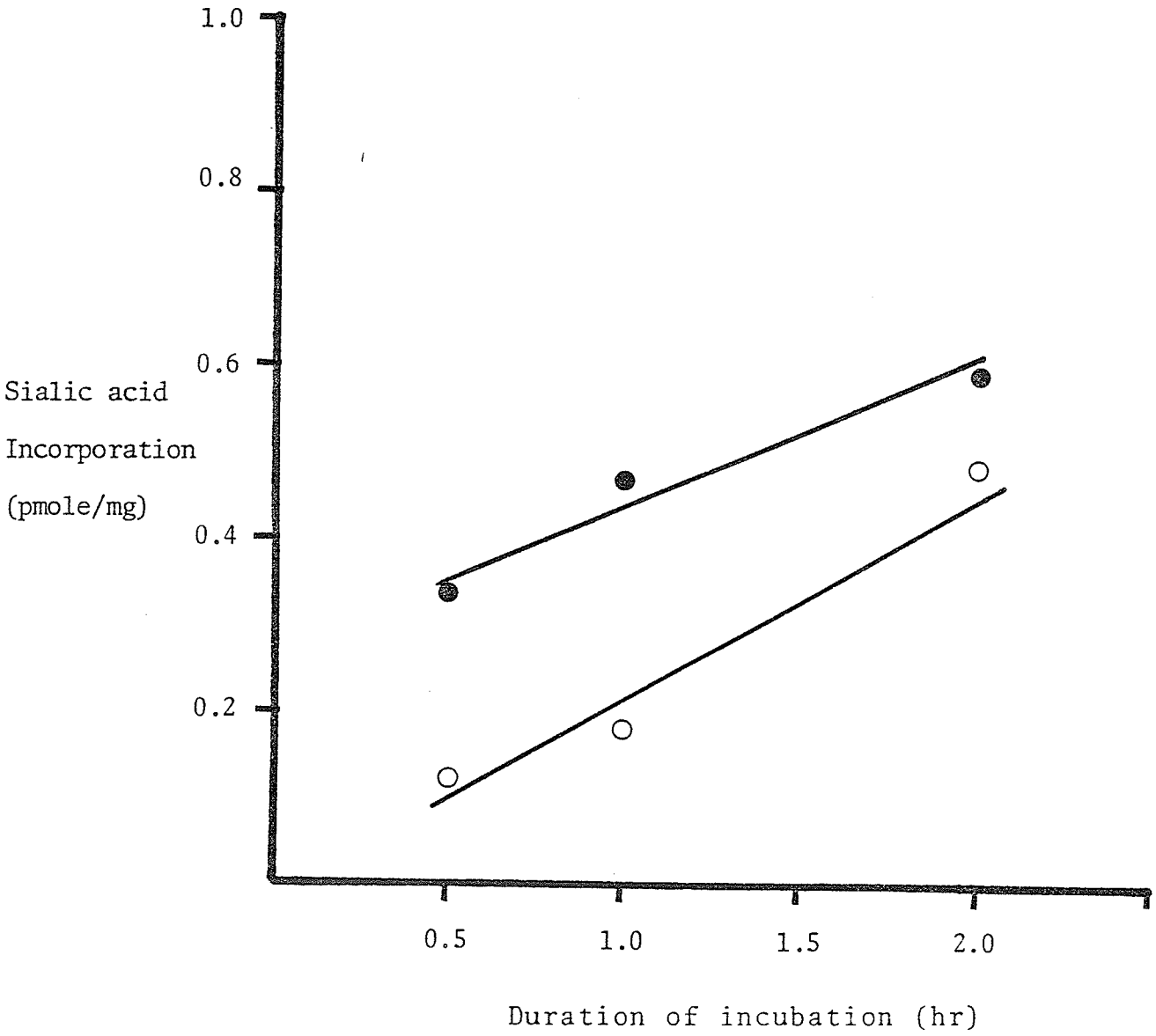
1.0
0.8
0.6
0.4
0.2
Sialic acid
Incorporation
(pmole/mg)
0.5
1.0
1.5
2.0
Duration of incubation (hr)

Table 23

Ionic and substrate influences on sialyltransferase activity of the cardiac cell fragments

	Treatment	Activity (pmole/mg/hr)	Δ Activity (pmole/mg/hr)
N-200 d	control[a]	0.44	-
	UDP 1 mM	0.18	- 0.26
	orotate 1 mM	0.48	+ 0.04
M-300 d	control[a]	0.62	-
	UDP 1 mM	0.35	- 0.27
	orotate 1 mM	0.89	+ 0.27
N-200 d	control[a]	1.40	-
	cation[b]- 100 mM Na	0.82	- 0.58
	cation[b]- 100 mM K	0.97	- 0.43
	cation[b]- 2 mM Ca	1.48	+ 0.08

[a] Control cation: Mg 10 mM, Mn 10 mM

[b] Control cation replaced by the specified cation

The sialyltransferase assay of the normal and cardiomyopathic (200-300 d) cardiac cell fragments indicated very low activity (Table 24). The sialyltransferase activity was lower in the cardiomyopathic hamster cardiac cell preparation but the difference was not statistically significant.

(d) Sialic acid concentration

Initial experiments indicated that TCA interfered with the spectrofluorometric assay of sialic acid (Figure 37). TCA linearly decreased the detectable sialic acid content such that every 100 µl of 10% TCA in the assayed sample caused a 12.5% reduction. The mechanism of this interference is not known. In any case, when TCA was used to precipitate protein, appropriate corrections were made for the estimation of sialic acid content.

Sucrose gives a false positive reaction in the spectrofluorometric assay of sialic acid. This precluded quantification of the soluble or released sialic acid content in the supernatant of the shock as well as the extraction mediums. In contrast to the pinkish color of the sialic acid reaction product, sucrose gives off a bright yellow color which also fluoreses at 570 nm. The spectrofluorescent profile of increasing concentration of sucrose (Figure 38) shows that 20 µl of 10% sucrose produces as much fluorescence as 1 nmole of sialic acid. Corresponding amounts of glucose solution (also in % solution, although it is at a higher molar concentration) produces little or no fluorescent material.

Table 24

Sialyltransferase activity of the cardiac cell fragments from the normal and cardiomyopathic hearts

Preparation (200-300 d)	Activity (pmole/mg/hr)
Normal	0.72±0.23 (3)
Cardiomyopathic	0.41±0.12 (3)
	P>0.05[a]

[a] t-test of two means with equal variance

Figure 37

TCA interference of the spectroflurometric assay of sialic acid. All samples contain 4 nmole sialic acid. Data points show apparent sialic acid reading with different amount of 10% TCA added.

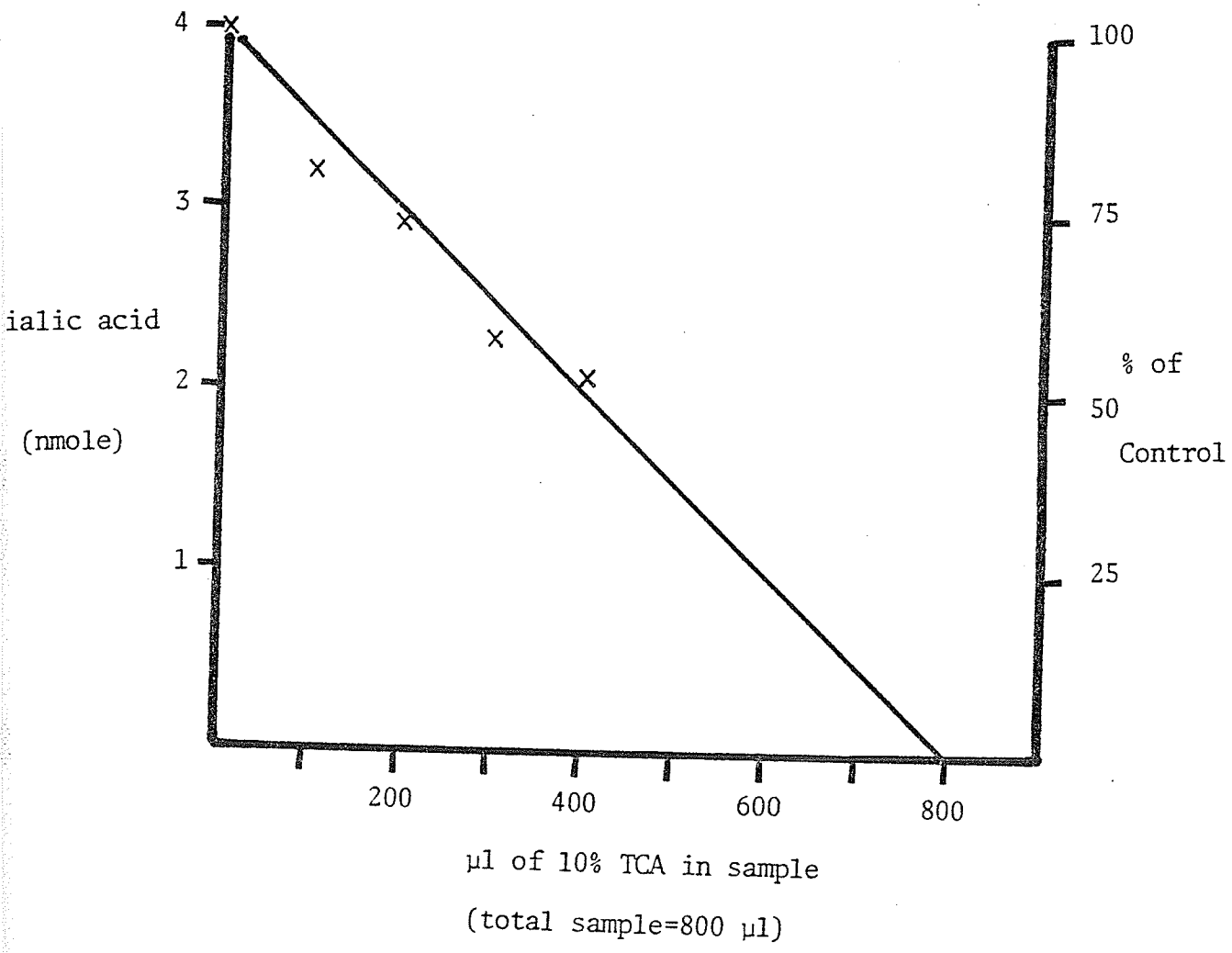
4
3
2
1
ialic acid
(nmole)
100
75
% of
50
Control
25
200
400
600
800
µl of 10% TCA in sample
(total sample=800 µl)

Figure 38

Sucrose and glucose interference with the spectrofluorometric assay of sialic acid.

(o) = sialic acid standard

(●) = 10% sucrose

(x) = 10% glucose

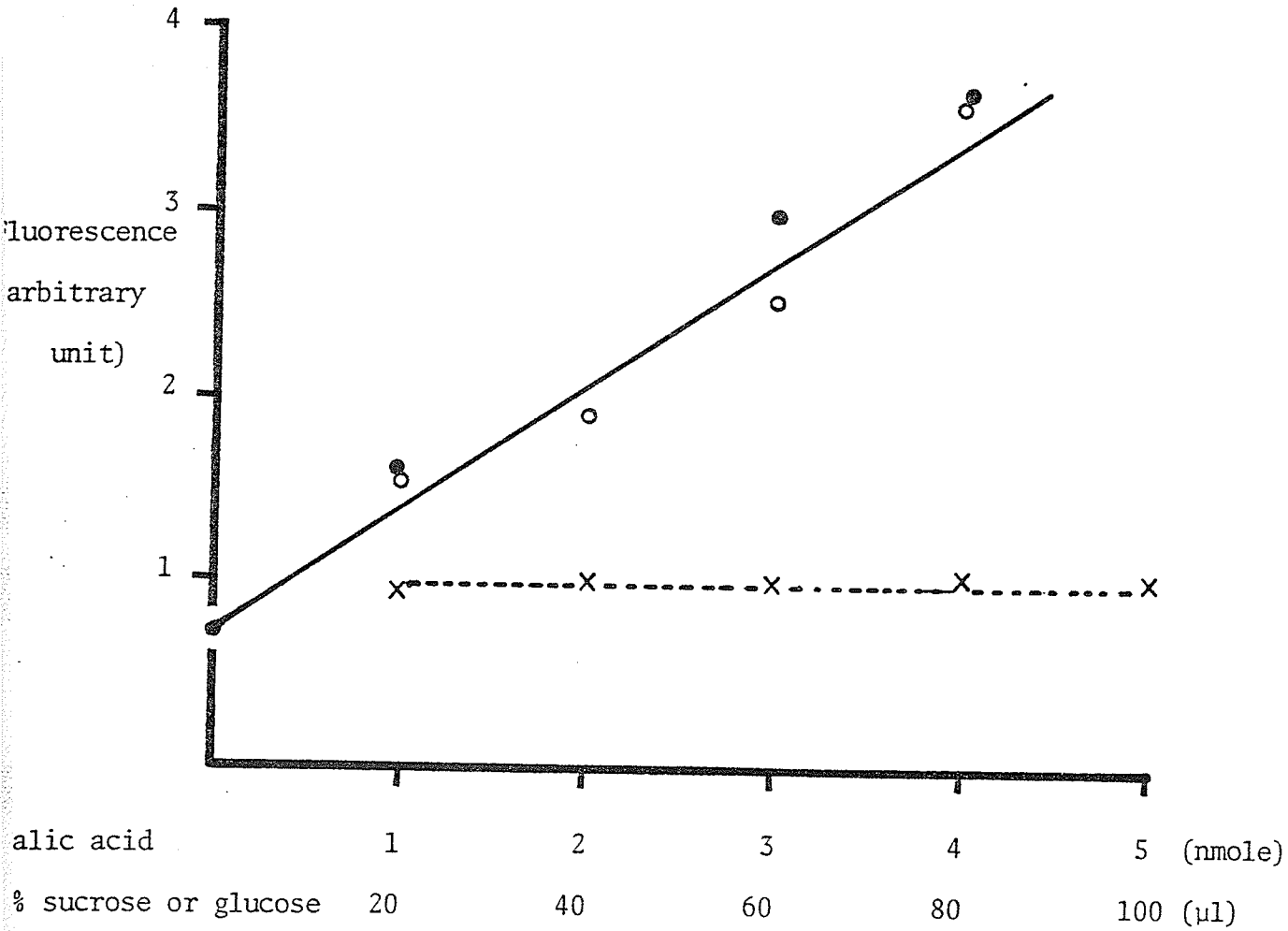
4
3
luorescence
arbitrary
unit)
2
1
alic acid 1 2 3 4 5 (nmole)
% sucrose or glucose 20 40 60 80 100 (µl)

Examination of the sialic acid content of the membrane fraction indicated two to three fold enrichment in the final sarcolemmal preparation from the normal hearts (Table 25). Enrichment in the myopathic hearts was not observed in the few experiments performed. Considerable variation was observed from experiment to experiment. This was probably due to the vary labile nature of the glycoprotein.

One experiment using normal and cardiomyopathic whole heart homogenates indicated the presence of an enzyme system active at pH 7.4 which was capable of hydrolyzing 80% of the sialic acid residues of extraneously added mucin in 2 hrs (Table 26). Spontaneous degradation of mucin at this pH and this length of time period was ruled out with control studies which showed negligible hydrolysis.

3. Ca binding

In previous section it was indicated that significant Ca binding to the glass and plastic connections of the perfusion apparatus occured which must be corrected before the kinetic data of Ca exchange could be interpreted. Therefore, Ca binding could also occur to the polyethylene incubation tubes used to assess Ca binding to the isolated sarcolemmal fraction.

(a) Ca binding to incubation tube

That quantity of Ca bound to the test tubes was evident from an experiment in which a fixed amount of ^{45}Ca was put into a series fo tubes which contained different concentration of ^{40}Ca. After equilibration, aliquots of the sample were

Table 25

Sialic acid content of membrane fraction

	Sialic acid (nmole/mg protein)	
	Homogenates	Sarcolemma
Normal 50 d	100	254
Normal 60 d	92	-
Normal 110 d	-	210
Normal 120 d	-	110
Normal 180 d	-	176
Normal 180-200 d	-	115
Normal 180-200 d	-	187
Normal 300 d	144	380
Myopathic 25 d	76	-
Myopathic 200-300 d	98	77
Myopathic 250 d	85	99
Myopathic 300 d	99	77

Table 26

Neuraminidase activity of the whole heart homogenate

	sialic acid hydrolyzed[a] nmole ; (% of total sialic acid residues)	
	½ hr	2 hr
normal homogenate[b] (0.163 mg)	13.1 (83.7%)	15.1 (96.5%)
myopathic homogenate[c] (0.158 mg)	12.1 (88.0%)	11.0 (80.0%)
normal homogenate (0.163 mg) + mucin (0.065 mg)[d]	16.5 (63.3%)	21.0 (80.6%)
myopathic homogenate (0.158 mg) + mucin (0.065 mg)	11.4 (47.2%)	17.4 (72.1%)

[a] Tris 5 mM, pH 7.4, 37°C

[b] 96 nmole sialic acid/mg protein

[c] 87 nmole sialic acid/mg protein

[d] 160 nmole sialic acid/mg protein

counted. The results are shown in Figure 39. The asymptototic increase in medium ^{45}Ca counts on a semi-logarithmic plot with increasing medium concentrations of ^{40}Ca indicates progressive displacement of ^{45}Ca from test tube binding sites by ^{40}Ca. In a different experiment with lower ranges of ^{40}Ca concentrations, the degree of ^{45}Ca binding to the test tubes was even more pronounced (Figure 40). The binding profile was not altered when either Li or K replaced Na in the medium.

Test tube binding of Ca cannot be corrected simply by subtracting the binding in the absence of the tissue from that in the presence of the tissue. The situation consists of two or more binding sites (one supplied by the test tube, one or more supplied by sarcolemmal preparation in equilibrium with the Ca ion).Thus the total amount of Ca avaiable for test tube binding is different in the absence as compared to the presence of tissue for a given total Ca input. This factor cannot be ignored when one or more binding sites can bind significant amounts of Ca as is true in this case, both with respect to sarcolemma and test tube.

The extraction values, or the total ^{45}Ca input minus the amount in medium after equilibration, could be plotted in the form of Scatchard plot and resolved into its two components with the computer program SKATCH.MB (Appendix 8B). However, one could not differentiate what was contributed by the test tube binding sites and what was contributed by the tissue binding sites. This problem was somewhat circumvented, in the studies of Ca binding to sarcolemmal membranes,

Figure 39

^{45}Ca displacement from test tube binding sites by increasing concentration of ^{40}Ca.

The medium contains 100 mM Na.

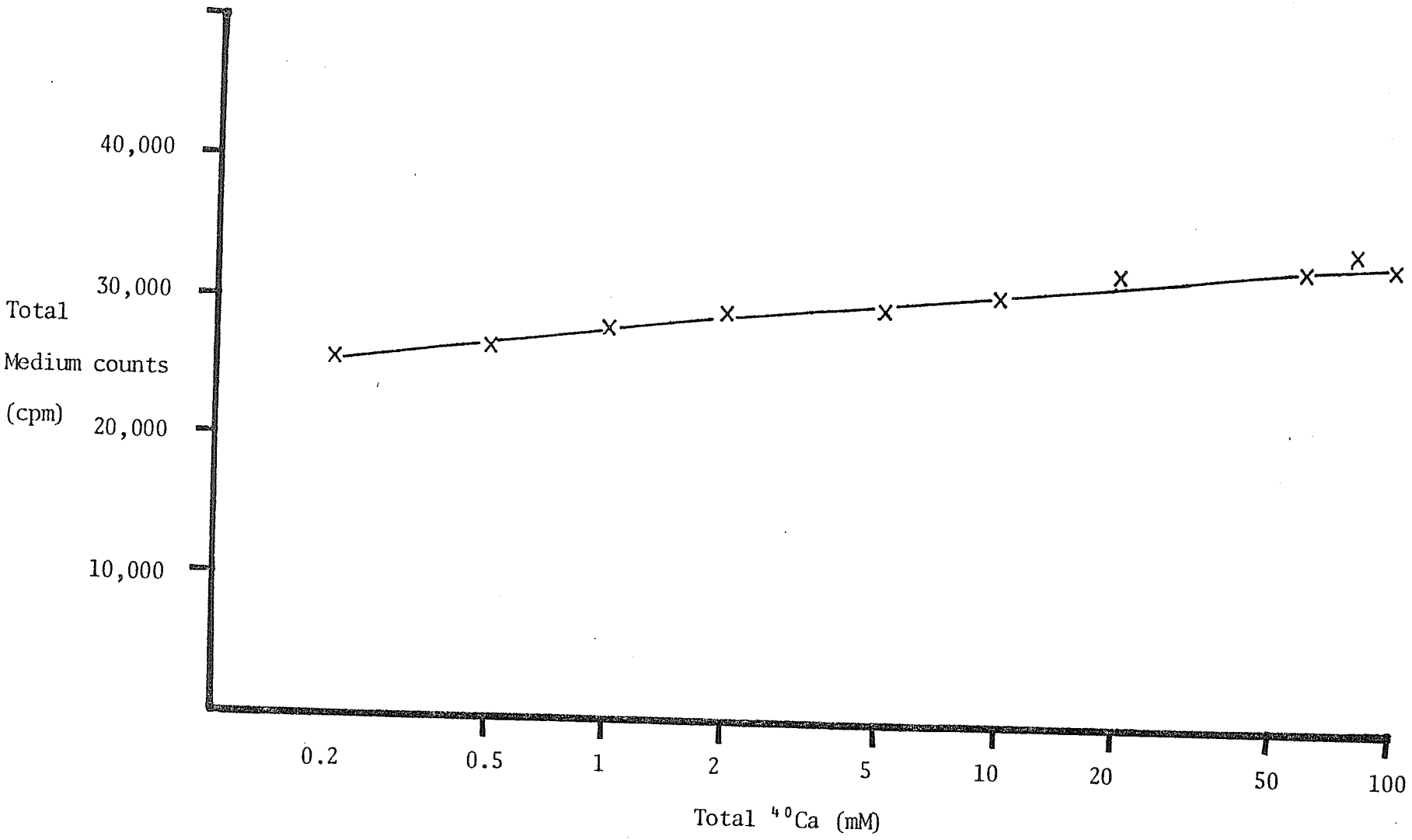
40,000
30,000
Total
Medium counts
(cpm)
20,000
10,000
0.2
0.5
1
2
5
10
20
50
100
Total ^{40}Ca (mM)

Figure 40

^{45}Ca displacement by ^{40}Ca from test tubes in the presence of different cations.

Closed circles (●) indicate 100 mM Li. Open circles (o) indicate 100 mM Na. Crosses (x) indicate 100 mM K.

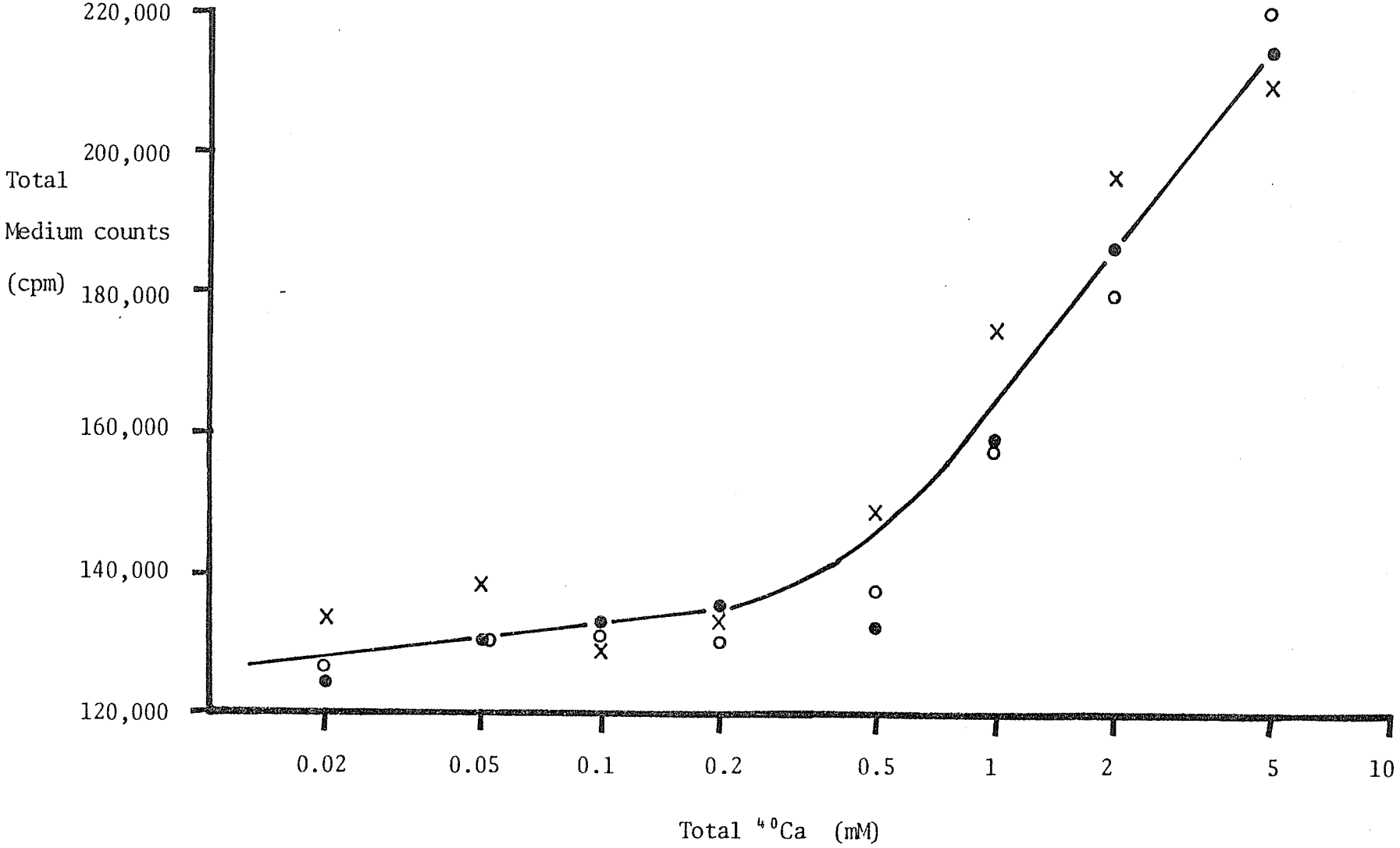
220,000
200,000
Total
Medium counts
(cpm)
180,000
160,000
140,000
120,000
0.02
0.05
0.1
0.2
0.5
1
2
5
10
Total ^{40}Ca (mM)

by dissolving the sarcolemmal pellet in a small volume of NaOH (see Methods), thus minimizing the contamination from ^{45}Ca bound to the test tube. Total free Ca at each total concentration of Ca, however, was lower, due to the binding by test tube, than if the test tube binding was absent. The end result was an overestimation of the bound to free atio (B/F) in Scatchard plot of the Ca binding to cardiac sarcolemma at low Ca concentration, when significant percentage of total input Ca was bound by test tube. At high concentrations of Ca this factor was less important as the percentage of free Ca to total Ca was large.

(b) Ca binding to mucin and fetuin

Figure 41 shows the Scatchard plot of Ca binding to mucin. The smooth curve is the least square best fit of the data points using the computer program SKATCH.MB. The program resolves the curve into two components. The low affinity binding site has a maximal binding capacity of 378.5 nmole of Ca per mg protein and has a dissociation constant(K_D) of 5.87 mM. The high affinity binding site has a maximal binding capacity of 6.5 nmole of Ca per mg protein and has a K_D of 0.039 mM. The results of this experiment indicate substantial Ca binding by a sialic acid-rich protein (mucin contains 160 nmole sialic acid residues per mg protein). The apparent 2:1 relationship between Ca bound and sialic acid residues is misleading as not all bindings are due to Ca-sialic acid interaction (see below for Ca binding to fetuin).

Figure 41

Scatchard plot of Ca binding to mucin

The smooth curve is the least square best fit of the data points using the computer program SKATCH.MB. The total reaction medium volume was 10 ml: 9 ml outside the dialysis bag and 1 ml within. The mucin concentration within the dialysis bag is 0.65 mg/ml. Data points represent Ca binding at total ^{40}Ca concentration of 20, 50, 100, 200, 500 µM, 1, 2, and 3 mM.

R=(bound Ca per mg)/(free Ca per l)

B= bound Ca in nmole/mg protein

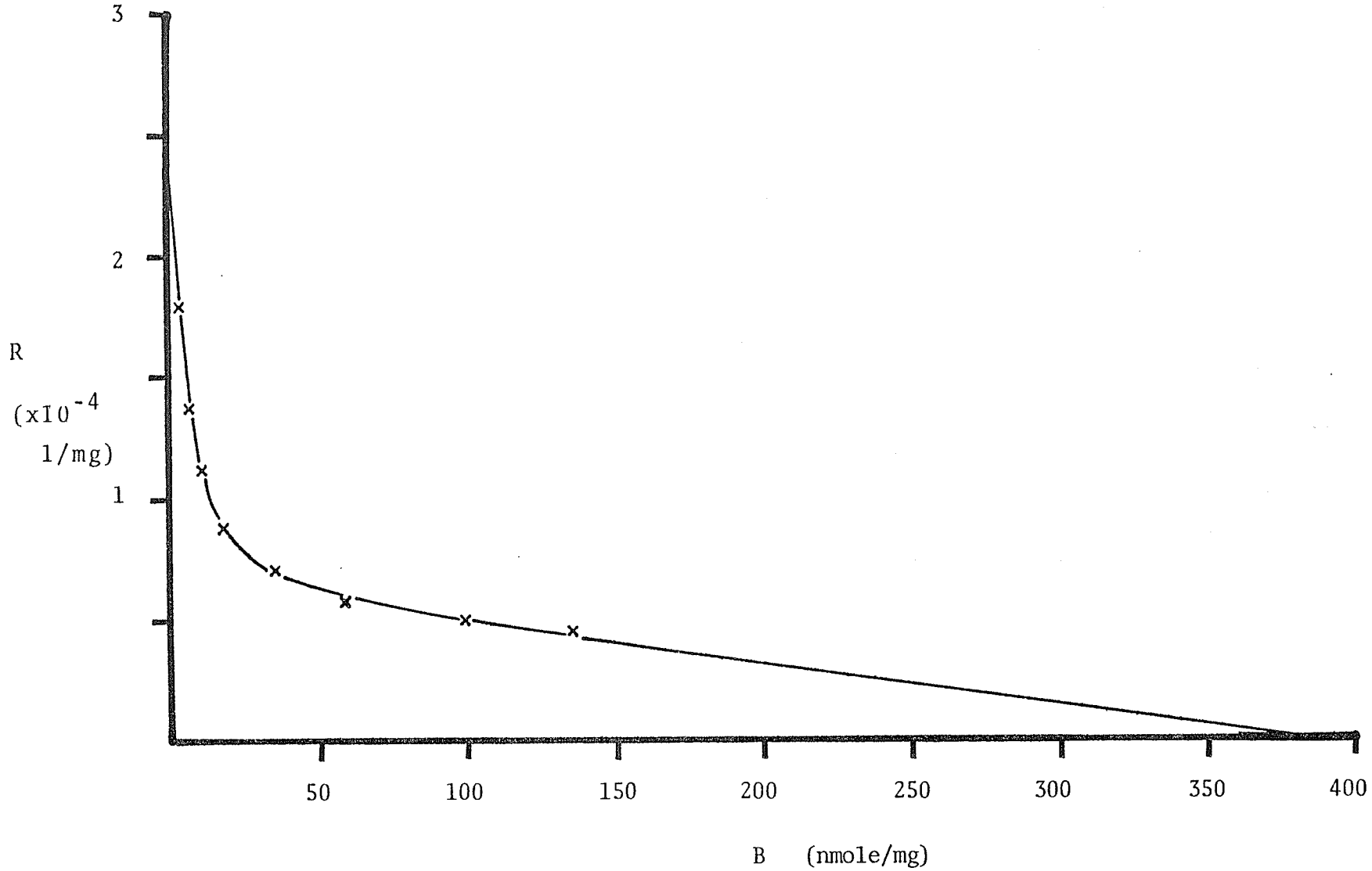
3
2
1
R
(x10-4
1/mg)
50
100
150
200
250
300
350
400
B (nmole/mg)

Attempts to remove the sialic acid residues by mild acid hydrolysis (0.1 N H_2SO_4, 1 hr) resulted in precipitation of the protein. For this reason, the exact quantity of Ca bound to sialic acid residues in mucin was not determined.

Fetuin, which also contains high level of sialic acid residues (216 nmole/mg protein), proves to be stable for acid hydrolysis treatment. Figure 42 shows the results of Ca binding to fetuin, asiolofetuin and a 1:1 mixture of the preceding two, expressed in the form of Scatchard plot. Kinetic analysis indicates a low affinity site with a capacity of 426.4 nmole of Ca per mg protein and with a K_D of 6.46 mM. Similar to mucin, fetuin also has a high affinity binding site with a capacity of 33.6 nmole of Ca per mg protein and a K_D of 0.21 mM.

Acid hydrolysis produced an essentially sialic acid free asialofetuin. Removal of sialic acid depressed the binding to both the high and low affinity sites. The low affinity capacity was reduced to 254 nmole of Ca per mg while low affinity capacity was reduced to 1 nmole of Ca per mg protein. The total binding capacity was reduced from 460 to 255 nmole of Ca per mg protein. This, together with the reduction of 200 nmole of sialic acid per mg of protein due to hydrolysis suggested a one to one correspondence between sialic acid residue and Ca binding site. The fact that total removal of sialic acid residues did not completely abolish Ca binding phenomenon indicated the importance of other anionic sites. This might explain the observation

Figure 42

Ca binding to fetuin, asialofetuin and a mixture of the two

The smooth curve is the least square best fit of the data points using the computer program SKATCH.MB. The total reaction medium volume was 10 ml: 9 ml outside the dialysis bag and 1 ml within. The protein concentration was 1 mg/ml. Data points represent Ca binding at total ^{40}Ca concentration of 20, 50, 100, 200, 500 μM, 1, 2, 3, 5, and 9 mM.

(x——x) = fetuin

(*——*) = asialofetuin

(o——o) = mixture

R = (bound Ca per mg)/(free Ca per l)

B = bound Ca in nmole/mg protein

R
($\times 10^{-4}$ l/mg)

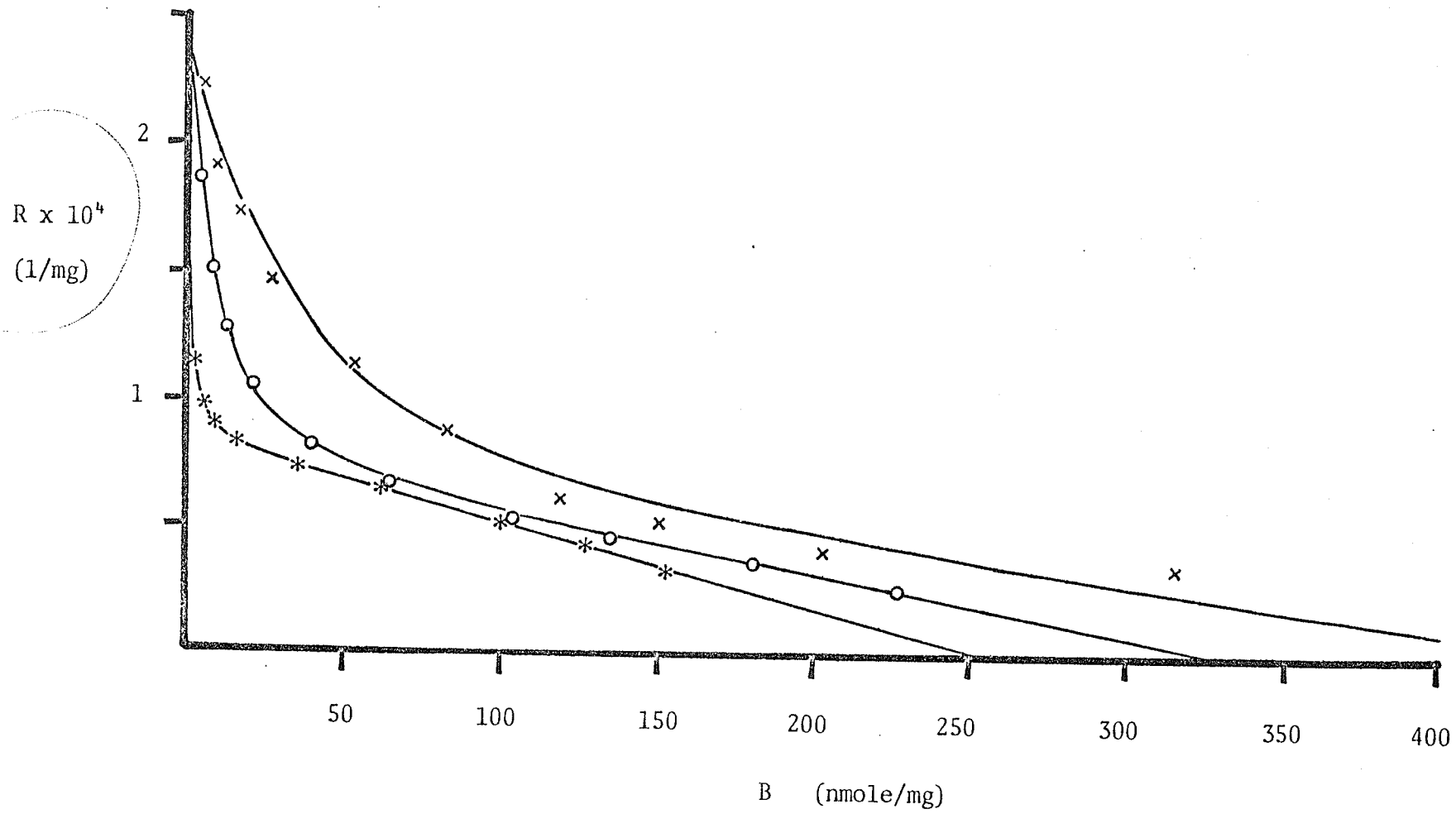

that removal of sialic acid also changed the K_D of the two binding sites to 3.03 and 0.01 mM respectively. Each of the two binding sites which was kinetically resolved may be an agglomeration of many different anionic binding groups each with similar binding constants.

To get another estimate of the relationship between sialic acid residue and bound Ca, a 1:1 mixture of fetuin and asialofetuin was made. A Ca binding study identical to the preceding two showed a total Ca binding capacity of 330 nmole of Ca per mg protein and a sialic acid content of 106 nmole per mg protein. Thus again with a reduction of sialic acid residue (110 nmole/mg), there was an equal quantity reduction of total Ca bound (130 nmole/mg), re-affirming the 1:1 sialic acid-Ca bound relationship observed earlier. The results directly validify the computer program SKATCH.MB.

(c) Ca binding to sarcolemmal fraction

Having established that sialic acid residue binds Ca ion, it is then possible to examine Ca binding to cardiac sarcolemmal preparation which has a high content of sialic acid residues (Table 25). K_D obtained in the preceding studies involving sialic acid-rich glycoproteins suggested the range for examining the Ca binding which is sialic acid dependent. Ca binding studies were done at total Ca concentrations of 20, 50, 100, 200, 500 μM and 1, 2, and 5 mM.

The interaction of different cations with Ca binding to sarcolemmal fraction was examined. One experiment each

of normal and cardiomyopathic hamster hearts sarcolemma derived from 10 animals was performed using the equilibrium centrifugation method described in the Methods section. Figure 43 shows the Scatchard plot of Ca binding to sarcolemmal preparation from 200 d normal hamster hearts. Kinetic analysis again resolved the curve into two components. Three different cations (100 mM Na, K, or Li) were tested to assess the influence of medium cation on the Ca binding profile of cardiac sarcolemma. No difference on Ca binding profile was observed when Na, K, or Li was used as the primary medium cation. With Na as the monovalent cation, the low affinity binding site had a capacity of 113.5 nmole of Ca per mg protein and a K_D of 1.02 mM. The high affinity binding site had a capacity of 3.8 nmole of Ca per mg protein and a K_D of 0.007 mM. The lack of any difference between Li, Na and K on Ca binding to sarcolemma protein was confirmed with a separate experiment using 200-300 d cardiomyopathic hearts. This is shown in Figure 44. With Na as the monovalent cation, the low affinity binding site has a capacity of 72.6 nmole of Ca per mg protein and a K_D of 1.8 mM. The high affinity binding site has a capacity of 3.4 nmole of Ca per mg protein and a K_D of 0.010 mM.

The effect of neuraminidase treatment and sialic acid removal on Ca binding was then examined. One experiment using pooled hearts from 10 normal hamsters (180-200 d) revealed a removal of 72.3 nmole of sialic acid per mg of sarcolemmal protein. Control at $4^{o}C$ showed a non-enzymic hydrolysis of

Figure 43

Scatchard plot of Ca binding to cardiac sarcolemma from 200 d normal hamsters under various ionic conditions

The smooth curve is the least square best fit of the data points (x) using the computer program SKATCH.MB. Total reaction medium volume is 1 ml which contains o.6 mg protein. Data points represent Ca binding at total ^{40}Ca concentrations of 20, 50, 100, 200, 500 μM, 1, 2, and 5 mM.

(o) = LiCl 100 mM

(x——x) = NaCl 100 mM

(Δ) = KCL 100 mM

R = (bound Ca per mg)/(free Ca per l)

B = bound Ca in nmole per mg protein

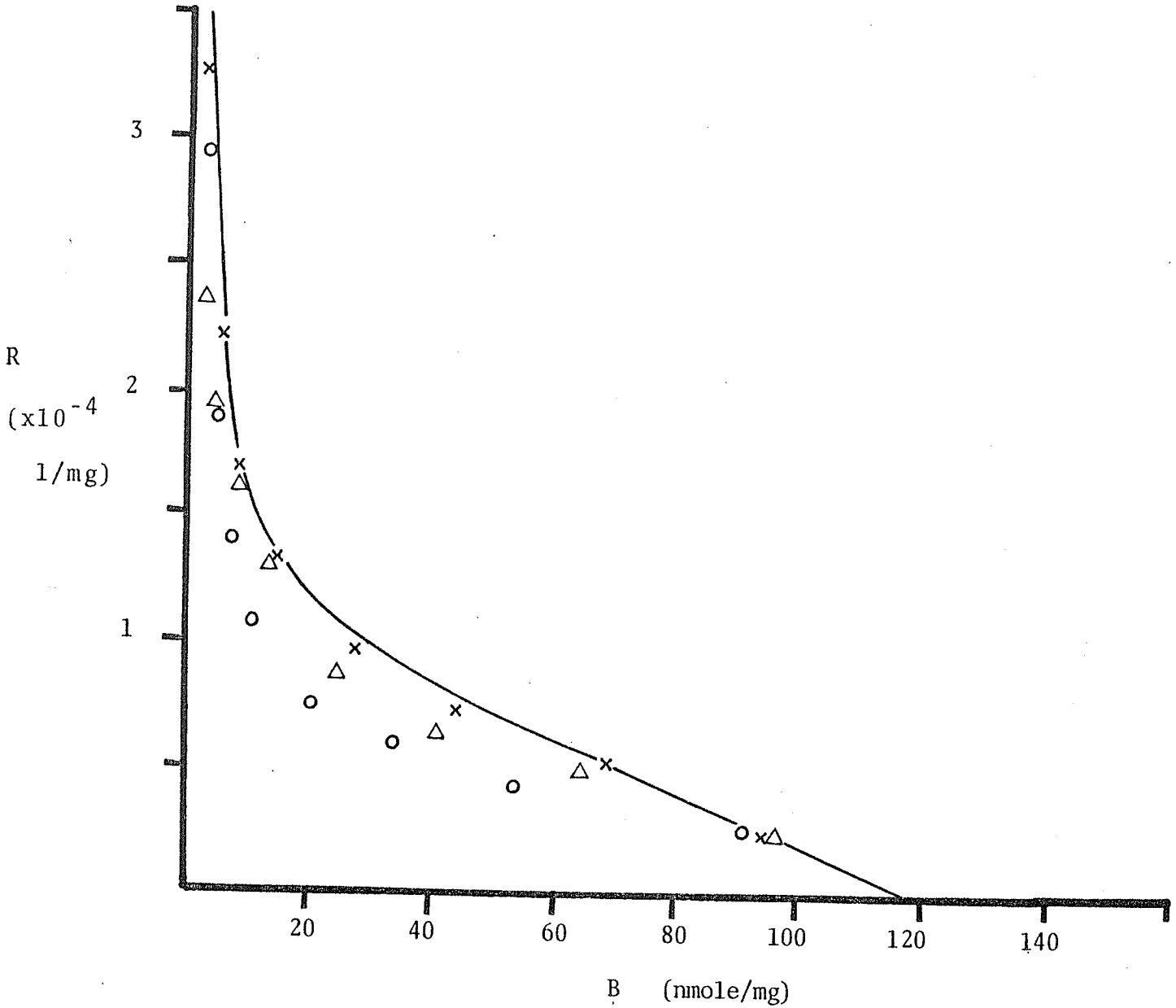
R
(x10⁻⁴
1/mg)
3
2
1
20
40
60
80
100
120
140
B (nmole/mg)

Figure 44

Scatchard plot of Ca binding to cardiac sarcolemma from 200-300 d cardiomyopathic hamsters under various ionic conditions

The smooth curve is the least square best fit of the data points (x) using the computer program SKATCH.MB. Total reaction medium volume is 1 ml which contains 1.2 mg protein. Data points represent Ca binding at total ^{40}Ca concentrations 0f 20,50,100,200,500 uM, 1, 2, and 5 mM.

(o) = LiCl 100 mM

(x——x) = NaCl 100 mM

(Δ) = KCl 100 mM

R = (bound Ca per mg)/(free Ca per l)

B = bound Ca in nmole/mg

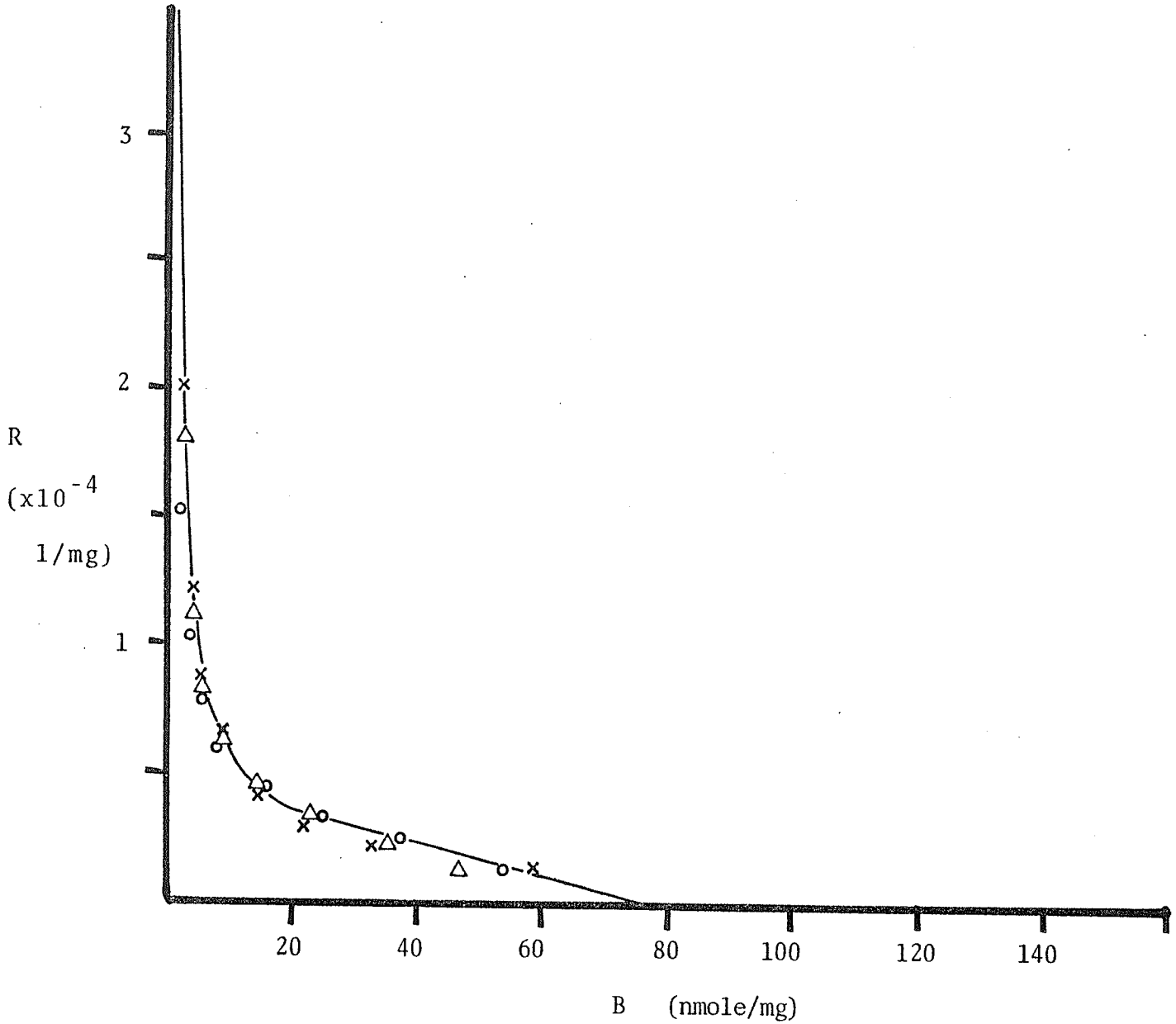
3
2
1
R
(x10^-4
1/mg)
20
40
60
80
100
120
140
B (nmole/mg)

16.9 nmole sialic acid per mg protein. The difference between the enzyme treatment and control was thus 55.4 nmole per mg protein or 30% of the total (186.7 nmole/mg).

The Ca binding profile of the control and neuraminidase treated sarcolemmal preparation is shown in Figure 45. Control sarcolemma consists of two types of binding site. The low affinity binding site has a capacity of 134.8 nmole of Ca per mg protein and a K_D of 2.17 mM. The high affinity binding site has a capacity of 5.2 nmole of Ca per mg protein and a K_D of 0.038 mM. Neuraminidase treatment reduced the total binding capacity by 90 nmole of Ca per mg protein, from 140 to 50 nmole of Ca per mg protein. For each sialic acid residue removed, there appeared to be a 1.6 Ca ion reduction in binding capacity.

Neuraminidase treatment reduced the low affinity binding capacity to 40.6 nmole Ca per mg protein but increased the high affinity binding capacity to 9.4 nmole of Ca per mg protein. Concurrently, the K_D were changed to 0.67 mM and 0.15 mM. The change of the K_D again suggested participation of other anionic groups in the process of Ca binding.

Table 27 summarizes the 4 experiments on Ca binding. It appears that the total binding sites is less in the cardiomyopathic hearts which is primarily a reflection of the low affinity, neuraminidase-sensitive binding sites. This is consistant with the previous observation(Table 25).

Figure 45

Ca binding to normal hamster heart (180-200 d) sarcolemma before and after neuraminidase treatment

The smooth curves are the least square best fit of the data points using the computer program SKATCH.MB. Total reaction medium volume is 1 ml which contains o.3 mg protein. Data points represent Ca binding at total ^{40}Ca concentrations of 20, 50, 100, 200, 500 μM, 1, 2, and 5 mM.

(x——x) = control

(o----o) = neuraminidase treated

R = (bound Ca per mg)/(free Ca per 1)

B = bound Ca in nmole/mg

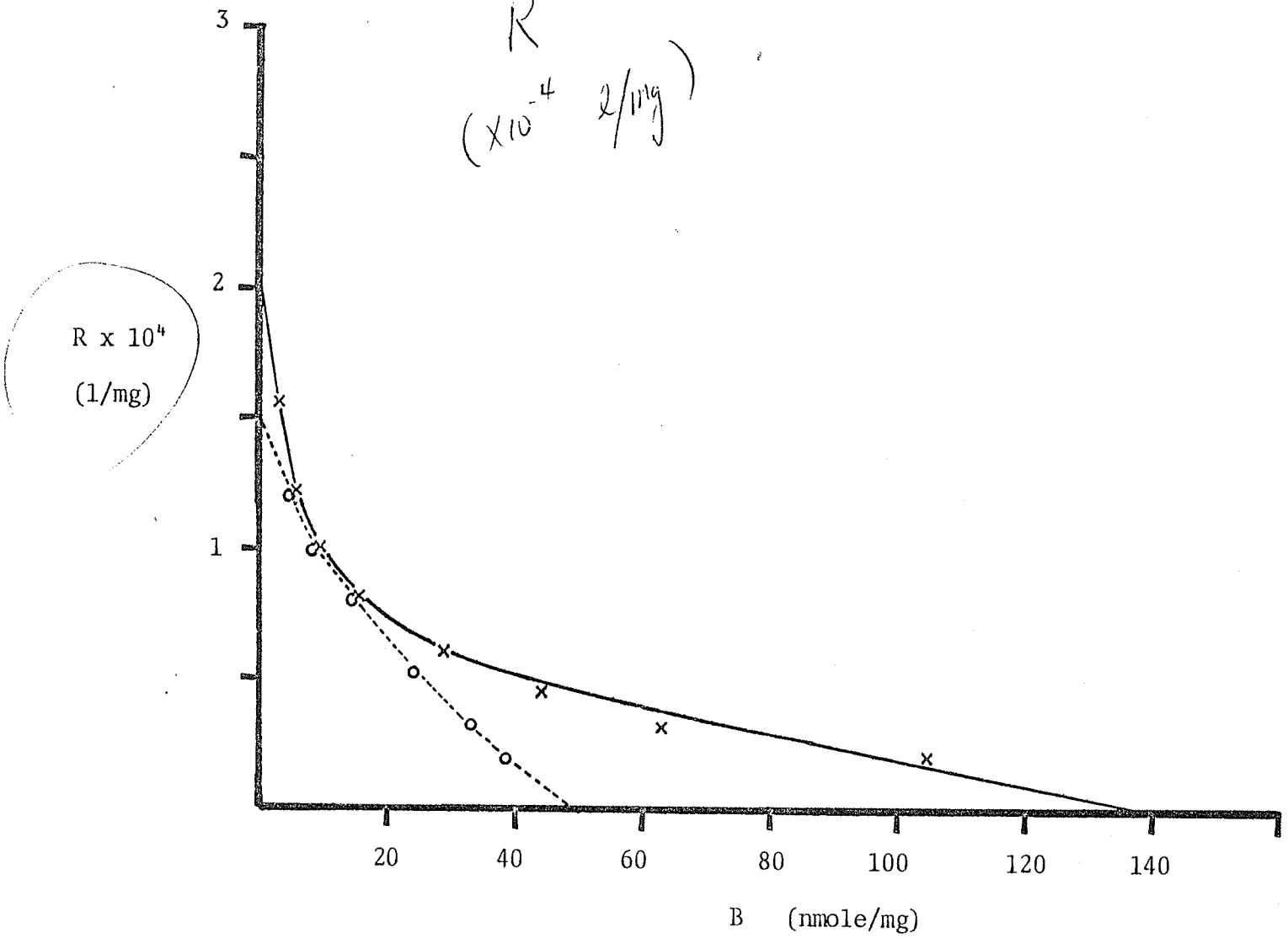
R
(x10^-4 2/mg)
R x 10^4
(1/mg)
3
2
1
20
40
60
80
100
120
140
B (nmole/mg)

Table 27

Ca binding to hamster cardiac sarcolemma

	nmole Ca/mg protein			mM	
	Q_2	Q_1	Q_T	$1/K_2$	$1/K_1$
Normal (180-200 d)[a]	114.2±11.7	4.9±0.6	119.0±11.6	1.51±0.34	0.019±0.009
Cardiomyopathic (200-300 d)	72.6	3.4	76.0	1.80	0.010

[a] n=3; mean±S.E.M.

Q_2, Q_1 = low and high affinity binding site capacities.

$1/K_2$, $1/K_1$ = dissociation constants for low and high affinity Ca binding sites.

SECTION IV

DISCUSSION

A. EXPERIMENTAL METHODS

1. Isolated heart

One of the important considerations in studying and quantifying the Ca exchange kinetics of a small piece of tissue (hamster heart wt range from 0.17 to 0.64 g in different stages of cardiomyopathy) is the realization that the perfusion apparatus represents a significant source or sink of exchangeable Ca. In this study Ca bound and adsorbed to the perfusion apparatus amounted to 94 nmole in the uptake and 165 nmole in the washout studies. The difference between the two is most likely the result of the fact that the technique is only sensitive to Ca extraction or washout and was not sensitive to contamination by a small amount of solution which adhered to the perfusion apparatus. This is best illustrated by an example. Consider a contamination of 50 µl which mixes with 1 ml of perfusion solution. If the perfusing ^{45}Ca containing solution is 10,000 cpm/ml, the dilution of 1 ml by 50 µl would give an apparent extraction of

$$10{,}000 \text{ cpm} - \frac{10{,}000 \text{ cpm}}{1.05} = 476 \text{ cpm}$$

in the uptake. On the other hand, the same ^{45}Ca contamination in the washout would appear simply as if 500 cpm have been washed out, i.e.,

$$10{,}000 \text{ cpm} \times 0.05 = 500 \text{ cpm}$$

Some contamination is also present on the isolated heart.

This is represented by a compartment with a $t_{\frac{1}{2}}$ of 2 sec or less and was ignored in all analyses.

The importance of the correction for the contamination is shown by the following calculation. For a heart of 0.15 g with total Ca washout of 2 mmole/kg, the total exchangeable Ca of the heart is 300 nmole, i.e.,

0.15 g X 2.0 mmole/kg = 300 nmole.

Consider that the perfusion apparatus can alone account for 165 nmole in the washout studies, it is immediately evident of the necessity of this correction. Similar arguments hold true for the uptake studies. For uptake studies, 94 nmole Ca with $t_{\frac{1}{2}}$ of 10 sec was subtracted from the uptake data before graphical analysis.

2. Isolated sarcolemma

There are many published methods for the isolation of an enriched cardiac sarcolemmal fraction (Stam et al, 1970; Tada et al, 1972; McNamara et al, 1974; Krause et al, 1975; Sulakhe et al, 1976). Continued efforts by a number of investigators in the development of new methods is a good indication that no one technique is yet acceptable to all as adequate. The most recent method developed by Sulakhe et al (1976) appeared to be milder than the previous techniques, however, for two reasons, it was not adopted for this investigation. First of all, the yield was too low (F_{3C}, or the enriched sarcolemma fraction, amounts to 1-2 mg protein/g ventricle). Secondly, the preparation consists of inhomogeneous population of vesicles (St. Louis and Sulakhe, 1976). Since one objective of this investiga-

tion was to study the Ca-binding characteristics of the basement membrane which is external to the sarcolemma, the possibility existed that some of the vesicles would reseal inside out and retain sufficient integrity (Besch et al, 1976) to serve as a barrier to the substrates, activators and inhibitors used for enzyme assays. In particular, asialofetuin (used as a substrate for sialyl-transferase catalyzed reaction) and neuraminidase (used to hydrolyze the sialic acid from the basement membrane) are proteins and would have difficulty in gaining access to the reaction sites in the inverted vesicles. Furthermore, although the procedure is considered mild in terms of preservation of enzyme activities, it is not clear how the extensive homogenization employed in making the vesicles would alter the basement membrane. Consequently, I have chosen and modified slightly the method of Tada et al (1972) for the isolation of sarcolemmal preparation which yields large membrane ghosts.

The membrane ATPase activities at different stages of isolation indicated progressive purification of the sarcolemmal membrane fraction. Although Mg-ATPase has been regarded as a sarcolemmal marker (Singh et al 1975), it is also a non-specific marker, since part of its activity can be attributed to mitochondrial activities which is azide sensitive (Besch et al, 1976). The initial homogenate activities in this investigation also showed a large (60%) azide sensitive fraction. In this context, the reduction of Mg-ATPase activities might be taken as indication of

the purification of the sarcolemmal fraction.

The level of the Na, K-activated and Na, K-activated, ouabain sensitive ATPase activities in the final sarcolemmal preparation approached the level reported in the original method on guinea pig hearts (Tada et al, 1972). On the other hand, the values are considerably lower than those reported by Sulakhe and Dhalla (1973) in normal hamster hearts (14.5 μmole/mg/hr in deoxycholate treated and 22.5 μmole/mg/hr in NaI treated).

Although the isolation procedure produces cardiac cell fragments, it is possible that the membranes are resealed and retain the relatively low, passive permeability to Na and ATP characteristic of intact sarcolemma. Winegrad (1971) has pointed out the risk of the sarcolemma healing over when medium Ca is elevated in chemically (EDTA) skinned multicellular cardiac preparation. In the present Na, K-ATPase assay, EDTA is not included and the multicellular fragments appear minimally disrupted when observed by phase contrast microscopy. With the membrane resealed, external Na and K could produce very low or variable ATPase activation by two mechanisms. First, the asymmetrical Na, K-activated ATPase (Besch, 1976) requires that Na and ATP be on the inside of the cell. This would be precluded by an intact permeability barrier. In the absence of Na, K activation, one can scarcely show any inhibition by ouabain. The high activity reported by Sulakhe and Dhalla (1973) probably

reflects the higher permeability state of their preparation after deoxycholate or NaI treatment. The small vesicular preparation employed by them also has a much larger surface to volume ratio as compared to that in the present cell-ghost preparation.

To test this hypothesis that the low Na, K-activated and ouabain inhibited ATPase activities observed in this investigation is due to deficiency of substrate, I decided to approach it in two ways. If low permeability to Na and ATP precluded activation, relatively long (2 hr) incubation at low temperature (4°C) should increase the level of substrate that penetrated the membrane. In addition, veratridine, which is known to increase Na permeability including that of the muscle membrane (Ulbricht, 1969, Varga et al, 1972 a, b), was included in some assays.

The results indicate that deficiency of substrate, especially Na, could be a significant factor in the previous observation of low Na, K-ATPase activities. Veratridine plus cold incubation resulted in about a two to three fold increase of enzyme activities in the cardiac cell fragments. The lack of effect of veratridine (and TTX) on the synaptosomal NaK-ATPase activities (ran as a parallel control of a source known to have high Na, K-ATPase activity), might be explained by the very low permeability to ATP in this preparation. In other words, the Na,K-ATPase activities assayed is that of the post-synaptic membrane and other extra-synaptosomal enzyme activities (White,

personal communication).

3. Non-steady state of Ca exchange - Permeability factor

Tracer studies of Ca fluxes under steady state conditions yield the kinetics of Ca exchange under a particular set of experimental conditions. It is nearly impossible, however, to correlate a specific Ca pool in the heart responsible for the maintenance of contractile force under such conditions. If the contractile state of the heart was manipulated by changing the frequency of stimulation or by inotropic interventions, then conceivably, under the new steady state, re-examination of Ca exchange kinetics might give information about a specific pool, whose content, for example, changed in parallel with that of the contractile activities of the heart. On the other hand, caution must be exercised in the interpretation of these results as these external influences might have produced a new homeostasis such that maintenance of the contractile state is modified or even dominated by a new Ca pool; for example, stair case is thought to increase cardiac contractility by increasing the capacity of an intracellular pool (Morad and Goldman, 1973) while digitalis (Nayler, 1973, 76) and adrenaline (Reuter, 1973) are thought to modify the more labile extracellular pool. In addition, steady state exchange is complicated by the factor of back-flux which cannot be easily quantified or analyzed.

A second and easier alternative is to use Ca-free

perfusion as a means of relating changes of contractile force with Ca-fluxes in the myocardium. Bailey and Dresel (1968) have shown that when the Ca steady state in the heart is disturbed by perfusion with a Ca-free K-H solution, the washout of a single Ca compartment which they have called Ca_{II}, was correlated directly to the decay of contractile force. The washout study of Bailey and Dresel's (1968) involves prior gas (95% O_2, 5% CO_2) perfusion. Subsequently Ong (1972) from the same laboratory have demonstrated some qualitative change of Ca exchange kinetics associated with gas perfusion, such as slower decay of contractile force and Ca washout when compared to kinetics studied in the absence of prolonged gas perfusion. The one-to-one correlation between contractile force decay and Ca washout from Ca_{II}, however remains valid in the latter case. In the present studies, gas perfusion is limited to 5-10 sec and serves only as a spacer to separate two different perfusion mediums. The technique established in kitten hearts is extended to identify and study the Ca pool responsible for the maintenance of cardiac contractile activity in healthy as well as in genetic cardiomyopathic hamster hearts.

Although non-steady state Ca removal has essentially eliminated the factor of back diffusion due to continuous Ca removal, it has also introduced its own complicating factor:possible membrane permeability changes. The conventional method of kinetic analysis assumes membranes

as barriers to exchange and membrane permeability as invariable constant characterized by exchange constants, K s. Thus, if membrane permeability to Ca does not remain constant during the Ca-free washout or its subsequent uptake, graphical analysis of calcium effluent curves is meaningless.

^{45}Ca influx measurements in various cardiac preparations (Winegrad and Shanes, 1962; Niedergerke et al, 1969) agree in showing a large increase in Ca permeability during excitation. Voltage clamp studies of mammalian ventricles (Table 2, Reuter, 1973) similarly show an increase in Ca influx per cm^2 during a single action potential. It is fortunate, in this regard, that Ca-free perfusion does not seem to alter the electrical activity of the heart (Gibbs and Vaughan, 1968; Ong, 1972).

Zimmerman and Hulsman (1966) reported that re-perfusion of Ca-containing medium to a Ca-depleted isolated rat heart resulted in an irreversible loss of mechanical and electrical activities. This "Ca paradox" phenomenon was thought to be the result of an excessive influx of calcium into cells during re-perfusion with Ca-containing medium (Zimmerman et al, 1967). However, isolated heart preparations of other species such as rabbit and cat appear to be less sensitive to Ca deprivation (Lee and Visscher, 1970,a,b, Shine et al 1971; Bailey et al, 1971, 1972). Even in the sensitive rat hearts, Yates and Dhalla showed that Ca-free perfusion at a relatively high perfusate flow rate of 10 ml/min, did not result in "Ca paradox" as long as the

deprivation was limited to three min. In this investigation with hamster hearts I have limited the Ca-free perfusion to 2 min prior to the uptake studies.

Ca uptake in the hamster hearts in this study was associated with an overshoot of contractility above steady state which then gradually returned to the steady level. The Ca uptake kinetics, however, remained bi-exponential, as in washout studies. The fact that net Ca uptake continued at a time when contractility started to decline toward a lower steady state, suggested (1) sequestration of part of the calcium which had entered the cells to some compartment that was not immediately available for E-C coupling, and (2) Ca deprivation had produced a transient supra-normal E-C coupling resulting in an overshoot. In 50% of the 220d cardiomyopathic hearts with congestive heart failure, uptake was associated with arrhythmias and transient elevation of base-line tension (reversible low amplitude contracture). The abnormal rhythmicity might be a result of AV block as atrial stimulation was used in the earlier studies, although age matched control did not show such abnormal rhythm. The elevation of base-line tension, on the other hand, might be interpreted to result from an excessive Ca influx. Although overshoot was also present in young normal and cardiomyopathic hamsters, abnormal rhythm or elevation of base-line tension were not present in Ca uptake studies. Young hamsters of either strain

(around 30 days of age) however, could be induced into sustained contracture by using 2xCa (3.6 mM) solution during the uptake studies. This may represent a less extensive developed relaxing system at the young age or and inability to regulate Ca influx, since identical treatment in adults could not precipitate contracture.

Since Ca uptake in this study was associated with overshoot, permeability alteration must be considered. Ca is known to have a membrane "stabilizing effect" modifying the excitability of many biological membranes by adsorption on the membrane's outer surface (Brink, 1954; Shanes, 1958; Frankenhaeuser and Hodgkin, 1956; Gilbert and Ehrenstern, 1969; Fishman et al, 1971; Hille, 1976). Reduction of extracellular Ca leads to an increase of Na and K permeability. With regard to transport across multi-cellular preparations, it is suggested that Ca plays an important role in maintaining the adherence of epthelial cells to one another which in turn may regulate ion, water and small molecule movement across the tissue (Zweifach, 1940; Hays et al, 1965). Saari and Johnson (1971, 1972) have suggested that the washout and uptake of contractile dependent Ca is limited by the capillary membrane permeability to Ca. To explain the faster rate of Ca uptake and contractility recovery in comparison to Ca removal and contractility decay they have postulated Ca removal increases capillary permeability to Ca. The observation of "Ca paradox" in rat heart tends to support the concept that

Ca regulates its own permeability. Langer et al (1976) have also observed an increase in Ca exchangeability in cultured heart cells (also from the rat) after removal of surface Ca-binding sialic acid residues.

Comparison of ^{14}C-mannitol exchange before and after Ca-free perfusion for 2 min in this study indicated no significant change in mannitol exchangeability. It is possible that after 5 min incubation, ^{14}C-mannitol may not have reached equilibrium. The calculated mannitol space of 16.9% wet ventricular weight is less than the 29.2% $^{35}SO_4$ space (5 min perfusion) reported by Frank and Langer (1974) (after 7% vascular space correction) in rabbit interventricular septa. It is, however, closer to the 23.9%measured by point-counting analysis of light micrographs in normal hamster heart (Lazarus et al, 1976), or to the 21% reported by Langer and Brady (1963) in perfused dog papillary muscle using ^{14}C-sucrose. It is larger, on the other hand, than the 12% $^{35}SO_4$ space (after 7% vascular space correction) reported in rat ventricle by Polimeni (1974). The fact that mannitol washout in this study was monoexponential (excluding glassware contamination) and had a volume of distribution within the range of reported interstitial water indicates that it indeed represents the washout from the interstitium. The $t_{\frac{1}{2}}$ of approximately 16 sec, however, is considerably faster than the 90 sec $t_{\frac{1}{2}}$ of exchange of sucrose reported in perfused papillary muscle by Langer and Brady (1963). The efflux of sucrose in the

latter study appears to have been flow limited.

Although ^{45}Ca exchange before and after Ca-free perfusion in this study showed some differences in the overall rate of Ca removal and extraction, the fact that steady state exchange did not involve change of cardiac contractility and is at the same time complicated by the factor of back-flux, may have contributed to the observed difference. Certainly, the statistical comparisons of the $t_{\frac{1}{2}}$ of both rapidly and slowly exchanging Ca compartments under steady and non-steady state conditions of Ca exchange do not indicate alteration of Ca permeability after Ca-free solution perfusion.

B. CONTRACTILE ACTIVITY ASSOCIATED WITH Ca POOLS

In agreement with previous findings from this laboratory in kitten hearts (Bailey and Dresel, 1968; Bailey et al, 1972; Ong, 1972; Pang, 1976), it was found in this investigation on hamster hearts that the decay of contractile force during Ca-free perfusion was monoexponential. The $t_{\frac{1}{2}}$ of contractility decay positively was correlated with that of the washout of a rapidly exchanging compartment $Ca_I(p)$ (or Ca_{II} in previous terminology). The slope of the regression lines, (in normals and cardiomyopathics) however, were not unity. The lines also do not pass through the origin, indicating the absence of a one-to-one correspondence. In general, this is represented by

a longer $t_{\frac{1}{2}}$ of $Ca_I(p)$ decay than the corresponding contractility decay. This might be the result of the fact that contractility in the myocardium is not maintained completely by a single Ca pool (Morad and Goldman, 1973). In addition, the assumption of an in-parallel model for Ca efflux may not be entirely correct despite the high correlation coefficient.

The $t_{\frac{1}{2}}$ of $Ca_I(p)$ efflux is about 15 sec which agrees closely with that of mannitol exchange ($t_{\frac{1}{2}}$ = 16 sec). Assuming a 20% interstitial space, a $[Ca]_o$ of 1.8 mM would give the interstitial Ca content 0.36 mmole/kg wet ventricular wt. This is considerably smaller than the content of $Ca_I(p)$ measured which ranged from 0.9-1.3 mmole/kg. This suggests part of the Ca_I arries from Ca bound to the cell membrane and possibly from intracellular sites.

Two lines of evidence suggest that the in-parallel model is inadequate in the kinetic analysis of uptake Ca. First, the $t_{\frac{1}{2}}$ of the rapidly exchanging compartment (approximately 6 sec, Table 28) is much faster than the interstitial Ca exchange ($t_{\frac{1}{2}}$ = 16 sec) in the present studies. Since the slowly exchanging compartment is presumably the rate limiting compartment, at least in terms of resolution by kinetic analysis, the fast rate of exchange indicates the choice of the in-parallel model may be in error. Second, a parallel model yields a rapidly exchanging Ca compartment in the uptake studies ($Ca_1(p)$) considerably smaller in size than $Ca_I(p)$ (Table 28).

Table 28

Comparison of the rapidly exchanging compartment content and $t_{\frac{1}{2}}$ in the uptake studies to that in the washout studies

	$Ca_I(p)$	$Ca_1(p)$	$Ca_1(s)$
	(mmole/kg)		
N-26	1.34 ± 0.19[@]	0.86 ± 0.16	1.35 ± 0.12
M-30	0.92 ± 0.04	0.37 ± 0.07	0.84 ± 0.09
N-44	1.30 ± 0.13	0.68 ± 0.11	1.40 ± 0.15
M-36	1.21 ± 0.12	0.50 ± 0.05	1.12 ± 0.12
N-60	1.21 ± 0.03	0.64 ± 0.09	1.25 ± 0.07
M-53	0.90 ± 0.07	0.40 ± 0.05	0.97 ± 0.03

	$t_{\frac{1}{2}}$ - $Ca_I(p)$	$t_{\frac{1}{2}}$ - $Ca_1(p)$
	(sec)	
N-26	15.0 ± 1.7[@]	6.5 ± 1.0
M-30	15.0 ± 2.3	4.1 ± 0.5
N-44	15.6 ± 1.0	5.1 ± 0.4
M-36	18.1 ± 0.8	5.9 ± 1.1
N-60	16.2 ± 1.2	6.6 ± 0.6
M-53	16.4 ± 1.2	6.5 ± 0.6

[@] mean ± S.E.M.

Both uptake and washout Ca kinetics are bi-exponential which indicates the presence of two compartments. Assuming the plasma membrane is the permeability barrier, it is likely that the fast exchanging compartment, irrespective of either uptake or washout studies, represents Ca external to the cell membrane. Indeed, after changing to an in-series model $Ca_1(s)$ closely approximated that of $Ca_I(p)$ in all age groups except the 220 d normals (Table 12). This exceptional case is intriguing and an explanation will be attempted although complete evidence is lacking.

In all age groups studied, the quantity of Ca washed out is less than that of the Ca taken up, even though the washout and uptake are carried out in the same experiment one subsequent to the other. The differences observed are modest in the young animals but are more pronounced in the older age groups (Table 11). In the 220 d age groups, the collection was only from the pulmonary artery. This resulted in an approximately 15% leakage through the aortic valve into the left ventricle. This perfusate was not collected. Considering the leakage and the resultant superfusion of the left ventricular cavity, it is conceivable some of the exchangeable Ca was lost this way. Since the Ca gradient for uptake is exponentially decreased as the muscle accumulates Ca whereas the Ca gradient for washout is always infinite with continuous replenishment of Ca-free medium, it is possible that a greater loss of recoverable Ca would be encountered in the

washout studies than in the uptake studies. Nevertheless, it is unlikely that this process can account completely for the difference between the quantity of Ca recovered in the uptake and washout in the 220 d age groups of hamster hearts. The collection of effluent in the young age groups consist of total drainage, including that of the aortic leak. Yet, consistently higher values for total Ca uptake are still observed. This suggests an alternative explanation. It is possible that net efflux of Ca occurs after 2-3 min of uptake, at a time when data variability prevented their inclusion in kinetic analysis. This redistribution of Ca, if it occurred, may contribute to the observed lower steady state contractility subsequent to the overshoot.

If the redistribution and net efflux of Ca occurred in the 220 d age group, then the rapidly exchanging compartment must have contained some intracellular Ca in addition to interstitial and extracellularly bound Ca, as it is less likely that there exists a sizeable extracellular reserve capacity. Indeed, it can be calculated (see below) that the size of the rapidly exchanging pool, $Ca_I(p)$ or $Ca_1(s)$, is too large to consist of interstitial and membrane bound Ca only.

Because of the error associated with collection in the 220 d age groups, the Ca washed out of the heart represents an underestimation of the true compartmental content. The washout kinetics, however, remain valid since the rate of change of effluent ^{45}Ca was not altered, even though

only a fraction of the Ca is collected. This is reflected in the positive correlation between the $t_{\frac{1}{2}}$ of contractility decay and that of $Ca_I(p)$ washout (Figure 19). On the other hand, the content of $Ca_1(s)$, though probably larger than the steady state level, nevertheless is closely correlated with steady state contractility (Figure 21). The high capacity of the rapidly exchanging pool $Ca_1(s)$ in the 220 d normal is associated with a higher level of cardiac contractility.

C. CARDIAC CONTRACTILITY

Examination of hamster heart contractility indicated a significant and gradual depression in the cardiomyopathic hamsters throughout its life span as compared to age-matched controls. This depression is present at the preclinic stage and is most pronounced during congestive heart failure(CHF). The ability of the heart to relax is similarly depressed in the cardiomyopathics.

Brink et al (1967, 1969) first reported depressed cardiac function in cardiomyopathic hamster hearts at age of 110-210 d. The isolated hearts in these studies were not paced, with the cardiomyopathics beating around 40 beats less per min than controls. The hearts were also stretched at the apex with 3.75 or 8.75 g of weight, which imposed unidirectional and rather unphysiological stretching of the myofilaments. Forman et al (1972) also showed depression of isolated papillary muscle contractility (dF/dt) of cardiomyopathic hamster from 60 to 320 d of age as compared

to age-matched controls. The system, however, was seriously affected by a slow rate of substrate diffusion. This was indicated by a depression of contractility above a stimulation rate of 3 per min. Examination of ventricular function *in vivo* in other studies indicated depressed dP/dt max during CHF in BIO 14.6 hamsters (Jeffrey et al, 1970), but only border line depression at an earlier stage of the disease in another strain of animals (Stauch and Lossnitzer, 1975; BIO 8262; 70 d).

In summary, cardiac contractility investigations in hamster cardiomyopathy by various investigators in the past were incomplete in terms of two factors. First, *in vivo* and *in vitro* studies were not controlled with respect to heart rate and *in vitro* studies were relatively unphysiologically stressed. Second, no examinations were made at the pre-clinic stage before the onset of cardiac lesions. The one study at relative early stage of the disease (Lochner et al, 1970, 35-42 d) showed no difference in cardiac contractility. Histological examination indicated that spontaneous myolytic lesion had already started at this age. Some mechanical damage was probably involved in this group of very small hearts (0.17-0.26 g) stretched with 5 g resting tension. This might explain the very low dP/dt max observed in this age group as compared to 90 d age groups of the same study.

The present study utilizing a saline-filled balloon in left ventricular cavity probably offers a more physiolo-

gical index of cardiac contractility. The measured control dP/dt max (30°C, 180 beats/min) is lower than that of *in vivo* measurement (37°C, 360 beats/min; Jeffrey et al, 1970; Stauch and Lossnitzer, 1975). Comparison between controls and cardiomyopathics was, however, more meaningful in this study because heart rate was controlled. The results indicate depressed cardiac function at the preclinic stage, before the development of myolytic lesions, hypertrophy or fibrotic tissue replacement. This suggests genetic transmitted abnormality at some step of the E-C coupling process which may predispose the heart to eventual contractile failure.

There was also the observation of a gradual decrease of the already depressed contractility as the disease progressed. This suggests that hypertrophy and fibrotic replacement further compounded the primary lesion and may have contributed to the final failure.

D. COMPARISON OF Ca-EXCHANGE KINETICS - NORMAL VS CARDIOMYOPATHIC HEARTS

Ca exchange profiles of the young normals indicated no difference in age group of 26, 44 and 60 d in both the uptake and washout studies. This suggested indirectly that the smaller hearts of the youngest age group were not handled differently when compared to the larger hearts of the older age groups. Differences exist between the young and 220 d age group normals, partly due to the

different methods of collection as discussed previously.

The total exchangeable Ca reported in cardiac muscle is different under different experimental conditions. With external [Ca] of 1.8-2.5 mM, heart rate of 100-240 beats per min, and at 37°C, the exchangeable Ca in rabbit cardiac muscle has been reported to be 2 mmole/kg wet weight in atria (Teiger and Farah, 1967) and 1.2-1.4 mmole/kg wet weight in myocardium (Saari and Johnson, 1971, 1972). At 26-28°C and heart rate of 30-37 beats/min, a higher value of 3.2 mmole/kg wet weight have been reported ($[Ca]_o$ = 2.5 mM; Shine et al, 1971). With isolated dog papillary muscle perfused at 24°C with 5 mM Ca, Langer (1964) reported a total exchangeable Ca content of 6 mmole/kg wet heart weight. In kitten hearts studied in this laboratory at 37°C and perfused with 5.0 mM Ca, the exchangeable Ca content is about 2 mmole/kg (Ong, 1972), whereas with 1.8 mM $[Ca]_o$, it is around 1.5 mmole/kg (Pang, 1976). In rat cultured heart cells, Langer and Frank (1972) and Langer et al (1976) reported an exchangeable Ca content of 2.56-2.77 mmole/kg wet weight when perfused with 1 mM Ca.

In this study the exchangeable Ca content was about 2-2.5 mmole/kg in the young hamsters and in 220 d cardiomyopathics but was 3.3 mmole/kg in the 220 d normals (uptake). The latter value was not associated with a rise in resting tension, and therefore, may be interpreted as representing Ca sequestration capacity. Part of the

higher Ca content may be due to the lower temperature (30°C) employed in this study. Shine et al (1971) reported a similar high exchangeable Ca content at low temperatures in rabbit heart.

With both washout and uptake studies of the cardiomyopathic hearts, the fast exchanging Ca compartment, $Ca_I(p)$ or $Ca_1(s)$, is reduced in content at 30 and 53 d age group, but not in 36 d age group. The 36 d age group is further distinguished by having a larger content of total exchangeable Ca than control. This sudden alteration at 36 d age group appears not to be accidental or artifactual. This age is co-incidental with the onset of spontaneous cardiac lesion (Bajusz et al, 1966, 1968) as well as an increase in RNA synthesis activity (Nair et al, 1972). The fact that total exchangeable Ca is elevated in this age group while contractility remains depressed suggests that in addition to the depression of the labile Ca pool associated with the disease (which occurs at the pre-clinic stage), some other stage of the E-C coupling may be abnormal in the cardiomyopathics such that deficiency of Ca utilization occurs.

The $t_{\frac{1}{2}}$ of the rapidly exchanging compartment in both washout and uptake (apparent $t_{\frac{1}{2}}$) studies were not different from control in the young age groups. This is consistent with the hypothesis that the rapidly exchanging compartment, $Ca_I(p)$ or $Ca_1(s)$, is extracellular in nature, thus unlikely to be a site of an alteration in exchange

kinetics. Compartment-2 ($Ca_{II}(p)$ or $Ca_2(s)$), on the other hand, exchanges more rapidly in the young cardiomyopathics, but only the 53 d age group was significantly different from control. Assuming compartment-2 is predominantly intracellular, this suggests an increase of membrane permeability to Ca in the cardiomyopathics. Compartment-2 content is significantly elevated in the 36 d cardiomyopathics in both the washout and uptake studies. ^{45}Ca uptake is known to be markedly increased during the myolytic stage (Lossnitzer et al, 1975), this increase is suggested in this study to be predominantly intracellular. The Ca-influx coefficient K_{01}, which may be explained as the extraction coefficient of Ca of the heart tissue, is in general depressed in the cardiomyopathics although this is only statistically signigicant in the 53 d age group.

Since K_{01} describes the entrance of Ca into compartment-1, this is the same as saying that the rapidly exchanging pool, $Ca_1(s)$, of the cardiomyopathics has a smaller capacity to take up Ca.

Compartmental exchange kinetics of the 220 d hamster, in contrast to that of the young hamsters, indicated no difference in the $t_{\frac{1}{2}}$ (or apparent $t_{\frac{1}{2}}$)of the slowly exchanging compartment, which suggests no gross increase of cell membrane permeability associated with the disease. In this age group, pronounced fibrotic replacement occurs in the dilated cardiomyopathic heart, it is possible that the fibrous tissue may complicate the true Ca exchange

kinetics of the cell. Bozler (1963) studied the ^{45}Ca exchange kinetics of Achilles tendon. The efflux curve indicated bi-exponential exchange with the slow exchanging compartment $t_{\frac{1}{2}}$ of 65 min or longer and fast exchanging compartment $t_{\frac{1}{2}}$ of about 3-4 min. The study might be diffusion limited but the overall picture suggested rather slow exchange of collagenous tissue. It is thus possible that the slow exchange kinetics of the collagenous tissue in the cardiomyopathic hearts may have masked any alteration of the membrane permeability.

The Ca content of the rapidly exchanging compartment is reduced by ½ in the 220 day cardiomyopathic hamster heart as compared to age matched controls. It might be argued that the normalizing factor of wet heart weight is not correct because the cardiomyopathic hearts contain a greater proportion of connective tissue. In normal hearts, the collagen content is about 4-19 mg/g wet heart weight according to different investigators (Bartosova et al, 1969, 4-8 mg/g;Skosey et al,1972, 6 mg/g; Cutilletta et al, 1975, 7 mg/g; Woessner, 1961, 10 mg/g; Buccino et al, 1969, 12-19 mg/g). Collagen content in hamster cardiomyopathy has not been measured but various other forms of experimental cardiac hypertrophy and necrosis have indicated a possible elevation of collagen content two to three fold above normal (Bartosova et al, 1969; Buccino et al, 1969; Skosey et al, 1972; Cutilletta et al, 1975). The exchangeable fraction of Ca bound to collagenous tissue

(Achilles tendon) has been estimated to be 1.4 μmole/g wet weight when equilibrated with 1 mM Ca (Bozler, 1963) and 6.55 μmole/g wet weight when equilibrated with 2 mM Ca (Villamil et al, 1973). For the present argument, I will assume the collagen binding capacity of 5 μmole/g, the normal cardiac collagen content of 10 mg/g and the cardiomyopathic cardiac collagen content of 30 mg/g. Calculation indicates that the Ca bound to collagen is about 0.05 mmole/kg in controls and 0.15 mmole/kg in the cardiomyopathics. Clearly this represents only a fraction of the rapidly exchanging Ca content. In addition, the failing hearts at this stage of cardiomyopathy have been reported to have signigicant tissue edema. The extracellular space of the left ventricle is estimated to be 24% (ml/100g wet weight) in controls and 36% in cardiomyopathic (Lossnitzer and Bajusz, 1974; assuming 80% cell water and after subtraction of 7% for the vascular space). The free interstitial Ca content in the normal hearts can thus be calculated to be 0.43 mmole/kg and that in the failing cardiomyopathic hearts 0.65 mmole/kg. This indicates that a reduction of rapidly exchanging Ca compartment in the failing cardiomyopathic hearts actually reflects a greater reduction of superficially bound Ca.

The larger interstitial space in cardiomyopathic hearts also suggests that even though the Ca influx coeffieient K_{01} does not differ from control, it is actually misleading since a smaller fraction of the total is

membrane bound.

A brief summary is in order. First, since cardiac contractility is related to the Ca content of a rapidly exchanging compartment $Ca_I(p)$ or $Ca_1(s)$, and since this Ca compartment is depressed in not only the failing but also in the pre-clinic cardiomyopathic hearts, it can be concluded that this depression is responsible for the observation of a depressed cardiac contractility throughout the life span of the cardiomyopathic hamster. Second, the kinetics of Ca exchange also suggest a greater permeability of the cardiomyopathic heart membrane to Ca. Since the Ca that is presumably intracellular appears less important in the regulation of E-C coupling than that outside of the cell membrane, an increased transmembrane Ca permeability might then impede cardiac cell relaxation. This may partly explain the observed reduction of negative dP/dt max of the cardiomyopathic heart. And finally, since the rapidly exchanging and presumably superficial and extracellular Ca compartment, $Ca_I(p)$ or $Ca_1(s)$, is too large to be accounted for by interstitial Ca alone, the depression of this Ca compartment in cardiomyopathic hearts suggests a possible reduction of sarcolemmal Ca binding capacity.

E. SIALIC ACID CONTENT AND SIALYLTRANSFERASE ACTIVITIES

In the glycoprotein, sialic acid is almost always terminally bound to oligosaccharides. Because the pKa

of sialic acid is around 2.3 to 2.6, it contributes to the overall net negative charges of the cell membrane at the physiological pH (Cook, 1968; Hughes, 1973). The subcellular distribution of sialic acid indicates that it is preferentially localized on the plasma membrane, as much as 65-70% of the total cell content may be found on cell surface structures (Patterson and Touster, 1962; Warren, 1976). In terms of specific concentration (nmoles sialic acid/mg protein), only lysosomal membrane is comparable to that of plasma membrance (Hughes, 1976).

Table 29 summarizes the sialic acid content of some of the tissues reported in the literature for purpose of comparison of the level observed in heart muscle in this investigation. It is clear that cardiac cells have one of the highest concentration of sialic acid, both in the homogenate and in sarcolemmal fraction. The high concentration of sialic acid in the final sarcolemmal fraction of the present study indicates a high degree of enrichment of the surface membrane.

The variabilities in the level of sialic acid assayed in this investigation might be a result of three different factors. First, the chelating agent EDTA utilized in the isolation procedure is known to strip off surface glycoproteins (Hughes, 1976). Beierle (1968) have reported the removal of glycoprotein from the BHK-21 cell coat by brief exposure to EDTA. Snow and Allen (1970) have reported a 13% extraction of cell glycoprotein from cultured baby

Table 29

Sialic acid concentration of various tissue cells

Whole tissue homogenates	Sialic acid (nmole/mg)
[a] chicken breast muscle	25
[b] rat liver homogenate	31
[c] pig synaptosome	65
[d] rat cultured heart cells	80
[e] rat synaptosome	120
hamster heart (this study)	110
Plasma membranes	
[f] rabbit gastric mucosa	10
[f] human platelets	18
[f] rat liver	27
[f] rat kidney brush border	34
[g] rat hepatoma	47
[f] rat erythrocyte	61
[a] calf thymocyte	66
[a] chicken breast muscle	72
[f] rabbit kidney brush border	74
[a] chicken embryo fibroblast	106
[h] mouse skeletal muscle	146
[a] mouse hepatoma - 147042	361
hamster heart (this study)	205

[a] Warren, 1976, Table 5
[b] Patterson and Touster, 1962
[c] Konnguth et al, 1971
[d] Langer et al, 1976
[e] Sample given by T. White, Dalhousie Univ.
[f] Hughes, 1976, Table 2.3
[g] Benedetti and Emmelot, 1967
[h] Boegman, 1974

hamster cells by exposure to 0.5 mM EDTA. Hughes et al (1975) have also shown the release of glycoproteins from cultured lens epithelial cells by EDTA treatment. Second, osmotic shock may also release cell membrane glycoprotein. Burger (1968) reported release of membrane glycoprotein from mouse leukemic cells after reduction of medium osmolarity from 0.15M NaCl to 0.12M NaCl. The I-ED buffer used in this investigation is hypo-osmolar, as was the suspension medium of 10 mM TriS. The low osmotic strength medium was then replaced with the 40%sucrose, high osmolar medium which was followed by volume dilution. It is likely the repeated osmotic shock released considerable amounts of membrane bound glycoproteins. Unfortunately sucrose gives fluorescence interference at the same wave length as sialic acid and the glycoprotein release could not be quantitated. Third, myocardial cells contain neuraminidase activity (Tallman and Brady, 1973). This is confirmed in the homogenate preparation of the present study which showed an intitial rate of approximately 150 nmole sialic acid released per mg protein per hr at 37°C and pH 7.4. This specific activity is 65 times that reported by Tallman and Brady (1973) in rat heart using ganglioside GM_2 as substrate and at pH 5. Although the present series of experiments have been conducted at 4°C, it is likely that some sialic acids are removed by this high activity system during the long process of isolation.

In spite of these complicating factors, there appears

to be a definite reduction of sialic acid content in the myopathic hearts which is even suggested at the homogenate level. The failure of enrichment of sialic acid residue concentration at the final sarcolemmal fraction in the myopathic hearts is perplexing. Since there is some suggestion that lysosomal enzyme activities is increased associated with myopathy, it is possible that a proportion of the homogenate sialic acid are contributed by the lysosomal membrane which is known to have a high concentration of sialic acid residues (Hughes, 1976). The question might be asked whether the lower concentration of sarcolemma sialic acid residues in the cardiomyopathic hearts is an experimental artifact due to higher level of degradation during the isolation process. This question might be better answered using some of the known neuraminidase inhibitors such as Cu, Hg, Zn ion at mM range (Rosenberg and Schengrund, 1976).

As far as the author is aware, there are only three reports in literature concerned with muscle sialic acid changes associated with dystrophy or necrosis. Andrew and Appel (1973) reported no change of muscle sialic acid content after denervation of a membrane fraction with high level of Na,K-ATPase activities. On the other hand, another fraction also identified as sarcolemma but with a low Na,K-ATPase activity indicated an elevated sialic acid level following denervation. A clear interpretation of these data is difficult because both membrane fraction appear to be

highly heterogenous. Boegman (1974) examined the sialic acid distribution in dystrophic and normal mouse skeletal muscle. No difference was observed on the fractions with the highest acetylcholinesterase activities which was used as the plasma membrane marker. It is not clear how to relate this negative finding to the results of this investigation. Perhaps the disease process is different in the dystrophic mouse as compared to cardiomyopathic hamster. Certainly the defects of the protein synthesis process are different in these two dystrophic models. Judd and Wexler (1974) investigated myocardial glycoprotein changes with isoproterenol-induced necrosis in the rat heart. They observed a delayed increase of serum and myocardial sialic acid content following the necrotic phase. The control myocardial sialic acid level reported in this study, however, was only about 7 nmole/mg cell protein (assuming 1 g of ventrical contains 100 mg cell protein), which is 10 times lower than that of the present study or that of Langer et al (1976). The qualitative change might still be valid and Judd and Wexler interpreted the data as a result of mobilization of sialic acid from liver (and from heart cells and proliferating fibroblasts) for the synthesis of cardiac cell ground substances.

With the high level of cardiac sialic acid content, it is perplexing that the sialyltransferase activities is so low. Two alternative explanations might account for this low activity: (1) Sialic acid acceptor (asialofetuin)

failed to get to the enzyme site; (2) degradation of the substrate (CMP-sialic acid) or product gave an apparent low activity. Unfortunately, these considerations could only be examined retrospectively, since none of the tests outlined below were done.

There is abundant evidence to suggest the presence of cell surface glycosyltransferase including that of sialyltransferase (Roth et al, 1971; Datta, 1974; Shur and Roth, 1975; Cerven, 1977; Durr, 1977). Nevertheless the bulk of the transferase is believed to reside in the Golgi apparatus (Schachter et al, 1970; Roseman,1970; Hughes, 1976). The carbohydrates are thought to be assembled in Golgi membranes and the finished glycoproteins are then transported to the outside of the cell membrane as Golgi particles which fuse with the sarcolemma (Rambourg et al, 1969; Bennett et al, 1974; Michaels and Le Blond, 1976). If the surface membrane arises, even in part, by evagination of Golgi vesicles, then the presence of cell surface glycosyltransferase is easily understandable. A predominant localization of the enzyme in the Golgi apparatus coupled with an intact permeability barrier in the cardiac cell fragments would then explain the low activities observed.

It is also possible that the cell fragments contain sufficient phosphatase activities to hydrolyze the CMP-^{14}C-sialic acid. And since the cell has high neuraminidase activities, it is also likely that degradation of the enzymatically transferred ^{14}C-sialic acid gives an apparent

low activities. The most direct way to test for this is to measure the degree of sugar donor breakdown or released with borate electrophoresis (Shur and Roth, 1975). In the present series of experiments, even the sarcolemmal fraction, which retained little neuraminidase activities, showed low sialyltransferase activities. However, it is to be remembered that the amount of CMP-^{14}C-sialic acid is very low in the assaying medium (0.45 nmole), and even if the sarcolemma retained 1/100 of the homogenate neuraminidase activities (which would be 1.5 nmole sialic acid released per mg per hr), considerable substrate hydrolysis can occur during the incubation period.

It is clear that using sub-optimal concentrations of substrate (CMP-sialic acid), not only is the reaction rate extremely slow, but the assay is also complicated by substrate and product degradation. But in spite of all these considerations, it is interesting that Roseman et al (1966) have reported that the striated muscle contained the lowest level of lactose-sialyltransferase activities among 9 tissue tested. The striated muscle activities amounted to only 40 cpm per mg protein per 5 hr incubation which was 2% of liver activities and 0.1% of mammary gland activities.

It might be hazardous to attach any significance, at this stage, to the lower activity of sialyltransferase activity observed in cardiomyopathic hearts in failure, but the depression, if confirmed, would suggest a mechanism for the observed reduction of surface sialic acid residues

and corresponding surface bound Ca.

F. Ca BINDING PROFILE OF THE SARCOLEMMA - RELATION TO SIALIC ACID RESIDUES

Sialic acid has been repeatedly implicated in the binding of Ca, not only from histochemical evidence (Gasic et al, 1968; Benedetti and Emmelot, 1967, 1968), but also from electrokinetic methods (Weiss, 1967; Cook, 1968), and from Ca binding to erythrocyte membrane (Long and Mouat, 1971; Duffy and Schwartz, 1974), liver cell membrane (Shlatz and Marinetti, 1972) and smooth muscle preparation (Ishiyama et al, 1975). The involvement of sialic acid residues in Ca binding in these studies was established by the ability of neuraminidase treatment to reduce or abolish the phenomenon in question.

The binding studies with sialic acid rich glycoprotein, mucin and fetuin, indicated a very large capacity for Ca binding. The observation of a 1:1 correspondence between sialic acid residue and Ca binding is perhaps surprising because the attraction is probably electrostatic (Cook, 1968) and sialic acid is monovalent while Ca is divalent, this would have suggested a 2:1 relationship. The data, however, is consistent with the recent study by Jaques et al (1977) on the interaction of sialic acid and Ca ion. Using an ion-selective electrode, it was found a 1:1 Ca-sialic acid complex occurs even at a ratio of 1:60 concentration. The low affinity dissociation constant (K_D)

of about 6 mM for mucin and fetuin is also quite close to the 4.4 or 8.3 mM (depending on the assumption of the Ca ion activity coefficient as unity or as the same as that of sialic acid) obtained by Jaques et al (1977) with Ca-sialic acid complex.

Cardiac sarcolemma have been reported to be able to bind (in the absence of Ca precipitating agent such as oxalate or phosphate: Will et al, 1973; Krause et al, 1973; Williamson et al, 1975; Dhalla et al, 1976; St. Louis et al, 1976) and accumulate(in the presence of precipitating anions: Sulakhe et al, 1976; St. Louis et al, 1976) Ca ions. In this study, the primary interest was in the binding of Ca to the terminal sialic acid of the sarcolemmal and basement membrane glycoprotein.

The millipore filtration method that has been utilized by some investigators in the study of Ca binding requires washing steps which may diminish the quantity of labile, easily exchanged, Ca. For example, the fast exchanging and superficial Ca compartment of this study has a $t_{\frac{1}{2}}$ of 15 sec. Similarly, using murexide-spectrophotometric technique, Nayler et al (1976) have reported saturation of plasma membrane Ca binding within 10 sec. On the other hand, millipore filtration technique usually involves 20-60 sec washing steps with 2-5 ml tracer-free medium. For this reason, the equilibrium-centrifugation method was used in studying the sarcolemmal Ca-binding characteristics.

The observation of a bi-phasic Scatchard plot of the sarcolemma Ca binding curve agrees with the reports of others (Williamson et al 1975; Will et al, 1976). Will et al (1976) examined the high affinity (K_D of about 1 μM) binding sites and observed complete inhibition by Na concentrations above 100 mM. They suggested that the binding sites involved are probably located on the internal side of the membrane and might be involved in a Na-coupled transport of Ca out of the cell. The low affinity binding sites (of their figure 1a and b) analyzed by SKATCH.MB yield a binding capacity of 16.6 nmole/mg with a K_D of 0.31 mM. These are one order of magnitude less than that of the normal hamster cardiac sarcolemma observed in this investigation. Williamson et al (1975) studied the Ca binding to guinea pig cardiac sarcolemma. They observed a low affinity site of 123 nmole/mg and a K_D of 0.8 mM (SKATCH.MB analysis gave a corresponding value of 103 nmole/mg and 0.78 mM). They further observed a specific inhibition of low affinity binding by verapamil. The binding capacity they demonstrated is approximately the same as that shown in the normal cardiac sarcolemma of this investigation (Average of 115 nmole/mg), although the dissociation constant was only half of that of the hamster heart (Average of 1.5 mM). Since the K_D for sialic acid and Ca complex is about 4-8 mM, the value of hamster heart sarcolemma K_D suggests greater participation of sialic acid residues in the Ca binding phenomenon of this tissue membrane.

The Ca-binding profile of hamster cardiac sarcolemma is distinguished by an insensitivity to changes in medium monovalent cation concentration of 100 mM. Na and K ion show no inhibition or activation of the sialic acid associated Ca binding (as compared to Li). Again, a value close to 1:1 association exists between sialic acid and Ca (actually a 1:1.6 relationship). The insensitivity to Na and K may be due to the unique way of association between sialic acid and Ca ion. Jaques and co-workers (1977) proposed participation of glycerol side chain in the binding of Ca ion based on NMR spectra study. Colominic acid, which is a polymer of sialic acid, does not have free glycerol groups because the monomers are linked together through α-2,8-ketosidic linkage, also has very small interaction with Ca ion. Thus the divalent Ca ion charges are neutralized by both the carboxy group and the glycerol hydroxy groups. Negligible interaction between sialic acid residue and Na or K ion has also been observed by Jaques et al (1977) and by Behr and Lehn (1972).

The observation that partial sialic acid removal by neuraminidase changed the dissociation constant of the remaining low affinity binding sites suggested participation of other anionic groups in the binding of Ca ions. Acidic phospholipids or the acidic groups associated with the protein at the surfaces of the membrane can bind Ca. The major binding sites are primary and secondary phosphates and carboxy groups (Bianchi, 1968). Recently, Feldman and

Weinhold (1977) have isolated a Ca binding lipoprotein component of rat heart plasma membrane. The lipoprotein has an extremely high Ca binding capacity, 4270 nmole/mg, with a K_D of 0.074 mM. This is compared to the plasma membrane capacity of 66 nmole/mg and a K_D of 0.35 mM in the same investigation. Assuming that the lipoprotein accounts for approximately 0.5% total protein in the plasma membrane, it was suggested that the lipoprotein might account for 33% of the Ca binding activity of the plasma membrane. The plasma membrane sialic acid concentration was 18 nmole/mg which is quite low compared to the hamster heart sarcolemma. It is possible that the lipoprotein component contributes to a lesser percentage of total Ca binding than that is claimed, in that case it might be equivalent to the high affinity binding sites observed in this investigation. The physiological role of this component with a K_D of 0.074 mM, however, is not clear.

Several other investigators have also examined the Ca binding characteristic of cardiac sarcolemma. Dhalla and co-workers (1976) observed a very high Ca binding by rat heart sarcolemma prepared by hypotonic shock LiBr treatment. The passive Ca binding using millipore filtration amounted to 250 nmole/mg protein at 1.25 mM Ca concentration. Unfortunately, the data could not be analyzed for K_D. Sulakhe et al (1976) and St. Louis et al (1976), on the other hand, have reported very low passive (<1 nmole/mg) and ATP dependent (35 nmole/mg) Ca binding. The

binding is further stimulated by K ion. Again K_D is unavailable and comparison to the present findings is difficult.

Schlatz and Marinetti (1972) have done an extensive investigation on Ca binding to liver plasma membrane. Similar to heart sarcolemma, they have demonstrated a low affinity binding sites of a capacity of 120 nmole/mg and with a K_D of 3.1 mM. The binding was sensitive to competition by Mg but insensitive to Na and K. Using phospholipase and neuraminidase digestion, it was determined that phospholipid accounts for 60-70% of the low affinity binding while sialic acid was responsible for only 30-40% of the binding. The amount contributed by the latter again suggested a 1:1 relationship between sialic acid and Ca, since liver plasma membrane contains baout 35-50 nmole sialic acid per mg (Benedetti and Emmelot, 1968; Ray, 1970).

Since anionic binding groups other than sialic acid can bind a considerable amount of Ca, the significance of sialic acid associated Ca in the heart E-C coupling may be questioned. The fact that cardiac sarcolemma contains a sialic acid concentration that is the highest amoung excitable tissues and five to ten fold higher than the rest of body tissue suggest some specific function. Kinetic studies of this investigation further showed the importance of a labile Ca pool, the quantity of which can not be entirely accounted for by the interstitial free Ca, in the main-

tenance of heart muscle E-C coupling. Figure 46 compares the saturation curve of Ca binding to cardiac sarcolemma and the cardiac muscle contractility as a function of $[Ca]_o$. The close correlation might be fortuitous but a definite relationship between the two is evident. The data may be interpreted to mean that cardiac contractility is a direct function of the saturation of superficial Ca binding. This is consistent with the observation of a linear correlation between cardiac contractility and fast exchanging Ca pool content in the kinetic studies.

Comparison of membrane sialic acid content and Ca binding characteristics is complicated by the factor of purity of the membrane proteins. The demonstration of lower sialic acid concentration and lower Ca binding capacity in the cardiomyopathic hearts could either be a true depression or an apparent depression due to contamination by other inert proteins. Since the yield in sarcolemmal protein in the normals (4.7 mg) and cardiomyopathics (5.2 mg) are not markedly different, it is suggested that the difference observed is not due to a different degree of purification of the sarcolemmal fraction. The possibility must still be considered, however, that the difference is manifested after isolation due to disproportionate enzyme degradation or abnormal fragility of the membrane glycoprotein.

I have established previously that the reduction of the cardiac contractility in the cardiomyopathic hearts

Figure 46

Comparison of the saturation curve of Ca binding to cardiac sarcolemma and cardiac muscle contractility as a function to [Ca] .

Solid curve indicates saturation of Ca binding to normal hamster cardiac sarcolemma using the average value of 115 nmoles Ca/mg protein and 1.5 mM for capacity and K_D respectively.

Open circle (o) indicates data from Shine et al (1971) representing dP/dt max (g/sec) of isolated blood perfused rabbit interventricular septum.

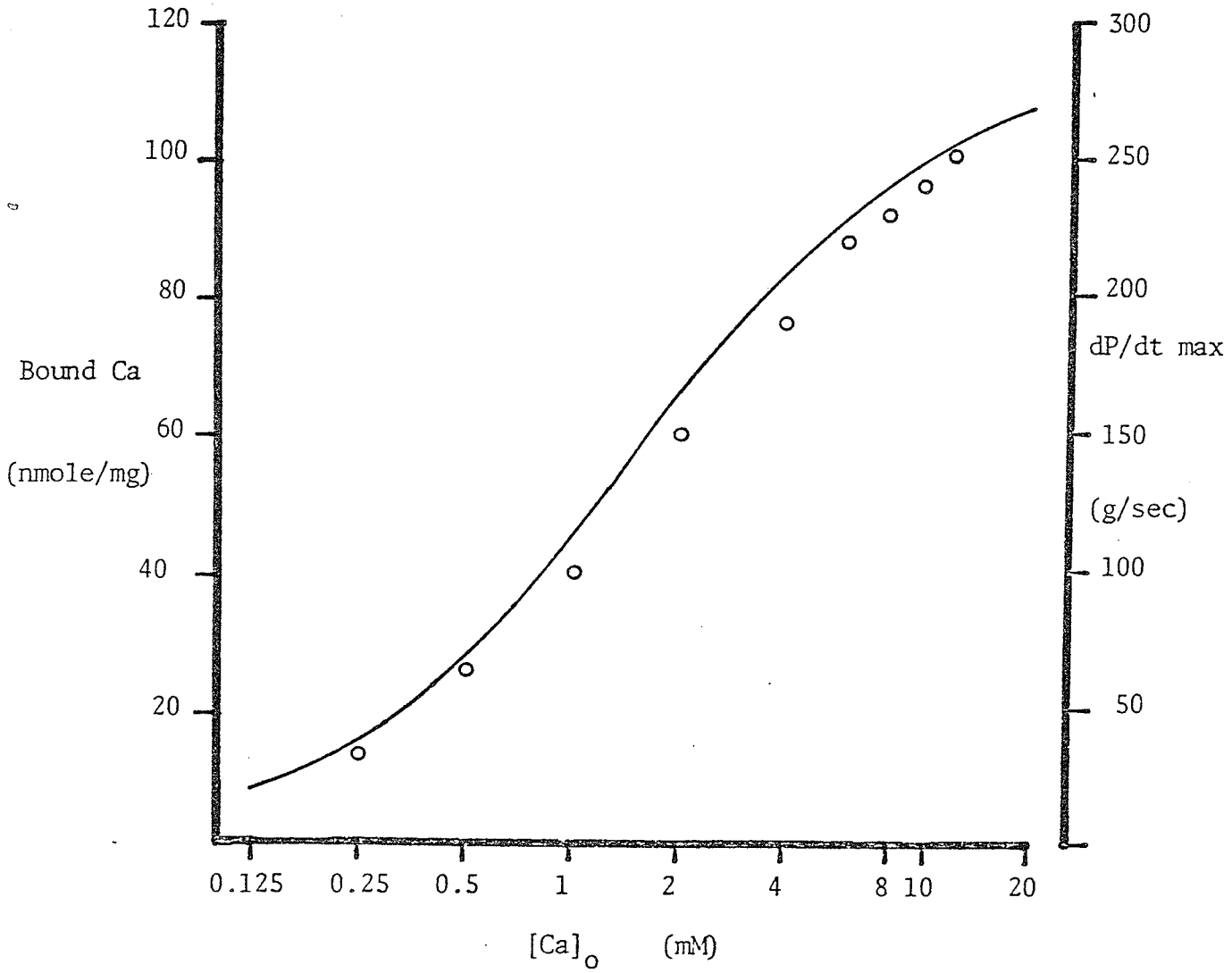
120
100
80
60
40
20
Bound Ca
(nmole/mg)
300
250
200
150
100
50
dP/dt max
(g/sec)
0.125
0.25
0.5
1
2
4
8
10
20
[Ca]o (mM)

can be explained in terms of a reduction of the content of a fast exchanging Ca pool, $Ca_1(s)$ or $Ca_I(p)$. Calculations indicated, however, that interstitial Ca alone can not account for the total quantity of Ca in this pool. This suggested, since this pool is likely to be extracellular, that a reduction of Ca binding capacity of the sarcolemma is present. The results from Ca-binding studies on cardiac sarcolemma of failing cardiomyopathic heart indeed showed a reduction of Ca binding capacity. This reduction was accompanied by a reduction of surface sialic acid residues.

In conclusion, it appears that surface sialic acid residues represent a binding site for Ca and functions as a rapidly exchanging Ca pool for cardiac muscle E-C coupling. The low K_D of this binding puts it in the range of interstitial [Ca] and supports the labile nature of this association (labile, superficial, fast exchanging Ca pool).

G. HYPOTHESIS OF HAMSTER CARDIOMYOPATHY

Since the hamster cardiomyopathy is genetically transmitted, it is likely that the many cellular abnormalities observed in this disease model are the result of one or at most a few basic biochemical defects. To explain the rather specific striated muscle tissue localization of the disease lesion, two hypothesis might be advanced: (1) the disease is manifested after tissue cell differentiation, and (2) the defect is present in all tissue cells

but is deleterious in only a few tissues due to their specific metabolic activities. The first possibility is deemed unlikely in the light of the work by Bester and Gevers (1973, a, b). They have demonstrated a functional reduction of the protein synthetic machinery in not only striated muscle tissue, but also in brain, liver and uterus. The defect is suggested to result from a higher endogenous exonuclease activity which non-specifically reduced the number of functional t-RNA. Subsequent studies (Bester and Gevers, 1975) confirmed the rather non-specific lesion in that both myofibrillar and soluble proteins synthesis were depressed as compared to controls. The retarded growth rate of cardiomyopathic hamster (Bajusz et al, 1966) is consistent with this observation. If the concept of a nonspecific tissue defect is accepted, it is then necessary to explain the localized lesion in skeletal and cardiac muscle cells.

The cardiac lesion is distinguished by spontaneous developed myolysis. This type of lesion is consistently observed in anoxia, hypoxia, or epinephrine toxicity (Bajusz et al, 1966; Buchner, 1971). Since the disease process can be reduced in intensities by Ca-deficient diet (Jasmin et al, 1975) and prevented during verapimil administration (Jasmin and Bajusz, 1975), it may be suggested that cardiac muscle cell death is a result of intracellular Ca overload due to excessive Ca influx. The fact that cardiac sympathetic tone is elevated co-incidental or

preceding the development of cardiac lesion (Sole et al, 1975) suggests the triggering factor of elevated Ca influx may be caused by augmented tissue sympathetic tone.

Lossnitzer and Bajusz (1974) have proposed that the localized myocytolysis involves predisposed immature cardiomyoblasts which exist in the pre-clinic stage of the cardiomyopathic hamster hearts (Buchner, 1970; Nadkarni et al, 1972). It is also possible that the localized lesions is due to the distribution of sympathetic nerve endings and local high concentration of amine as a result of elevated nervous activities in the heart (Reichenbach and Benditt, 1970).

What is then the triggering factor for the high sympathetic outflow? It is clear a reduced cardiac contractility would reflexly induce high cardiac sympathetic activity. The observation of a depressed cardiac function in the pre-clinic cardiomyopathic hearts of this investigation suggests the possible triggering factor.

The cardiomyopathic hearts are supersensitive to the adverse action of catecholamine (Bajusz et al, 1969 d). This suggests, possibly, an abnormal membrane permeability to Ca. Based on data on kinetic studies and on subcellular biochemical analysis, I propose that the basic functional defect in hamster cardiomyopathy is a deficiency of striated muscle basement membrane sialic acid residues.

This hypothesis would both explain the decreased cardiac contractility and the abnormal sensitivity to

catecholamine. I have established that cardiac contractility is intimately correlated to the content of a fast exchanging Ca pool which include interstitial and sarcolemmal bound Ca. I have further demonstrated a correlation between Ca-binding capacity of the cardiac sarcolemma and membrane sialic acid content. The reduced content of fast exchanging Ca in the young cardiomyopathic hearts suggests a deficiency of sarcolemmal Ca binding sites and I have shown some evidence of membrane sialic acid deficiency and reduced Ca binding in the older age group of cardiomyopathic hamster hearts. As a corollary to the observation that the removal of surface sialic acid can result in elevated Ca permeability (Langer et al, 1976) it is possible that the deficiency of membrane sialic acid residues renders the cells excessively sensitive to the change of interstitial Ca or the action of catecholamine. The kinetic studies of this investigation support an increased Ca permeability in the cardiomyopathic hearts.

If the functional defect in hamster cardiomyopathy is a deficiency of sarcolemmal sialic acid residues, what then is the underlying defect? Two possibilities exist: (1) there is a deficiency of membrane glycoprotein synthesis and (2) there is an elevation of tissue breakdown. Based on the finding of an elevated exonuclease activities in the cardiomyopathics, it is possible that there is lesser amount of enzymes present involved in glycoprotein synthesis. If this is true, there should be a general depres-

sion of other amino sugars in the basement membrane of the cardiomyopathics. It is unfortunate that I could not obtain a reasonable activity of sialyltransferase. It is possible that muscle sialyltransferase differs from that of the other tissues and requires special factors for activation. Nevertheless, some depression of the sialyltransferase activity, albeit statistically nonsignificant, was observed in the cardiomyopathic hearts in failure. Serum sialic acid level in the cardiomyopathic hamster indicates the reduction of surface sialic acid is not due to a lack of this substrate.

If the hypothesis advanced is accepted, there remains a few observations that must be discussed. These are: (1) the phenomena of low blood pressure and bradycardia in cardiomyopathic hamster in the face of high sympathetic outflows, (2) the non-progressive nature of the spontaneous cardiac lesions, (3) the beneficial effect of K-orotate, K-aspartate and parabiosis, (4) the presence of lesions in skeletal muscle, and (5) the absence of lesions in smooth muscle and other tissues.

The hemodynamics in hamster cardiomyopathy have only been examined in the stages post cardiac necrosis and hypertroph (Abelman et al 1972, 1973; Jeffrey et al, 1970). At those times, the cardiac NE turn over rate is elevated in the cardiomyopathics indicating high sympathetic outflow (Sole et al, 1976). The apparent paradox of hypotension and bradycardia can not be easily explained. It would be inter-

esting to examine the hemodynamics in the young hamster when cardiac lesions and elevated sympathetic outflow first occured. It is perhaps relevant that the isolated cardiomyopathic hearts *in vitro* showed a slower spontaneous sinus rhythm than control (Brink et al, 1967, 1969).

The non-progressive nature of spontaneous cardiac lesions is equally difficult to explain unless they only involve the predisposed immature cardiomyoblasts. Bajusz et al (1966) have also reported loss of sensitivity of the cardiomyopathic hamster heart to the necrotic effect of catecholamines after the necrotic phase of the disease. It seems some cellular metabolic adaptations have occured, though what is involved is not at all clear.

The observation that only certain K-salts influenced the outcome of the cardiomyopathy suggested that the organic moiety of these salts plays an important role in the therapeutic effect. The failure of Na-salt might be explained in terms of the imposed Na load while the negative effect of Mg-salt might be a result of failure of absorption. It might be significant that aspartate is the immediate precursor of orotate which in turn is the building block of *de novo* pyrimidine synthesis.

Other functions of the aspartate salt may also participate in the beneficial effect. For example, aspartate has been reported to inhibit NaK-ATPase (Fedelesova et al, 1972); K-Mg aspartate has been found to have higher protection value against asphyxia than equal molar amount of other salts of K-Mg (Hochrein and Lossnitzer, 1969); as-

partate has been found to produce positive inotropic effects in isolated heart preparation (Lamarche and Royer, 1965). In addition, the metabolic significance of the malate-aspartate cycle in heart has been recently emphasized (Safer and Williamson, 1972; Safer, 1975, Williamson et al 1976b). K-Mg aspartate may also act by maintaining electrolyte balance (Kenter and Falkenhahn, 1966; Pillen, 1966) and act as the intracellular Ca-antagonist (Slezak and Tribulova, 1975; Fedelesova et al, 1975).

Similar to aspartate, orotate also has a large spectrum of pharmacological effect. Orotate is positive inotropic in the isolated dog heart (Buckley et al, 1961). Orotic acid administration has been shown to enhance protein synthesis in experimental cardiac hypertrophy and to promote a change of cardiac contractility, (Kolos et al, 1974; Donohoe et al, 1974). The observation of increased cardiac contractility associated with cardiac hypertrophy is against the conventional concept of hypertrophy (Braunwald et al, 1976) and suggest some special functional role. Since pyrimidine UDP has been shown to activate liver sialyltransferase (Bernacki, 1975), it was hoped that UDP or orotate can also activate cardiac sialyltransferase. The results (Table 24) did not support this concept. And finally, orotate has been shown to promote scar organization of the necrotic cardiac tissue (Nikolaeva et al, 1974).

The beneficial effect of parabiosis may act through transfer of orotate and aspartate from the healthy partner.

Meerson (1969) has proposed that during the acute phase of adjustment of the heart to stress, there might be a relative deficiency of co-factors. Parabiosis may simply act as a reservoir of necessary co-factors.

Since skeletal muscle is not sympathetically innervated and since its lesions develop much earlier than that of the heart, some other triggering factor must be present in skeletal muscle at least. Mendell et al (1971) have reported that functional ischema (reduced blood supply plus Serotonin injection) can produce skeletal muscle lesions characteristic of dystrophy in normal rats. Although no elevation of plasma serotonin level is observed in subsequent studies (Murphy et al, 1973) of patients with Duchenne muscular dystrophy, the possibility of functional ischema in hamster myopathy exists in the light of the observation by Jasmin and Bajusz (1975) that dibenamine, an α-blocker, was efficient in reducing the severity of skeletal muscle lesions in hamster dystrophy.

Finally, it might be asked why clinical lesions do not develop in other tissues, especially smooth muscle? For the sake of completeness, the following speculation is advanced, without strong supporting evidence. Assume Ca overload is the final course of the muscle death. Skeletal, cardiac and smooth muscle show decreasing order in SR development and increasing order in surface to volume ratio (Langer, 1973; Somlyo and Somlyo, 1968). It is possible that skeletal muscle tends to sequester excessive intracellular

Ca whereas smooth muscle tends to eliminate excess Ca by Na-Ca exchange (Ma and Bose, 1976). Heart muscle probably disposes of excess Ca by both mechanisms (Reuter and Seitz, 1968). This may then explain why skeletal and cardiac muscle, but not smooth muscle, are damaged by a membrane abnormality.

To sum up, it is proposed that the basic functional defect in hamster cardiomyopathy involves a deficiency of surface membrane sialic acid residues. This might arise from a deficiency of sialyltransferase due to a higher exonuclease activities. The defect results in depressed cardiac contractility which reflexly increases sympathetic output. Because of the deficiency of surface sialic acid, the membrane is proposed to have higher passive Ca permeability. This could result in a supersensitivity to the necrotic effect of released NE. Myolysis ensues. Fibrotic and calcified scar formations further depress cardiac contractility. NE turn over increases until cardiac NE are depleted. CHF then sets in leading to death.

H. SUMMARY

The objectives of this study were (1) to study the Ca exchange kinetics and cardiac contractility changes in the normal and cardiomyopathic hamster hearts as a function of the course of the disease, and (2) to study the Ca binding characteristics of hamster cardiac sarcolemma in normals and in myopathics and to relate this to a Ca compartment in kinetic studies.

Since a short period of Ca-free perfusion did not result in marked change of Ca permeability, it was deemed valid to use non-steady state Ca exchange in order to correlate Ca exchange to contractility change.

A fast exchanging Ca pool, $Ca_I(p)$ in the washout study with $t_{\frac{1}{2}}$ of around 15 sec was found to be related to changes of cardiac contractility. The content of this compartment was considerably larger than interstitial Ca.

A fast exchanging Ca pool, $Ca_1(s)$, in the uptake studies was similarly found to correlate with cardiac contractility. The size of this compartment was smaller than that of the washout studies using an in-parallel model of exchange, but was approximately equal to that of the washout studies using in-series model of exchange.

The size of the rapidly exchanging compartment was decreased in the cardiomyopathic hearts. Cardiac contractility was also observed to be depressed in the cardiomyopathics. The defect was apparent at 30 d of age, or before the onset of cardiac lesions in these animals. The magnitude of change of both the Ca pool and contractility was most pronounced in hamsters with CHF.

The sarcolemma fraction obtained by osmotic shock, salt extraction technique revealed high levels of sialic acid residues. An average of 200 mole sialic acid per mg sarcolemma protein is amongst the highest concentration reported on surface membranes of different tissues.

Ca binding of the cardiac sarcolemma indicated two

binding sites. The low affinity binding sites had a capacity of 115 nmole Ca/mg protein and a K_D of 1.5 mM and was sensitive to sialic acid removal. The Ca binding exhibited a 1:1 relationship to sialic content and was insensitive to medium Na or K.

A reduction of sarcolemmal sialic acid content and Ca binding capacity was observed in cardiomyopathic hearts in failure. It suggests that this depression corresponds to that in the kinetic studies and is responsible for the reduced contractility.

It is proposed that the primary functional defect in hamster cardiomyopathy is a deficiency of surface sialic acid residues and its associated Ca binding. Myocardial lesions may result from a reflex elevation of sympathetic output due to depressed cardiac contractility, coupled with a supersensitivity to NE action due to deficiency of surface sialic acid residues, which have been shown to regulate membrane Ca permeability.

SECTION V

BIBLIOGRAPHY

Abdullah F, Pennington RJ: Ribonucleases in normal and dystrophic human muscle. Clin Chim Acta 20:365, 1968

Abelmann WH, Jeffrey FE, Wagner R: Hemodynamics of the hereditary cardiomyopathy of syrian hamsters. Rec Adv Stud Cardiac Struc Metab 1:225, 1972

Abelmann WH, Wagner RL, Bajusz E: Serial hemodynamic observations in hereditary cardiomyopathy of the Syrian hamster. Rec Adv Stud Cardiac Struc Metab 2:509, 1973

Albers RW: Biochemical aspects of active transport. Ann Rev Biochem 36:727, 1967

Andersson KE, Edman KAP: Effects of lanthanum on the coupling between membrane excitation and contraction of isolated frog muscle fibers. Acta Physiol Scand 90:113, 1974

Andrew CG, Appel SH: Macromolecular characterization of muscle membrane. J Biol Chem 248:5156, 1973

Angelakos ET, King MP, Millard RW: Regional distribution of catecholamines in the hearts of various species. Ann NY Acad Sci 156:219, 1969

Angelakos ET, Carballo LC, Daniels JB, King MP, Bajusz E: Adrenergic neurohumors in the heart of hamsters with hereditary myopathy during cardiac hypertrophy and failure. Rec Adv Stud Cardiac Struc Metab 1:262, 1972

Angelakos ET, King MP, Carballo L: Cardiac adrenergic innervation in hamsters with hereditary myocardiopathy: chemical and histochemical studies. Rec Adv Stud Cardiac Struc Metab 2:519, 1973

Argus MF, Arcos JC, Sardesai VM, Overby JL: Oxidative rates and phosphorylation in sarcosomes from experimentally-induced failing rat heart. Proc Soc Exp Biol Med 117:380, 1964

Awapara J, Seale B: Distribution of transaminases in rat organs. J Biol Chem 194:497, 1952

Baieve D, Florini JR: Effect of muscular dystrophy on the rate of RNA synthesis in chicken. Arch Biochem Biophys 139:393, 1970

Bailey LE, Dresel PE: Correlation of contractile force with a calcium pool in the isolated cat heart. J Gen Physiol 52:969, 1968

Bailey LE, Sures HA: The effect of ouabain on the washout and uptake of Ca in the isolated cat heart. J Pharmacol Exp Ther 178:259, 1971

Bailey LE, Ong SD, Queen GM: Calcium movement during contraction in the cat heart. J Mol Cell Cardiol 4:121, 1972

Bajusz E: The role of some essential nutrients in the pathogenesis of cardiac necrosis (studies on K, Mg, Na, and Cl-deficiencies). Rev Canad Biol 20:713, 1961

Bajusz E, Jasmin G: Action of parathyroidectomy and dihydrotachysterol on myocardial calcification due to coronary vein obstruction. Proc Soc Exp Biol Med 112:752, 1963a

Bajusz E, Jasmin G, Mongeau A: Thyroid-parathyroid interrelationship in processes governing myocardial calcification. Endocrinol 73:92, 1963b

Bajusz E, In: Nutritional aspects of cardiovascular diseases. Crosby Lockwood and Son, 1965a

Bajusz E, ed. In: Electrolytes and cardiovascular diseases vol 1, fundamental aspects. S Karger, Basel, 1965b

Bajusz E, Homburger F, Baker JR: The heart muscle in muscular dystrophy with special reference to involvement of the cardiovascular system in the hereditary myopathy of the hamster. Ann NY Acad Sci 138:213, 1966

Bajusz E: Interrelationship between reparative processes in myocardium and the development of congestive heart failure. Rev Canad Biol 27:45, 1968a

Bajusz E, Lossnitzer K: A new disease model of chronic congestive heart failure: studies on pathogenesis. Trans NY Acad Sci 30:939, 1968b

Bajusz E: Hereditary cardiomyopathy: A new disease model. Am Heart J 77:686, 1969a

Bajusz E, Baker JR, Nixon CW, Homburger F: Spontaneous hereditary myocardial degeneration and congestive heart failure in a strain of Syrian hamsters. Ann NY Acad Sci 156:105, 1969b

Bajusz E: Dystrophic calcification of myocardium as conditioning factor in genesis of congestive heart failure. Am Heart J 78: 202, 1969c

Bajusz E, Homburger F, Baker JR, Bogdonoff P: Dissociation of factors influencing myocardial degeneration and generalized cardiocirculatory failure. Ann NY Acad Sci 156:386, 1969d

Balasubramanian V, McNamara DB, Singh JN, Dhalla NS: Biochemical basis of heart function. X. Reduction of Na, K stimulated ATPase activity in failing rat heart due to hypoxia. Can J Physiol Pharmacol 51:504, 1973

Bartosova D, Shuapil M, Konecky B, Poupa K, Rakusan K, Turek Z, Vizek M: The growth of the muscular and collagenous parts of the rat heart in various forms of cardiomegaly. J Physiol 200:285, 1969

Battelle B, Florini JR: Protein synthesis in chicken muscular dystrophy. Biochem 12:635, 1973

Beeler GW Jr, Reuter H: Voltage clamp experiments on ventricular myocardial fibers. J Physiol 207:165, 1970a

Beeler GW Jr, Reuter H: Membrane Ca current in ventricular myocardial fibers. J Physiol 207:191, 1970b

Beeler GW Jr, Reuter H: The relation between membrane potential, membrane currents and activation of contraction in ventricular myocardial fibers. J Physiol 207: 211, 1970c

Behr J-P, Lehn J-M: Stability constants for the complexation of alkali and alkaline-earth cations by N-acetylneuraminic acid. FEBS Lett 22:178, 1972

Beierle JW: Cell proliferation: enhancement by extracts from cell surface of polyoma-transformed cells. Sci 161:798, 1968

Benedetti EL, Emmelot P: Studies on plasma membrane. IV. The ultrastructural localization and content of sialic acid in plasma membrane isolated from rat liver and hepatoma. J Cell Sci 2:499, 1967

Benedetti EL, Emmelot P: Structure and function of plasma membranes isolated from liver. In: The membranes; ultrastructure in biological systems. Dalton AJ, Haguenau F ed. 4:33, 1968

Bennett SH: Morphological aspects of extracellular polysaccharides. J Histochem Cytochem 11:14, 1963

Bennett G, LeBlond CP, Haddad A: Migration of glycoproteins from the Golgi apparatus to the surface of various cell types as shown by radioautography after labelled fucose injection into rats. J Cell Biol 60:258, 1974

Bernacki RJ: Regulation of rat-liver glycoprotein: N-acetylneuraminic acid transferase activity by pyrimidine nucleotides. Eur J Biochem 58:977, 1975

Berson SA, Yalow RS: Quantitative aspects of the reaction between insulin and insulin-binding antibody. J Clin Invest 38:1996, 1959

Bosch HR Jr, Jones LR, Watanabe AM: Intact vesicles of canine cardiac sarcolemma: Evidence from vectorial properties of Na, K-ATPase. Circ Res 39:586, 1976

Bester AJ, Gevers W: Cell-free protein synthesis in heart and skeletal muscles from polymyopathic hamsters. Biochem J 132:193, 1973a

Bester AJ, Gevers W: Evidence for defective transfer ribonucleic acid in polymyopathic hamsters and its inhibitory effect on protein synthesis. Biochem J 132:202, 1973b

Bester AJ, Gevers W: The synthesis of myofibrillar and soluable proteins in cell-free systems and in intact cultured muscle cells from newborn polymyopathic hamsters. J Mol Cell Cardiol 7:325, 1975

Bianchi PC, In: Cell calcium. Mol Biol Med Ser. New York, Appleton-Century-Crofts, 1968

Bing RJ, WUC, Gudbjarnason S: Mechanism of heart failure. Circ Res 15, suppl II:64, 1964

Bloodworth JMB Jr, Von Haam E: The tissue catecholamine concentration of the human heart, determined by the aluminum hydroxide-arsenomolybdic acid method. Circ 13:573. 1956

Boas EP, Lowenberg H: The heart rate in progressive muscular dystrophy. Arch Int Med 47:376, 1931

Boegman RJ: The isolation and partial characterization of membranes from dystrophic and normal muscle. Comp Biochem Physiol 48A:237, 1974

Borowski IFM, Harrow JAC, Pritchard ET, Dhalla NS: Changes in electrolyte and lipid contents of the myopathic hamster (UM-X 7.1) skeletal and cardiac muscles. Res Commun Chem Pathol Pharmacol 7:443, 1974

Boutet M, Huttner I, Rona GR: Permeability alteration of sarcolemmal membrane in catecholamine-induced cardiac muscle cell injury; in vivo studies with fine structural diffusion tracer horseradish peroxidase. Lab Invest 34: 482, 1976

Bozler E: Distribution and exchange of Ca in connective tissue and smooth muscle. Am J Physiol 205:608, 1963

Braunwald E, Ross J Jr, Sonnenblick EH, In: Mechanisms of contraction of the normal and failing heart. Little and Brown, 1976

Briggs NF, Gertz EW, Hess ML: Calcium uptake by cardiac vesicles: inhibition by amytal and reversal by ouabain. Biochim Zeit 345:122, 1966

Briggs NF, Solaro JR, Gertz EW: Estimation of the amount of sarcoplasmic reticulum in cardiac muscle. In: Cardiac hypertrophy Alpert NR ed. Academic Press. pp 167-175, 1971

Brink AJ, Lochner A: Work performance of the isolated perfused beating heart in the hereditary myocardiopathy of the Syrian hamster. Circ Res 21:391, 1967

Brink AJ, Lochner A: Contractility and tension development of the myopathic hamster (BIO 14.6) heart. Cardiovasc Res 3:453, 1969

Brink F: The role of calcium ions in neural processes. Pharmacol Rev 6:243, 1954

Buccino PA, Harris E, Spann JF, Sonnenblick EH: Response of myocardial connective tissue development of experimental hypertrophy. Am J Physiol 216:425, 1969

Buchner F: Quantitative morphology of heart failure. Meth Achievm Exp Path 5:60, 1971

Buckley NM, Tsuboi KK, Zeig NJ: Inotropic effects of purine and pyrimidines on the isolated heart. Circ Res 9:242, 1961

Burch GE, Carlson FD, Davies JNP, DePasquale N, Ferrans V, Fowler NO, Hibbs R, Mattingly TW, Mogabgab W, Sjoerdsma A, Walsh J: Primary myocardial disease (heart muscle disease, cardiomyopathy). In: The heart and circulation, Second National Conference on Cardiovascular diseases. Andrus EC, Maxwell CH ed. Washington D.C. Fed Am Soc Exp Biol 1:488, 1965

Burch GE, DePasquale NP: Recognition and prevention of cardiomyopathy from the inter-society commission for heart disease resources. Circ 62:A47, 1970

Burger MM: Isolation of a receptor complex for a tumour specific agglutinin from the neoplastic cell surface. Nature 219:499, 1968

Cantin M, Leone A, Bajusz E: Participation of renal electrolytes in the mechanism of edema in congestive heart failure: studies on cardiomyopathic hamsters. Rec Adv Stud Cardiac Struc Metab 1:303, 1972

Carafoli E, Azzi A: The affinity of mitochondria for calcium. Experientia 27:906, 1972a

Carafoli E: Mitochondria in the contraction and relaxation of heart. Rec Adv Stud Cardiac Struc Metab 4:393, 1972b

Carafoli E, editorial: Mitochondrial, Ca transport and the regulation of heart contraction and metabolism. J Mol Cell Cardiol 7:83, 1975

Carsten ME: The cardiac calcium pump. Proc Nat Acad Sci USA 52:1456, 1964

Caruso G, Buchtal F: Refractory period of muscle and electromyographic findings in relatives of patients with muscular dystrophy. Brain 88:29, 1965

Cerven E: Determination of sialyl transfer from exogenons CMP-N-acetyl-(^{14}c) Neuraminic acid to cell membrane-bound acceptor molecules at the surface of intact Ehrlich ascites tumor cells. Biochim Biophys Acta 467:72, 1977

Chance B: The energy-linked reaction of Ca with mitochondria. J Biol Chem 240:2729, 1964

Chidsey CA, Braunwald E, Morrow AG, Mason DT: Myocardial norepinephrine concentration in man - effects of congestive heart failure. New Eng J Med 269:653, 1963

Chidsey CA, Kaiser GA, Sonnenblick EH, Spann JF, Braunwald E: Cardiac norepinephrine stores in experimental heart failure in the dog. J Clin Invest 43:2386, 1964

Chidsey CA, Weinbach EC, Pool PE, Morrow AG: Biochemical studies of energy production in the failing human heart. J Clin Invest 45:40, 1966a

Chidsey CA, Braunwald E: Sympathetic activity and neurotransmitter depletion in congestive heart failure. Pharmacol Rev 18:685, 1966b

Cook GMW, Heard DH, Seaman GVF: Sialic acids and the electrokinetic charge of the human erythrocyte. Nature 191:44, 1961

Cook GMW: Glycoproteins in membranes. Biol Rev 43:363, 1968

Covell JW, Chidsey CA, Braunwald E: Reduction of the cardiac response to postganglionic sympathetic nerve stimulation in experimental heart failure. Circ Res 19:51, 1966

Cutilletta AF, Dowell RT, Rudnik M, Arcilla RA, Zak R: Regression of myocardial hypertrophy. I. Experimental model, changes in heart weight, mucleic acids and collagen. J Mol Cell Cardiol 7:767, 1975

Datta P: Labeling of the external surface of hamster and mouse fibroblasts with (^{14}c) sialic acid. Biochem 13: 3987, 1974

DeDuve C: The lysosome in retrospect, In: Lysosomes in biology and pathology Dingle JT, Fell HB ed. 1:1, 1969, North Holland, Amsterdam

DeQuattro V, Nagatsu T, Mendoz A, Verska J: Determinants of cardiac noradrenaline depletion in human congestive failure. Cardiovasc Res 7:344, 1973

Dhalla NS: Defects in Ca regulatory mechanism in heart failure. Rec Adv Stud Cardiac Struc Metab 4:521, 1972

Dhalls NS, Singh JN, Fedelesova M, Balasubramanian V, McNamara DB: Biochemical basis of heart function X II. Sodium-potassium stimulated adenosine triphosphatase activity in the perfused rat heart made to fail by substrate lack. Cardiovasc Res 8:227, 1974a

Dhalla NS, Sulakhe PV, Fedelesova M, Yates JC: Molecular abnormalities in cardiomyopathy. Adv Cardiol 13:282, 1974b S Karger, Basel

Dhalla NS, Editorial: Involvement of membrane systems in heart failure due to intracellular Ca overload and deficiency. J Mol Cell Cardiol 8:661, 1976a

Dhalla NS, McNamara DB, Anand MB: Heart sarcolemma as a dynamic excitable membrane. Rec Adv Stud Cardiac Struc Metab 9:1, 1976b

Dhalla NS, Anand MB, Harrow JAC: Calcium binding and ATPase activities of heart sarcolemma. J Biochem 79:1345, 1976c

Doggenweiler CF, Frank S: Staining properties of lanthanum on cell membranes. Proc Nat Acad Sci 53:425, 1965

Donohoe JA, Williams JF, Kolos G, Hickie JB: The action of orotic acid as a positive inotropic agent during the acute phase of myocardial hypertrophy. Aust N Z J Med 4:542, 1974

Duffy MJ, Schwartz V: Molecular groups responsible for the binding of Ca ions in the erythrocyte membrane. Biochem Soc Trans 2:403, 1974

Durr R, Shur B, Roth S: Sperm-associated sialyltransferase activity. Nature 265:547, 1977

Ebashi S, Endo M: Calcium ion and muscle contraction. Prog Biophys Mol Biol 18:123, 1968

Ebashi S: Excitation-contraction coupling. Ann Rev Physiol 38:293, 1976

Endo M, Tanaka M, Ebashi S: Release of Ca from SR in skinned fibers of the frog. Proc Intern Congr Physiol Sci 24th 7:126, 1968

Endo M, Tanaka M, Ogawa Y: Ca induced release of Ca from the SR of skinned skeletal muscle fibre. Nature 228:34, 1970

Endo M: Calcium release from the sarcoplasmic reticulum. Physiol Rev 57:71, 1977

Fabiato A, Fabiato F: Activation of skinned cardiac cells: subcellular effects of cardioactive drugs. Eur J Cardiol 1/2:143, 1973

Fabiato A, Fabiato F: Contractions induced by a Ca-triggered release of Ca from the SR of single skinned cardiac cell. J Physiol 249:469, 1975

Fabiato A, Fabiato F: Ca release from the SR. Circ Res 40:119, 1977

Fanburg B, Finkel RM, Martonosi A: The role of Ca in the mechanism of relaxation of cardiac muscle. J Biol Chem 239:2298, 1964

Farmer TW, Buchthal F, Rosenfalck P: Refractory and irresponsive periods of muscle in progressive muscular dystrophy and paresis due to lower motor neuron involvement. Neurol 9:747, 1959

Fedelesova M, Sulakhe PV, Yates JC, Dhalla NS: Biochemical basis of heart function. IV. Energy metabolism and calcium transport in hearts of vitamin E deficient rats. Can J Physiol Pharmacol 49:909, 1971

Fedelesova M, Dzurba A, Ziegelhoffer A: Inhibition of sodium-potassium-activated adenosine triphosphatase by K-Mg-aspartate. Rec Adv Stud Cardiac Struc Metab 4:155, 1972

Fedelesova M, Ziegelhoffer A, Luknarova O, Kostolansky S: Prevention by K-Mg aspartate of isoproterenol-induced metabolic changes in the myocardium. Rec Adv Stud Cardiac Struc Metab 6:59, 1975

Fejfar Z: Cardiomyopathies - an international problem. Cardiologia 52:9, 1968

Feldman HA: Mathematical theory of complex ligand-binding systems at equilibrium - some methods for parameter fitting. Anal Biochem 48:317, 1972

Feldman DA, Weinhold PA: Calcium binding to rat heart plasma membranes: isolation and purification of a lipoprotein component with a high calcium binding capacity. Biochem 16:3470, 1977

Ferrans VJ, Morrow AG, Roberts WC: Myocardial ultrastructure in idiopathic hypertrophic subaortic stenosis. A study of operatively excised left ventricular outflow tract muscle in 14 patients. Circ 45:769, 1972

Ferrans VJ, Massumi RA, Shugoll GI, Ali N, Roberts WC: Ultrastructural studies of myocardial biopsies in 45 patients with obstructive or congestive cardiomyopathy. Rec Adv Stud Cardiac Struc Metab 2:231, 1973

Fisher JE, Horst WD, Kopin IJ: Norepinephrine metabolism in hypertrophied rat hearts. Nature 207:951, 1965

Fisherman SN, Khodorov BI, Volkenstein MV: Molecular mechanisms of membrane ionic permeability changes. Biochim Biophys Acta 225:1, 1971

Ford LE, Podolsky RJ: Force development and Ca movements in skinned muscle fibers. Fed Proc 27:375, 1968

Ford LE, Podolsky RJ: Regenerative Ca release within muscle cells. Sci 167:58, 1970

Forman R, Parmley WW, Sonnenblick EH: Myocardial contractility in relation to hypertrophy and failure in myopathic Syrian hamsters. J Mol Cell Cardiol 4:203, 1972

Fox AC, Reed GE: Exchanges of nucleotide phosphate in normal and in failing canine hearts. Am J Physiol 110: 1383, 1966

Fozzard HA: Heart: Excitation-contraction coupling. Ann Rev Physiol 39:201, 1977

Frank JS, Langer GA: The myocardial interstitium: its structure and its role in ionic exchange. J Cell Biol 60: 586, 1974

Frankenhaeuser B, Hodgkin AL: The action of Ca on the electrical properties of squid axons. J Physiol 137:218, 1957

Fruton JS: Cathepsins, In: The enzymes, Boyer PD, Lardy H, Myrback K ed. 4:233, 1960. Academic Press, New York

Gailani S, Danowski TS, Fisher DS: Muscular dystrophy. Circ 17:583, 1958

Gambhir KK, McMenamy RH: Location of the indole binding site in human serum albumin. J Biol Chem 248:1956, 1973

Gasic G, Berwick L: Hale stain for acid-containing mucins. J Cell Biol 19:223, 1963

Gasic G, Berwick L, Sarrentino M: Positive and negative colloidal iron as cell surface electron stains. Lab Invest 18:63, 1968

Gertler MM: Production of experimental congestive heart failure in the guinea pig. Proc Soc Exp Biol Med 102:396, 1959

Gertler MM: Differences in efficiencies of energy transfer in mitochondrial systems derived from normal and failing hearts. Proc Soc Exp Biol Med 106:109, 1961

Gertler MM, Saluste E, Spencer F: Biochemical analysis of human papillary muscles and guinea-pig heart ventricles in failure. Proc Soc Exp Biol Med 135:817, 1970

Gertz EW, Hess ML, Lain RF, Briggs FN: Activity of the vesicular calcium pump in the spontaneously failing heart-lung preparation. Circ Res 20:477, 1967

Gertz EW, Stam AC, Sonnenblick EH: A quantitative and qualitative defect in the sarcoplasmic reticulum in the hereditary cardiomyopathy of the Syrian hamster. Biochem Biophys Res Commun 40:746, 1970

Gertz EW: Cardiomyopathic Syrian hamster: Possible model of human disease. In: Pathology of the Syrian hamster: Progress in experimental tumor research 16: 242, 1972a Homburger F ed. S Karger, Basel

Gertz EW, Stam A Jr, Bajusz E, Sonnenblick EH: A biochemical defect in the function of the sarcoplasmic reticulum in the hereditary cardiopathy of the Syrian hamster. Rec Adv Stud Cardiac Struc Metab 1:243, 1972b

Gibbs CL, Vaughan P: The effect of calcium depletion upon the tension-independent component of cardiac heat production. J Gen Physiol 52:532, 1968

Gilbert DL, Ehrenstein G: Effect of divalent cations on potassium conductance of squid axons: determination of surface charge. Biophys J 9:447, 1969

Gilroy J, Cahalan JL, Berman K, Newman M: Cardiac and pulmonary complications in Duchenne's progressive muscular dystrophy. Circ 27:484, 1963

Globus JH: Pathological findings in the heart in progressive muscular dystrophy. Arch Neurol Psychiat 9:59, 1923

Greenwood FC, Hunter WM: The preparation of ^{131}I-labelled human growth hormone of high specific radioactivity. Biochem J 89:114, 1963

Hammond KS, Papermaster DS: Fluorometric assay of sialic acid in the picomole range: a modification of the thiobarbituric acid assay. Anal Biochem 74:292, 1976

Harigaya S, Schwartz A: Rate of calcium binding and uptake in normal animal and failing human cardiac muscle. Circ Res 25:781, 1969

Hartree EF: Determination of protein: a modification of the Lowry method that gives a linear photometric response. Anal Biochem 48:422, 1972

Haugaard N, Haugaard ES, Lee NH, Horn RS: Possible role of mitochondria in regulation of cardiac contractility. Fed Proc 28:1657, 1969

Hays RM, Singer B, Malamed S: The effect of calcium withdrawal on the structure and function of the toad bladder. J Cell Biol 25:195, 1965

Hille B: Gating in sodium channels of nerve. Ann Rev Physiol 38:139, 1976

Hochrein H, Lossnitzer K: The interrelation between myocardial metabolism and heart failure. Ann NY Acad Sci 156:387, 1969

Homburger F, Baker JR, Nixon CW, Whitney R: Primary, generalized polymyopathy and cardiac necrosis in an inbred line of Syrian hamsters. Med Exp (Basel) 6:339, 1962

Homburger F, Nixon CW, Eppenberger M, Baker JR: Hereditary myopathy in the Syrian hamster: studies on pathogenesis. Ann NY Acad Sci 138:14, 1966

Homburger F, Bajusz E: New models of human disease in the Syrian hamster. JAMA 212:604, 1970

Howland JL: Abnormal potassium conductance associated with genetic muscular dystrophy. Nature 251:724, 1974

Howse, HD, Ferrans VJ, Hibbs RG: A comparative histochemical and electron microscopic study of the surface coating of cardiac muscle cells. J Mol Cell Cardiol 1:157, 1970

Hughes BP: Lipid changes in Duchenne muscular dystrophy. J Neurol Neurosurg Psychiat 35:658, 1972

Hughes RC: Glycoproteins as components of cellular membranes. Prog Biophys Mol Biol 26:189, 1973

Hughes RC, Laurent M, Lonchampt MO, Courtois Y: Lens glycoproteins: biosynthesis in cultured epithetical cells of bovine lens. Eur J Biochem 52:143, 1975

Hughes RC, In: Membrane glycoproteins: A review of structure and function. Butterworth, 1976

Inesi G, Ebashi S, Watanabe S: Preparation of vesicular relaxing factor from bovine heart tissue. Am J Physiol 207:1339, 1964

Ionasescu V, Zellweger H, Conway TW: A new approach for carrier detection in Duchenne muscular dystrophy. Neurol 21:703, 1971a

Ionasescu V, Zellweger H, Conway TW: Ribosomal protein synthesis in Duchenne muscular dystrophy. Arch Biochem Biophys 144:51, 1971b

Ishiyama Y, Yabu H, Miyazaki E: Changes in contractility and calcium binding of guinea pig taenia coli by treatment with enzymes which hydrolyze sialic acid. Jap J Physiol 25: 719, 1975

Jansons VK, Burger MM: Isolation and characterization of agglutinin receptor sites. II. Isolation and partial purification of a surface membrane receptor for wheat germ agglutinin. Biochim Biophys Acta 291:127, 1973

Jacques LW, Brown EB, Barrett JM, Brey WS Jr, Weltner W Jr: Sialic acid: a calcium-binding carbohydrate. J Biol Chem 252:4533, 1977

Jasmin G, Bajusz E: Myocardial lesions in strain 129 dystrophic mice. Nature 193:181, 1962

Jasmin G, Solymoss B: Prevention of hereditary cardiomyopathy in the hamster by verapamil and other agents. Proc Soc Exp Biol Med 149:193, 1975a

Jasmin G, Solymoss B, Eu EY: Effect of thyroparathyroidectomy and of a low Ca diet on the cardiomyopathy of the Syrian hamster. Rec Adv Stud CardiacStruc Metab 10:717, 1975b

Jasmin G, Bajusz E: Prevention of myocardial degeneration in hamster with hereditary cardiomyopathy. Rec Adv Stud Cardiac Struc Metab 6:219, 1975c

Jeffrey FE, Wagner R, Abelmann WH: Left and right ventricular pressures in the normal and the cardiomyopathic Syrian hamster. Proc Soc Exp Biol Med 135:940, 1970

Judd JT, Wexler BC: Myocardial glycoprotein changes with isoproterenol-induced necrosis and repair in the rat. Am J Physiol 226:597, 1974

Kako JK, Thornton MJ, Heggtveit AH: Depressed fatty acid and acetate oxidation and other metabolic defects in homogenates from hearts of hamsters with hereditary cardiomyopathy. Circ Res 34:570, 1974

Kako JK, Heggtveit AH: Metabolic changes in the myocardium of hamsters with hereditary muscular dystrophy. Rec Adv Stud Cardiac Struc Metab 6:269, 1975

Katz AM, Repke DI: Quantitative aspects of dog cardiac microsomal calcium binding and calcium uptake. Circ Res 21:153, 1967

Kenter H, Falkenhahn A: Management of myocardial infarction with potassium magnesium aspartate. In: Electrolytes and cardiovascular diseases. Bajusz E ed. 2:420, 1966 S Karger, Basel

Kohlhardt M, Bauer B, Krause H, Fleckenstein A: Selective inhibition of the transmembrane Ca conductivity of mammalian myocardial fibres by Ni, Co and Mn ions. Pflugers Arch 338:115, 1973

Kolos G, Williams JF, Hickie JB: Biochemical studies in myocardial hypertrophy and metabolic support of the acutely stressed myocardium. Adv Cardiol 12:106, 1974

Kornguth SE, Flangos AL, Siegal FL, Geison RL, O'Brien JF, Lamar C Jr, Scott G: Chemical and metabolic characteristics of synaptic complexes from brain isolated by zonal centrifugation in a cesium chloride gradient. J Biol Chem 246:1177, 1971

Krause EG, Will H, Schirpke B, Wollenberger A: Cyclic AMP-enhanced protein phosphorylation and calcium binding in a cell-membrane-enriched fraction from myocardium. Adv Cyclic Nucleotide Res 5:473, 1975 Drummond GI, Greengard P, Robison GA ed. Raven Press, New York

Kubler W, Shinebourne EA: Calcium and the mitochondria. In: Calcium and the heart. Harris P, Opie L ed. Academic Press, 1971, p 93

Kunze D, Olthoff D, Schellnack K: Changes of lipid content of skeletal muscle in progressive muscular dystrophy as a basis of a hypothesis of primary enzyme defect. Acta Biol Med Ger 21:669, 1968

Kunze D, Reichmann G, Egger E, Leuschner G, Eckhardt H: Erythrozythenlipide bei progressiver muskeldystrophie. Clin Chim Acta 43:333, 1973

Kunze D: Lipid composition and phospholipid metabolism of muscle in progressive muscular dystrophy. In: Basic Research Myology, Proc 2nd Inter Congr Muscle Disease Kakulas BA ed. Excerpta Medica Amsterdam 1973, p 161

La Due JS, Wroblewski F, Karmen A: Serum glutamic oxaloacetic transaminase activity in human transmural myocardial infarction. Sci 120:497, 1954

Lain RF, Hess ML, Gertz EW, Briggs FN: Calcium uptake activity of canine myocardial sarcoplasmic reticulum in the presence of anesthetic agents. Circ Res 23:597, 1968

Lamarche M, Royer R: Aspartic acid salts and the cardiovascular diseases. In: Electrolytes and cardiovascular diseases. Bajusz E ed. p 104, 1965. S Karger, Basel

Langer GA: Kinetic studies of Ca distribution in ventricular muscle of the dog. Circ Res 15:393, 1964

Langer GA: Ion fluxes in cardiac excitation and contraction and their relation to myocardial contractility. Physiol Rev 48:708, 1968

Langer GA, Frank JS: Lanthanum in heart tissue culture. J Cell Biol 54:441, 1972

Langer GA: Heart: Excitation-contraction coupling. Ann Rev Physiol 35:5, 1973

Langer GA: Events at the cardiac sarcolemma: localization and movements of contractile-dependent calcium. Fed Proc 35:1274, 1976

Langer GA, Frank JS, Nudd LM, Seraydarian K: Sialic acid: effect of removal on Ca exchangeability of cultured heart cells. Sci 193:1013, 1976

La Raia PJ, Gertz EW, Sonnenblick EH: Adenyl cyclase in hamster cardiomyopathy. Clin Res 19:324, 1971

Lazarus ML, Colgan JA, Sachs HG: Quantitative light and electron microscopic comparison of the normal and cardiomyopathic Syrian hamster heart. J Mol Cell Cardiol 8:431, 1976

Lee SH, Dusek J, Rona G: Electron microscopic cytochemical study of glutamic oxalaacetic transaminase activity in ischemic myocardium. J Mol Cell Cardiol 3:103, 1971

Lee YCP, Visscher MB: Perfusate cations and contracture and Ca, Cr, PCr, and ATP in rabbit myocardium. Am J Physiol 219:1637, 1970a

Lee YCP, Visscher MB: Influx of Ca into rabbit myocardium in relation to its ionic environment. Proc Nat Acad Sci 66:603, 1970b

Lehninger AL: Esterification of inorganic phosphate coupled to electron transport between dihydrodiphosphopyridine nucleotide and oxygen. J Biol Chem 178:625, 1949

Lehninger AL, Carafoli E, Rossi CS: Energy-linked ion movements in mitochondrial systems. Adv Enzymol 29:259, 1967

Lehninger AL, In: Biochemistry. Worth Publishers 1975

Levin S, Baens GS, Weinberg T: The heart in pseudo-hypertrophic muscular dystrophy. J Pediat 55:460, 1959

Li YT, Li SC, Shetlar MR: Carbohydrate content in subcellular fractions of rat liver and Walker 256 carcinosarcoma. Cancer Res 25:1225, 1965

Lindenmayer GE, Sordahl LA, Schwartz A: Reevaluation of oxidative phosphorylation in cardiac mitochondria from normal animals and animals in heart failure. Circ Res 23:439, 1968

Lindenmayer GE, Sordahl LA, Harigaya S, Allen JC, Besch HR Jr, Schwartz A: Some biochemical studies on subcellular systems isolated from fresh recipient human cardiac tissue obtained during transplantation. Am J Cardiol 27:277, 1971

Lochner A, Brink AJ, Van der Walt JJ: The significance of biochemical and structural changes in the development of the myocardiopathy of the Syrian hamster. J Mol Cell Cardiol 1:47, 1970

Lochner A, Van der Welt JJ, Bajusz E, Brink A, Kotze JCN: Effects of potassium-glucose-insulin treatment on the histology, protein synthesis, and mechanical activity of the myopathic hamster heart. Rec Adv Stud Cardiac Struc Metab 2:543, 1973

Locke FS, Rosenheim O: Contributions to the physiology of the isolated heart. The consumption of dextrose by mammalian cardiac muscle. J Physiol 36:205, 1907

Long C, Mouat B: The binding of calcium ion by erythrocytes and 'Ghost'-cell membranes. Biochem J 123:829, 1971

Lossnitzer K, Bajusz E: Water and electrolyte alterations during the life course of the BIO 14.6 Syrian golden hamster. A disease model of a hereditary cardiomyopathy. J Mol Cell Cardiol 6:163, 1974

Lossnitzer K, Janke J, Hein B, Stauch M, Fleckenstein A: Disturbed myocardial calcium metabolism; a possible pathogenetic factor in the hereditary cardiomyopathy of the Syrian hamster. Rec Adv Stud Cardiac Struc Metab 6:207, 1975

Luttgau HC, Niedergerke R: The antagonism between Ca and Na ions on the frog's heart. J Physiol 143:486, 1958

Lyon AF: Primary myocardial disease in the adult. A clinical analysis. In: Electrolytes and cardiovascular diseases. Bajusz E ed. 2:1, 1966, S Karger, Basel

Ma TS, Bose D: Sodium in smooth muscle relaxation. Am J Physiol 232:C59, 1977

Macbeth RAL, Bekesi JG: Tissue glycoproteins in rats bearing Walker 256 carcinoma. Cancer Res 24:614, 1964

Manasek FJ: Macromolecules of the extracellular compartments of embryonic and mature hearts. Circ Res 38: 331, 1976

Maron BJ, Ferrans VJ, Roberts WC: Ultrastructural features of degenerated cardiac muscle cells in patients with cardiac hypertrophy. Am J Path 79:387, 1975

Matheson DW, Howland JL: Erythrocyte deformation in human muscular dystrophy. Sci 184:165, 1974

Mattingly TW: Changing concepts of myocardial diseases. JAMA 191:127, 1965

Mawatari S, Takagi A, Rowland LP: Adenyl cyclase in normal and pathologic human muscle. Arch Neurol 30:96, 1974

McCollum WB, Crow C, Harigaya S, Bajusz E, Schwartz A: Calcium binding by cardiac relaxing system isolated from myopathic Syrian hamster (strain 4.6, 80.62, 40.54). J Mol Cell Cardiol 1:445, 1970

McGill HC, Thatcher JL: Unexpected hypertrophy of the heart in infants and children. J Louisiana Stat Med Soc 107:223, 1955

McKinney B, In: Pathology of the cardiomyopathies. Butterworths, 1974

McNamara DB, Sulakhe PV, Singh JN, Dhalla NS: Properties of heart sarcolemmal Na, K-ATPase. J Biochem (Tokyo) 75:795, 1974

Mead RJ, Peterson MB, Welty JO: Sarcolemmal and sarcoplasmic reticulum ATPase activities in the failing canine heart. Circ Res 29:14, 1971

Meerson FZ, Manukhin BN, Pshenichnikova MG, Rozanova LS: Mediator metabolism in myocardium in compensatory hyperfunction and hypertrophy of heart. Fed Proc (Trans Suppl) 23:T593, 1964 (Patologicheskaya Fiziologiya: Eksperimental' naya Terapiya 7:32, 1963)

Meerson FZ, Zaletayeva TA, Lagutchev SS, Pshennikova MD: Structural and mass of mitochondria in the process of compensatory hyperfunction and hypertrophy of the heart. Exp Cell Res 36:568, 1964

Meerson FZ: The myocardium in hyperfunction, hypertrophy and heart failure. Circ Res 24-25, Suppl II:1, 1969

Mendell JR, King Engel W, Derrer EC: Duchenne muscular dystrophy: functional ischemia reproduces its characteristic lesions. Sci 172:1143, 1971

Mezon BJ, Wrogemann K, Blanchaer MC: Differing populations of mitochondria isolated from the skeletal muscle of normal and dystrophic hamsters. Can J Biochem 52:1024, 1974

Miale TD, Frias JL, Lawson DL: Erythrocytes in human muscular dystrophy. Sci 187:453, 1975

Michaels JE, Le Blond CP: Transport of glycoprotein from Golgi apparatus to cell surface by means of "carrier" vesicles, as shown by radioautography of mouse coloric epithelium after injection of ^{3}H-fucose. J Microscop Biol Cell 25:243, 1976

Miller SE, Rases AD, Appel SH: Scanning electron microscopy studies in muscular dystrophy. Arch Neurol 33:172, 1976

Mokri B, Engel AG: Duchenne dystrophy: electron microscopic findings pointing to a basic or early abnormality in the plasma membrane of the muscle fiber. Neurol 25:111, 1975

Monckton G, Nihei T: Some biochemical changes occuring in muscular dystrophy and their possible genetical significance. Ann NY Acad Sci 138:329, 1966

Monckton G, Nihei T: A correlation of histology and amino acid incorporation studies in Duchenne muscular dystrophy. Neurol 19:415, 1969

Monckton G, Marusyk H: Myofibrillar incorporation of ^{3}H(G)L-leucine in progressive muscular dystrophy and motor neurone disease. Neurol 26:234, 1976

Morad M, Trautwein W: The effect of the duration of the action potential on contraction in the mammalian heart tissue. Pflugers Arch 229:66, 1968

Morad M, Goldman Y: Excitation-contraction coupling in heart muscle: membrane control of development of tension. Prog Biophys Mol Biol 27:259, 1973

Morse PF, Howland JL: Erythrocytes from animals with genetic muscular dystrophy. Nature 245:156, 1973

Muir JR, Dhalla NS, Orteza JM, Olson RE: Energy-linked calcium transport in subcellular fraction of the failing rat heart. Circ Res 26:429, 1970

Murphy DL, Mendell JR, King Engel W: Serotonin and platelet function in Duchenne muscular dystrophy. Arch Neurol 28:239, 1973

Nad Karni BB, Hunt B, Heggtveit HA: Early ultrastructural and biochemical changes in the myopathic hamster heart. Rec Adv Stud Cardiac Struc Metab 1:251, 1972

Nair KG,Umali T, Potts J: RNA polymerase and adenyl cyclase in cardiac hypertrophy and cardiomyopathy. Rec Adv Stud Cardiac Struc Metab 3:479, 1972

Nair KG, Umali T, Potts J: Metabolic adaptation in cardiac hypertrophy. Circ Res 34-35 Suppl II:33, 1974

Naylor WG: An effect of ouabain on the superficially-located stores of calcium in cardiac muscle cells. J Mol Cell Cardiol 5:101, 1973

Naylor WG, Dunnett J, Sullivan A: Drug-induced changes in the superficially located sotes of calcium in heart sarcolemma. Rec Adv Stud Cardiac Struc Metab 9:53, 1976

New W, Trautwein W: Inward currents in mammalian myocardium. Pflugers Arch 343:1, 1972

Niedergerke R: Movements of Ca in beating ventricles of the frog heart. J Physiol 167:551, 1963

Niedergerke R, Page S, Talbot MS: Calcium fluxes in frog heart ventricles. Pflugers Arch ges Physiol 306:357, 1969

Nihei T, Monckton G: Some aspects of ribosomal and nuclear activity in normal and dystrophic muscle. In: 2nd Inter Congr Neuro-genetics p 23, 1967

Nihei T, Tataryn D, Filipenko C: The reduction of myosin synthesis in muscle of dystrophic mice. In: Basic Research Myology, Kakulas BJ ed. Amsterdam, Excerpta Medica p 204, 1973

Nikolaeva LF, Cherpachenko NM, Veselova SA, Sokolova RI: Mechanisms of drug action on recovery processes of cardiac muscle in myocardial infarction. Circ Res 34-35 Suppl III:202, 1974

Norris FH Jr, Moss AJ, Yu PN: On the possibility that a type of human dystrophy commences in myocardium. Ann NY Acad Sci 138:342, 1966

Okada R, Nasu T: Idiopathic myocardiopathy and allied cardiac disease in Japan. Pathol Microbiol 35:56, 1970

Ong SD: Studies on excitation-contraction coupling in cardiac muscle. PhD Thesis. Univ of Manitoba, 1972

Owens K, Hughes BP: Lipids of dystrophic and normal mouse muscle: whole tissue and particulate fractions. J Lipid Res 11:486, 1970

Owens K, Weglicki WB, Sonnenblick EH, Gertz EW: Phospholipid and cholesterol content of ventricular tissue from the cardiomyopathic Syrian hamster. J Mol Cell Cardiol 4:229, 1972

Owens K, Weglicki WB, Ruth RC, Stam AC, Sonnenblick EH: Lipid composition, Ca uptake and Ca-stimulated ATPase activity of sarcoplasmic reticulum of the cardiomyopathic hamster. Biochim Biophys Acta 296:71, 1973

Owens K, Weglicki WB, Ruth RC, Sonnenblick EH: Abnormalities of myopathic subcellular fractions: composition and function. Adv Cardiol 13:81, 1974

Owens K, Weglicki WB, Ruth RC, Gottwik MG, McNamara DB, Sonnenblick EH: Structural and functional characteristics of membrane fractions from cardiomyopathic and dystrophic muscle. Rec Adv Stud Cardiac Struc Metab 6:245, 1975

Pang CCY: Modification by practolol of changes in Ca metabolism induced by hypoxia and by isoproterenol. PhD Thesis. Univ of Manitoba, 1976

Pare JA, Fraser RG, Pirozynski WJ, Shanks JA, Stubington D: Hereditary cardiovascular dysplasia - a form of familial cardiomyopathy. Am J Med 31:37, 1961

Patriarca P, Carafoli E: A study of the intracellular transport of calcium in rat heart. J Cell Physiol 72:29, 1968

Patterson MK Jr, Touster O: Intracellular distribution of sialic acid and its relationship to membranes. Biochim Biophys Acta 56:626, 1962

Pearce GW: The sarcolemmal and sarcotubular systems in normal and dystrophic muscle. In: Research in Muscular dystrophy JB Lippincott Co p 146, 1965

Pennington RJ, In: Disorders of voluntary muscle p 488 Walton JN ed. Churchill Livingston, London, 1974

Perloff JK, deLeon AC Jr, O'Doherty D: Cardiomyopathy of progressive muscular dystrophy. Circ 33:625, 1966

Petryshyn R, Nicholls DM: Protein synthesis in dystrophic muscle. Activity of the pH 5 supernatant fraction of muscle in dystrophic mice. Biochim Biophys Acta 435: 391, 1976

Pillen D: Experiences with potassium magnesium aspartate therapy. In: Electrolytes and cardiovascular diseases. Bajusz E ed. vol 2. p 386, S Karger, Basel, 1966

Polimeni PI: Extracellular space and ionic distribution in rat ventricle. Am J Physiol 227:676, 1974

Pool PE, Covell JW, Levitt M, Gibb J, Braunwald E: Reduction of cardiac tyrosine hydroxylase activity in experimental congestive heart failure. Circ Res 20: 349, 1967

Pretorius PJ, Pohl WG, Smithen CS, Inesi G: Structural and functional characterization of dog heart microsomes. Circ Res 25:487, 1969

Raab W: The pathogenic significance of adrenaline and related substances in the heart muscle. Exp Med Surg 1:188, 1943

Raab W, Gigel W: Norepinephrine and epinephrine content or normal and diseased human hearts. Circ 11:593, 1955

Raab W: Metabolic protection and reconditioning of the heart muscle through habitual physical exercise. Ann Intern Med 53:87, 1960a

Raab W: Key position of catecholamines in functional and degenerative cardiovascular pathology. Am J Cardiol 5:571, 1960b

Rambourg A, Le Blond CP: Electron microscope observations on the carbohydrate-rich cell coat present at the surface of cells in the rat. J Cell Biol 32:27, 1967

Rambourg A, Hernandez W, Le Blond CP: Detection of complex carbohydrates in the Golgi apparatus of rat cells. J Cell Biol 40:395, 1969

Ray TK: A modified method for the isolation of the plasma membrane from rat liver. Biochim Biophys Acta 196:1, 1970

Reichenback DD, Benditt EP: Catecholamines and cardiomyopathy. Human Pathol 1:125, 1970

Reuter H, Seitz N: The dependence of Ca-efflux from cardiac muscle on temperature and external ion composition. J Physiol 195:451, 1968

Reuter H: Divalent cations as charge carriers in excitable membranes. Prog Biophys Mol Biol 26:3, 1973

Revel JP: A stain for the ultrastructural localization of acid mucopolysaccharides. J Microscopie 3:535, 1964

Riggs DS, In: The mathematical approach to physiological problems. The Williams and Wilkins Co. Baltimore, 1963

Ringer S: A further contribution regarding the influence of the different constituents of the blood on the contraction of the heart. J Physiol 4:29, 1883

Rona G, Boutet M, Huttner I: Membrane permeability alterations as manifestation of early cardiac muscle cell injury. Rec Adv Stud Cardiac Struc Metab 6: 439, 1975

Roseman S: The synthesis of complex carbohydrates by multiglycosyltransferase systems and their potential function in intercellular adhesion. Chem Phys Lipids 5:270, 1970

Rosenberg A, Schengrund C-L: Sialidases, In: Biological roles of sialic acid. Rosenberg A, Schengrund C-L ed. Plenum Press p 295, 1976

Rosenthal HE: A graphic method for the determination and presentation of binding parameters in a complex system. Anal Biochem 20:525, 1967

Roth S, McGuire EJ, Roseman S: Evidence for cell-surface glycosyltransferases: their potential role in cellular recognition. J Cell Biol 51:536, 1971

Saari JT, Johnson JA: Decay of Ca content and contractile force in the rabbit heart. Am J Physiol 221:1572, 1971

Saari JT, Johnson JA: Build-up of calcium content and contractile force in the rabbit heart. Can J Physiol Pharmacol 50:1206, 1972

Safer B, Williamson JR: Functional significance of the malate-aspartate shuttle for the oxidation of the cytoplasmic reducing equivalents in rat heart. Rec Adv Stud Cardiac Struc Metab 1:34, 1972

Safer B: The metabolic significance of the malate-aspartate cycle in heart. Circ Res 37:527, 1975

Sassa H: Mechanism of myocardial catecholamine depletion in cardiac hypertrophy and failure in rabbits. Jap Circ J 35:391, 1971

Scatchard G: The attraction of proteins for small molecules and ions. Ann NY Acad Sci 51:660, 1949

Schachter H, Jabbal I, Hudgin RL, Pinteric L, McGuire EJ, Roseman S: Intracellular localization of liver sugar nucleotide glycoprotein glycosyltransferases in a Golgi-rich fraction. J Biol Chem 245:1090, 1970

Schlesinger MJ, Reiner L: Focal myocytolysis of the heart. Am J Pathol 31:443, 1955

Schmalbruch H: Segmental fibre breakdown and defects of the plasmalemma in diseased human muscles. Acta Neuropathol 33:129, 1975

Schotland DL, Bonilla E, Van Meter M: Duchenne dystrophy: alteration in muscle plasma membrane structure. Sci 196: 1005, 1977

Schwartz A, Lee KS: Study of heart mitochondria and glycolytic metabolism in experimentally induced cardiac failure. Circ Res 10:321, 1962

Schwartz A: Calcium and the sarcoplasmic reticulum. In: Calcium and the heart. Harris P, Opie L ed. Academic Press, p 66, 1970

Schwartz A, Nagano K, Nakao M, Lindenmayer GE, Allen JC, Matsui H: The sodium- and potassium-activated adenosine-triphosphatase system. In: Methods in pharmacology vol 1, p 361, Schwartz A ed. Meredith Corp 1971a

Schwartz A: Studies on mitochondria from normal, hypertrophic, and failing myocardium. In: Cardiac hypertrophy. Alpert NR ed. Academic Press p 511, 1971b

Schwartz A, Sordahl LA, Crow CA, McCollum WB, Harigaya S, Bajusz E: Several biochemical characteristics of the cardiomyopathic Syrian hamster. Rec Adv Stud Cardiac Struc Metab 1:235, 1972

Seaman GVF, Jackson LJ, Uhlenbruck G: Action of α-amylase preparations and some proteases on the surface of mammalian erythrocytes. Arch Biochem Biophys 122:605, 1967

Sekiguchi M, Konno S: Diagnosis and classification of primary myocardial disease with the aid of endomyocardial biopsy. Jap Circ J 35:737, 1971

Sekiguchi M: Electron microscopical observations of the myocardium in patients with idiopathic cardiomyopathy using endomyocardial biopsy. J Mol Cell Cardiol 6:111, 1974

Shaafi RI, Rodan SB, Hintz RL, Fernandez SM, Rodan GA: Abnormalities in membrane microviscosity and ion transport in genetic muscular dystrophy. Nature 254:525, 1975

Shanes AM: Electrochemical aspects of physiological and pharmacological action in excitable cells. Pharmacol Rev 10:59, 1958

Shea SM: Lanthanum staining of the surface coat of cells. Its enhancement by the use of fixatives containing Alcian blue or cetylpyridinium chloride. J Cell Biol 51:611, 1971

Shlatz L, Marinetti GV: Calcium binding to the rat liver plasma membrane. Biochim Biophys Acta 290:70, 1972

Shine KI, Serena SD, Langer GA: Kinetic localization of contractile Ca in rabbit myocardium. Am J Physiol 221: 1408, 1971

Shur BO, Roth S: Cell surface glycosyltransferases. Biochim Biophys Acta 415:473, 1975

Singh JN, Dhalla NS, McNamara DB, Bajusz E, Jasmin G: Membrane alteration in failing hearts of cardiomyopathic hamsters. Rec Adv Stud Cardiac Struc Metab 6:259, 1975

Skelton CL, Sonnenblick EH: Heterogeneity of contractile function in cardiac hypertrophy. Circ Res 34-35 Suppl II:83, 1974

Skou JC: Enzymatic basis for active transport of Na and K across cell membrane. Physiol Rev 45:596, 1965

Skosey JL, Zak R, Martin AF, Aschenbrenner V, Rabinowitz M: Biochemical correlates of cardiac hypertrophy. V. Labeling of collagen, myosin, and nuclear DNA during experimental myocardial hypertrophy in the rat. Circ Res 31:145, 1972

Slezak J, Tribulova N: Morphological changes after simultaneous administration of isoproterenol and K-Mg aspartate as a physiological Ca antagonist. Arzneim-Forsch (Drug Res) 25:918, 1975

Smith AL, Bind JWC: Distribution and particle properties of the vacuolar apparatus of cardiac muscle tissue. I. Biochemical characterization of cardiac muscle lysosomes and the isolation and characterization of acid, neutral and alkaline proteases. J Mol Cell Cardiol 7:39, 1975

Snow C, Allen A: The release of radioactive nucleic acids and mucoproteins by trypsin and ethylenediaminetetraacetate treatment of baby-hamster cells in tissue culture. Biochem J 119:707, 1970

Sobel BE, Spann JF, Pool PE, Sonnenblick EH, Braunwald E: Normal oxidative phosphorylation in mitochondria from the failing heart. Circ Res 21:355, 1967

Sobel BE, Henry PD, Robison A, Bloor C, Ross J Jr: Depressed adenyl cyclase activity in the failing guinea pig heart. Circ Res 24:507, 1969

Sole MJ, Lo C-M, Laird CW, Sonnenblick EH, Wurtman RJ: Norepinephrine turnover in the heart and spleen of the cardiomyopathic Syrian hamster. Circ Res 37:855, 1975

Sole MJ, Wurtman RJ, Lo C-M, Kamble AB, Sonnenblick EH: Tyrosine hydroxylase activity in the heart of the cardiomyopathic Syrian hamster. J Mol Cell Cardiol 9:225, 1977

Solaro RJ, Wise RM, Shiner JS, Briggs FN: Ca requirements for cardiac myofibrillar activation. Circ Res 34:525, 1974

Somlyo AP, Somlyo AV: Vascular smooth muscle. Pharmacol Rev 20:197, 1968

Spann JF, Chidsey CA, Braunwald E: Reduction of cardiac stores of norepinephrine in experimental heart failure. Sci 145: 1439, 1964

Spann JF, Chidsey CA, Pool PE, Braunwald E: Mechanism of norepinephrine depletion in experimental heart failure produced by aortic constriction in the guinea pig. Circ Res 17:312, 1965

SrivastavaU: Biochemical changes in progressive muscular dystrophy. VIII. Protein synthesis in skeletal muscle of mouse as a function of muscular dystrophy. Arch Biochem Biophys 135:236, 1969

Srivastava U: Biochemical changes in progressive muscular dystrophy. IX. Synthesis of native myosin, actin, and tropomyosin in the skeletal muscle of mouse as a function of muscular dystrophy. Can J Biochem 50:409, 1972

St. Louis PJ, Sulakhe PV: Isolation of sarcolemmal membranes from cardiac muscle. Int J Biochem 7:547, 1976

St. Louis PJ, Sulakhe PV: Adenosine triphosphate-dependent calcium binding and accumulation by guinea-pig cardiac sarcolemma. Can J Biochem 54:946, 1976

Stam AC, Weglicki WB Jr, Feldman D, Shelburne JC, Sonnenblick EH: Canine myocardial sarcolemma: its preparation and enzymic activity. J Mol Cell Cardiol 1:117, 1970

Stauch M, Lossnitzer K: Left ventricular function in Syrian hamsters of different ages with hereditary cardiomyopathy. Rec Adv Stud Cardiac Struc Metab 6:283, 1975

Sulakhe PV, Dhalla NS: Adenyl cyclase activity in failing hearts of genetically myopathic hamsters. Biochem Med 6:471, 1972

Sulakhe PV, Dhalla NS: Alterations in the activity of cardiac Na-K stimulated ATPase in congestive heart failure. Exp Mol Path 18:100, 1973

Sulakhe PV, Leung NLK, St. Louis PJ: Stimulation of calcium accumulation in cardiac sarcolemma by protein kinase. Can J Biochem 54:438, 1976

Sulakhe PV, Dhalla NS: Alterations in the activity of cardiac Na-K stimulated ATPase in congestive heart failure. Exp Mol Pathol 18:100, 1973

Sundermeyer JP, Gudbjarnason S, Wendt VE, den Bakker PB, Bing RJ: Myocardial metabolism in progressive muscular dystrophy. Circ 24:1348, 1961

Szekeres L, Schein M: Cell metabolism of the overloaded mammalian heart in situ. Cardiologia 34:19, 1959

Tada M, Finney JO Jr, Swartz MH, Katz AM: Preparation and properties of plasma membranes from guinea pig hearts. J Mol Cell Cardiol 4:417, 1972

Tallman JF, Brady RO: The purification and properties of a mammalian neuraminidase (sialidase). Biochim Biophys Acta 293:434, 1973

Tappel A, Zalkin H, Caldwell AK, Desai ID, Shibko S: Increased lysozomal enzymes in genetic muscular dystrophy. Arch Biochem 96:340, 1962

Taussky HH, Shoir E: A microcalorimetric method for the determination of inorganic phosphorus. J Biol Chem 202:675, 1953

Teiger DG, Farah A: Calcium movements in resting and stimulated isolated rabbit atria. J Pharmacol Exp Ther 157:8, 1967

Trautwein W: The slow inward current in mammalian myocardium. Eur J Cardiol 1/2:169, 1973

Ulbricht W: The effect of veratridine on excitable membranes of nerve and muscle. Ergebn Physiol 61:18, 1969

Van der Walt JJ: Comparative histopathological studies in hamster and human cardiomyopathies. Rec Adv Stud Cardiac Struc Metab 2:293, 1973

Varga E, Kovacs L, Gesztely I: Depolarizing effect of veratrine on frog skeletal muscle. Acta Physiol Acad Sci Hung 41:81, 1972a

Varga E, Kovacs T, Szabo B: The effect of veratrine on the ion transport of frog skeletal muscle. Acta Physiol Acad Sci Hung 41:265, 1972b

Villamil MF, Rettori V, Yeyati N: Ca exchange and distribution in the arterial wall. Am J Physiol 224:1314, 1973

Wallach ST, Ballavia JV, Schorr J, Schaffer A: Tissue distribution of electrolyte ^{47}Ca and ^{28}Mg in experimental hyper- and hypoparathyroidism. Endocrinol 78:16, 1965

Walton JN, Nattrass FJ: On the classification, natural history and treatment of the myopathies. Brain 77:169, 1954

Warren L: The distribution of sialic acids within the eukaryotic cells. In: Biological roles of sialic acid. Rosenberg A, Schengrund C-L ed. Plenum Press, 1976 p 103

Weber A, Herz R, Reiss I: On the mechanism of relaxing effect of fragmented sarcoplasmic reticulum. J Gen Physiol 46:679, 1963

Weber A, Herz R, Reiss I: The nature of the cardiac relaxing factor. Biochim Biophys Acta 131:188, 1967

Weinstock IM, Goldrich AD, Milhorat AT: Enzyme studies in muscular dystrophy. I. Muscle proteolytic activity and vitamin E-deficiency. Proc Soc Exp Biol Med 88: 257, 1955

Weinstock IM,Epstein S, Milhorat AT: Enzyme studies in muscular dystrophy. III. In hereditary muscular dystrophy in mice. Proc Soc Exp Biol 99:272, 1958

Weinstock IM, Iodice AA: Acid hydrolase activity in muscular dystrophy and denervation atrophy. In: Lysosomes in biology and pathology. 1:450, 1969 Dingle JT, Fell HB ed. North Holland, Amsterdam

Weinstock IM, Soh TS, Freidman HS, Cutler ME: Amino acid incorporation into proteins of developing breast muscle of the normal and dystrophic chicken. Biochem Med 2: 345, 1969

Weinstock IM, Markiewicz L: Muscle protein synthesis during development of the normal and dystrophic chicken. Biochim Biophys Acta 374:197, 1974

Weisenfeld S, Messinger WJ: Cardiac involvement in progressive muscular dystrophy. Am Heart J 43:170, 1952

Weiss L, In: The cell periphery. Metastatis and other contact phenomena. North-Holland, Amsterdam, 1967

Wendt VE, Stock TB, Hayden RO, Bruce TA, Gudbjarnason S, Bing RJ: Hemodynamics and cardiac metabolism in cardiomyopathies. Med Clin N Amer 46:1445, 1962

Wilde WS, O'Brien JM, Bay I: Time relation between potassium ^{42}K outflow, action potential and contraction phase of heart muscle as revealed by the effluogram. Proc Inter Conf Peaceful Uses Atomic Energy, Geneva 12:318, 1956

Will H, Schirpke B, Wollenberger A: Binding of calcium to a cell membrane-enriched preparation from pig myocardium: Increase in calcium affinity upon membrane protein phosphorylation enhanced by a membrane-bound cAMP-dependent protein kinase. Acta Biol Med Ger 31:K45, 1973

Williams JF, Donohoe J, Lykke A, Kolos G: Studies using orotic acid for improving the controlled development of myocardial hypertrophy. Aust N Z J Med 6 Suppl 2: 60, 1976

Williamson JR, Woodrow ML, Scarpa A: Calcium binding to cardiac sarcolemma. Rec Adv Stud Cardiac Struc Metab 5:61, 1976a

Williamson JR, Ford C, Illingworth J, Safer B: Coordination of citric acid cycle acticity with electron transport flux. Circ Res 38 Suppl I:39, 1976b

Winegrad S, Shanes AM: Calcium flux and contractility in guinea pig atria. J Gen Physiol 45:371, 1962

Winegrad S: Studies of cardiac muscle with a high permeability to Ca produced by treatment with ethylenediamine tetraacetic acid. J Gen Physiol 58:71, 1971

Woessner JF: The determination of hydroxyproline in tissue and protein samples containing small proportions of amino acid. Arch Biochem Biophys 93:440, 1961

Wollenberger AW, Kleitke B, Raabe G: Some metabolic characteristics of mitochondria from chronically overloaded hypertrophied hearts. Exp Mol Path 2:251, 1965

Wrogemann K, Blancher MC, Jacobson BE: Oxidative phosphorylation at various stages of genetically determined cardiomyopathy in the Syrian hamster. Rec Adv Stud Cardiac Struc Metab 3:467, 1972

Wrogemann K, Blancher MC, Thakar JH, Mezon BJ: On the role of mitochondria in the hereditary cardiomyopathy of the Syrian hamster. Rec Adv Stud Cardiac Struc Metab 6:231, 1975

Wrogemann K, Jacobson BE, Blanchaer MC: Sarcolemmal ATPase activities in normal and BIO 14.6 dystrophic hamster skeletal muscle. Can J Biochem 52:500, 1974

Yamazaki N, Ogawa K: Cardiac catecholamine metabolism in heart failure. Jap Circ J 35: 965, 1971

Yates JC, Dhalla NS: Structural and functional changes associated with failure and recovery of hearts after perfusion with Ca-free medium. J Mol Cell Cardiol 7:91, 1975

Zutuchni J, Aegerter EE, Moltham L, Shuman SR: The heart in progressive muscular dystrophy. Circ 3:846, 1951

Zimmerman ANE, Hulsmann WC: Paradoxical influence of calcium ions on the permeability of the cell membrane of the isolated rat heart. Nature 211:646, 1966

Zimmerman ANE, Daems W, Hulsmann WC, Shijder J, Wisse E, Durrer D: Morphological changes of heart muscle caused by successive perfusion with Ca-free and Ca-containing solutions (Ca-paradox). Cardiovas Res 1:201, 1967

Zweifach BW: The structural basis of permeability and other functions of blood capillaries. Cold Spring Harbor Symp Quart Biol 8:216, 1940

SECTION VI

APPENDICES

APPENDIX 1

Interaction between fast and slow compartment

To estimate the degree of contamination of the fast compartment on the slow compartment at time t, we first assume $K_1 = 3K_2$, which is the least rate constant difference necessary for the separation of 2 compartments (Riggs, 1963). The ratio of the quantity derived from Compartment 1 to that from Compartment 2 at time t is given by

$$\frac{A_1(t)}{A_2(t)} = \frac{A_{10}\, e^{-K_1 t}}{A_{20}\, e^{-K_2 t}} = \frac{D_1\ K_1}{D_2\ K_2} \cdot e^{-t(K_1-K_2)} \qquad (1a)$$

where D_1, D_2 are the contents of compartment one and two respectively and $D_1 = A_{10}/K_1$, $D_2 = A_{20}/K_2$. Since we have assumed $K_1 = 3K_2$, therefore

$$\frac{A_1(t)}{A_2(t)} = 3\frac{D_1}{D_2} \cdot e^{-t\cdot 2K_2}$$

$$= 3\frac{D_1}{D_2} \cdot e^{-t\cdot(2\cdot 0.693/t_{\frac{1}{2}})} \qquad (1b)$$

We will examine the degree of contamination at $t = t_{\frac{1}{2}}$, $2t_{\frac{1}{2}}$, $3t_{\frac{1}{2}}$, where $t_{\frac{1}{2}}$ is the half time of exchange of compartment 2.

at $t = t_{\frac{1}{2}}$

$$\frac{A_1(t)}{A_2(t)} = 3\frac{D_1}{D_2} \cdot e^{-2\cdot 0.693} \qquad (1c)$$

at $t = 2t_{\frac{1}{2}}$

$$\frac{A_1(t)}{A_2(t)} = 3\,\frac{D_1}{D_2}\cdot e^{-4\cdot 0.693} \tag{1d}$$

at $t = 3t_{\frac{1}{2}}$

$$\frac{A_1(t)}{A_2(t)} = 3\,\frac{D_1}{D_2}\cdot e^{-6\cdot 0.693} \tag{1e}$$

APPENDIX 2

Simulation of two compartments in series (uptake)

The sum of the change of the content of compartment 1 and 2 can be expressed as:

$$\frac{dD_1(t)}{dt} + \frac{dD_2(t)}{dt} = A_1 e^{-K_1 t} + A_2 e^{-K_2 t} \qquad (2a)$$

where A_1 and A_2 are the intercepts and K_1 and K_2 are the rate constants of the uptake curve analyzed according to parellel model (curve-peeling method).

From derivations in the method section, we have

$$D_1(\infty) + D_2(\infty) = C_1(\infty)V_1 + C_2(\infty)V_2 = A_1/K_1 + A_2/K_2 \qquad (2b)$$

$$\frac{dD_1(t)}{dt} = V_1 \frac{dC_1(t)}{dt} = 1.8\ K_{01} + K_{21} C_2(t) - (K_{10} + K_{12}) C_1(t) \qquad (2c)$$

$$\frac{dD_2(t)}{dt} = V_2 \frac{dC_2(t)}{dt} = K_{12} C_1(t) - K_{21} C_2(t) \qquad (2d)$$

$$1.8\ K_{01} = C_1(\infty)\ K_{10} \qquad (2e)$$

$$C_1(\infty)\ K_{12} = C_2(\infty)\ K_{21} \qquad (2f)$$

$$D_1(\infty) = \frac{(A_1+A_2)^2}{A_1K_1 + A_2K_2} \qquad (2g)$$

$$D_2(\infty) = \frac{A_1}{K_1} + \frac{A_2}{K_2} - D_1(\infty) \qquad (2h)$$

By taking the second time derivative of equation 2c, 2d (or third time derivative of D(t)), equating their sum to the

second time derivative of equation 2a, and set time to zero, we get

$$A_1K_1^2 + A_2K_2^2 = 1.8\,\frac{K_{01}\,K_{10}\,(K_{10} + K_{12})}{V_1^2} \qquad (2i)$$

By assuming $K_{12} = K_{21}$ and applying equation 2f, we get

$$C_1(\infty) = C_2(\infty) \qquad (2j)$$

And by assigning $V_1 + V_2 = 0.8\ H$ (which is irrelevant in the generation of figure 12 but which makes K_{10}, K_{12}, K_{21} soluable, where H is the wet heart weight), we have (2k)

$$C_1(\infty) = (A_1/K_1 + A_2/K_2)/0.8\ H \qquad (2l)$$

$$C_2(\infty) = C_1(\infty) \qquad (2m)$$

$$K_{01} = (A_1 + A_2)/1.8 \qquad (2n)$$

$$K_{10} = (A_1 + A_2)/C_1(\infty) \qquad (2o)$$

$$D_1(\infty) = \frac{(A_1 + A_2)^2}{A_1K_1 + A_2K_2} \qquad (2p)$$

$$D_2(\infty) = A_1/K_1 + A_2/K_2 - D_1(\infty) \qquad (2q)$$

$$K_{12} = \frac{V_1(A_1K_1^2 + A_2K_2^2)}{(A_1K_1 + A_2K_2)} - K_{10} \qquad (2r)$$

$$K_{21} = K_{12} \qquad (2s)$$

From 2c and 2d we can find the expression for the new values of $C_1(t)$ and $C_2(t)$ when the increment of time is Δt.

$$C_1(t+\Delta t) = C_1(t) + \frac{dC_1(t)}{dt}\,\Delta t$$

$$= C_1(t) + \frac{1}{V_1}(1.8\ K_{01} + K_{21}C_2(t) - (K_{10} + K_{12})C_1(t))\ \Delta t \qquad (2t)$$

$$C_2(t+\Delta t) = C_2(t) + \frac{dC_2(t)}{dt}\,\Delta t$$

$$= C_2(t) + \frac{1}{V_1}\left(K_{12}\,C_1(t) - K_{21}\,C_2(t)\right)\,\Delta t \qquad (2u)$$

The functions of $C_1(t)$ and $C_2(t)$ can be generated by the computer using $C_1(o) = C_2(o) = 0$ and $\Delta t = 0.1$ sec. These can in terms be used to generate the functions $\frac{dD_1(t)}{dt}$ and $\frac{dD_2(t)}{dt}$ of equation 2c and 2d which underlies the figure 12.

APPENDIX 2B

```
OLD
OLD FILE NAME--RK1:COMPA3.BAS

READY

LIST

COMPA3  01-AUG-77  BASIC V01B-02A

10 REM--                COMPAN.BAS                      MARCH 22,1977
20 REM--
30 REM-- TO SIMULATE 2 COMPARTMENTS IN-SERIES
40 REM--
50 REM--INPUT A1,A2,K1,K2,HEART WT (H)
60 PRINT "INPUT A1,A2 (MMOLES/SEC)";\INPUT A1,A2
70 PRINT "INPUT K1,K2 (L/SEC)";\INPUT K1,K2
80 PRINT "INPUT HEART WT (KG)";\INPUT H
90 REM--
100 REM--CALCULATION OF C1,C2 (MMOLES/L)
110 C1=(A1/K1+A2/K2)/(.8*H)
120 C2=C1
130 REM--
140 REM--CALCULATION OF K01,K10 (L/SEC)
150 K3=(A1+A2)/1.8
160 K4=(A1+A2)/C1
170 REM--
180 REM--CALCULATION OF D1,D2 (MMOLES)
190 D1=(A1+A2)^2/(A1*K1+A2*K2)
200 D2=A1/K1+A2/K2-D1
210 REM--
220 REM--CALCULATION OF V1,V2 (L)
230 V1=D1/C1
240 V2=D2/C2
250 REM--
260 REM--CALCULATION OF K12, K21 ( L/SEC)
270 K5=V1*(A1*K1^2+A2*K2^2)/(A1*K1+A2*K2)-K4
280 K6=K5
290 REM--
300 REM--CALCULATION OF C1(T), C2(T)
301 REM--INTERVAL OF CALCULATION=0.1 SEC
310 DIM C1(1000),C2(1000)
320 C1(0)=0\C2(0)=0
330 FOR I=0 TO 999
340 C1(I+1)=(1.8*K3+K5*C2(I)-K4*C1(I)-K5*C1(I))*.1/V1+C1(I)
350 C2(I+1)=(K5*C1(I)-K6*C2(I))*.1/V2+C2(I)
360 NEXT I
```

```
361 REM--
362 REM--CALCULATION OF D1(T),D2(T),D(T).INTERVAL=0.1 SEC
363 DIM D1(1000),D2(1000),D(1000)
364 FOR I=0 TO 1000
365 D1(I)=1.8*K3+K6*C2(I)-(K4+K5)*C1(I)
366 D2(I)=K5*C1(I)-K6*C2(I)
367 D(I)=1.8*K3-K4*C1(I)
368 NEXT I
370 REM--
420 REM--OUTPUT K01,K10,K12,K21,V1,V2,D1,D2,V1+V2,V1/V2
421 PRINT \PRINT
422 PRINT " K(01)= ";K3;TAB(15);"L/SEC"
423 PRINT " K(10)= ";K4;TAB(15);"L/SEC"
424 PRINT " K(12)= ";K5;TAB(15);"L/SEC"
425 PRINT " K(21)= ";K6;TAB(15);"L/SEC"
426 PRINT " V1    = ";V1;TAB(15);"L"
427 PRINT " V2    = ";V2;TAB(15);"L"
428 PRINT " D1    = ";D1/H;TAB(22);"MMOLES/KG"
429 PRINT " D2    = ";D2/H;TAB(22);"MMOLES/KG"
430 PRINT " V1+V2= ";V1+V2;TAB(15);"L"
431 PRINT " V1/V2= ";V1/V2
432 PRINT \PRINT
433 REM--
440 REM--OUTPUT T, C1(T),C2(T),V1*C1(T),V2*C2(T)
450 PRINT TAB(4);"SEC";TAB(20);"MM";TAB(35);"MM";
460 PRINT TAB(43);"MMOLES/KG";TAB(57);"MMOLES/KG"
470 PRINT TAB(3);"TIME";TAB(18);"C1(T)";TAB(33);"C2(T)";
471 PRINT TAB(44);"V1*C1(T)";TAB(58);"V2*C2(T)"
472 PRINT " ***********   ";" ***********   ";
473 PRINT " ***********   ";" ***********   ";
474 PRINT " ***********   "
490 FOR I=0 TO 1000 STEP 20
500 PRINT I/10,C1(I),C2(I),V1*C1(I)/H,V2*C2(I)/H
510 NEXT I
520 REM--
530 REM--OUTPUT T,D1(T),D2(T),D(T)
540 PRINT \PRINT
550 PRINT TAB(4);"SEC";TAB(16);"MMOLES/KG";
560 PRINT TAB(31);"MMOLES/KG";TAB(46);"MMOLES/KG"
570 PRINT TAB(3);"TIME";TAB(18);"D1(T)";
580 PRINT TAB(33);"D2(T)";TAB(48);"D(T)"
590 PRINT " ***********   ";" ***********   ";
591 PRINT " ***********   ";" ***********   "
595 FOR I=0 TO 1000 STEP 20
600 PRINT I/10,D1(I),D2(I),D(I)
700 NEXT I
710 STOP\END

READY
```

```
RUN

COMPA3  01-AUG-77  BASIC V01B-02A

INPUT A1,A2 (MMOLES/SEC)?5E-6,1E-5
INPUT K1,K2 (L/SEC)?.1386,.0231
INPUT HEART WT (KG)?3E-4


 K(01)=  8.33333E-06 L/SEC
 K(10)=  7.67631E-06 L/SEC
 K(12)=  5.99711E-06 L/SEC
 K(21)=  5.99711E-06 L/SEC
 V1   =  1.24615E-04 L
 V2   =  1.15385E-04 L
 D1   =  .811688      MMOLES/KG
 D2   =  .751563      MMOLES/KG
 V1+V2=  2.40000E-04 L
 V1/V2=  1.08
```

SEC TIME	MM C1(T)	MM C2(T)	MMOLES/KG V1*C1(T)	MMOLES/KG V2*C2(T)
**********	**********	**********	**********	**********
0	0	0	0	0
2	.21753	.0108002	.0903586	4.15391E-03
4	.393757	.0399942	.163561	.0153824
6	.538214	.0821518	.223566	.0315968
8	.658135	.133208	.273379	.0512338
10	.759014	.190129	.315283	.0731266
12	.845029	.25066	.351012	.0964075
14	.919363	.31313	.381889	.120435
16	.984442	.376315	.408922	.144736
18	1.04212	.439319	.43288	.168969
20	1.09382	.5015	.454354	.192884
22	1.14062	.562401	.473798	.216308
24	1.18339	.621707	.49156	.239118
26	1.22276	.679209	.507914	.261234
28	1.25924	.734775	.523069	.282606
30	1.29324	.78833	.537193	.303204
32	1.32507	.839843	.550415	.323017
34	1.35499	.889315	.562841	.342044
36	1.38319	.936768	.574556	.360295
38	1.40984	.982241	.585627	.377785
40	1.43509	1.02578	.596112	.394531
42	1.45903	1.06745	.606058	.410557
44	1.48177	1.1073	.615505	.425886
46	1.5034	1.14541	.624488	.440542
48	1.52398	1.18183	.633037	.454552
50	1.54358	1.21664	.641178	.46794

52	1.56225	1.2499	.648935	.480732
54	1.58005	1.28168	.65633	.492952
56	1.59703	1.31203	.66338	.504626
58	1.61322	1.34102	.670105	.515775
60	1.62866	1.3687	.676521	.526424
62	1.6434	1.39514	.682643	.536593
64	1.65747	1.42039	.688486	.546304
66	1.67089	1.4445	.694062	.555578
68	1.6837	1.46753	.699384	.564434
70	1.69593	1.48951	.704464	.57289
72	1.70761	1.51051	.709313	.580964
74	1.71875	1.53055	.713943	.588674
76	1.72939	1.54969	.718363	.596036
78	1.73955	1.56797	.722582	.603065
80	1.74925	1.58542	.726611	.609776
82	1.75851	1.60208	.730457	.616185
84	1.76735	1.61799	.734129	.622303
86	1.77579	1.63318	.737636	.628146
88	1.78385	1.64768	.740983	.633724
90	1.79154	1.66153	.744179	.63905
92	1.79889	1.67475	.747231	.644136
94	1.8059	1.68738	.750144	.648991
96	1.8126	1.69943	.752926	.653628
98	1.819	1.71094	.755583	.658054
100	1.8251	1.72193	.758119	.662281

SEC TIME	MMOLES/KG D1(T)	MMOLES/KG D2(T)	MMOLES/KG D(T)
**********	**********	**********	**********
0	1.50000E-05	0	1.50000E-05
2	1.20904E-05	1.23978E-06	1.33302E-05
4	9.85584E-06	2.12156E-06	1.19774E-05
6	8.13344E-06	2.73506E-06	1.08685E-05
8	6.79991E-06	3.14805E-06	9.94795E-06
10	5.76191E-06	3.41167E-06	9.17358E-06
12	4.94879E-06	3.56450E-06	8.51330E-06
14	4.30704E-06	3.63565E-06	7.94269E-06
16	3.79612E-06	3.64701E-06	7.44312E-06
18	3.38531E-06	3.61506E-06	7.00037E-06
20	3.05134E-06	3.55219E-06	6.60353E-06
22	2.77655E-06	3.46767E-06	6.24422E-06
24	2.54751E-06	3.36845E-06	5.91596E-06
26	2.35404E-06	3.25971E-06	5.61375E-06
28	2.18840E-06	3.14528E-06	5.33368E-06
30	2.04467E-06	3.02802E-06	5.07268E-06
32	1.91835E-06	2.90998E-06	4.82833E-06
34	1.80599E-06	2.79270E-06	4.59869E-06
36	1.70496E-06	2.67724E-06	4.38221E-06
38	1.61323E-06	2.56438E-06	4.17761E-06
40	1.52921E-06	2.45464E-06	3.98385E-06

42	1.45170E-06	2.34835E-06	3.80005E-06
44	1.37973E-06	2.24573E-06	3.62546E-06
46	1.31256E-06	2.14690E-06	3.45946E-06
48	1.24960E-06	2.05188E-06	3.30147E-06
50	1.19037E-06	1.96066E-06	3.15103E-06
52	1.13449E-06	1.87319E-06	3.00768E-06
54	1.08164E-06	1.78940E-06	2.87103E-06
56	1.03156E-06	1.70918E-06	2.74073E-06
58	9.84033E-07	1.63242E-06	2.61645E-06
60	9.38868E-07	1.55902E-06	2.49788E-06
62	8.95918E-07	1.48884E-06	2.38475E-06
64	8.55029E-07	1.42176E-06	2.27679E-06
66	8.16088E-07	1.35766E-06	2.17375E-06
68	7.78980E-07	1.29641E-06	2.07539E-06
70	7.43603E-07	1.23791E-06	1.98151E-06
72	7.09864E-07	1.18203E-06	1.89189E-06
74	6.77683E-07	1.12865E-06	1.80634E-06
76	6.46982E-07	1.07768E-06	1.72466E-06
78	6.17685E-07	1.02899E-06	1.64668E-06
80	5.89724E-07	9.82508E-07	1.57223E-06
82	5.63035E-07	9.38116E-07	1.50115E-06
84	5.37562E-07	8.95727E-07	1.43329E-06
86	5.13248E-07	8.55249E-07	1.36850E-06
88	4.90036E-07	8.16597E-07	1.30663E-06
90	4.67879E-07	7.79693E-07	1.24757E-06
92	4.46720E-07	7.44457E-07	1.19118E-06
94	4.26522E-07	7.10809E-07	1.13733E-06
96	4.07235E-07	6.78685E-07	1.08592E-06
98	3.88825E-07	6.48010E-07	1.03684E-06
100	3.71248E-07	6.18722E-07	9.89970E-07

STOP AT LINE 710

READY

APPENDIX 3A

Simulation of two compartments in series (washout)

The change of the sum of the content of compartment 1 and 2 can be expresses as:

$$-\left(\frac{dD_1(t)}{dt} + \frac{dD_2(t)}{dt}\right) = A_1 e^{-K_1 t} + A_2 e^{-K_2 t} , \qquad (3a)$$

where A_1, A_2 are the intercepts and K_1, K_2 are the rate constants of the washout curve analyzed according to parallel model (by automatic computer program PEEL65). The negative sign indicates that the change observed in the effluent is opposite to that in the compartments.

Intergration of equation 3a from time zero to infinity with $D_1(\infty) = D_2(\infty) = 0$ gives

$$D_1(o) + D_2(o) = C_1(o)V_1 + C_2(o)V_2 = \frac{A_1}{K_1} + \frac{A_2}{K_2} . \qquad (3b)$$

The two differential equations which describe the model shown in figure 13 are as follows:

$$\frac{dD_1(t)}{dt} = K_{21}C_2(t) - (K_{10} + K_{12})C_1(t)$$

$$= V_1 \frac{dC_1(t)}{dt} \qquad (3c)$$

$$\frac{dD_2(t)}{dt} = K_{12}C_1(t) - K_{21}C_2(t)$$

$$= V_2 \frac{dC_2(t)}{dt} \qquad (3d)$$

Summing equation 3c, 3d and equating to 3a at time zero gives us

$$K_{10} C_1(o) = A_1 + A_2 \qquad (3e)$$

By taking the first time derivative of equations 3a, 3c, 3d and equating the first equation so derived with the sum of the following two at time zero we get

$$V_1 = \frac{K_{10}^2 C_1(o)}{A_1 K_1 + A_2 K_2} \qquad (3f)$$

Since the content of compartment 1 equals its concentration times the volume of distribution or $D_1(o) = C_1(o)\ V$, (3g) equation 3e and 3f when substituted into 3g let us express the content in terms of the constants A_1, A_2, K_1 and K_2.

$$D_1(o) = \frac{(A_1 + A_2)^2}{A_1 K_1 + A_2 K_2} \qquad (3h)$$

Notice this is identical to that derived for uptake process (equation 16). The content of compartment 2 is given by equation 3b

$$D_2(o) = \frac{A_1}{K_1} + \frac{A_2}{K_2} - D_1(o) \qquad (3i)$$

If we make the further assumption of $K_{12} = K_{21}$, the steady state condition

$$C_1(o)\ K_{12} = C_2(o)\ K_{21}$$

leads to $C_1(o) = C_2(o)$. (3j)

By taking the second time derivative of equation 3a, 3c, 3d and equating the first equation so derived with the sum of

the following two, setting the time to zero, and substituting equation 3j into the result, we get

$$A_1K_1^2 + A_2K_2^2 = \frac{K_{10}^2 C_1(o)\ (K_{10} + K_{12})}{V_1^2} \qquad (3k)$$

From equations 3b and 3j, assuming $V_1 + V_2 = 0.8\ H$, where H is the wet ventricular weight (this assumption is not necessary for the generation of curves in figure 14; the dummy term is later cancelled out, but it is necessary for an estimate of the rate constants K_{10}, K_{12} and K_{21} to be made), we get

$$C_1(o) = C_2(o) = \frac{A_1/K_1 + A_2/K_2}{0.8\ H} \qquad (31)$$

From 3e we get

$$K_{10} = \frac{A_1 + A_2}{C_1(o)} \qquad (3m)$$

The volumes of distribution of the two compartments are respectively:

$$V_1 = D_1(o)/C_1(o) \qquad (3n)$$

$$V_2 = D_2(o)/C_2(o) \qquad (3o)$$

From equation 3k we get

$$K_{12} = K_{21} = V_1 \frac{(A_1K_1^2 + A_2K_2^2)}{A_1K_1 + A_2K_2} - K_{10} \qquad (3p)$$

The generation of the curves in figure 14 is now possible with the following derivations.

From equations 3c and 3d

$$C_1(t+\Delta t) = C_1(t) + \frac{dC_1(t)}{dt}\Delta t$$

$$= C_1(t) + \frac{1}{V_1}(K_{21}C_2(t) - (K_{10}+K_{12})\,C_1(t))\Delta t \qquad (3q)$$

$$C_2(t+\Delta t) = C_2(t) + \frac{dC_2(t)}{dt}\Delta t$$

$$= C_2(t) + \frac{1}{V_2}(K_{12}C_1(t) - K_{21}C_2(t))\Delta t \qquad (3r)$$

The functions of $C_1(t)$ and $C_2(t)$ can be generated by the computer using equation 31 and $\Delta t = 0.1$ sec. These can in terms be used to generate the functions $-\frac{dD_1(t)}{dt}$ and $-\frac{dD_2(t)}{dt}$ of equations 3c and 3d which underlies the figure 14. Notice again the negative sign necessary to show that the changes in the effluent is opposite to that of the changes of the compartments.

APPENDIX 3B

```
OLD
OLD FILE NAME--RK1:SERIWA.BAS

READY

LIST

SERIWA  01-AUG-77  BASIC V01B-02A

5 REM--                                  TONY MA
10 REM--          SERIWA.BAS                    MARCH 27,1977
20 REM--
30 REM--          TO SIMULATE 2 COMPARTMENTS IN SERIES (WASH)
40 REM--
50 REM--INPUT A1,A2,K1,K2,H
60 PRINT "INPUT A1,A2 (MMOLES/SEC)";\INPUT A1,A2
70 PRINT "INPUT K1,K2 (1/SEC)";\INPUT K1,K2
80 PRINT "INPUT HEART WT (KG)";\INPUT H
90 REM--
100 REM--CALCULATION OF C1(0),C2(0)  (MMOLES/L AT BEGINING OF WASH)
110 C1=(A1/K1+A2/K2)/(.8*H)
120 C2=C1
130 REM--
140 REM--CALCULATION OF K(10) (L/SEC)
160 K4=(A1+A2)/C1
170 REM--
180 REM--CALCULATION OF D1,D2 (MMOLES)
190 D1=(A1+A2)^2/(A1*K1+A2*K2)
200 D2=A1/K1+A2/K2-D1
210 REM--
220 REM--CALCULATION OF V1,V2 (L)
230 V1=D1/C1
240 V2=D2/C2
250 REM--
260 REM--CALCULATION OF K12, K21 ( L/SEC)
270 K5=V1*(A1*K1^2+A2*K2^2)/(A1*K1+A2*K2)-K4
280 K6=K5
290 REM--
370 REM--
420 REM--OUTPUT K(10),K(12),K(21),V1,V2,D1,D2,V1+V2,V1/V2
421 PRINT \PRINT
423 PRINT " K(10)= ";K4;TAB(15);"L/SEC"
424 PRINT " K(12)= ";K5;TAB(15);"L/SEC"
425 PRINT " K(21)= ";K6;TAB(15);"L/SEC"
426 PRINT " V1    = ";V1;TAB(15);"L"
427 PRINT " V2    = ";V2;TAB(15);"L"
428 PRINT " D1    = ";D1/H;TAB(22);"MMOLES/KG"
429 PRINT " D2    = ";D2/H;TAB(22);"MMOLES/KG"
430 PRINT " V1+V2= ";V1+V2;TAB(15);"L"
431 PRINT " V1/V2= ";V1/V2
432 PRINT " C1(0)= ";C1;TAB(15);"MM"
433 PRINT " C2(0)= ";C2;TAB(15);"MM"
434 PRINT \PRINT
```

```
435 REM--
440 REM--OUTPUT T, C1(T),C2(T),V1*C1(T),V2*C2(T)
450 PRINT TAB(4);"SEC";TAB(20);"MM";TAB(35);"MM";
460 PRINT TAB(43);"MMOLES/KG";TAB(57);"MMOLES/KG"
470 PRINT TAB(3);"TIME";TAB(18);"C1(T)";TAB(33);"C2(T)";
471 PRINT TAB(44);"V1*C1(T)";TAB(58);"V2*C2(T)"
472 PRINT " **********   ";" **********   ";
473 PRINT " **********   ";" **********   ";
474 PRINT " **********   "
475 DIM C1(1000),C2(1000)
480 C1(0)=C1\C2(0)=C2\A=0
485 GOSUB 800 \GOSUB 840
490 C1(0)=C1(1000)\C2(0)=C2(1000)\A=1000
495 GOSUB 800 \GOSUB 840
500 C1(0)=C1(1000)\C2(0)=C2(1000)\A=2000
505 GOSUB 800 \GOSUB 840
510 I=1000
515 PRINT (A+I)/10,C1(I),C2(I),V1*C1(I)/H,V2*C2(I)/H
520 REM--
530 REM--OUTPUT T,D1(T),D2(T),D(T)
540 PRINT \PRINT
550 PRINT TAB(4);"SEC";TAB(16);"MMOLES/KG";
560 PRINT TAB(31);"MMOLES/KG";TAB(46);"MMOLES/KG"
570 PRINT TAB(3);"TIME";TAB(18);"D1(T)";
580 PRINT TAB(33);"D2(T)";TAB(48);"D(T)"
590 DIM D1(1000),D2(1000),D(1000)
591 PRINT " **********   ";" **********   ";
592 PRINT " **********   ";" **********"
600 C1(0)=C1\C2(0)=C2\A=0
610 GOSUB 890
620 C1(0)=C1(1000)\C2(0)=C2(1000)\A=1000
630 GOSUB 890
640 C1(0)=C1(1000)\C2(0)=C2(1000)\A=2000
650 GOSUB 890
660 I=1000
670 PRINT (A+I)/10,D1(I),D2(I),D(I)
680 STOP
800 FOR I=0 TO 999
810 C1(I+1)=C1(I)+(K6*C2(I)-(K4+K5)*C1(I))*.1/V1
820 C2(I+1)=C2(I)+(K5*C1(I)-K6*C2(I))*.1/V2
830 NEXT I\RETURN
840 FOR I=0 TO 950 STEP 50
850 PRINT (A+I)/10,C1(I),C2(I),V1*C1(I)/H,V2*C2(I)/H
860 NEXT I
870 RETURN
890 GOSUB 800
900 FOR I=0 TO 1000
910 D1(I)=(K6*C2(I)-(K4+K5)*C1(I))*(-1)
920 D2(I)=(K5*C1(I)-K6*C2(I))*(-1)
930 D(I)=K4*C1(I)
940 NEXT I
950 FOR I=0 TO 950 STEP 50
960 PRINT (A+I)/10,D1(I),D2(I),D(I)
970 NEXT I
980 RETURN
1000 END
```

```
READY

RUN

SERIWA  01-AUG-77  BASIC V01B-02A

INPUT A1,A2 (MMOLES/SEC)?2.36E-5,2.8E-6
INPUT K1,K2 (1/SEC)?3.98799E-2,6.67203E-3
INPUT HEART WT (KG)?6.07E-4


 K(10)=  1.26748E-05 L/SEC
 K(12)=  1.00251E-06 L/SEC
 K(21)=  1.00251E-06 L/SEC
 V1    =  3.48614E-04 L
 V2    =  1.36986E-04 L
 D1    =  1.19624       MMOLES/KG
 D2    =  .470056       MMOLES/KG
 V1+V2=  4.85600E-04 L
 V1/V2=  2.54488
 C1(0)=  2.08287 MM
 C2(0)=  2.08287 MM
```

SEC TIME	MM C1(T)	MM C2(T)	MMOLES/KG V1*C1(T)	MMOLES/KG V2*C2(T)
**********	**********	**********	**********	**********
0	2.08287	2.08287	1.19624	.470056
5	1.73841	2.07656	.998406	.468632
10	1.45526	2.05922	.835787	.46472
15	1.22235	2.03325	.702021	.458859
20	1.03061	2.00059	.591903	.451489
25	.872628	1.96284	.50117	.442969
30	.742314	1.92127	.426328	.433587
35	.634691	1.87693	.364518	.42358
40	.545679	1.83065	.313396	.413136
45	.471937	1.78311	.271044	.402408
50	.410726	1.73487	.235889	.39152
55	.359805	1.68634	.206644	.380569
60	.317335	1.63789	.182253	.369634
65	.281812	1.58977	.161851	.358776
70	.252003	1.54222	.144731	.348044
75	.226895	1.49538	.130311	.337475
80	.20566	1.4494	.118115	.327098
85	.18762	1.40437	.107754	.316935
90	.172216	1.36036	.0989075	.307002
95	.158992	1.31741	.0913128	.29731
100	.147574	1.27557	.0847549	.287867
105	.137653	1.23484	.0790572	.278676
110	.128977	1.19525	.0740746	.269741
115	.121339	1.15679	.0696879	.261061
120	.114569	1.11945	.0657994	.252634

125	.108525	1.08322	.0623285	.244458
130	.103094	1.04809	.059209	.23653
135	.098179	1.01403	.0563864	.228844
140	.0937028	.981034	.0538156	.221397
145	.0896007	.949066	.0514597	.214183
150	.0858192	.918107	.0492879	.207196
155	.082314	.888129	.0472748	.200431
160	.0790486	.859107	.0453994	.193881
165	.0759925	.831014	.0436442	.187541
170	.0731203	.803825	.0419946	.181405
175	.0704108	.777512	.0404385	.175467
180	.0678463	.752051	.0389657	.169721
185	.0654119	.727415	.0375675	.164161
190	.063095	.703579	.0362369	.158782
195	.060885	.680518	.0349676	.153578
200	.0587727	.658209	.0337545	.148543
205	.0567503	.636627	.032593	.143672
210	.0548113	.61575	.0314794	.138961
215	.0529497	.595555	.0304102	.134403
220	.0511606	.57602	.0293827	.129995
225	.0494395	.557124	.0283942	.12573
230	.0477825	.538847	.0274426	.121606
235	.0461861	.521168	.0265257	.117616
240	.0446472	.504068	.0256419	.113757
245	.043163	.487528	.0247895	.110024
250	.0417309	.471531	.023967	.106414
255	.0403486	.456058	.0231731	.102922
260	.039014	.441092	.0224066	.0995446
265	.037725	.426617	.0216663	.0962779
270	.0364799	.412617	.0209512	.0931184
275	.0352769	.399076	.0202603	.0900625
280	.0341145	.385979	.0195927	.0871068
285	.032991	.373312	.0189475	.0842481
290	.0319051	.36106	.0183238	.0814832
295	.0308554	.349211	.0177209	.078809
300	.0298406	.33775	.0171381	.0762226

SEC TIME	MMOLES/KG D1(T)	MMOLES/KG D2(T)	MMOLES/KG D(T)
**********	**********	**********	**********
0	2.64000E-05	0	2.64000E-05
5	2.16950E-05	3.39001E-07	2.20340E-05
10	1.78397E-05	6.05481E-07	1.84452E-05
15	1.46801E-05	8.12941E-07	1.54931E-05
20	1.20904E-05	9.72420E-07	1.30628E-05
25	9.96747E-06	1.09295E-06	1.10604E-05
30	8.22680E-06	1.18192E-06	9.40872E-06
35	6.79926E-06	1.24536E-06	8.04462E-06
40	5.62821E-06	1.28820E-06	6.91640E-06
45	4.66726E-06	1.31447E-06	5.98173E-06
50	3.87842E-06	1.32747E-06	5.20589E-06
55	3.23060E-06	1.32987E-06	4.56047E-06
60	2.69831E-06	1.32387E-06	4.02218E-06

65	2.26068E-06	1.31125E-06	3.57193E-06
70	1.90064E-06	1.29346E-06	3.19410E-06
75	1.60418E-06	1.27168E-06	2.87586E-06
80	1.35984E-06	1.24687E-06	2.60671E-06
85	1.15824E-06	1.21981E-06	2.37805E-06
90	9.91683E-07	1.19113E-06	2.18281E-06
95	8.53871E-07	1.16133E-06	2.01520E-06
100	7.39648E-07	1.13083E-06	1.87048E-06
105	6.44783E-07	1.09995E-06	1.74473E-06
110	5.65816E-07	1.06895E-06	1.63477E-06
115	4.99909E-07	1.03805E-06	1.53796E-06
120	4.44738E-07	1.00740E-06	1.45214E-06
125	3.98398E-07	9.77143E-07	1.37554E-06
130	3.59328E-07	9.47368E-07	1.30670E-06
135	3.26248E-07	9.18155E-07	1.24440E-06
140	2.98109E-07	8.89560E-07	1.18767E-06
145	2.74051E-07	8.61625E-07	1.13568E-06
150	2.53367E-07	8.34378E-07	1.08775E-06
155	2.35479E-07	8.07839E-07	1.04332E-06
160	2.19911E-07	7.82018E-07	1.00193E-06
165	2.06275E-07	7.56919E-07	9.63193E-07
170	1.94248E-07	7.32540E-07	9.26788E-07
175	1.83568E-07	7.08878E-07	8.92446E-07
180	1.74018E-07	6.85924E-07	8.59941E-07
185	1.65420E-07	6.63666E-07	8.29086E-07
190	1.57627E-07	6.42093E-07	7.99720E-07
195	1.50518E-07	6.21190E-07	7.71708E-07
200	1.43992E-07	6.00942E-07	7.44934E-07
205	1.37968E-07	5.81333E-07	7.19302E-07
210	1.32377E-07	5.62348E-07	6.94725E-07
215	1.27162E-07	5.43968E-07	6.71130E-07
220	1.22275E-07	5.26178E-07	6.48453E-07
225	1.17679E-07	5.08960E-07	6.26639E-07
230	1.13338E-07	4.92298E-07	6.05636E-07
235	1.09227E-07	4.76175E-07	5.85402E-07
240	1.05322E-07	4.60575E-07	5.65897E-07
245	1.01602E-07	4.45482E-07	5.47084E-07
250	9.80523E-08	4.30880E-07	5.28933E-07
255	9.46586E-08	4.16754E-07	5.11412E-07
260	9.14079E-08	4.03089E-07	4.94496E-07
265	8.82897E-08	3.89869E-07	4.78159E-07
270	8.52952E-08	3.77082E-07	4.62377E-07
275	8.24166E-08	3.64713E-07	4.47130E-07
280	7.96470E-08	3.52749E-07	4.32396E-07
285	7.69798E-08	3.41176E-07	4.18156E-07
290	7.44099E-08	3.29982E-07	4.04392E-07
295	7.19321E-08	3.19155E-07	3.91087E-07
300	6.95420E-08	3.08683E-07	3.78225E-07

STOP AT LINE 680

READY

APPENDIX 4A

```
OLD
OLD FILE NAME--DATA.MA

READY

LIST

DATA     01-AUG-77  BASIC V01B-02A

5 REM-- DATA.MA                    MAY 20/77
6 REM--CONVERT CPM(PER 1 SEC SAMPLE) OF WASHOUT OR UPTAKE DATA
7 REM-- INTO MMOLES/KG/SEC AFTER FIRST SUBTRACTING
8 REM-- CA EXCHANGE OF PERFUSION APPARATUS
9 REM-- UPTAKE 94 NMOLES,10 SEC;WASHOUT 165 NMOLES,20SEC
10 DIM X(100),Y(100)
15 PRINT "FILE NAME(EXP.ID.)";
20 INPUT H$
30 OPEN H$ FOR OUTPUT AS FILE #1
40 PRINT "COMMENT"
50 INPUT C$
55 C$=H$&","&C$
56 PRINT #1:C$
60 PRINT "HOW MANY DATA POINTS";
70 INPUT N
80 PRINT #1:N,0
85 PRINT "HEART WT(G)";\INPUT H
86 PRINT "STANDARD CPM(PER SEC SAMPLE),STANDARD ML/MIN";
87 INPUT S1,S2
88 C=(1.80000E-03*S2)/(60*S1)\REM-- C IN MMOLES/SEC
90 PRINT "UPTAKE OR WASHOUT (U OR W)";
95 INPUT Q$
100 IF Q$="W"GO TO 150
110 IF Q$="U"GO TO 120 \GO TO 90
120 A=9.40000E-05*.693/10\REM-- A=APPARATUS UPTAKE AT 0-TIME
121 T=10
130 GOSUB 1000 \GO TO 200 \REM--        WITH UNITS MMOLES/SEC
150 A=1.65000E-04*.693/20\REM-- A=APPARATUS WASHOUT AT 0-TIME
151 T=20
160 GOSUB 1000 \REM--       WITH UNITS MMOLES/SEC
200 FOR I=1 TO N
210 PRINT #1:X(I);",";Y(I)
220 NEXT I\PRINT \PRINT
300 PRINT "SEC";TAB(13);"MMOLES/KG/SEC"
310 PRINT "*****";TAB(13);"**************"
320 FOR I=1 TO N
330 PRINT X(I),Y(I)
340 NEXT I
345 PRINT #1:1;",";0
346 PRINT #1:0
350 CLOSE #1
```

```
360 PRINT "ARE YOU DONE(Y OR N)";\INPUT R$
370 IF R$="Y"GO TO 1200
380 IF R$="N"GO TO 10
390 GO TO 360
1000 PRINT "SEC,CPM"
1010 FOR I=1 TO N
1015 PRINT I;")";
1020 INPUT X(I),Y(I)
1030 NEXT I
1040 PRINT "ANY CORRECTION (Y OR N)";\INPUT P$
1050 IF P$="N"GO TO 1090
1060 IF P$="Y"GO TO 1065 \GO TO 1040
1065 PRINT "DATA NUMBER,SEC,CPM";
1070 INPUT N1,X(N1),Y(N1)
1080 GO TO 1040
1090 FOR I=1 TO N
1100 Y(I)=(Y(I)*C-A*EXP(-.693*X(I)/T))/(H*1.00000E-03)
1110 NEXT I
1120 RETURN
1200 STOP\END

READY
```

```
RUN

DATA     01-AUG-77   BASIC V01B-02A

FILE NAME(EXP.ID.)?RK1:M30E1.W2
COMMENT
?3/30/76 M-30 EXP-1 O-CA WASH
HOW MANY DATA POINTS?100
HEART WT(G)?0.18
STANDARD CPM(PER SEC SAMPLE),STANDARD ML/MIN?9930,1
UPTAKE OR WASHOUT (U OR W)?W
SEC,CPM
 1 )?2,4400
 2 )?3,4950
 3 )?4,4800
 4 )?5,4450
 5 )?6,4275
 6 )?7,4200
 7 )?8,3900
 8 )?9,3750
 9 )?10,3450
 10 )?12,3050
 11 )?14,2525
 12 )?16,2325
 13 )?18,2075
 14 )?20,1820
 15 )?22,1640
 16 )?24,1400
 17 )?26,1300
 18 )?28,1250
 19 )?30,1175
 20 )?32,1040
 21 )?34,950
 22 )?36,925
 23 )?38,890
 24 )?40,825
 25 )?42,740
 26 )?44,660
 27 )?46,600
 28 )?48,590
 29 )?50,515
 30 )?52,465
 31 )?54,420
 32 )?56,380
 33 )?58,345
 34 )?60,317
 35 )?62,290
 36 )?64,260
 37 )?66,240
 38 )?68,223
 39 )?72,204
 40 )?74,183
 41 )?76,170
 42 )?78,160
 43 )?82,135
 44 )?84,127
```

```
 45 )?86,117
 46 )?88,111
 47 )?92,111
 48 )?94,105
 49 )?96,98
 50 )?98,95
 51 )?100,87
 52 )?102,84
 53 )?104,77
 54 )?106,75
 55 )?108,72
 56 )?110,81
 57 )?112,81
 58 )?114,81
 59 )?116,80
 60 )?124,45
 61 )?128,40
 62 )?132,35
 63 )?136,45
 64 )?140,34
 65 )?144,34
 66 )?148,33
 67 )?152,32
 68 )?156,31
 69 )?160,30
 70 )?164,28
 71 )?168,27
 72 )?172,26
 73 )?176,26
 74 )?180,25
 75 )?184,23
 76 )?188,23
 77 )?204,19
 78 )?208,19
 79 )?212,17
 80 )?216,16
 81 )?220,16
 82 )?224,17
 83 )?228,18
 84 )?232,18
 85 )?236,18
 86 )?240,17
 87 )?244,18
 88 )?248,18
 89 )?252,18
 90 )?256,18
 91 )?260,17
 92 )?264,17
 93 )?268,17
 94 )?272,16
 95 )?276,16
 96 )?280,15
 97 )?284,15
 98 )?288,15
 99 )?292,15
100 )?296,16
ANY CORRECTION (Y OR N)?N
```

SEC	MMOLES/KG/SEC
*****	**********
2	.0442144
3	.054455
4	.0529123
5	.0479796
6	.045952
7	.0455718
8	.0413853
9	.0396875
10	.0354442
12	.0302344
14	.0228259
16	.0207783
18	.0178038
20	.0146636
22	.0127059
24	9.66995E-03
26	8.91735E-03
28	8.94198E-03
30	8.48916E-03
32	6.97534E-03
34	6.16645E-03
36	6.40155E-03
38	6.42497E-03
40	5.90397E-03
42	5.00912E-03
44	4.16259E-03
46	3.61852E-03
48	3.88266E-03
50	3.02691E-03
52	2.56377E-03
54	2.15937E-03
56	1.81541E-03
58	1.53344E-03
60	1.34851E-03
62	1.16128E-03
64	9.05894E-04
66	8.01736E-04
68	7.32426E-04
72	8.03151E-04
74	6.26155E-04
76	5.71685E-04
78	5.56605E-04
82	4.12527E-04
84	4.02341E-04
86	3.50278E-04
88	3.57600E-04
92	5.52440E-04
94	5.39484E-04
96	5.03869E-04
98	5.29908E-04
100	4.66913E-04

```
  102             4.83066E-04
  104             4.27629E-04
  106             4.51959E-04
  108             4.55628E-04
  110             6.57090E-04
  112             7.04120E-04
  114             7.48001E-04
  116             7.72159E-04
  124             3.22848E-04
  128             2.94895E-04
  132             2.59699E-04
  136             4.69958E-04
  140             3.22261E-04
  144             3.54410E-04
  148             3.65614E-04
  152             3.73195E-04
  156             3.77624E-04
  160             3.79306E-04
  164             3.61815E-04
  168             3.59027E-04
  172             3.54427E-04
  176             3.65035E-04
  180             3.57486E-04
  184             3.31957E-04
  188             3.38956E-04
  204             2.91856E-04
  208             2.95356E-04
  212             2.64834E-04
  216             2.50703E-04
  220             2.53012E-04
  224             2.71807E-04
  228             2.90341E-04
  232             2.91865E-04
  236             2.93192E-04
  240             2.77562E-04
  244             2.95352E-04
  248             2.96227E-04
  252             2.96989E-04
  256             2.97653E-04
  260             2.81446E-04
  264             2.81949E-04
  268             2.82386E-04
  272             2.65983E-04
  276             2.66315E-04
  280             2.49820E-04
  284             2.50071E-04
  288             2.50290E-04
  292             2.50481E-04
  296             2.67431E-04
ARE YOU DONE(Y OR N)?Y

STOP AT LINE 1200

READY
```

APPENDIX 4B

```
OLD
OLD FILE NAME--SUMRAY.MA

READY

LIST

SUMRAY  01-AUG-77  BASIC V01B-02A

5 REM--  SUMRAY.MA                              MAY 26/77
6 REM--                  SUMMARY OF IN-PARALLEL & IN-SERIES ANALYSIS
10 PRINT \PRINT \PRINT \PRINT "COMMENT"
20 INPUT H$\PRINT
25 PRINT "INPUT INTERCEPT A1,A2 (MMOLES/KG/SEC)"
26 INPUT A1,A2\PRINT
30 PRINT "INPUT TIME CONSTANT(1/SEC)"
31 INPUT K1,K2\PRINT
40 C1=A1/K1\REM--   IN-PARALLEL CONTENT
41 C2=A2/K2
42 D=C1+C2
50 D1=(A1+A2)^2/(A1*K1+A2*K2)\REM--IN-SERIES CONTENT
51 D2=D-D1
60 K0=(A1+A2)/1.8
70 PRINT \PRINT \PRINT H$
71 PRINT
80 PRINT TAB(6);"IN PARALLEL";TAB(36);"IN SERIES";TAB(55);"TOTAL CA"
81 PRINT "     D1              D2              D1              D2         (MM
ES/KG)"
82 PRINT "************  ************  ************  ************  ****
******"
90 PRINT C1,C2,D1,D2,D
91 PRINT \PRINT
100 PRINT TAB(6);"IN PARALLEL";TAB(36);"IN SERIES";TAB(57);"K-01"
101 PRINT "  T1/2(1)        T1/2(2)        T1/2(1)        T1/2(2)        (
SEC)"
102 PRINT "************  ************  ************  ************  ***
*******"
110 PRINT .693/K1,.693/K2,.693/((A1+A2)/D1),.693/K2,K0
111 PRINT \PRINT
120 PRINT "ARE YOU DONE(Y OR N)";
121 INPUT Q$
122 IF Q$="Y"GO TO 200
123 IF Q$="N"GO TO 10
124 GO TO 120
200 STOP\END

READY
```

```
RUN

SUMRAY  01-AUG-77  BASIC V01B-02A



COMMENT
?M30E1.W2 0-CA WASH

INPUT INTERCEPT A1,A2 (MMOLES/KG/SEC)
?7.19852E-2
?6.83648E-4

INPUT TIME CONSTANT(1/SEC)
?7.49602E-2
?3.63975E-3



M30E1.W2 0-CA WASH

      IN PARALLEL                    IN SERIES                TOTAL CA
      D1            D2               D1            D2          (MMOLES/KG)
************  ************  ************  ************  ************
 .960312       .187828       .978188       .169952       1.14814

      IN PARALLEL                    IN SERIES                 K-01
  T1/2(1)       T1/2(2)          T1/2(1)       T1/2(2)        (1/SEC)
************  ************  ************  ************  ************
 9.24491       190.398       9.3284        190.398       .0403716

ARE YOU DONE(Y OR N)?Y

STOP AT LINE 200

READY
```

APPENDIX 5

Scatchard plot of calcium binding to cardiac sarcolemma

Reversible binding reaction between calcium (a ligand) and a binding site Q (eg. one or more sialic acid groups) is described by

$$Ca + Q \rightleftharpoons Ca - Q \tag{5a}$$

The system is generally assumed to behave according to second-order chemical kinetics, i.e., the association-dissociation reaction reaches equilibrium, in such a way that

$$K_{eq} = \frac{[Ca - Q]}{[Ca]\ [Q]} \tag{5b}$$

K_{eq} is a physical constant characteristic of Ca and Q. $[Ca]$, $[Q]$, and $[Ca - Q]$ are the equilibrium concentrations of free Ca, free Q, and Ca − Q complex.

If we define

$$[Q_{tot}] = [Q] + [Ca - Q] \tag{5c}$$

$$[Ca_{tot}] = [Ca] + [Ca - Q] \tag{5d}$$

where Q_{tot} is the total binding sites and Ca_{tot} is the total calcium, then equation 5b becomes:

$$K_{eq} = \frac{[Ca - Q]}{[Ca]\ ([Q_{tot}] - [Ca - Q])} \tag{5e}$$

This can be re-arranged to become

$$\frac{[Ca - Q]}{[Ca]} = K_{eq}\ [Q_{tot}] - K_{eq}\ [Ca - Q] \tag{5f}$$

The graphical representation of $[Ca - Q] / [Ca]$ as a function of $[Ca - Q]$ produces a straight line with x and y intercepts respectively $[Q_{tot}]$ and $K_{eq}[Q_{tot}]$. This is called a Scatchard plot.

In the case when more than one binding sites are available, the Scatchard plot is no longer linear but rather a concave curve as is shown in figure 16.

Consider the case where there are two binding sites in equilibration with one ligand Ca:

$$Ca + Q_1 \rightleftharpoons Ca - Q_1 \tag{5g}$$

$$Ca + Q_2 \rightleftharpoons Ca - Q_2 \tag{5h}$$

where the equilibrium constants of the 2 systems are described by

$$K_1 = [Ca - Q_1] / [Ca] [Q_{1\text{-}tot}] \tag{5i}$$

$$K_2 = [Ca - Q_2] / [Ca] [Q_{2\text{-}tot}] \tag{5j}$$

The Scatchard version of equation 5i and 5j are:

$$\frac{[Ca - Q_1]}{[Ca]} = K_1[Q_{1\text{-}tot}] - K_1[Ca - Q_1] \tag{5k}$$

$$\frac{[Ca - Q_2]}{[Ca]} = K_2[Q_{2\text{-}tot}] - K_2[Ca - Q_2] \tag{5l}$$

Thus on each point of the curve in figure 16, the concentration of free ligand is in equilibrium with the concentrations of ligand bound to each of the two groups of binding sites. Consequently, $[Ca - Q] / [Ca]$ at a point on the curve is the sum of $[Ca - Q_1]/[Ca]$ and $[Ca - Q_2]/[Ca]$ at a constant value of $[Ca]$.

$$\frac{[Ca - Q]}{[Ca]} = \frac{[Ca - Q_1]}{[Ca]} + \frac{[Ca - Q_2]}{[Ca]}$$

$$= \frac{[Ca - Q_1] + [Ca - Q_2]}{[Ca]} \qquad (5m)$$

Substituting $[Ca - Q_1]$ and $[Ca - Q_2]$ from equation 5k and 51 into equation 5m, we get

$$\frac{[Ca - Q]}{[Ca]} = \frac{K_1[Q_{1\text{-tot}}]}{K_1[Ca] + 1} + \frac{K_2[Q_{2\text{-tot}}]}{K_2[Ca] + 1} \qquad (5n)$$

As $[Ca]$ approaches large value $K_1[Ca] >> 1$ and equation 5n becomes

$$\frac{[Ca - Q]}{[Ca]} = \frac{[Q_{1\text{-tot}}] + [Q_{2\text{-tot}}]}{[Ca]} \qquad (5o)$$

or

$$[Ca - Q] = [Q_{1\text{-tot}}] + [Q_{2\text{-tot}}] \qquad (5p)$$

On Scatchard plot, the extrapolated x-intercept is therefore the total binding sites of component 1 and 2.

On the other hand, at very low $[Ca]$ (and consequently very low $[Ca - P]$), $K_1[Ca] << 1$ and equation 5n becomes

$$\frac{[Ca - Q]}{[Ca]} = K_1[Q_{1\text{-tot}}] + K_2[Q_{2\text{-tot}}] \qquad (5q)$$

Thus on Scatchard plot, the extrapolated y-intercept is $(K_1[Q_{1\text{-tot}}] + K_2[Q_{2\text{-tot}}])$.

Feldman (1972) gave a different derivation but arrived at the same expression as equation 5n. One important aspect

of this derivation necessitates some detailed discussion. Based on this, essentially, I have developed the computer program for separating the curvalinear Scatchard plot into its two components.

The general equation developed by Feldman (1972) for n ligands and m binding groups is given by

$$R_i = \sum_{j=1}^{m} \frac{K_{ij} Q_j}{1 + \sum_{i=1}^{n} K_{ij} F_i} \quad , i = 1,---, n. \tag{5r}$$

where Q_j is the total concentration of j^{th} binding group and F_i is the free concentration of i^{th} type ligand.

In the specific case of one ligand (n = 1) and two binding groups (m = 2), equation 5r can be reduced to the form of equation 5n.

$$R = \frac{b}{F} = \frac{K_1 Q_1}{1+K_1 F} + \frac{K_2 Q_2}{1+K_2 F} \tag{5s}$$

where I have abbreviated R_1, K_{11}, K_{12} and F_i as R, K_1, K_2 and F respectively. The total bound ligand is shown as b. Q_1 and Q_2 are total binding sites of the two binding groups.

Equation 5s can be cross-multiplied to get rid of denominators, multiplied with R on both sides and R x F can be substituted with b to yield:

$$K_1K_2b^2 + (K_1+K_2)Rb + R^2 - K_1K_2(Q_1+Q_2)b - (K_1Q_1 + K_2Q_2)R = 0. \tag{5t}$$

This equation has the general quadratic form

$$Ax^2 + Bxy + Cy^2 + Dx + Ey + F = 0 \tag{5u}$$

where

$$x = b$$
$$y = R$$
$$A = K_1K_2$$
$$B = K_1 + K_2$$
$$C = 1$$
$$D = -K_1K_2(Q_1+Q_2)$$
$$E = -K_1Q_1 - K_2Q_2$$
$$F = 0$$

Because the discriminant $B^2 - 4AC = (K_1 - K_2)^2$ is positive, the Scatchard plot (R vs b) is a hyperbola. The hyperbola intersects the y-axis at $K_1Q_1 + K_2Q_2$ (or when b=0 in equation 5t) as argued before.

The asymptotes of the hyperbola are the lines $y = -K_1(x - Q_1)$ and $y = -K_2(x - Q_2)$. The first asymptote has a y-intercept of K_1Q_1 while the other has a y-intercept of K_2Q_2. Thus the y-intercept of the Scatchard curve equals the sum of the y-intercepts of its asymptotes.

Equation 5t is a quadratic of R and can be solved explicitly in terms of b.

$$R = \tfrac{1}{2}\{ K_1(Q_1-b) + K_2(Q_2-b) + \sqrt{\{K_1(Q_1-b) - K_2(Q_2-b)\}^2 + 4K_1K_2Q_1Q_2}\ \} \qquad (5v)$$

Equations 5t and 5v allow me to develop a computer program using systematic approximation and least square fitting for resolution of the two components under a Scatchard curve. The approach and derivations are given in Appendix 6.

APPENDIX 6

Solution for Scatchard plot: successive approximation

From equation 4s in Appendix 4, we have

$$R = \frac{K_1 Q_1}{1+K_1 F} + \frac{K_2 Q_2}{1+K_2 F} \qquad (6a)$$

where R indicates different value of bound/free ligand ratio at different free ligand (F) concentrations. From previous discussion, we also have the x- and y-intercepts

$$x_0 = Q_1 + Q_2 \qquad (6b)$$

and

$$y_0 = K_1 Q_1 + K_2 Q_2. \qquad (6c)$$

Equations 6b and 6c can be rearranged and substituted to give

$$Q_1 = x_0 - Q_2 \qquad (6d)$$

$$K_1 = (y_0 - Q_2 K_2)/(x_0 - Q_2). \qquad (6e)$$

Substitution of 6d and 6e into equation 6a eliminates Q_1 and K_1 and yields an equation in terms of K_2 and Q_2 only.

$$(Fx_0Q_2 - RF^2Q_2)K_2^2 + (RFx_0 + RF^2y_0 - Fx_0y_0 - 2RFQ_2)K_2 + (Rx_0 - RQ_2 + RFy_0 - x_0y_0 + y_0Q_2) = 0 \qquad (6f)$$

This is a simple quadratic equation of the form

$$Ax^2 + Bx + C = 0 \qquad (6g)$$

where

$$A = Fx_0Q_2 - RF^2Q_2$$
$$B = RFx_0 + RF^2y_0 - Fx_0y_0 - 2RFQ_2$$
$$C = Rx_0 - RQ_2 + RFy_0 - x_0y_0 + y_0Q_2$$
$$x = K_2.$$

The solution of K is simply

$$K_2 = \frac{-B \pm \sqrt{B^2 - 4AC}}{2A} \tag{6h}$$

Consequently, given R, F, x_0, y_0, and a guessed Q_2 we can calculate the other constants Q_1, K_1 and K_2. The goodness of the guess can then be evaluated by least-square estimation.

I have developed the computer program (Appendix 7B) by assigning the initial Q_2 value half of the total binding sites

$$Q_2 = x_0/2. \tag{6i}$$

After taking the precaution that only positive K_1 and K_2 are accepted (negative K_1 and K_2 are meaningless), the mean of the different K_1 as well as that of K_2, as estimated from each data point (R, F and x_0, y_0), are determined and used as the final K_1 and K_2 values respectively. Together with Q_1 and Q_2 values, these are used to calculate the estimated R for each data point b, according to equation 5v. The sum of the square of the difference (SS) between estimated and given R is shown by equation 6j.

$$SS = \sum_{i=1}^{n} \{R_i(\text{estimated}) - R_i(\text{given})\}^2 \tag{6j}$$

where i indicates the i^{th} data point.

Successive approximation to get the best fit is achieved by a computer loop which looks at new values of Q in both increasing and decreasing direction according to

$$Q_2(\text{new}) = Q_2(\text{old}) \pm (\tfrac{1}{2})^i x_0 \qquad i = 1 \text{ to } 30 \tag{6k}$$

where i is the successive increments of the loop. For example, on the first time through the loop, two values of new Q_2 are evaluated; namely,

$$Q_2(\text{new}) = Q_2(\text{old}) + \tfrac{1}{2}\, x_0 \tag{61}$$

and

$$Q_2(\text{new}) = Q_2(\text{old}) - \tfrac{1}{2}\, x_0 \tag{6m}$$

Whether an increasing or a decreasing Q_2 is adopted depends on which value gives a lower SS. The loop is evaluated 30 times unless the difference between the new SS and the last evaluated SS is less than 0.1% of the latter, in which case the iteration terminates. In the case when the two new estimates of Q_2 provides no better fit, step increments (or decrements) of Q_2 by one-twentith of the normal step $(\tfrac{1}{2})^i x_0$ is scanned to find a better guess of Q_2.

Appendix 7A shows a computer program utilizing equation 5v for the generation of a Scatchard curve. Appendix 7B gives the computer program for resolving the Scatchard curve into its two components using successive approximations as outlined in Appendix 5 and 6. Using data generated by computer program SCATGN.BA (Appendix 7A), it is clear that the program SKATCH.BA can precisely resolve the Scatchard curve into its two components within 20 steps of successive approximations.

APPENDIX 7A

```
LIST

SCATGN  31-JUL-77  BASIC V01B-02A

1 REM--          SCATGN.BA
2 REM--GENERATE SCATCHARD PLOT                    JULY 31,77
3 DIM B(20)
5 PRINT "INPUT Q1,Q2,K1,K2"
10 INPUT Q1,Q2,K1,K2
15 PRINT "INPUT X-, Y-INTERCEPTS"
20 INPUT X,Y
25 PRINT \PRINT
30 PRINT "   R              B              F"
35 PRINT "---------    ----------    ----------"
40 B(0)=0
45 I=0\GOSUB 1100
50 PRINT S1,B(0)
55 FOR I=1 TO 20
60 B(I)=B(I-1)+(X/20)
65 GOSUB 1100
70 PRINT S1,B(I),B(I)/S1
75 NEXT I
80 STOP
1100 S1=(K1*(Q1-B(I))-K2*(Q2-B(I)))^2
1101 S1=SQR(S1+4*K1*K2*Q1*Q2)
1102 S1=.5*(S1+K1*(Q1-B(I))+K2*(Q2-B(I)))
1104 RETURN
1105 END

READY
```

```
RUN

SCATGN  31-JUL-77  BASIC V01B-02A

INPUT Q1,Q2,K1,K2
?2,8,5,.5
INPUT X-, Y-INTERCEPTS
?10,14
```

R	B	F
14	0	
12.2216	.5	.040911
10.6189	1	.094172
9.21066	1.5	.162855
8	2	.25
6.97267	2.5	.358543
6.10272	3	.491584
5.36034	3.5	.652944
4.7178	4	.847853
4.1521	4.5	1.08379
3.64531	5	1.37163
3.18387	5.5	1.72746
2.75765	6	2.17576
2.35907	6.5	2.75532
1.98245	7	3.53099
1.62346	7.5	4.61975
1.27882	8	6.25576
.945959	8.5	8.98559
.622875	9	14.4491
.307978	9.5	30.8464
0	10	

```
?DVO AT LINE 70

READY
```

APPENDIX 7B

```
LIST

SKATCH  31-JUL-77  BASIC V01B-02A

1 REM--                    SKATCH.BA              JULY 28,77
2 REM--      CA BINDING DATA ANALYSIS
3 REM--  ACCORDING TO SCATCHARD PLOT
4 REM--   AND LEAST SQUARE FITTING
5 REM--
8 DIM R1(20),B(20),F(20)
9 PRINT "NO. OF SCATCHARD PAIR DATA";\INPUT N
10 PRINT "INPUT (BOUND/FREE), (BOUND), (FREE)"\PRINT
16 FOR I=1 TO N
18 INPUT R1(I),B(I),F(I)\REM--  R1(I)=EXP R
20 NEXT I\PRINT
22 PRINT "INPUT X-INTERCEPT";\REM-- X=TOTAL BINDING SITES
24 INPUT X\REM--  =Q1+Q2
26 PRINT "INPUT Y-INTERCEPT";\REM--  Y=K1*Q1 +K2*Q2
28 INPUT Y
29 PRINT \PRINT
30 REM--FIRST ESTIMATION OF CURVE FIT
32 REM--ASSIGN Q2=X/2
34 REM-- SOLVE K2 AND Q1, K1
36 REM--A, B, C ARE QUADRAIC EQUATION COEFFICIENTS
38 REM--FOR SOLVING K2
39 Q2=X/2
40 GOSUB 1200 \REM--RETURN FROM 1232
42 REM-- OUTPUT FORMAT
44 PRINT "  Q2          Q1          K2          K1          SS"
46 PRINT "---------   --------   ----------   ----------   --------"
48 PRINT Q2,Q1,K2,K1,S9
49 X9=S9
50 REM--    SECOND AND SUBSEQUENT FIT
52 REM--         30 ITERATIONS
54 FOR J=2 TO 30
55 X9=S9\V1=Q1\V2=Q2\V3=K1\V4=K2
56 Q3=Q2
60 Q2=Q2+(1/2)^J*X
62 GOSUB 1200 \REM-- RETURN FROM 1232
64 X1=Q1\X2=Q2\X3=K1
66 X4=K2\X5=S9
68 Q2=Q3
70 Q2=Q2-(1/2)^J*X
72 GOSUB 1200 \REM-- RETURN FROM 1232
74 IF S9<X9GO TO 90
75 IF X5<X9GO TO 80
77 GOSUB 1300 \REM-- RETURN FROM 1340,1380
78 GO TO 100
80 Q1=X1\Q2=X2\K1=X3\K2=X4\S9=X5
85 GO TO 100
90 IF S9<X5GO TO 100
95 GO TO 80
100 PRINT Q2,Q1,K2,K1,S9
```

```
110 NEXT J
115 PRINT \PRINT
116 PRINT "    R                B"
117 PRINT "----------   ------------"
120 FOR I=1 TO N
125 GOSUB 1100 \REM-- RETURN FROM 1104
127 PRINT S1,B(I)
130 NEXT I
135 PRINT \PRINT
137 PRINT "         ANALYZED CURVE"
140 PRINT "----------------------------"
142 B(0)=0
143 I=0\GOSUB 1100 \REM-- RETURN FROM 1104
144 PRINT S1,B(0)
145 FOR I=1 TO 20
150 B(I)=B(I-1)+(X/20)
155 GOSUB 1100 \REM-- RETURN FROM 1104
160 PRINT S1,B(I)
165 NEXT I
200 STOP
989 REM-------------------------------------------------------------
990 REM-- SUBROUTINE TO SOLVE K2,K1,Q1, WITH Q2
1000 A=F(I)*X*Q2-R1(I)*F(I)^2*Q2
1002 B=R1(I)*F(I)*X+R1(I)*F(I)^2*Y
1003 B=B-F(I)*X*Y-2*R1(I)*F(I)*Q2
1004 C=R1(I)*X-R1(I)*Q2+R1(I)*F(I)*Y
1005 C=C-X*Y+Y*Q2
1006 Q1=X-Q2
1008 Y8=B^2-4*A*C
1010 IF Y8<0GO TO 1014
1012 S=SQR(Y8)\GO TO 1018
1014 M=M+1\Y7=1\GO TO 1080
1018 P1=(-B+S)/(2*A)\REM--          P1 & P2 ARE TEMPORARY K2
1020 P2=(-B-S)/(2*A)
1022 T1=(Y-Q2*P1)/(X-Q2)\REM--       T1 & T2 ARE TEMPORARY K1
1024 T2=(Y-Q2*P2)/(X-Q2)
1026 IF P1<0GO TO 1050
1028 IF P2<0GO TO 1056
1030 REM--P1>0 & P2>0
1031 IF T1<0GO TO 1060
1032 IF T2<0GO TO 1044
1033 K2=P1\K1=T1
1034 GOSUB 1100 \REM-- RETURN FROM 1104
1036 S3=(S1-R1(I))^2
1037 K2=P2\K1=T2
1038 GOSUB 1100 \REM-- RETURN FROM 1104
1040 S4=(S1-R1(I))^2
1042 IF S3>S4GO TO 1046
1044 K2=P1\K1=T1\GO TO 1048
1046 K2=P2\K1=T2
1048 GO TO 1080
1050 IF P2>0GO TO 1064
```

```
1052 REM-- P1<0 & P2<0
1054 M=M+1\Y7=1\GO TO 1080
1056 IF T1<0GO TO 1054
1058 GO TO 1044
1060 IF T2<0GO TO 1054
1062 GO TO 1046
1064 IF T2<0GO TO 1054
1066 GO TO 1046
1080 RETURN\REM-- RETURN TO 1204
1088 REM-------------------------------------------------------------
1090 REM-- SUBROUTINE TO FIND ESTIMATED R
1100 S1=(K1*(Q1-B(I))-K2*(Q2-B(I)))^2
1101 S1=SQR(S1+4*K1*K2*Q1*Q2)
1102 S1=.5*(S1+K1*(Q1-B(I))+K2*(Q2-B(I)))
1104 RETURN\REM-- RETURN TO 127,144,160,1036,1040,1228
1105 REM-------------------------------------------------------------
1190 REM-- SUBROUTINE TO FIND SS USING MEAN Q1,Q2,K1,K2
1200 A1=0\A2=0\B1=0\B2=0\M=0
1201 FOR I=1 TO N\Y7=0
1202 GOSUB 1000 \REM-- RETURN FROM 1080
1204 IF Y7=1GO TO 1212
1208 A1=A1+Q1\A2=A2+Q2
1210 B1=B1+K1\B2=B2+K2
1212 NEXT I
1213 IF (N-M)<=0GO TO 1240
1214 Q1=A1/(N-M)\Q2=A2/(N-M)
1216 K1=B1/(N-M)\K2=B2/(N-M)
1218 REM-- FIND SUM OF SQUARE OF THE DIFFERENCE
1220 REM-- BETWEEN ESTIMATED AND EXP. R
1222 S9=0
1224 FOR I=1 TO N
1226 GOSUB 1100 \REM-- RETURN FROM 1104
1228 S9=S9+(S1-R1(I))^2
1230 NEXT I
1232 RETURN\REM-- RETURN TO 42,64,74,1325,1365
1233 REM-------------------------------------------------------------
1240 S9=9.09494E+37
1242 GO TO 1232
1295 REM-------------------------------------------------------------
1298 REM--WHEN THE TWO NEW ESTIMATES ARE NO BETTER THAN THE LAST
1299 REM-- SUBROUTINE TO FIND A BETTER ESTIMATE OR  EXIT
1300 Q2=Q3
1305 IF S9<X5GO TO 1350
1310 FOR K=1 TO 20
1315 Q2=Q2+((1/2)^J*X)/20
1320 GOSUB 1200 \REM-- RETURN FROM 1232
1325 IF S9<=X9GO TO 1340
1326 D=SQR((S9-X9)^2)
1327 IF D<(1.00000E-03*S9)GO TO 115
1330 NEXT K
1335 Q1=V1\Q2=V2\K1=V3\K2=V4\S9=X9\GO TO 115
1340 RETURN\REM-- RETURN TO 78
```

```
1350 FOR L=1 TO 20
1355 Q2=Q2-((1/2)^J*X)/20
1360 GOSUB 1200 \REM-- RETURN FROM 1232
1365 IF S9<=X9GO TO 1380
1366 D=SQR((S9-X9)^2)
1367 IF D<(1.00000E-03*S9)GO TO 115
1370 NEXT L
1375 Q2=Q3\GO TO 1310
1380 RETURN\REM-- RETURN TO 78
1400 END

READY
```

```
RUN

SKATCH  01-AUG-77  BASIC V01B-02A

NO. OF SCATCHARD PAIR DATA?10
INPUT (BOUND/FREE), (BOUND), (FREE)

?12.2216,0.5,.040911
?10.6189,1.0,.094172
?9.21066,1.5,.162855
?8,2,.25
?6.97267,2.5,.358543
?6.10272,3,.491584
?5.36034,3.5,.652944
?4.7178,4,.847853
?4.1521,4.5,1.08379
?3.64531,5,1.37163

INPUT X-INTERCEPT?10
INPUT Y-INTERCEPT?14
```

Q2	Q1	K2	K1	SS
5	5	2.16131	.638687	54.2326
7.5	2.5	.417834	4.3465	.191817
7.5625	2.4375	.428008	4.41567	.146736
8.1875	1.8125	.531513	5.32317	.0282401
7.875	2.125	.47925	4.81219	.0121023
8.03125	1.96875	.505216	5.05015	7.67317E-04
8.02734	1.97266	.504564	5.04381	5.87219E-04
7.98828	2.01172	.498046	4.98155	1.07527E-04
8.00781	1.99219	.501303	5.01241	4.77823E-05
7.99805	2.00195	.499674	4.99691	3.00376E-06
7.99829	2.00171	.499715	4.9973	2.30267E-06
8.00073	1.99927	.500122	5.00116	4.17174E-07
7.99951	2.00049	.499918	4.99923	1.93287E-07
8.00012	1.99988	.50002	5.0002	1.32018E-08
8.00011	1.99989	.500017	5.00017	1.06305E-08
7.99995	2.00005	.499992	4.99993	4.55140E-09
8.00003	1.99997	.500005	5.00005	2.93045E-09
7.99999	2.00001	.499998	4.99999	2.48252E-09
8.00001	1.99999	.500001	5.00002	2.46661E-09

R	B
12.2216	.5
10.6189	1
9.21066	1.5
8	2
6.97267	2.5
6.10272	3
5.36034	3.5
4.7178	4
4.1521	4.5
3.64531	5

ANALYZED CURVE

14	0
12.2216	.5
10.6189	1
9.21066	1.5
8	2
6.97267	2.5
6.10272	3
5.36034	3.5
4.7178	4
4.1521	4.5
3.64531	5
3.18388	5.5
2.75765	6
2.35907	6.5
1.98245	7
1.62347	7.5
1.27882	8
.945962	8.5
.622876	9
.30798	9.5
1.60933E-06	10

```
STOP AT LINE 200

READY
```

APPENDIX 8A

```
READY

OLD
OLD FILE NAME--MAT1.BA

READY

15 W=1.15
20 C=0
22 V=10.1E-3
25 D=3.48E6
LIST

MAT1          BASIC V01B-02A

1 REM-- X   :  UMOLAR 40-CA
2 REM-- A   :  TISSUE 45-CA
3 REM-- F   :  MEDIUM 45-CA
4 REM-- W   :  TISSUE IN MG
5 REM-- C   :  VOLUME OF MEDIUM CONTAMINATION OF TISSUE , IN ML
6 REM-- V   :  VOLUME OF TOTAL REACTION MEDIUM , IN L
7 REM-- D   :  TOTAL 45-CA INPUT
10 INPUT X,A,F
12 X=X*1000\REM-NMOLAR
15 W=1.15
20 C=0
22 V=.0101
25 D=3.48000E+06
35 B=A-(F/(V*1000))*C
50 R=(B/F)/W*V
60 B2=((B/D)*V)*X/W
70 PRINT TAB(20);"R= ";R;"   B=";B2;" NMOLE/MG"
80 GO TO 10
90 END

READY
```

```
RUN

MAT1        BASIC V01B-02A
?20,82500,3.257E6
                    R=  2.22464E-04   B= 4.16417  NMOLE/MG
?30,77500,3.257E6
                    R=  2.08981E-04   B= 5.86769  NMOLE/MG
?50,71300,3.259E6
                    R=  1.92145E-04   B= 8.99713  NMOLE/MG
?70,67100,3.261E6
                    R=  1.80715E-04   B= 11.854   NMOLE/MG
?100,64800,3.264E6
                    R=  1.74361E-04   B= 16.3538  NMOLE/MG
?200,55000,3.272E6
                    R=  1.47629E-04   B= 27.7611  NMOLE/MG
?300,49000,3.277E6
                    R=  1.31324E-04   B= 37.0989  NMOLE/MG
?500,42600,3.287E6
                    R=  1.13824E-04   B= 53.7556  NMOLE/MG
?700,36900,3.294E6
                    R=  9.83844E-05   B= 65.1882  NMOLE/MG
?1000,32900,3.304E6
                    R=  8.74539E-05   B= 83.031   NMOLE/MG
?2000,23600,3.337E6
                    R=  6.21125E-05   B= 119.12   NMOLE/MG
?3000,19900,3.364E6
                    R=  5.19542E-05   B= 150.667  NMOLE/MG
?5000,16100,3.403E6
                    R=  4.15516E-05   B= 203.161  NMOLE/MG
?7000,14200,3.432E6
                    R=  3.63383E-05   B= 250.86   NMOLE/MG
?9000,13900,3.455E6
                    R=  3.53339E-05   B= 315.72   NMOLE/MG
?^C
```

APPENDIX 8B

```
READY

LIST

SKATCH      BASIC V01B-02A

 1 REM                  SKATCH.MB
 2 REM--      CA BINDING DATA ANALYSIS
 3 REM--   ACCORDING TO SCATCHARD PLOT
 4 REM--    AND LEAST SQUARE FITTING
 5 REM--
 8 DIM R1(20),B(20),F(20)
 9 PRINT "NO. OF SCATCHARD PAIR DATA";\INPUT N
10 PRINT "INPUT (B/F), (B)"
16 FOR I=1 TO N
18 INPUT R1(I),B(I)
19 F(I)=B(I)/R1(I)
20 NEXT I\PRINT
22 PRINT "INPUT X-INTERCEPT";\REM-- X=TOTAL BINDING SITES
24 INPUT X\REM--   =Q1+Q2
26 PRINT "INPUT Y-INTERCEPT";\REM--  Y=K1*Q1 +K2*Q2
28 INPUT Y
29 PRINT \PRINT
30 REM--FIRST ESTIMATION OF CURVE FIT
32 REM--ASSIGN Q2=X/2
34 REM-- SOLVE K2 AND Q1, K1
36 REM--A, B, C ARE QUADRAIC EQUATION COEFFICIENTS
38 REM--FOR SOLVING K2
39 Q2=X/2
40 GOSUB 1200 \REM--RETURN FROM 1232
42 REM-- OUTPUT FORMAT
44 PRINT "  Q2           Q1           K2           K1           SS"
46 PRINT "----------    --------    ----------    ----------    --------"
49 X9=S9
50 REM--     SECOND AND SUBSEQUENT FIT
52 REM--              20 ITERATIONS
54 FOR J=2 TO 20
55 X9=S9\V1=Q1\V2=Q2\V3=K1\V4=K2
56 Q3=Q2
60 Q2=Q2+(1/2)^J*X
62 GOSUB 1200 \REM-- RETURN FROM 1232
64 X1=Q1\X2=Q2\X3=K1
66 X4=K2\X5=S9
68 Q2=Q3
70 Q2=Q2-(1/2)^J*X
72 GOSUB 1200 \REM-- RETURN FROM 1232
74 IF S9<X9GO TO 90
75 IF X5<X9GO TO 80
77 GOSUB 1300 \REM-- RETURN FROM 1340,1390
78 GO TO 100
80 Q1=X1\Q2=X2\K1=X3\K2=X4\S9=X5
85 GO TO 100
90 IF S9<X5GO TO 100
95 GO TO 80
```

```
100 REM
110 NEXT J
115 PRINT Q2,Q1,K2,K1,S9\PRINT \PRINT
116 PRINT "    R                B"
117 PRINT "----------   ------------"
118 GO TO 22
120 FOR I=1 TO N
125 GOSUB 1100 \REM-- RETURN FROM 1104
127 PRINT S1,B(I)
130 NEXT I
135 PRINT \PRINT
137 PRINT "         ANALYZED CURVE"
140 PRINT "------------------------------"
141 DIM B1(20)
142 B(0)=0
143 I=0\GOSUB 1100 \REM-- RETURN FROM 1104
144 PRINT S1,B(0)
145 FOR I=1 TO 20
146 B1(I)=B(I)
150 B(I)=B(I-1)+(X/20)
155 GOSUB 1100 \REM-- RETURN FROM 1104
160 PRINT S1,B(I)
165 NEXT I
170 FOR I=1 TO N
175 B(I)=B1(I)
180 NEXT I
185 PRINT \PRINT "K2*Q2=";K2*Q2
190 PRINT "K1*Q1=";K1*Q1
200 STOP
989 REM-----------------------------------------------------------------
990 REM-- SUBROUTINE TO SOLVE K2,K1,Q1, WITH Q2
1000 A=F(I)*X*Q2-R1(I)*F(I)^2*Q2
1002 B=R1(I)*F(I)*X+R1(I)*F(I)^2*Y
1003 B=B-F(I)*X*Y-2*R1(I)*F(I)*Q2
1004 C=R1(I)*X-R1(I)*Q2+R1(I)*F(I)*Y
1005 C=C-X*Y+Y*Q2
1006 Q1=X-Q2
1008 Y8=B^2-4*A*C
1010 IF Y8<0GO TO 1014
1012 S=SQR(Y8)\GO TO 1018
1014 M=M+1\Y7=1\GO TO 1080
1018 P1=(-B+S)/(2*A)\REM--          P1 & P2 ARE TEMPORARY K2
1020 P2=(-B-S)/(2*A)
1022 T1=(Y-Q2*P1)/(X-Q2)\REM--       T1 & T2 ARE TEMPORARY K1
1024 T2=(Y-Q2*P2)/(X-Q2)
1026 IF P1<0GO TO 1050
1028 IF P2<0GO TO 1056
1030 REM--P1>0 & P2>0
1031 IF T1<0GO TO 1060
1032 IF T2<0GO TO 1044
1033 K2=P1\K1=T1
```

```
1034 GOSUB 1100 \REM-- RETURN FROM 1104
1036 S3=(S1-R1(I))^2
1037 K2=P2\K1=T2
1038 GOSUB 1100 \REM-- RETURN FROM 1104
1040 S4=(S1-R1(I))^2
1042 IF S3>S4GO TO 1046
1044 K2=P1\K1=T1\GO TO 1048
1046 K2=P2\K1=T2
1048 GO TO 1080
1050 IF P2>0GO TO 1064
1052 REM-- P1<0 & P2<0
1054 M=M+1\Y7=1\GO TO 1080
1056 IF T1<0GO TO 1054
1058 GO TO 1044
1060 IF T2<0GO TO 1054
1062 GO TO 1046
1064 IF T2<0GO TO 1054
1066 GO TO 1046
1080 RETURN\REM-- RETURN TO 1204
1088 REM-------------------------------------------------------------------
1090 REM-- SUBROUTINE TO FIND ESTIMATED R
1100 S1=(K1*(Q1-B(I))-K2*(Q2-B(I)))^2
1101 S1=SQR(S1+4*K1*K2*Q1*Q2)
1102 S1=.5*(S1+K1*(Q1-B(I))+K2*(Q2-B(I)))
1104 RETURN\REM-- RETURN TO 127,144,160,1036,1040,1228
1105 REM-------------------------------------------------------------------
1190 REM-- SUBROUTINE TO FIND SS USING MEAN Q1,Q2,K1,K2
1200 A1=0\A2=0\B1=0\B2=0\M=0
1201 FOR I=1 TO N\Y7=0
1202 GOSUB 1000 \REM-- RETURN FROM 1080
1204 IF Y7=1GO TO 1212
1208 A1=A1+Q1\A2=A2+Q2
1210 B1=B1+K1\B2=B2+K2
1212 NEXT I
1213 IF (N-M)<=0GO TO 1240
1214 Q1=A1/(N-M)\Q2=A2/(N-M)
1216 K1=B1/(N-M)\K2=B2/(N-M)
1218 REM-- FIND SUM OF SQUARE OF THE DIFFERENCE
1220 REM-- BETWEEN ESTIMATED AND EXP. R
1222 S9=0
1224 FOR I=1 TO N
1226 GOSUB 1100 \REM-- RETURN FROM 1104
1228 S9=S9+(S1-R1(I))^2
1230 NEXT I
1232 RETURN\REM-- RETURN TO 42,64,74,1325,1365
1233 REM-------------------------------------------------------------------
1240 S9=9.09494E+37
1242 GO TO 1232
```

```
1295 REM-----------------------------------------------------------------
1298 REM--WHEN THE TWO NEW ESTIMATES ARE NO BETTER THAN THE LAST
1299 REM-- SUBROUTINE TO FIND A BETTER ESTIMATE OR  EXIT
1300 Q2=Q3
1305 IF S9<X5GO TO 1350
1310 FOR K=1 TO 20
1315 Q2=Q2+((1/2)^J*X)/20
1320 GOSUB 1200 \REM-- RETURN FROM 1232
1325 IF S9<=X9GO TO 1340
1326 D=SQR((S9-X9)^2)
1327 IF D<(1.00000E-03*S9)GO TO 115
1330 NEXT K
1335 Q1=V1\Q2=V2\K1=V3\K2=V4\S9=X9\GO TO 115
1340 RETURN\REM-- RETURN TO 78
1350 FOR L=1 TO 20
1355 Q2=Q2-((1/2)^J*X)/20
1360 GOSUB 1200 \REM-- RETURN FROM 1232
1365 IF S9<=X9GO TO 1380
1366 D=SQR((S9-X9)^2)
1367 IF D<(1.00000E-03*S9)GO TO 115
1370 NEXT L
1375 Q2=Q3\GO TO 1310
1380 RETURN\REM-- RETURN TO 78
1400 END

READY
```

```
OLD FILE NAME--SKATCH.MB

READY

RUN

SKATCH      BASIC V01B-02A

NO. OF SCATCHARD PAIR DATA?15
INPUT (B/F); (B)
?2.22464E-4,4.16417
?2.08981E-4,5.86769
?1.92145E-4,8.99714_3
?1.80715E-4,11.854
?1.74361E-4,16.3538
?1.47629E-4,27.7611
?1.31324E-4,37.0989
?1.13824E-4,53.7556
?9.83844E-5,65.1882
?8.74539E-5,83.031
?6.21125E-5,119.12
?5.19542E-5,150.667
?4.15516E-5,2-0__03.161
?3.63383E-5,250.86
?3.53338E-5,315.72

INPUT X-INTERCEPT?350
INPUT Y-INTERCEPT?2.5E-4

   Q2          Q1          K2          K1          SS
---------   --------   ----------   ----------   -------
 335.283      14.7175     2.76694E-07  1.06832E-05  1.22814E-09

    R           B
----------  ----------
INPUT X-INTERCEPT?365
INPUT Y-INTERCEPT?2.4E-4

   Q2          Q1          K2          K1          SS
---------   --------   ----------   ----------   -------
 19.4731      345.527     7.95490E-06  2.46272E-07  9.03688E-10

    R           B
----------  ----------
INPUT X-INTERCEPT?365
INPUT Y-INTERCEPT?2.35E-4

   Q2          Q1          K2          K1          SS
---------   --------   ----------   ----------   -------
 22.8125      342.188     6.71248E-06  2.39259E-07  8.56319E-10
```

```
     R                B
----------    ------------
INPUT X-INTERCEPT?370
INPUT Y-INTERCEPT?2.35E-4

  Q2            Q1            K2             K1             SS
--------      --------    ----------    ----------    -------
 23.125         346.875       6.66578E-06    2.33092E-07    8.10876E-10

     R                B
----------    ------------
INPUT X-INTERCEPT?^C

.RE

READY

GOTO120
 2.17171E-04    4.16417
 2.10305E-04    5.86769
 1.98370E-04    8.99713
 1.88259E-04    11.854
 1.73862E-04    16.3539
 1.45168E-04    27.7611
 1.28449E-04    37.0989
 1.09220E-04    53.7556
 9.85493E-05    65.1892
 8.71213E-05    83.031
 7.06292E-05    119.12
 5.94364E-05    150.667
 4.35205E-05    203.161
 3.04291E-05    250.86
 1.36079E-05    315.72
```

```
        ANALYZED CURVE
-------------------------------
 2.35000E-04    0
 1.67640E-04    18.5
 1.28602E-04    37
 1.06577E-04    55.5
 9.24817E-05    74
 8.21773E-05    92.5
 7.38749E-05    111
 6.67333E-05    129.5
 6.03174E-05    148
 5.43927E-05    166.5
 4.87826E-05    185
 4.34241E-05    203.5
 3.82453E-05    222
 3.32040E-05    240.5
 2.82698E-05    259
 2.34210E-05    277.5
 1.86411E-05    296
 1.39177E-05    314.5
 9.24116E-06    333
 4.60399E-06    351.5
 0              370

K2*Q2= 1.54146E-04
K1*Q1= 8.08537E-05

STOP AT LINE 200

READY

PRINT 1/K2*1E-6,     1/K1*1E-6
 .15002          4.29015
```